EXPERIMENTAL ANALYSIS OF AN AUXILIARY AIR CONDITIONING SYSTEM USED IN AN ARMORED VEHICLE

A THESIS SUBMITTED TO
THE GRADUATE SCHOOL OF NATURAL AND APPLIED SCIENCES
OF
MIDDLE EAST TECHNICAL UNIVERSITY

BY

ALPER KORKMAZ

IN PARTIAL FULFILLMENT OF THE REQUIREMENTS
FOR
THE DEGREE OF MASTER OF SCIENCE
IN
MECHANICAL ENGINEERING

JUNE 2015

Approval of the thesis:

EXPERIMENTAL ANALYSIS OF AN AUXILIARY AIR CONDITIONING SYSTEM USED IN AN ARMORED VEHICLE

submitted by **ALPER KORKMAZ** in partial fulfillment of the requirements for the degree of **Master of Science in Mechanical Engineering Department, Middle East Technical University** by,

Prof. Dr. M. Gülbin Dural Ünver _____
Dean, Graduate School of **Natural and Applied Sciences**

Prof. Dr. Tuna Balkan _____
Head of Department, **Mechanical Engineering**

Assoc. Prof. Dr. Cemil Yamalı _____
Supervisor, **Mechanical Engineering Dept., METU**

Assist. Prof. Dr. Özgür Bayer _____
Co-Supervisor, **Mechanical Engineering Dept., METU**

Examining Committee Members:

Prof. Dr. Kahraman Albayrak _____
Mechanical Engineering Dept., METU

Assoc. Prof. Dr. Cemil Yamalı _____
Mechanical Engineering Dept., METU

Assoc. Prof. Dr. İlker Tarı _____
Mechanical Engineering Dept., METU

Assist. Prof. Dr. Özgür Bayer _____
Mechanical Engineering Dept., METU

Prof. Dr. Mecit Sivrioğlu _____
Mechanical Engineering Dept., Gazi University

Date: 03.07.2015

Thereby declare that all information in this document has been obtained and presented in accordance with academic rules and ethical conduct. I also declare that, as required by these rules and conduct, I have fully cited and referenced all material and results that are not original to this work.

Name, Last Name : Alper KORKMAZ

Signature :

ABSTRACT

EXPERIMENTAL ANALYSIS OF AN AUXILIARY AIR CONDITIONING SYSTEM USED IN AN ARMORED VEHICLE

Korkmaz, Alper
M.Sc., Department of Mechanical Engineering
Supervisor : Assoc. Prof. Dr. Cemil Yamalı
Co-Supervisor : Assist. Prof. Dr. Özgür Bayer

June 2015, 162 Pages

In this thesis study, the theoretical design phases and experiments are performed about the air conditioning unit for a specific military vehicle, which is designed to be driven by an Auxiliary Power Unit (APU) system. The purpose is to determine the vapor compression refrigeration cycle characteristics under different load conditions on both the evaporator and the condenser as well as observe the particular mass flow rates considering the vapor and liquid phases of the refrigerant. Additionally, all experiment results are compared in terms of pressures, temperatures, relevant mass flow rates as well as performance characteristics such as COP, volumetric, isentropic and exergetic efficiencies, condenser heat rejection rate, evaporator cooling capacity and compressor work.

The APU systems are commonly used in military vehicles to power the any required units/systems, desired to run externally. Details of the APU system are explained in the following chapters. In present study, APU is purposed to run the compressor of the

A/C system. Accordingly, A/C system has also other main components such as; evaporator unit with expansion valve and receiver-filter-dryer, and condenser module. Considering these, the thermodynamic cycle analysis of the whole A/C system is conducted as well as componentwise analysis.

In the tests, the temperatures and the pressures at the inlet/outlet of the components are recorded. In addition, mass flow rates in the both high-pressure (liquid) and low-pressure (vapor) sides are observed. All these data are internally compared according to the experiments results to observe the efficiency of refrigeration vapor compression cycle as well as for better understanding the dynamics of the A/C system.

In conclusion, test setup is prepared to perform six different load configurations on the evaporator and condenser, and relevant results are presented accordingly.

Keywords: APU, A/C system, compressor, evaporating unit, condenser module

ÖZ

ZIRHLI ARAÇLAR İÇİN YARDIMCI KLİMA SİSTEMİ DENEYSEL ANALİZİ

Korkmaz, Alper
Yüksek Lisans, Makine Mühendisliği Bölümü
Tez Yöneticisi : Doç. Dr. Cemil Yamalı
Ortak Tez Yöneticisi : Yrd. Doç. Dr. Özgür Bayer

Haziran 2015, 162 Sayfa

Bu tezde, özel bir askeri araç için tasarlanan ve bir harici güç ünitesi ile sürülen (HGÜ) klima sisteminin teorik tasarım aşamaları ve testleri gerçekleştirilmiştir. Amaç, kondenser ve evaporator üniteleri üzerinde oluşturulan farklı ısı yükleri altında buhar sıkıştırma döngüsü karakterini belirlerken, soğutucu akışkanın sıvı ve gaz hallerindeki kütlesel debilerini gözlemlemektir. Ek olarak, yapılan bütün testlerin sonuçları basınçlar, sıcaklıklar, ilgili kütlesel debiler dikkate alınarak karşılaştırılmıştır. Bunun yanında, deney sonuçlarının karşılaştırılmasında testlerin performans özelliklerinden olan performans katsayısı, kütlesel, izentropik ve eksergetik verimleri ve kondenser ısı uzaklaştırma oranı, evaporator soğutma kapasitesi ve kompresör gücü de sonuç bölümünde sunulmuştur.

Harici güç üniteleri, herhangi bir birimi veya sistemi dışardan enerjilendirmek/çalıştırmak için askeri araçlarda sıklıkla kullanılan sistemlerdir. Harici güç ünitesini detayları ilerleyen bölümlerde anlatılacaktır. Bu çalışmada, HGÜ,

klima sisteminde yer alan kompresörü çalıştırmak için kullanılmıştır. Benzer şekilde, klima sistemi, genleşme valfli ve kurutucu filtreli evaporator ünitesi ve kondenser ünitesi şeklinde başka ana bileşenlere de sahiptir. Bu elemanlar da göz önünde bulundurularak, bütün klima sisteminin döngüsel termodinamik analizi yanı sıra birleşen bazlı analizleri de gerçekleştirilmiştir.

Testlerde, elemanların giriş ve çıkış bağlantılarındaki sıcaklık ve basınçlar kaydedilmiştir. Ek olarak, yüksek ve alçak basınç bölgelerindeki sıvı ve gaz fazlardaki kütlesel akış debileri gözlemlenmiştir. Bütün bu deney sonuçları hem soğutucu buhar sıkıştırma döngüsünün verimini gözlemlemek hem de klima sistemi dinamiklerini anlamak için karşılaştırmalı olarak belirtilmiştir.

Sonuç olarak, evaporator ve kondenser üzerinde oluşturulan altı farklı ısıl yük konfigürasyonlarını uygulamak için deney düzeneği kurulmuş olup, ilgili test sonuçları buna göre sunulmuştur.

Anahtar kelimeler: HGÜ, Klima sistemi, kompresör, evaporator ünitesi, kondenser ünitesi

To My Parents;

Mrs. Salime KORKMAZ

Mr. Muzaffer KORKMAZ

ACKNOWLEDGEMENTS

I would like to express deepest gratitude to my supervisor Assoc. Prof. Dr. Cemil Yamalı and co-supervisor Assist. Prof. Dr. Özgür Bayer for their guidance, advices, criticisms, encouragements and insights throughout the research.

The technical assistance of Mr. Serhat Başaran, Mr. Tonguç Yalçın, Mr. N. Tayfun Yılmaz and Mr. Çağdaş İnan are gratefully acknowledged.

I would also like to thank my dearest friends Hilmi, Emrah, Eren, Evren, Sedat and Emine, who gave great support in every step of this study.

This study was supported by FNSS SAVUNMA SİSTEMLERİ A.Ş.

TABLE OF CONTENTS

LIST OF TABLES

TABLES

LIST OF FIGURES

FIGURES

LIST OF SYMBOLS

SYMBOLS

AFV……...Armored Fighting Vehicle

ACV……...Armored Command-Post Vehicle

APU……..Auxiliary Power Unit

MMI……...…Man-Machine Interface Unit

A/C……..Air Conditioning System

COP…….....Coefficient of Performance

T_L……...…….Low Temperature Reservoir

T_H……...High Temperature Reservoir

T…….....…….. Temperature, °C

T_0…….……..Reference Temperature, K

P…….Pressure, kPa

s……...……..Entropy, kJ/kg.K

h……..……Enthalpy, kJ/kg

ρ……...….Density, kg/m^3

c_v…….Constant Volume Specific Heat, kJ/kg.K

c_p……...….Constant Pressure Specific Heat, kJ/kg.K

η_s……...…Isentropic Efficiency

η_v…….…Volumetric Efficiency

η_x……....Exergetic Efficiency

N_{rpm}……...Compressor Speed

$\dot{m}_{comp}$……..Mass Flow Rate, kg/s

k…….....…Isentropic Exponent

c_r……...….Compressor Clearance Ratio

Q_{evap}…….…..Evaporator Cooling Capacity, kW

Q_{cond}……...Condenser Heat Rejection, kW

W_{comp}……..Compressor Work, kW

x……....Exergy Destruction, kW

σ_T……...……Uncertainty in Temperature, °C

σ_P…….……Uncertainty in Temperature, kPa

σ_{flow}……Uncertainty in Mass Flow Rate, kg/s

σ_{cond}…….……Uncertainty in Condenser Heat Rejection, kW

CHAPTER 1

INTRODUCTION

1.1. 8x8x8 ARMORED FIGHTING VEHICLE

8x8x8 Armored Fighting Vehicles are the multi-purposes wheeled tactical military systems, designed to accomplish related number of operations with their mission objectives. 8x8x8 simply represents the eight-wheeled, eight-wheel drive and eight-wheel steering respectively. This property provides the vehicle stabilized-drive dynamics on any surfaces such as sandy road or rocky terrain. Furthermore, eight-wheel steering, indeed, brings vehicle the high maneuverability capabilities in any conditions. Besides these drive related properties, 8x8x8 vehicles are designed to carry out wide variety of utility missions having several different operational variants. [1] To clarify, during the operations, one vehicle specifically focuses on pre-defined duties. Hence, these types of vehicles can be designed as having multi-discipline variants such as; Infantry Carrier Vehicle, Infantry Fighting Vehicle, Mortar, Command Post, Recovery and Fitters, Armored Ambulance and so on. In the figure 1, common variants of tactical wheeled vehicles can be seen. Another remarkable feature of vehicle is the advance technology hull protection systems. The hull, basic vehicle shell, is produced from hard steel or armor steel. Depending on the mission requirements, overall hull can be assembled with the modular armor shields. Additionally, against the attacks from below the vehicles, the protection for crew is reinforced with both underbody hull geometry and the mine-protection seats.

Figure 1 8x8x8 Armored Fighting Vehicle Common Variants [2]

A further characteristic of the tactical wheeled vehicles is the amphibiousness. Vehicles, having this property, can also move in the water by using their water jet propellers assembled on the rear of vehicle. During past years, the significance of this property has been well understood by the ground vehicle military industry society and nowadays modern warfare systems are figured amphibiousness as essential property.

Figure 2 Amphibious Operation, IFV [3]

On the other hand, considering all these vital features, an AFV is consist of the sub-systems providing vehicle to gain above abilities which are the building blocks of the whole system. Practically, they give vehicle to contain automotive or military abilities,

stated above, that can be used by utilizer actively or done by the system automatically. For instance, going with the above prominent properties, an AFV may be equipped with Central Tire Inflation System (CTIS), Integrated Auxiliary Power Unit (APU), Self-recovery Winch, Air Conditioning (A/C), Nuclear-Biological-Chemical Protection (NBC), Automatic Fire Suppression System, Land Navigation System and Independent Air Suspension System with Ride Height Adjustment etc. [4] During land or water operations, all these sub-systems run within an integrity for the success of mission. Indeed, the one of the main topic of this thesis study is the Integrated Auxiliary Power Unit (APU) system. Although the some general specifications of the APU will be indicated in the following section, in the name of giving some basic of the APU in ACV, it has two major objects. First one, can be classified as key feature, is the supplying electrical power for the vehicle batteries when the main engine is either ON or OFF. Other feature is that the APU is in charge of supplying the power for the vehicle personnel cabin A/C.

At the same time, while the general situation is as above, it is better to get familiar the vehicle AV-8 ACV on which the APU-driven air conditioning system is used as a vital sub-system. The "AV-8" is the name of the project that is signed to design and manufacture a set of wheeled armored vehicle for the Malaysian Army by the FNSS Savunma Sistemleri A.Ş. As stated above, "ACV" is the armored command-post vehicle variant in the project. In details, to have a look of its main properties, ACV is the vehicle that commands and guides the other vehicles in the operation. It has common features of 8x8x8 Armored Personnel Carrier, such as eight-wheeled, eight-wheel drive and eight-wheeled steering. Besides, from the modularity perspective of the project, ACV has high level of ballistic protected hull, adjustable ride height air suspensions, amphibious feature, compact power pack and drivetrain systems, self-recovery winch system and interconnected electrical control modules with CAN-Bus technology and so on. [5] In figure 3, general view and some aspects of the ACV variant can be seen.

Figure 3 General View of AV-8 ACV

Along with the modular features of the vehicle, ACV has also variant specific sub-systems. As indicated previously, Integrated Auxiliary Power Unit (APU), Remote Control Weapon System (RCWS), and Commander Communication Unit are the major systems that are designed to meet the ACV operation requirements. For the following, the general technical and performance specifications of the vehicle can be found.

Table 1 AV-8 ACV Technical Specifications [5]

TECHNICAL	
Engine	550 hp Diesel Engine
Transmission	Fully Automatic 6 Forward 1 Reverse
Power to Weight Ratio	≥ 20 hp/tones
Number of Axles	4
Driven Axles	All
Steered Axles	1,2,3,4
Suspension	Semi-Automatic, Pneumatic & Adjustable
Electrical System	Integrated CAN-Bus, MIL-STD 1275

Table 2 AV-8 ACV Performance Specifications [5]

PERFORMANCE	
Max. Road Speed	100 km/h
Creep Speed	3 km/h
Swimming	8 km/h (with Propellers)
Range	700 km
Angle of Approach	> 50°
Angle of Departure	> 40°
Gradient	60%
Side Slope	30%
Vertical Obstacle	0.70 m
Turning Radius	< 8.00 m
Ground Clearance	0.2 to 0.5 m (Adjustable)

1.2. AUXILIARY POWER UNITS

The Auxiliary Power Units (APU) are the secondary power sources in the systems that can be used during any emergency case or their functions can be limited in the frame of specific operations rather than main propulsion units. In this point of view, historically, initiatory APU was used during World War I by the British Army, of the duty by supplying electrical power for the aircraft's radio transmitter and mechanical power for an air blower. By proving their necessity for critical circumstances, furthermore, APU systems had been also started to be used in WV II and nowadays, they have been ranking among the necessary components of all types of vehicle. In modern world, APU systems can be used in some large aircrafts, naval ships, as well as military vehicles. [6] Indeed, APU systems are defined as subsidiaries of main power systems for supplying electric, hydraulics or pneumatic power depending on system needs, as well as it is desired that the both system can run simultaneously or in the scope of specific mission requirements. In detail, followings indicate the types of APU manufactured around the worldwide.

Figure 4 APIC APS3200 APU for Airbus A320 [6]

1.2.1. APU SYSTEM DETAILS

In this section, the common components of the APU systems are explained and furthermore, some examples of the APU manufacturers and their products' specifications are presented.

In general, an APU system can be consists of;

- Diesel engine as main power supply
- Embedded cooling system for engine
- Exhaust system
- Air intake system
- Alternator for electrical power
- Compressor for A/C system
- Electrical system of APU

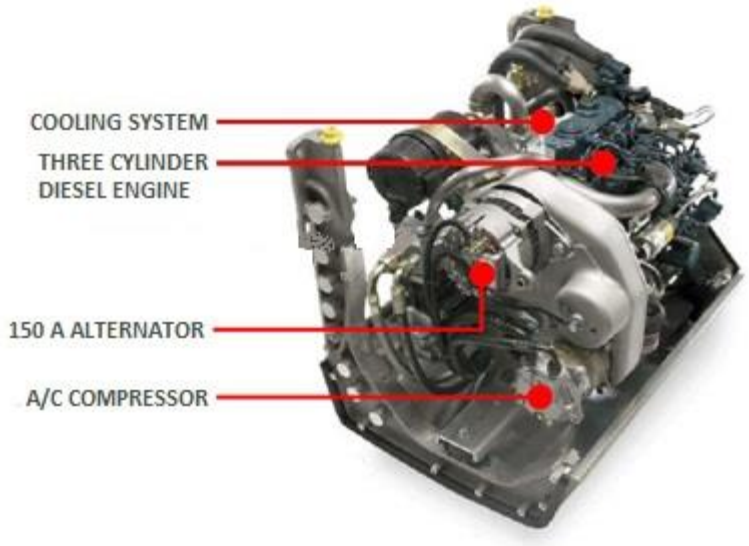

Figure 5 Common Components of APU [7]

In details, small size diesel engines are considerably used as the main power supplies in APU systems. They are basically three-cylinder engines providing power output around 9-40 kW. These all diesel engines are compatible with the ASTM No 2-D [8] fuel specification, such as F54 and F34 fuels. Deutz AG, Kubota and Mitsubishi are among the well-known engine suppliers around the world. For the supportive sub-systems, which can be shortly classified as cooling system, exhaust system and air intake system, either they all can be designed specifically for the related APU system according to the requirements of the engine or on-the-shelf products can be utilized. Furthermore, alternators, one of the primary components of the system, are responsible for D/C electric generation in the unit. Their ranges are varying around 40-500 A, for example for military vehicles, depending the system needs. The alternators of Prestolite Electric, and C.E. Neihoff are commonly used in the military vehicle for their reliability and long service life. Later on, electrical systems utilized in APU's are usually designed for unit sensitive. Since every APU is a sub-system of upper tract, compromise is crucial property, which is reached by consistent electrical systems algorithm. For exemplifying, further sections are shortly describes the specifications of APU'S, designed by leading companies around the world.

GENERAL DYNAMICS LAND SYSTEMS

General Dynamics is one of the most important suppliers for the designing and producing the combat vehicles and weapon systems. Accordingly, their solutions for the specific needs are also well-known around the world. For the case in the point, here what is seen in Figure 6 is that the APU system is design by GD for the HMMWV 1123 (known also as Humvee). It provides 508 A at 28 vDC electrical output, in the environmental conditions as an altitude up to 3650 meters and temperatures from -32 °C to 55 °C. Its general dimension are 965 x 635 x 1600 mm (L x W x H) and consumes fuel types of DF-2, JP8 and Ultra Low Sulfur Diesel (ULSD). [9]

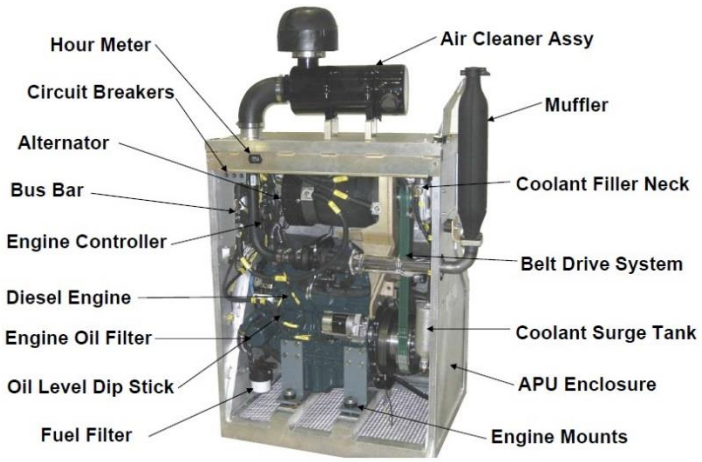

Figure 6 APU for HMMWV 1123 by General Dynamics [9]

MARVIN-LAND SYSTEMS

Marvin Land Systems is dealing with the manufacturing the original equipment such as environmental control units (ECU), auxiliary power units, generator, NBC systems, etc. for the military vehicles. As shown in Figure 7, their one of the most common products is the APU system for the Expeditionary Fighting Vehicle (EFV). As a main feature, the APU system supplies the 300 A at 28 vDC rated current output, from the temperature of -32°C to 51 °C, covering the altitude up to 3000 meters. Its gross weight is maximum 90 kg with dimensions 635 x 480 x 760 mm (L x W x H). Compatible with the fuel types of DF-1, DF-2, JP-4 and JP-8, APU uses the diesel engine of Kubota D722, Turbocharged. [10]

Figure 7 APU for EFV by Marvin Land Systems [10]

FISHER PANDA GENERATORS

The company defines themselves as the manufacturer of generator sets for the use special applications in military, marine and automotive industries. One of the prominent products, shown in Figure 8, is the "Panda AGT 5000 PE-150N designed for M577 Command Post Vehicle (CPV). APU has the property of panel mounted assembly, which can be located outside of the vehicle. The system's electrical output is 180 A at 28 vDC with operating temperature from -32°C to 50 °C, in the altitude up to 3000 meters. Max. dry weight of the APU is 240 kg and the overall dimensions are 734 x 867 x 518 mm (L x W x H). The system uses the F34 and F54 diesel fuels in its 3-cylinder turbocharged engine. [11]

Figure 8 Panda AGT 5000 PE-150N for M577 APC by Fisher Panda [11]

FNSS APU

FNSS SAVUNMA SİSTEMLERİ A.Ş. (FNSS) [12] designs, develops, and supports tailored, reliable and cost-effective land combat system solution, aiming to become the number one supplier of land combat system solutions for the Turkish Armed Forces and preferred local supplier around the world. In the Figure 9, APU system designed for AV8 Command Post vehicle, described above, can be seen. This APU is the power supply for the air conditioning system, as well as the electrical system, which is actually the main research topic of the thesis study.

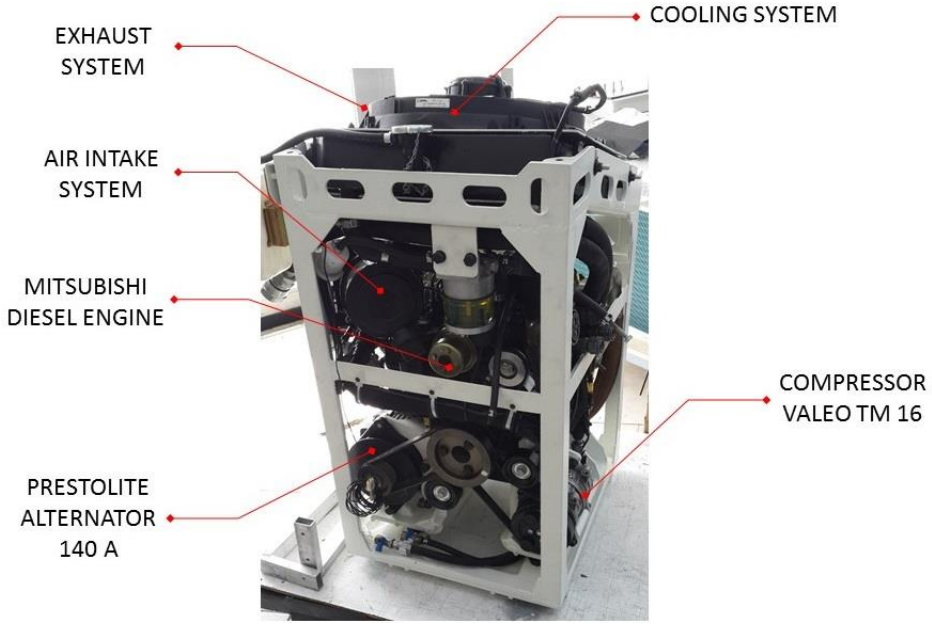

Figure 9 APU for AV-8 ACV by FNSS

Basically, FNSS APU is designed for primarily the supplying electrical power for charging the vehicle batteries during routine operational conditions and, in addition, if desired by the user, it can be used in any emergency cases, that is the lighting the load of batteries. Second primary task of the APU is the drive of the air conditioning system's compressor in the meaning of supplying mechanical power. APU has "Mitsubishi" three-cylinder diesel engine for mechanical power supply and in relation to that, as APU sensitive design, embedded cooling system, air intake and exhaust systems are located. At the same time, Prestolite 140 amps alternator and Valeo TM 16 A/C system compressor are found in the layout of the APU. Besides, for the control system, all these components are operable in the scope of automated safety features, which can also be observed on the APU Control Unit. In details, general specifications of the APU can be seen in Table 3.

Table 3 General Specifications of FNSS APU

SPECIFICATIONS	
Engine	Mitsubishi L3E 17.7 kW, 3-cylinder, water cooled, diesel
Alternator	Prestolite 140 A
Compressor	Valeo TM 16
Net Weight	225 kg
Exterior Dimensions (L x W x H)	540 x 500 x 1000 mm
Net Electrical Output	Max. 70 A @ 28 vDC
Fuel Type	Diesel F34, F54 (compatible with ASTM No: 2-D)
Operation Temperature	+44 °C, - 32 °C
Operation Altitude	Sea level to 3000 m

1.3. VEHICLE AIR CONDITIONING SYSTEMS

The main topic of the thesis study, air conditioning systems, is described generally in the scope of introduction for clear understanding. An air conditioning system is basically a vapor compression refrigeration cycle, in that, commonly, the refrigerant R134a goes through the components, causing to change its intensive properties. Generally, in the A/C system, there exist main components as compressor, condenser, evaporator and expansion valve. For improve the system efficiency, there can be also added some components such as, liquid receiver drier, accumulator, hot gas by-pass line etc.

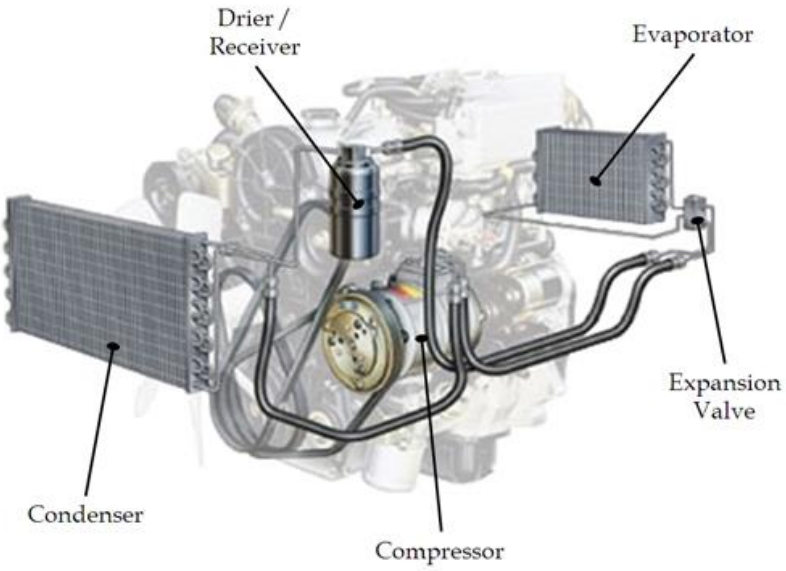

Figure 10 Common Components of A/C System [13]

In details, theoretical ideal vapor compression refrigeration cycle by considering above components is processed as following. Assuming the beginning of cycle at the inlet of evaporator, the refrigerant firstly enters the evaporator as a two-phase liquid-vapor mixture. In the evaporator, the refrigerant passes from liquid to vapor phase by gaining the heat from air to be cooled in the vehicle. During the process, temperature and pressure of the refrigerant remain constant. Then, refrigerant, leaving the evaporator as vapor, is compressed by the compressor adiabatically at a higher pressure hence higher temperature. After that, the superheated vapor passes through the condenser

with constant pressure by transfer the heat to the ambient air. During the process, refrigerant passes from vapor to liquid phase by decreasing its temperature. Finally, liquid refrigerant is throttled in the expansion valve to the two-phase liquid-vapor mixture by decreasing both its pressure and temperature. Then, the cycle is restarting by going through the evaporator. [14] To sum up, following processes describes the ideal vapor compression cycle step by step with the help of Figure 11.

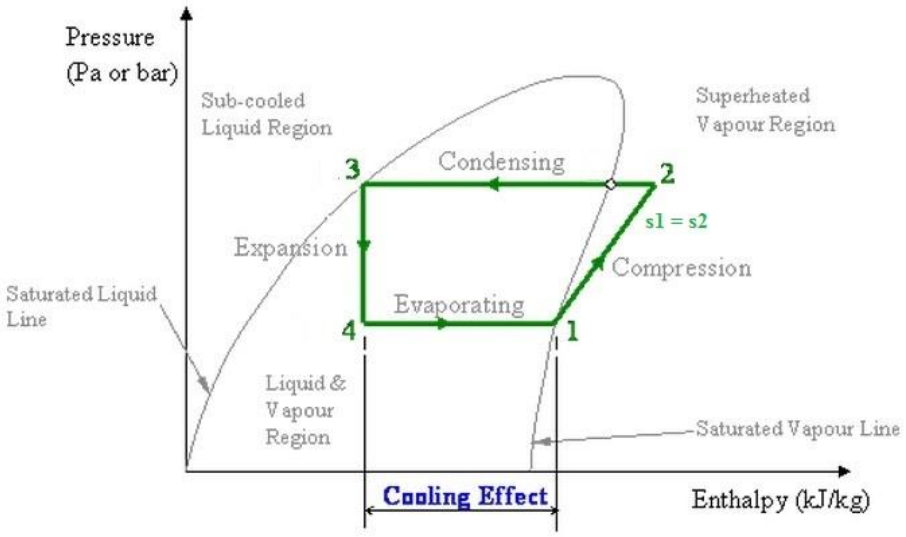

Figure 11 P-h Diagram of Ideal Vapor Compression Refrigeration Cycle [15]

Process 1-2 : Isentropic compression of refrigerant

Process 2-3 : Heat transfer **from** the refrigerant at constant pressure

Process 3-4 : Throttling from liquid phase to two-phase liquid-vapor mixture

Process 4-1 : Heat transfer **to** the refrigerant at constant pressure

1.3.1. APU-DRIVEN A/C SYTEM

Similar to the general types of the A/C systems, stated as above, an APU-driven A/C system has same components such as compressor, condenser, expansion valve and evaporator. The different thing is that, as stated in APU system introduction, they have all primarily the duty of supplying the electrical power. In this case and as most of the

APU designs have, the mechanical power to run the compressor is obtained from APU engine rather than the main engine. Indeed, for the AV-8 ACV, the crew cabin has two different A/C systems, fed by different engines such as one is run by FNSS APU engine and the other is fed by main engine. Both systems have separate hosing/tubing for compressors, condensers and expansion valves. However, two systems meet in the evaporator unit by means of not mixing the fluids of each. For detail, the evaporator unit contains two different heat exchangers in it, which are blown by same centrifugal types of fans, in the way of one for the APU A/C system and the other for the main engine A/C system. As noted earlier, the side of the FNSS APU A/C system will be the main topic of this thesis study. Although the details of the analysis and the components in the A/C system are evaluated in the Chapter 2, below figure shows the general views of components as CAD models.

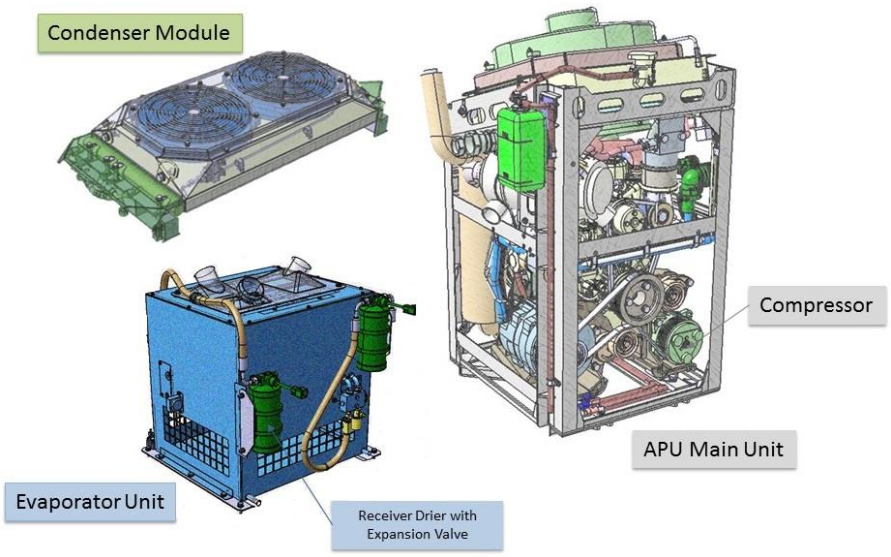

Figure 12 Components of APU-driven A/C System

1.4. LITERATURE SURVEY ON THESIS SUBJECT

The studies about the A/C system in the literature are herewith investigated for better understanding of the concepts, which are considered in this study. As stated previously, the aim of current work is to design and test the A/C system used in an armored personnel carrier. In this point of view, over the years, similar activities have been conducted by the researchers to understand or improve the dynamics of the system. These needs are actually came from the characteristics of both dynamics behaviors of the components in the A/C cycle and the fluid, refrigerant R134a in this case, used in the system. Since refrigerant in the system appears in two-phase flow in the cycle, such as the vapor in the compressor or two-phase liquid vapor mixture in the evaporator or in the condenser, behavior of refrigerant for one step beyond is more difficult to predict. On this basis, to clarify the conditions of the refrigerant in the A/C components, Lil and Alleyne [16] were proposed a modeling concept for the refrigerant flow during the start-up and shut-down periods, called "Switched Moving-Boundary Framework". In their work, the possible conditions of refrigerant in evaporator and condenser during the start-up and shut-down periods are modeled by considering the effects of compressor and expansion valve. The model was tested, whose results were considerably compatible with the test results of system transient behaviors.

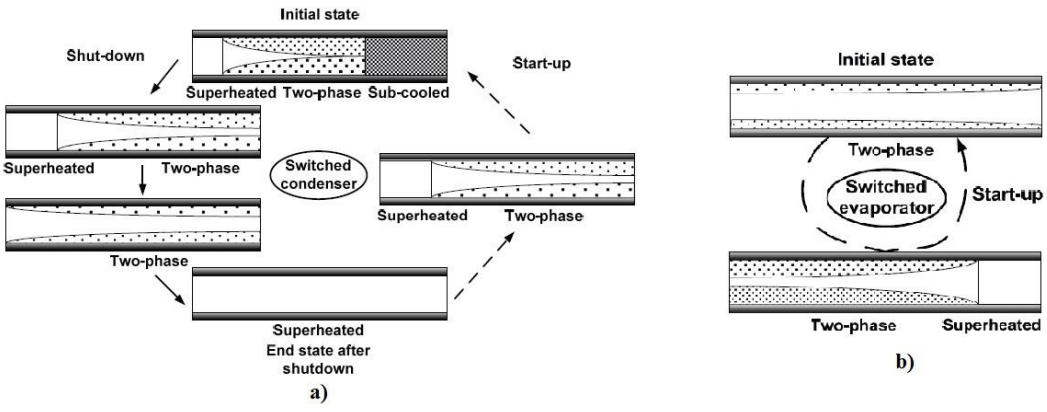

Figure 13 Switched Moving-Boundary Models for a) Condenser, b) Evaporator [17]

Another study about the transient simulation model for dynamic performance of vapor-compression cycle was conducted by Browne and Bansal. [18] They applied the thermal capacitance approach during the modeling heat exchangers i.e. condenser and evaporator, and simulation was capable of changing heat transfer coefficient through the heat exchangers for real-time performance estimation and accuracy of the model. Validating the results with two screw chillers, although the estimations appeared pretty good enough, ± 10% accuracy could be considered open to improvements. Besides the simulations, Lei and Zaheeruddin [19] were proposed a mathematical model about the dynamics of refrigeration system. Their model depended on mass and energy balance equations in the concept of lumped-capacitance method dealing with both transient and steady-state responses of the overall water-chiller system. What they concluded from the work was that the refrigerant side of the system could be more stable than the water side, meaning that the overall system had a two time-scale domain. Similarly, another numerical study was conducted by Ismail and et al. [20] comparing the transient and steady-state models. In the study, formulation was obtained with concepts of mass, energy and momentum balance. While transient model was used to estimate the start-up condition of the system only, steady-state approach covered the whole cycle. At the end of the study, consistencies of both models were obtained by investigating the start-up period initially. All these work are done with the commonly used refrigerant R134a by aiming to modeling and, if need, validating the simulation with a suitable tests. However, as stated above, to understand the dynamics of the refrigeration cycle, some other researchers have focused on the different refrigerants in the cycle. One of them is Chandrasekharan [21] was conducted a study about the using different refrigerant in the vapor compression cycle based on coefficient of performance and the exergitic efficiency. For his model, R12 and R134a were defined as fluids in the system and center of attention was the effects of these refrigerants on the efficiencies while changing with evaporating temperatures and sub-cool temperatures. Obtained results were that the depending on the refrigerant type, efficiencies could be varying with changes of the temperatures. For evaporating temperature, R134a had higher COP that the R12 for lower temperature; on the other hand, R12 was getting higher COP for higher temperatures. For sub-cool temperature, R134a had higher COP and exergitic efficiency than those of R12 as the temperature

increased. Apart from the modeling studies, there have been experimental efforts on the air conditioning systems in the scope of real-size and real-time concepts. Actually, considering the scope of this thesis study, below work would be beneficial to describing the inputs for our test setup. In detail, an experimental analysis was conducted by Wang and Gu [22] purposing the measurement of COP, evaporator cooling capacity, compressor power consumption, vapor and liquid mass flow rates, pressure and temperature on the each side of components i.e. inlet and outlet. While measuring the above properties of refrigerant R134a, they also applied some disturbances in the system such as, refrigerant charging, changing of air-side temperature of evaporator and water-side temperature of condenser. Consequently, their findings were remarkable to guide the future works as same as now. Shortly, results obtained are listed below;

- The total mass flow increases with increase of refrigerant charge, evaporator air-side temperature, condenser water-side temperature. [22]

- The cooling capacity does not change with the refrigerant charge but increases with the increase of evaporator air-side temperature and decrease with the increase of condenser water-side temperature. [22]

- The compressor volumetric efficiency increases with increase of refrigerant charge and the evaporator air-side temperature decreases with increase of condenser water-side temperature. [22]

Another experimental analysis was implemented by Hoşöz and et al. [23], investigating the effects of compressor rpm and the temperature of air-side at the inlet of condenser and evaporator on the A/C system. Measurements were taken every 5 °C air inlet temperature increments in the range of 25 °C to 40 °C on the condenser and evaporator, and at two different compressor rpms such as 850 rpm and 2250 rpm. After applying COP and exergy analysis by the help of measurements, the below results were found as;

- The cooling capacity and the power consumption of compressor increase with increase of compressor rpm and the air inlet temperature of condenser and evaporator. [23]

- COP and the exergy of the system decreases with increase of compressor rpm and the air inlet temperature of condenser and evaporator. [23]

- The heat transfer to the ambient on the condenser increases with increase of compressor rpm and the air inlet temperature of condenser and evaporator. [23]

While above mentioned studies are very stimulating, the last two experiments provide many advantages to shape the general form of thesis work. Indeed, current study is formed of initially an "Introduction" chapter, three main chapters and, finally a "Conclusion" chapter. After the "Introduction" chapter, "Analysis of the Vapor Compression System" illustrates the main focus points of this study. In addition, the design requirements of the overall system and, on this basis, the thermodynamic cycle analysis of the A/C system are presented here. Furthermore, the mathematical modeling of the components depending on thermodynamic cycle analysis is prepared by using Matlab® environment. Advancing chapter, "Experiments", defines the technical specifications of the components used in the test setup. After that, the details of test bench and test conditions are illustrated here. The following chapter, "Comparison of the Experimental Results", includes the comparisons of performance variables of the tests in the scope of design requirements and the critical properties of the A/C system such as heat transfer rates, COP, mass flow rates, cooling capacity, compressor volumetric efficiency, etc. Finally, "Conclusion" chapter summarizes the works-done in the great scheme of the study. Additionally, some comments about the comparisons of the results are provided here to reveal some opinions for the future studies or new challenging questions for the interested people dealing with the subject.

CHAPTER 2

ANALYSIS OF THE VAPOR COMPRESSION SYSTEM

In chapter 2, the thermodynamic analysis of the vapor compression refrigeration cycle is processed within the frame of components' ideal operation conditions. While executing analyses, some predictable and modelable disturbances are tried to be got involved in the system, in order to make the cycle converge to actual operational states. For better understanding, the properties of the components in the cycle and the disturbances are shown in the following parts.

2.1. DESIGN REQUIREMENTS

Before getting in the analyses, the design requirements of the A/C system are presented as following. In the formal explanation, the minimum cooling capacity of the cycle shall be determined when the evaporator air side inlet temperature is at 33 °C with the humidity level of 30%-40% and the maximum expected evaporator air side outlet temperature yields to 18 °C. In addition to above explanation, depending on the evaluation of personnel cabin heat input estimations, the minimum evaporator cooling capacity shall be stated as 8.5 kW. In the highlight of the above information, cycle analyses of the vapor compression refrigeration system are performed by taking the refrigerant side into account.

2.2. VAPOR COMPRESSION CYCLES

Vapor compression cycles are widely used in industry or household applications to meet the cooling or heating demands of the systems as well as in case of automotive applications. In the cycle, a refrigerant, commonly R134a in automotive applications, flows through the components, which are mainly compressor, condenser, expansion valve and the evaporator, as medium to absorb or reject the heat over the cycle by changing its intensive properties. In details, the vapor compression cycles are mainly generated from the "Reversed Carnot Vapor Power Cycle". The cycle operates between hot reservoir and cold reservoir with the components; compressor, condenser, turbine and evaporator. For ideal operation, refrigerant is compressed to saturated vapor by the compressor, temperature from T_L to T_H. Then, it passes through the condenser while changing its phase to saturated liquid as a result of heat transfer to hot reservoir at temperature T_H. Afterwards, refrigerant is expanded adiabatically to two phase liquid-vapor mixture in the turbine from temperature T_H to T_L. Finally, getting heat transfer from cold reservoir, refrigerant passes through the evaporator while some of refrigerant changes from liquid to vapor at temperature T_L and returns the start of cycle. Below figure shows the diagram for reversed Carnot vapor power cycle.

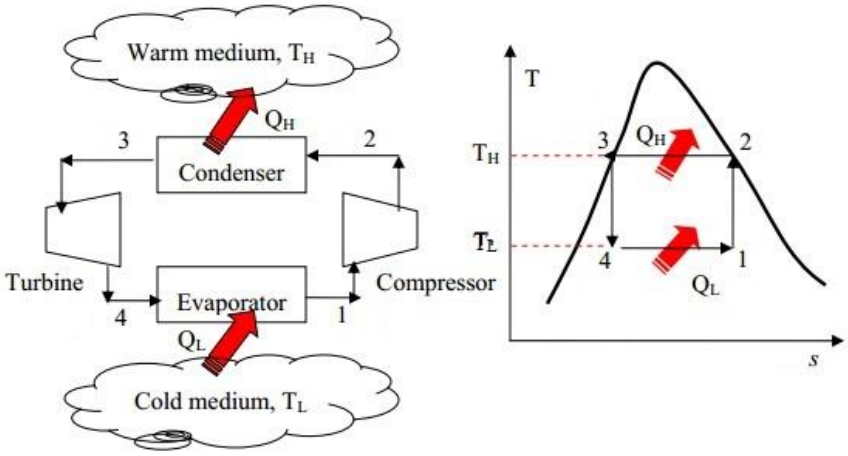

Figure 14 Reversed Carnot Vapor Power Cycle [24]

Similarly, the vapor compression refrigeration cycles operates between hot and cold reservoir, T_H and T_L respectively. In the cycle, an expander, expansion valve, is used instead of turbine for expanding the refrigerant from T_H to T_L. However, refrigeration cycles are departed from reversed Carnot vapor cycles regarding some features listed below;

- The reversed Carnot power cycles are made up for reversible processes. Indeed, in actual system, process is not taken into consideration as reversible due to some loses in the components. In the point of view of desired heat transfer rates, the evaporator needs the temperature T'_L which is considerable below T_L. Likewise, for the condenser, in order to maintain sufficient heat rejection, temperature T'_H, more above of T_H, is needed for condenser operation. In figure 15, layout of T_H & T_L and T'_H & T'_L can be seen on T-s diagram. [14]

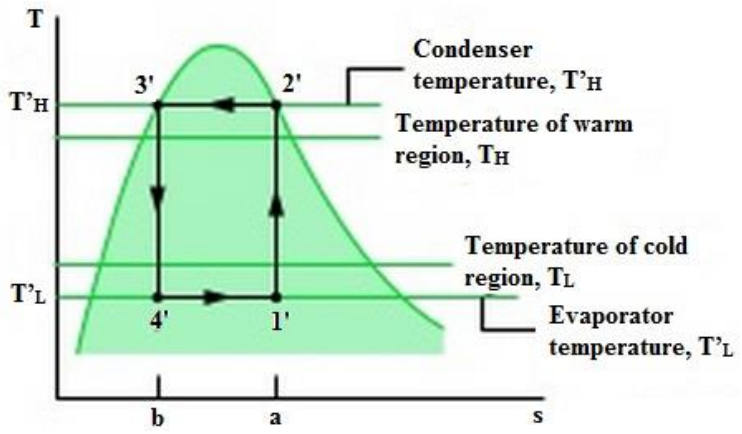

Figure 15 Comparison of the Condenser and Evaporator Temperatures with those of the Warm and Cold Regions [14]

- Another departure is the properties of the refrigerant under compression process and the compressor operational affectivity. When the compression process is figured from state 1' to state 2' as two phase liquid-vapor to saturated vapor, existence of liquid in the inlet of compressor (state 1') may be harmful hence, decreasing the operational life of the compressor. In actual system, in the scope of maintenance and the life cycle, the compressor can be more efficient when they only operate with vapor.

- Other important feature of the actual refrigeration cycle is related with expansion process. In the reversed Carnot vapor power cycle, expansion of the refrigerant is done by a turbine. This process generates small amount of work output compared to the work input of compressor. In the opinion of financial efficiency, work output of the turbine can be disregarded and sacrificed by the simple throttling valve, which provides the advantages of saving initial and maintenance cost. [14]

In the highlights above knowledge, the ideal vapor compression refrigeration cycle can be built up as being operates under dry compression process (only vapor at the inlet of compressor) and expansion occurring in a throttling valve, "expansion valve". For visualization, following figures show vapor compression refrigeration cycle's components and ideal T-s & P-h diagrams.

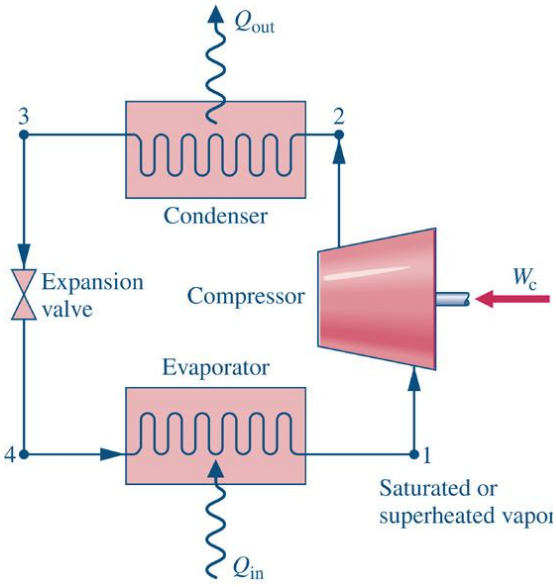

Figure 16 Components of the Vapor Compression Refrigeration System [25]

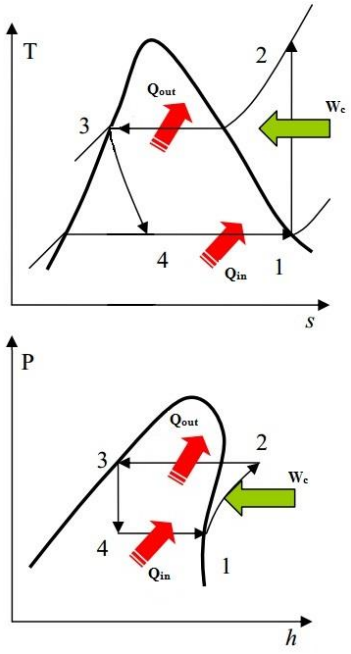

Figure 17 Ideal Vapor Compression Refrigeration Cycle T-s & P-h Diagrams [24]

As seen in figure 17 for ideal vapor compression cycle, compression process occurs as reversible and adiabatic (isentropic), where the heat transfers to/from surroundings are ignored. Hence, the entropy during compression of the refrigerant remains constant.

Furthermore, condensation and evaporation of refrigerant take place internally reversible at a constant pressure. For condensation, refrigerant goes under cooling process from superheat vapor to saturated liquid phase. On the other hand, in the evaporator, heat from surroundings make the refrigerant pass from the two phase liquid-vapor mixture to saturated vapor phase. Besides, throttling valve in the cycle expands the refrigerant from saturated liquid to two phase liquid vapor state. Indeed, the expansion takes place as irreversible where the temperature and pressure of refrigerant decrease at a constant enthalpy. Also, heat transfers to/from surroundings are ignored.

Inversely, in practical life, implementation of above procedures to an actual cycle seems nearly impossible. Since the perfect insulation from the surrounding and the ignorance the friction of refrigerant inside the cycle are inevitably out of the question. Indeed, the heat transfer to/from surrounding actually occurs hence; irreversible and non-adiabatic compression takes place, meaning the entropy at the end of the compression increased.

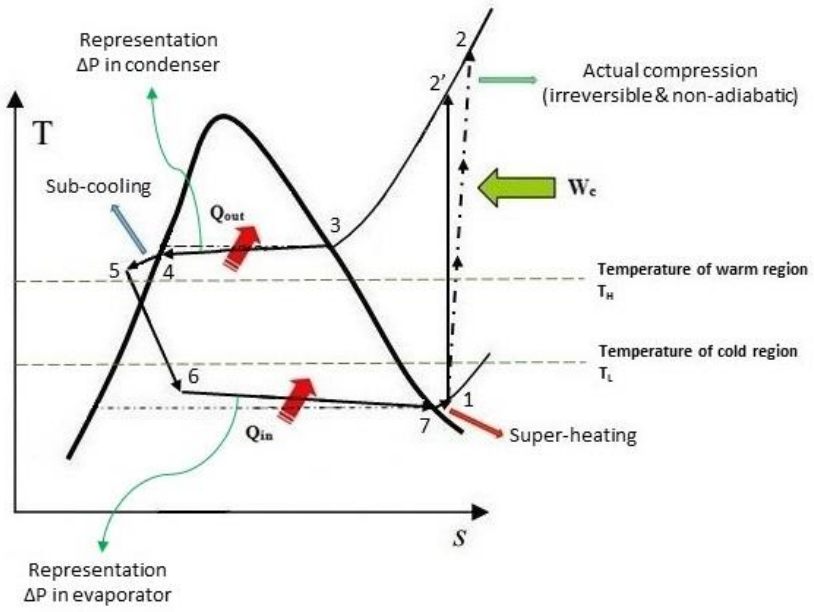

Figure 18 Actual Vapor Compression Refrigeration Cycle T-s Diagram

Similarly, since there exists friction loses in the condenser, evaporator and the connection pipes, pressure drops during condensation and evaporation are inevitable. Thus, heat transfers between hot and cold regions (condensation and evaporation) don't take place as reversible. As clarified in figure 15, explanation of differences between reversed Carnot vapor power cycle and vapor compression refrigeration cycles, the condensation temperature is greater than hot region temperature and of which of evaporation is less than that of the cold region in order to accomplished to obtain desired cooling capacity of the cycle. These cases are the main departures from the ideal cycle. In addition to all above, the outlet temperatures of the condenser and the evaporator are also major impact on the performance of the actual cycle, considering the operation life and the efficiencies of the both the expansion valve and the compressor. For the effect of condenser outlet temperature, refrigerant leaving the condenser is actually desired on sub-cooled state. The reason behind the idea is to prevent to formation of vapor bubble at the inlet of expansion valve hence decreasing the expansion process efficiency. Furthermore, since the heat transfer from surrounding is inevitable, it is not desired to refrigerant to change its state to the vapor from outlet of the condenser to the inlet of the expansion valve. In this case, the expansion valve can be prevented from the measuring of needed liquid refrigerant into the evaporator for planned cooling capacity hence, may cause the decrease of overall system performance. Similarly for the temperature of the evaporator outlet, state of the refrigerant leaving the evaporator is important for the efficiency and the operational life of the compressor. In actual systems, compressor can only handle the refrigerant at vapor state for the best operation. If the some of the refrigerant is liquid at the outlet of the evaporator and going through the compressor, this may cause slugging, damaging the compressor valves or internal mechanical components. Indeed, both sub-cool and super-heat temperature are organically depended each other serving to obtain best system performance. The adjustment of these temperatures is directly related both amount of refrigerant fed in the cycle and, the design of the condenser and evaporator. Assuming the desired condenser and evaporator exist, the changing the amount of refrigerant affects the cycle sub-cool and super-heat temperatures. If the mass of refrigerant is increased in the system, super-heat temperature shows most likely decrease manner while sub-cool temperature increases. Adversely, undercharge of the

refrigerant shall cause the increase of super-heat temperature, conversely decrease of sub-cool temperature. For clarification, figure 18 T-s diagram and figure 19 P-h diagram show the irreversible and non-adiabatic compression due to heat transfer to/from surroundings, pressure drops in the condenser and evaporator due to friction, sub-cool and super-heat temperatures related with the irreversibilities in real life.

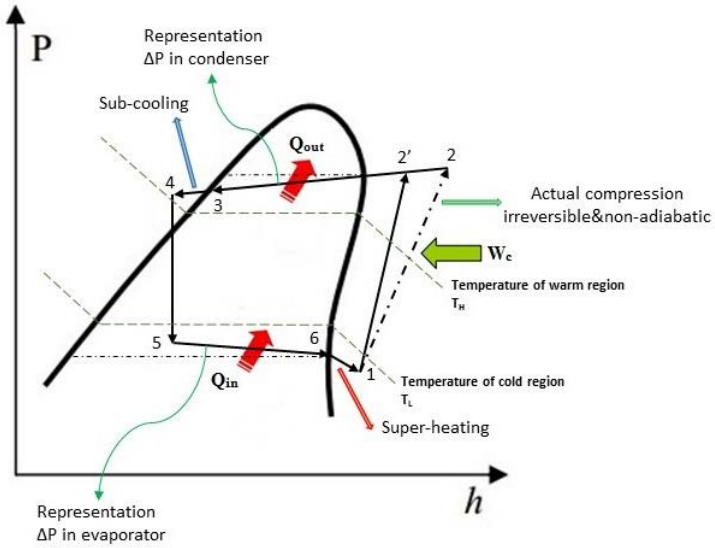

Figure 19 Actual Vapor Compression Refrigeration Cycle P-h Diagram

2.3. PERFORMANCE EVALUATION OF THE REFRIGERATION CYCLE

System based performance evaluations of the refrigeration cycle are carried out by considering behavior of COP, system cooling capacity, compressor work, condenser heat rejection rate, and efficiencies of the cycle with respect to change of condensing temperature and pressure, and the compressor speed. A MATLAB® code, called 'analysis.m', is written and accompanied for the related simulations of the cycle by combining the program called 'miniREFPROP' [26]. The 'miniREFPROP' is used for obtaining the thermodynamic properties of the refrigerant at relevant states. The code 'analysis.m' and the 'miniREFPROP' is linked via 'refpropm.m' [27] MATLAB® code, written for combining the MATLAB® and the 'miniREFPROP'. For the proper usage of the 'analysis.m', the 'refpropm.m' should be located in the same directory with it. Further information and the use of 'refpropm.m' can be found in the relevant reference. [27]

2.3.1. ASSUMPTIONS USED IN THE ANALYSES

When analyzing the refrigeration cycle, it should be noted that the overall system is actually two-sided. One is ambient air environment in which the cycle is located and the other is the refrigerant side flowing through the compression system. For this analysis, only the refrigerant side is considered.

As stated in section 2.2. Vapor Compression Cycle; there exist some differences between ideal and actual refrigeration cycles due to the environmental or systemic impacts. For the analysis, the ideal refrigeration cycle is tried to be actualized to some extend by assuming or modeling the disturbances which can be pre-estimated. For the reason, those below are assumed as for simplification of the analysis.

- The viscous friction inside the condenser and the evaporator with the refrigerant are neglected. Thus, the condensing and evaporation of refrigerant occurs at constant pressures respectively, characterized as internally reversible processes.

- Compression process is not isentropic. Indeed, the polytrophic compression occurs with an assumed relations related with the isentropic efficiency. In detail, Jain and Bullard [28] claim that the isentropic efficiency of the compressor varies with the ratio of discharge pressure to suction pressure as well as compressor rpm. Indeed, the overall isentropic efficiency is the product of these two relations. Details of the formulation will be given in further sections.

- The expansion of the refrigerant in the expansion valve is isenthalpic. Hence, the temperature and pressure of the refrigerant decreases up to a state at inlet of the evaporator by with a constant enthalpy line.

- The super-heat temperature can be defined as the difference between the temperature at the outlet of the evaporator and the evaporating temperature of refrigerant. Indeed, usual operable super-heat temperature is between 5 °C -10 °C. [29] For the analysis, the super-heat temperature is assumed as 10 °C.

- The sub-cool temperature can be defined as the difference between the temperature at the outlet of the condenser and the condensation temperature of refrigerant. Indeed, usual operable sub-cool temperature can be achieved up 10 °C. [30] For the analysis, the sub-cool temperature is assumed as 5 °C.

- For initializing the analysis of the refrigeration cycle, the evaporating temperature should be analyzed. The study conducted by Holder [31] deals with the effect of temperature differences between the air-side and the refrigerant-side of the evaporator for the best cooling performance. As said, the evaporating temperature should be far enough from the temperature of the cold region temperature. Indeed, the temperature difference between air and the refrigerant is greatest at the inlet of the evaporator and the less at the outlet of the evaporator. Thus, through the evaporator, heat transfer between air and refrigerant approaches to zero. From the requirements of the cycle as, maximum air outlet temperature from the evaporator should be 18 °C, it is determined that the evaporating temperature is far away from the design requirement as possible.

  On the other hand, it is well-known fact that the evaporating temperature below 0 °C (freezing temperature of the water) may cause the frost accumulation on the evaporator. This may lead up both the clogging of evaporator with frost and the decrease of the overall heat transfer coefficient, apparently decreasing the efficiency of the evaporator cooling performance.

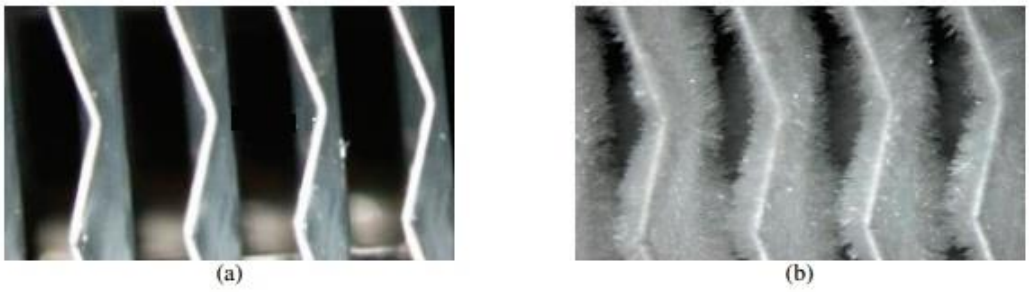

Figure 20 Frost Formation [32]

For the solution, one of the defrosting methods can be used such as off-cycle defrosting, electrical defrosting, hot-gas defrosting, reverse cycle defrosting etc.; however, implementing one of the above methods may cause the increase of the initial and maintenance costs dramatically. As a conclusion from above information, approach of the evaporating temperature to cold region temperature may cause the decrease of cooling capacity of system as well as the decrease of it may lead the increase of operational cost of the system. Hence, evaporating temperature is assumed as fixed on the 0 °C for getting the optimum efficiency from evaporator in terms of both financial and operational.

- Through the cycle, mass flow rate of the refrigerant supplied by the compressor is assumed as constant.

To sum up, considering the above assumptions, analyses for refrigeration cycle are performed in following section. For figuring out, the cycle studied has the pressure-enthalpy diagram below. Condensing temperature is specified as 50 °C for visualization.

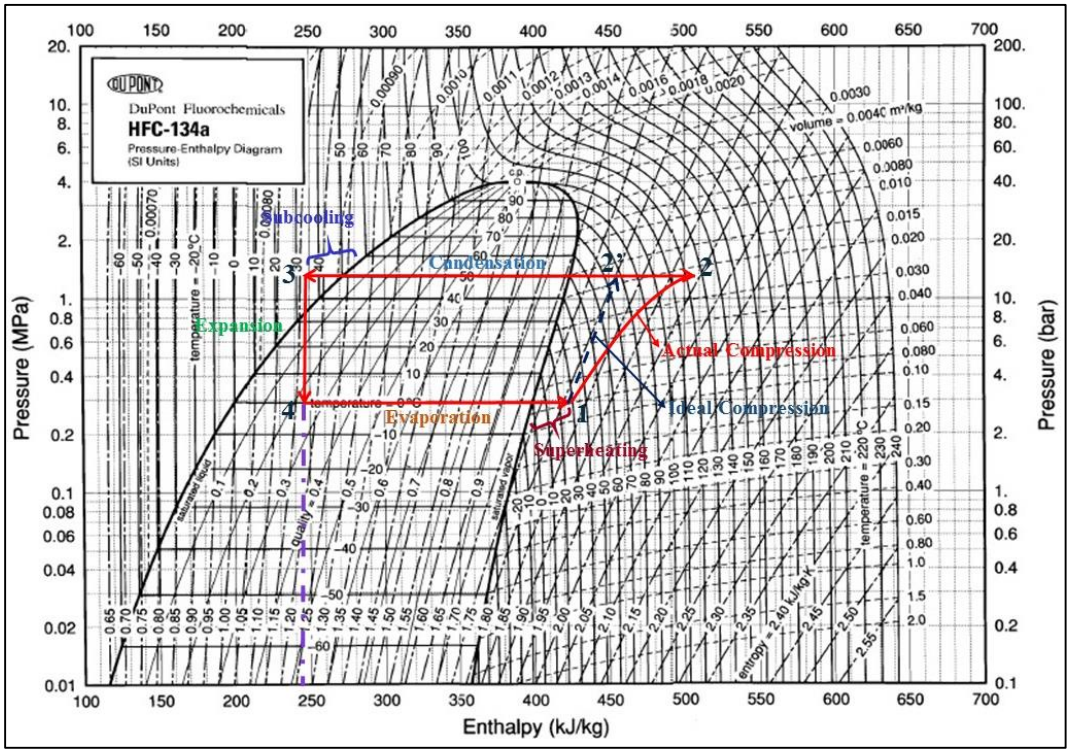

Figure 21 Actualized Refrigeration Cycle, P-h Diagram

2.3.2. THERMODYNAMICS PERFORMANCE ANALYSIS OF THE REFRIGERATION CYCLE

Based upon above assumptions, the refrigeration cycle analysis is performed as following. Initially, state 1, the evaporator outlet-compressor inlet, is set using the evaporating temperature and super-heat temperature, which are the 0 °C and 10 °C respectively. Afterwards, the initial set value of condensing temperature is assumed as 20 °C; furthermore, the pressure in the condenser is found accordingly from the pressure-enthalpy diagram. State 3, condenser outlet-expansion valve inlet, is determined depending on pre-defined sub-cool temperature and the condensation pressure which are the 5 °C and the pressure at the 20 °C condensing temperature for the moment. Since the state 3 is set, it is possible to find the state 4, expansion valve outlet-evaporator inlet, by isenthalpic expansion process, where $h_3=h_4$. Later on, by the help of thermodynamic properties on state 1 and 3, the state 2, condenser outlet-evaporator inlet, can be set by considering the isentropic compression process on the compressor. It is clear that entropies of state 1 and state 2 should be equal for isentropic process. When the isentropic state 2 is defined, enthalpy of it also can be found. However, for actual process, the heat transfer to/from surroundings cannot be neglected; refrigerant experiences the polytrophic compression, stated before. Hence, actual state 2 is determined according to the below formulation of isentropic efficiency.

$$\eta_s = \frac{h_{2\ \text{isentropic}} - h_1}{h_{2\ \text{actual}} - h_1} \quad (1)$$

η_s = Isentropic efficiency

$h_{2\ \text{isentropic}}$ = Ideal enthalpy @ compressor outlet (kJ/kg)

$h_{2\ \text{actual}}$ = Actual enthalpy @ compressor outlet (kJ/kg)

h_1 = Enthalpy @ compressor inlet – evaporator outlet (kJ/kg)

In the formula, η_s is formulated by the hypothesis of Jain and Bullard [28] as following. As said, the isentropic efficiency is related with the ratio of compressor inlet and outlet pressure as well as compressor rpm.

- Isentropic efficiency is linearized with the ratio of suction and discharge pressure of compressor in the interval of 7.5 to 8.5.

$$\eta_{s1} = -0{,}123\frac{P_{discharge}}{P_{suction}} + 0.8714 \quad (2)$$

η_{s1} = Isentropic efficiency (pressure ratio linearized)
$P_{discharge}$ = Pressure @ compressor outlet (kPa)
$P_{suction}$ = Pressure @ compressor inlet (kPa)

- Compressor speed interval is assumed as 600 to 7000 rpm. Isentropic efficiency is normalized with the quadratic function of compressor speed at the average of 3800 rpm.

$$\eta_{s2} = -0.08\left(\frac{N_{rpm}}{3800}\right)^2 + 0.1411\left(\frac{N_{rpm}}{3800}\right) + 0.9337 \quad (3)$$

η_{s2} = Isentropic efficiency (comp. speed normalized)
N_{rpm} = Compressor speed (rpm)

Finally, the overall isentropic efficiency is calculated by the product of η_{s1} and η_{s2} as following.

$$\eta_s = \eta_{s1}\eta_{s2} \quad (4)$$

η_s = Overall isentropic efficiency

Finally, using (1) and (4), the actual state of compressor outlet-condenser inlet could be found.

Up to now, all the state of the cycle are determined by following the steps above. After that point, heat transfer on the condenser and the evaporator and, the compressor work are calculated. In order to do that, mass flow rate flowing in the system need to be calculated. Related formula is given below as;

$$\dot{m}_{comp} = V_s \eta_v \rho_1 N_{rpm} \tag{5}$$

$\dot{m}_{comp}$ = Mass flow rate (kg/min)
V_s = Compressor displacement volume (m^3/rev)
η_v = Volumetric efficiency
ρ_1 = Density @ compressor inlet (kg/m^3)
N_{rpm} = Compressor speed (rpm)

Except volumetric efficiency, all other term is either calculated or assumed. For the volumetric efficiency;

$$\eta_v = 100 - c_r \left\{ \left(\frac{P_{discharge}}{P_{suction}} \right)^{\frac{1}{k}} - 1 \right\} \tag{6}$$

η_v = Volumetric efficiency (%)
$P_{discharge}$ = Pressure @ compressor outlet (kPa)
$P_{suction}$ = Pressure @ compressor inlet (kPa)
c_r = Compressor clearance ratio
k = Isentropic exponent

where;

$$k = \frac{c_p(T_1)}{c_v(T_1)} \tag{7}$$

c_v = Constant volume specific heat @ compressor inlet (kJ/kgK)
c_p = Constant pressure specific heat @ compressor inlet (kJ/kgK)

Depending on compressor type, the clearance ratio may vary. In this study, the piston type reciprocating compressor is operated and the related clearance volume is assumed as 5%. [33] Furthermore, compressor displacement volume is researched among commercial products and taken as 163 cc/rev. [34] After all, using (5) and (6), mass flow rate is calculated accordingly.

For the calculation of evaporator cooling capacity, condenser heat rejection and the compressor work, following formulas are occupied.

$$Q_{evap} = \dot{m}_{comp}(h_1 - h_4) \quad (8)$$

$$Q_{cond} = \dot{m}_{comp}(h_2 - h_3) \quad (9)$$

$$W_{comp} = \dot{m}_{comp}(h_2 - h_1) \quad (10)$$

where;

Q_{evap} = Evaporator cooling capacity (kW)
Q_{cond} = Condenser heat rejection (kW)
W_{comp} = Compressor work (kW)
$\dot{m}_{comp}$ = Mass flow rate (kg/s)
h_1 = Enthalpy @ evaporator outlet - compressor inlet (kJ/kg)
h_2 = Enthalpy @ compressor outlet - condenser inlet (kJ/kg)
h_3 = Enthalpy @ condenser outlet - expansion valve inlet (kJ/kg)
h_4 = Enthalpy @ expansion valve outlet - evaporator inlet (kJ/kg)

After calculating the performance variables above, overall system coefficient of performance can be calculated as;

$$COP = \frac{Q_{evap}}{W_{comp}} \Rightarrow \frac{h_1 - h_4}{h_2 - h_1} \quad (11)$$

COP = Coefficient of performance

Furthermore, depending on the study conducted by Wu and Lee [35], second law analysis of the refrigeration cycle is performed as following. Firstly, irreversibilities presented in the system can be calculated on the basis of components as below. General formula of exergy destruction is simplified.

For compressor;

$$x_{comp} = \dot{m}_{comp} T_0 \, (s_2 - s_1) \tag{12}$$

For condenser;

$$x_{cond} = T_0 \left[\frac{\dot{m}_{comp} \, (h_2 - h_3)}{T_0} + \dot{m}_{comp} (s_3 - s_2) \right] \tag{13}$$

For expansion valve;

$$x_{ex\_val} = \dot{m}_{comp} T_0 \, (s_4 - s_3) \tag{14}$$

For evaporator;

$$x_{evap} = T_0 \left[\frac{\dot{m}_{comp} \, (h_4 - h_1)}{T_0} + \dot{m}_{comp} (s_1 - s_4) \right] \tag{15}$$

x_{comp} = Exergy destruction in compressor (kW)

x_{cond} = Exergy destruction in condenser (kW)

x_{ex_valve} = Exergy destruction in expansion valve (kW)

x_{evap} = Exergy destruction in evaporator (kW)

T_0 = Reference temperature (K)

In the analysis, reference temperature is assumed as same with the ambient temperature. Hence, the overall exergy destruction in the system is the sum of the irreversibilities in each component above.

$$x_{total} = x_{comp} + x_{cond} + x_{ex\_valve} + x_{evap} \tag{16}$$

x_{total} = Overall exergy destruction in refrigeration cycle (kW)

Afterwards, the exergetic efficiency of the cycle is calculated by using (10) and (16) in relevant formula below such as the ratio of available reversible work to compressor work accordingly;

$$\eta_x = \left[1 - \frac{x_{total}}{W_{comp}}\right] \quad (17)$$

η_x = Exergetic efficiency

Upon calculating the performance variables above, the design requirements should be re-checked. Indeed, it is stated before that the minimum evaporator cooling capacity shall be 8.5 kW. On this basis, if the evaporator cooling capacity is between 8.4 and 8.6 kW, the calculated variables are recorded and relevant graphical information are supplied. At this point, code completes the one cycle of execution with the pre-defined condensing temperature. For further calculations, condensing temperature are increased by ΔT, which is 2 °C for the moment, and the above formulations are repeated once again until the condensing temperature reaches to 90 °C. For clarification, below table shows the assumptions that are applied in the coding.

Table 4 Refrigeration Cycle Analysis - Input Variables

VARIABLE	VALUE	UNIT
Initial Condensing Temperature	20	°C
Condensing Temperature Increment	2	°C
Evaporating Temperature	0	°C
Evaporating Pressure	291.2	kPa
Compressor Displacement Volume	163	cm^3/rev
Compressor Clearance Ratio	5	%
Initial Compressor Isentropic Efficiency	80	%
Evaporator Cooling Capacity	8.4 - 8.6	kW
Super-heat Temperature	10	°C
Sub-cool Temperature	5	°C
Reference Temperature	33	°C

For further information, the code “analysis.m” is supplied in the Appendix A. Also, the below flow chart explains the overall coding algorithm step by step.

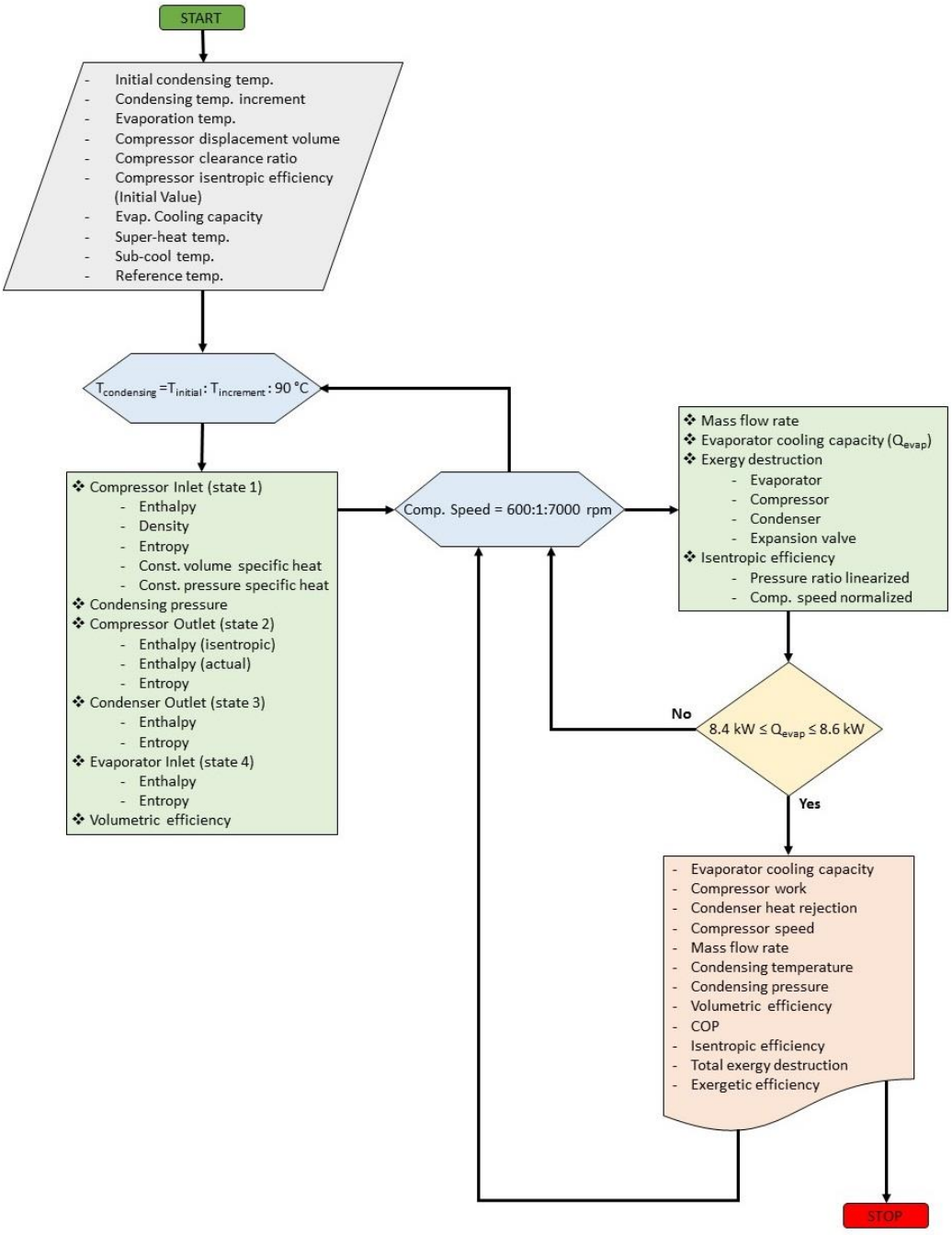

Figure 22 Flow Chart of Coding Algorithm

2.4. RESULTS OF THE ANALYSES

Analyses as per assumptions and formulas above are performed and hereby, following results are obtained. The graphical representations of refrigeration cycle's characteristics are provided for comparing the behavior of variables.

Previously, calculated variables are recorded if the evaporator cooling capacity is between 8.4 – 8.6 kW. Following graph shows that the requirement is satisfied by describing the change of cooling capacity regarding the compressor speed that is recorded for each $T_{condensing} = T_{condensing} + \Delta T_{condensing}$ appeared in each vertical lines set.

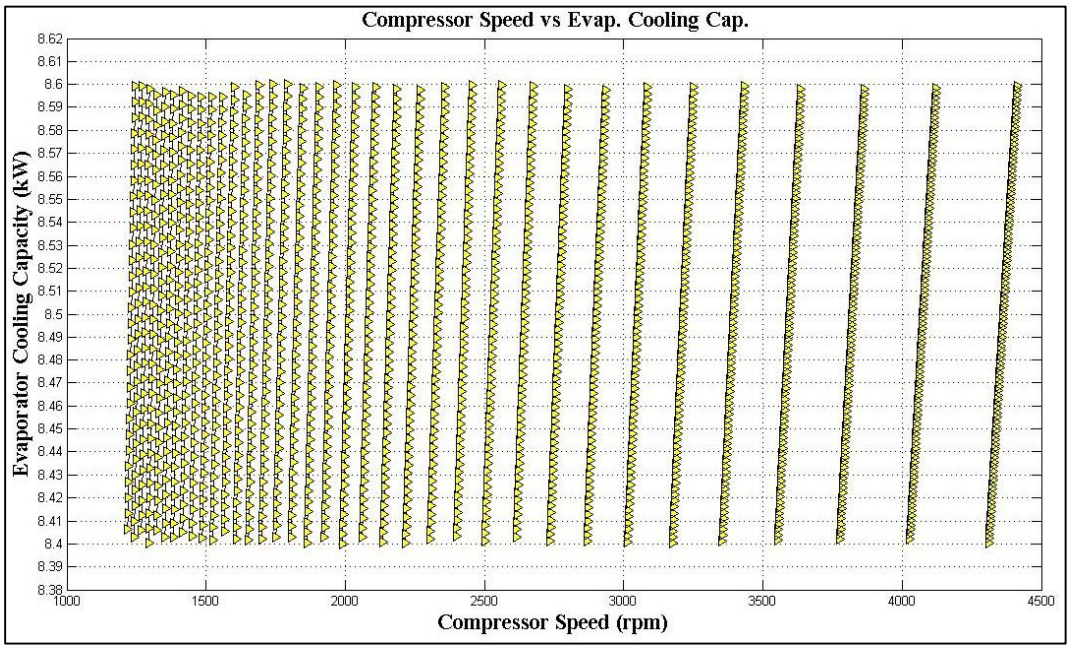

Figure 23 Compressor Speed vs Evaporator Cooling Capacity

After the cooling capacity is guaranteed as above between 8.4 and 8.6 kW, the compressor work and the condenser heat rejection show the characteristics in figure 24 and figure 25. As the condensing temperature increases, the rate of increase of condenser heat rejection and the compressor work input increase. Upward vertical lines in each curve in figure 24 also show that the condenser heat rejection and compressor work has linear relations with increasing compressor speed, indeed, mass flow rate supplied by compressor itself.

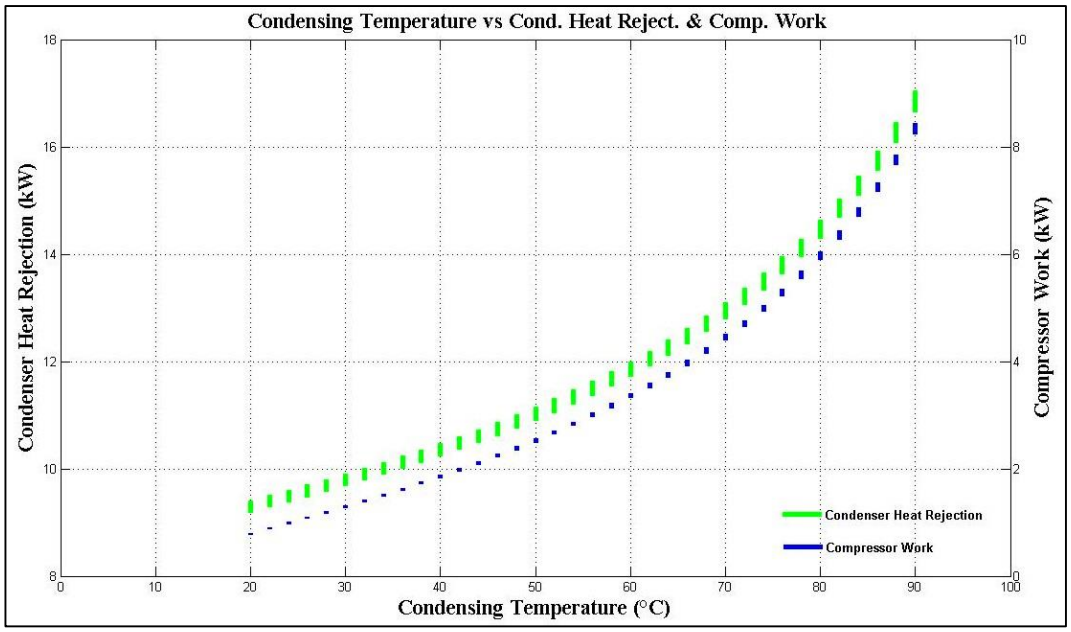

Figure 24 Condensing Temp. vs Condenser Heat Reject. & Compressor Work

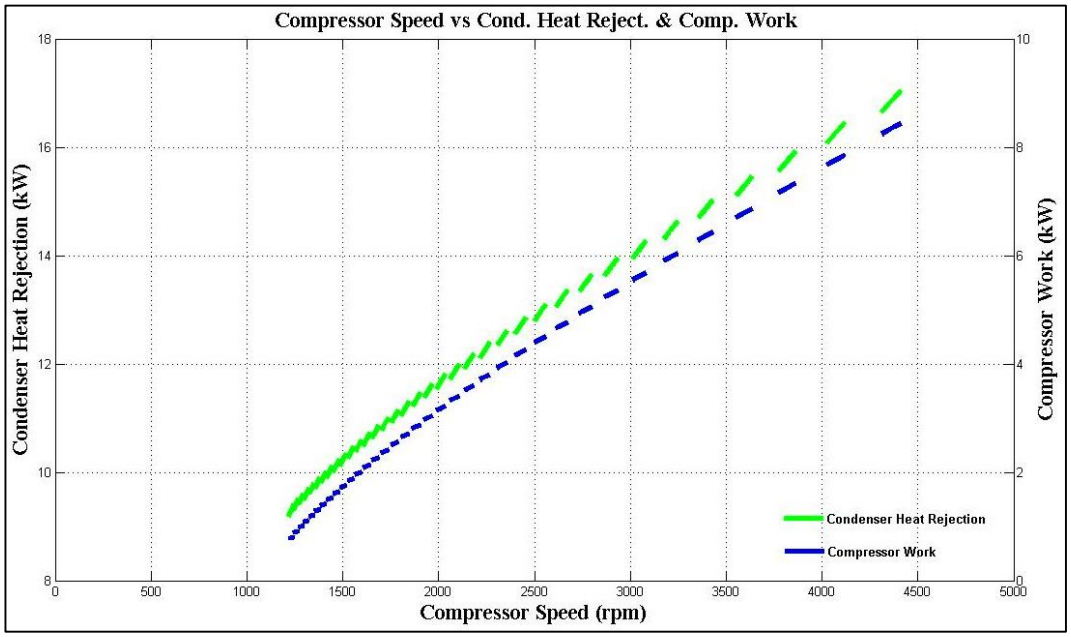

Figure 25 Compressor Speed vs Condenser Heat Reject. & Compressor Work

In figure 25, while the compressor speed increases, the rate of increase for both condenser heat rejection and compressor work seem to have decreasing rate of increase up around 1800 rpm. After that speed, increase rates of both appear to be constant.

While the compressor work and the condenser heat rejection show the above behaviors accordingly, below figure shows the efficiencies of the refrigeration cycle with respect to condensing temperature. While volumetric and isentropic efficiencies have increasing rate of decrease with respect to increasing condensing temperature. Indeed, increase of condensing temperature, registering the increase of condensing pressure, causes the decrease of isentropic efficiency in the view of temperature seen in formula (2). Similarly, the increase of compressor speed, indeed the mass flow rate of refrigerant, makes the second coefficient of isentropic efficiency decrease, seen in formula (3). Accordingly, overall isentropic efficiency decreases. In addition, the volumetric efficiency is related with the discharge pressure on the compressor, meaning the increase of discharge pressure decrease the volumetric efficiency. On the other hand, as the condensation temperature increases, the rate of decrease of exergetic efficiency decreases.

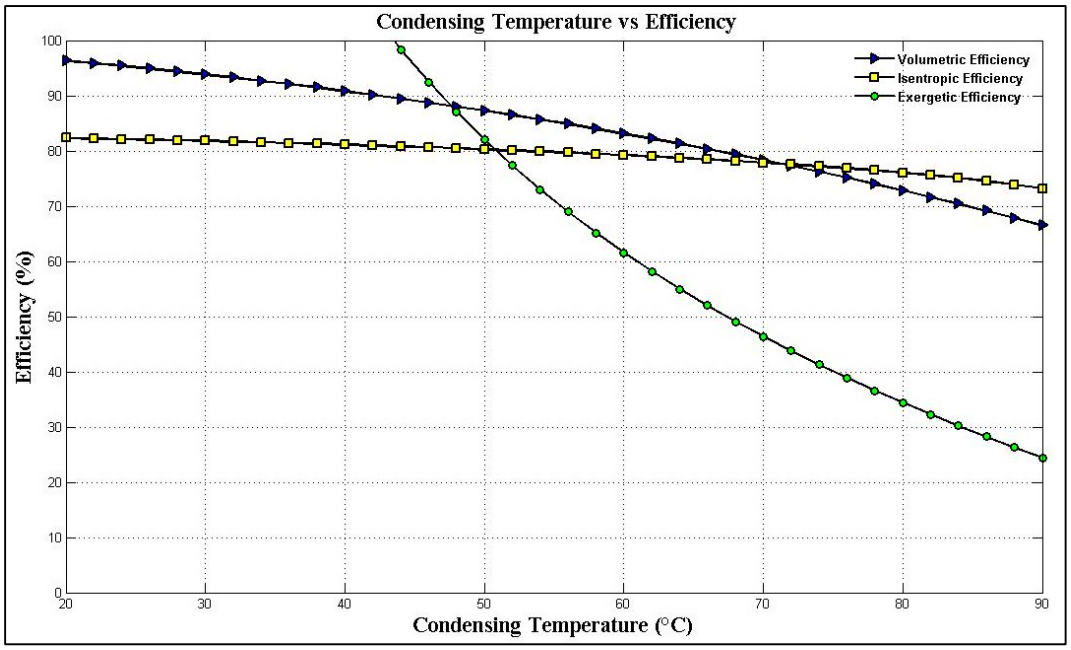

Figure 26 Condensing Temperature vs Efficiencies

The exergetic efficiency is an important parameter for the refrigeration cycle. It is directly related with the condensing temperature and compressor speed in terms of enthalpy and the mass flow rate of the refrigerant as it could be seen in formulae of exergy destruction in each components. The comment, of decrease of exergetic efficiency with respect to increasing condensing temperature, clarifies that as the

increase of the condensing temperature escalates the total exergy destruction in the system as well as the compressor work. However, since the rate of exergy destruction is clearly higher than the increase of the compressor work for each condensing temperature, the exergetic efficiency decreases simultaneously.

Another commitment about the refrigeration cycle is the evaluation of feasible operation points in which the system can operate in terms of interval of condensing temperature. From figure 26, it is clearly seen that the condensing temperature below 43 °C approximately is not possible for the cycle. The fundamental reason behind this though is that the exergetic efficiency is clearly higher than 100%, at which is the ultimate point that the exergetic efficiency can reach. Furthermore, same viewpoint can be concluded from the figure 27, which shows the behavior of exergetic efficiency with respect to compressor speed. As considering the values of exergetic efficiency below 1600 rpm, it is noticeable to have higher values than 100%. Hence, it is also induced that at lower than 1600 rpm compressor speed, there is no possibility to run the cycle as seen below. Also, the effect of compressor speed on the exergetic efficiency is similar to that of condensing temperature in the view of decrease behavior of the efficiency. However, the increasing compressor speed affects the behavior of the isentropic and volumetric efficiencies adversely. While the compressor speed increases, the isentropic and volumetric efficiencies have decreasing rate of decrease with respect to the variable.

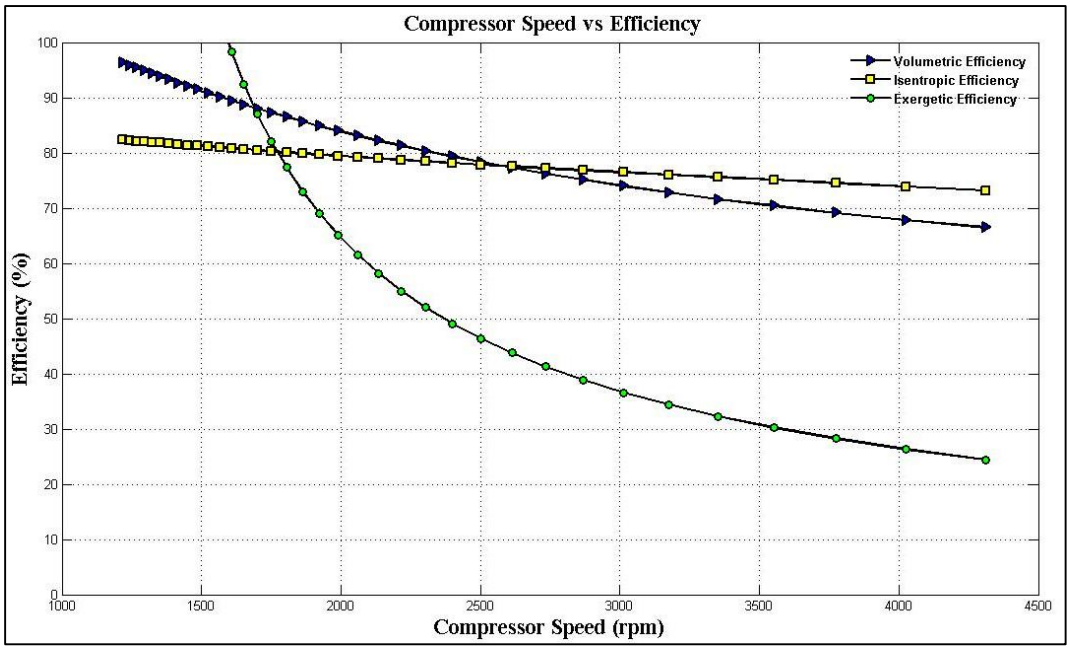

Figure 27 Compressor Speed vs Efficiencies

As in the case of refrigeration cycle operation points in terms of exergetic efficiency, same phenomenon can be observed in figure 28 and figure 29. In the graphs, the change of total exergy destructed with respect to condensing temperature and compressor speed are represented. For certain cycles, Clausius inequality states that the exergy destruction either equals to zero, meaning the system is reversible, or is bigger than zero, indicating that there exist irreversibilities within the system. [14] However, for condensing temperature below 43 °C and for compressor speed below 1600 rpm, total exergy destruction within the system is negative which contracts the above statement. Hence, it could be concluded that the system, having total exergy destruction with negative sign, is impossible. Passing those mentioned condensing temperature and compressor speed points above, the destruction of exergy within the cycle increases by increasing rate with respect to increasing condensing temperature, and increases with almost constant slope according to the increasing compressor speed.

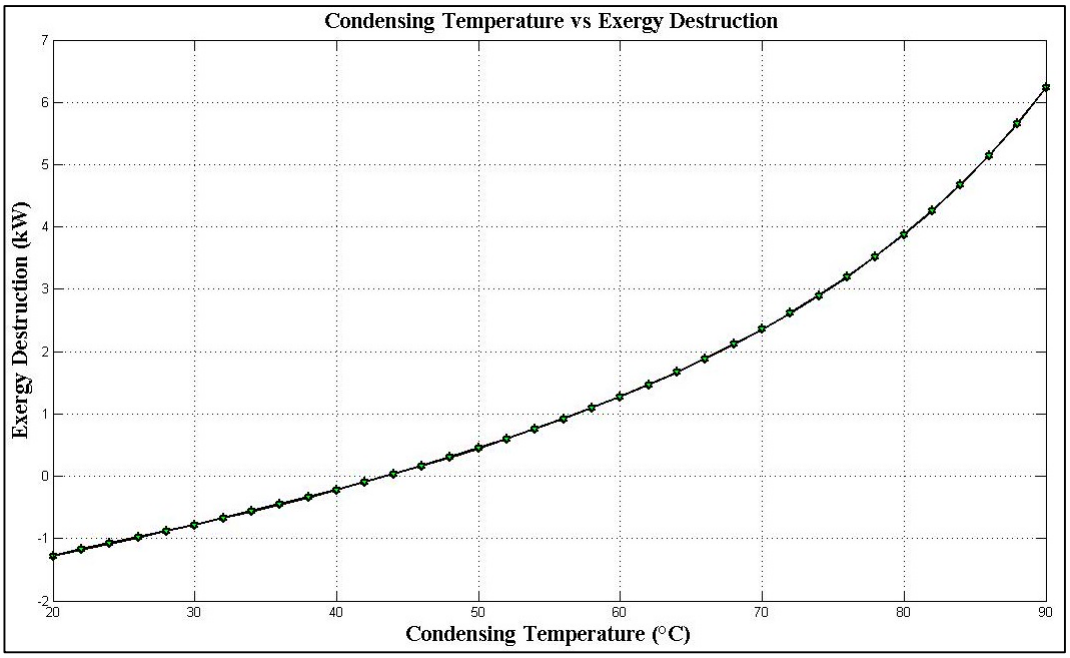

Figure 28 Condensing Temperature vs Exergy Destruction

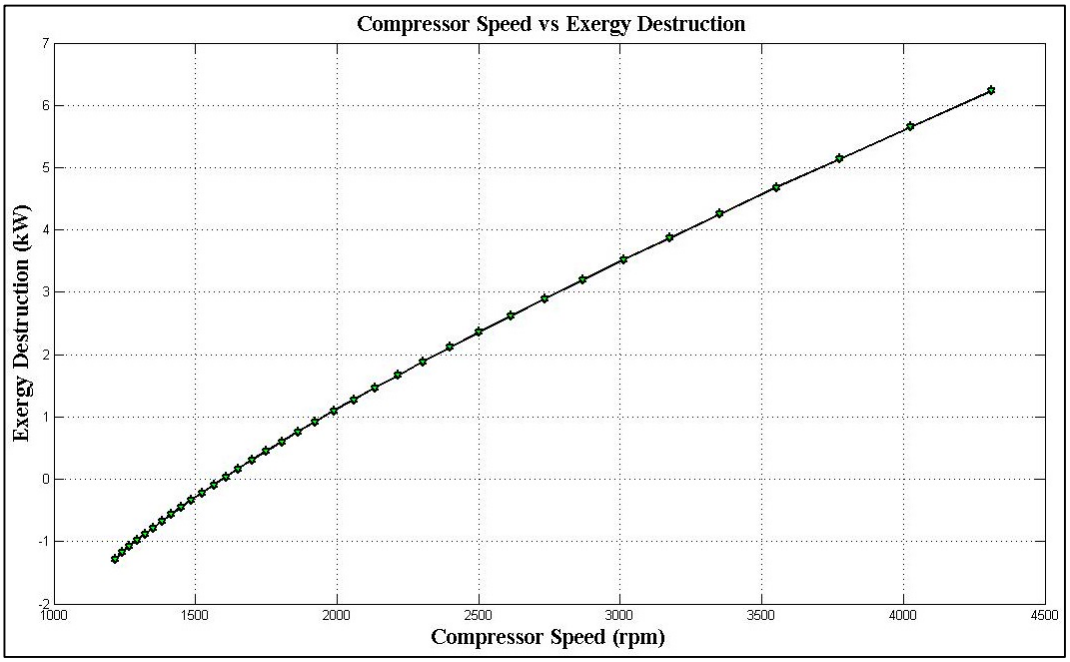

Figure 29 Compressor Speed vs Exergy Destruction

Another and, probably the most important, variable for the refrigeration cycle is the system coefficient of performance. Indeed, COP is the representation of how optimum and feasible that system meets the requirements correspondingly. In detail, the COP is the measurement of the output of the system, which is the evaporator cooling capacity, compared to the supplied input work to the cycle, actually the compressor work. As it is seen in formula (11), what is gained from the cycle in exchange for what is given to the system is the proportion of evaporator cooling capacity to compressor work. For graphical representation, the behavior of COP with respect to condensing temperature is given in figure 30. As the condensing temperature increases, the COP of the cycle tends to decrease because of the increase of refrigerant enthalpy at the inlet of the evaporator. From formula (11), as the condensing temperature is increased, with the consideration of pre-defined sub-cool temperature, the evaporator cooling capacity decreases and the compressor work increases adversely, resulting increase of COP as seen in below figure. In addition, with the help of figure 26, the reasonable COP values for the cycle can be taken into account around 43 °C in which is as close as possible to related possible exergetic efficiency.

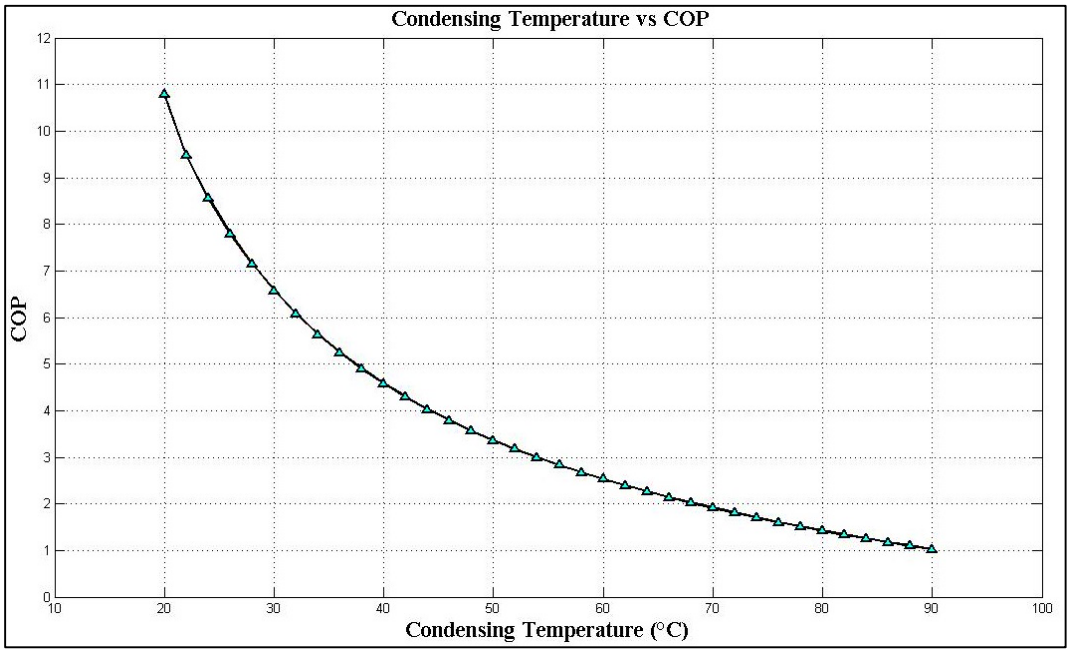

Figure 30 Condensing Temperature vs COP

For the relation of compressor speed and the COP of the cycle, the increase of compressor speed causes, more likely, the decrease of COP of the system in some manner. In real life, as the compressor speed is increased, the refrigerant passing through the compressor is pressurized at higher levels, causing the increase of its temperature, which is actually condensing temperature. When the condensing temperature increases, it is possible to increase of refrigerant enthalpies at both outlet of the compressor and the inlet of the evaporator with assumed sub-cool temperature. Indeed, this effect can be also prescribed in figure 30. However, the current coding algorithm does not contain any relation between compressor speed and the COP. As it is stated before, those of all performance variables are recorded only when the evaporator cooling capacity is between 8.4-8.6 kW and the change of COP values only depends on condensing temperature. Considering the flow chart of the coding, below figure is graphed by recorded COP values with respect condensing temperature as the compressor speed runs from 600 to 7000 rpm, which has actually no impact on COP values at all. However, figure 31 may be noticed as assistance for the understanding of relation between compressor speed and the COP of the cycle as well as behavior of the rate of COP decrease compared to that of in figure 30.

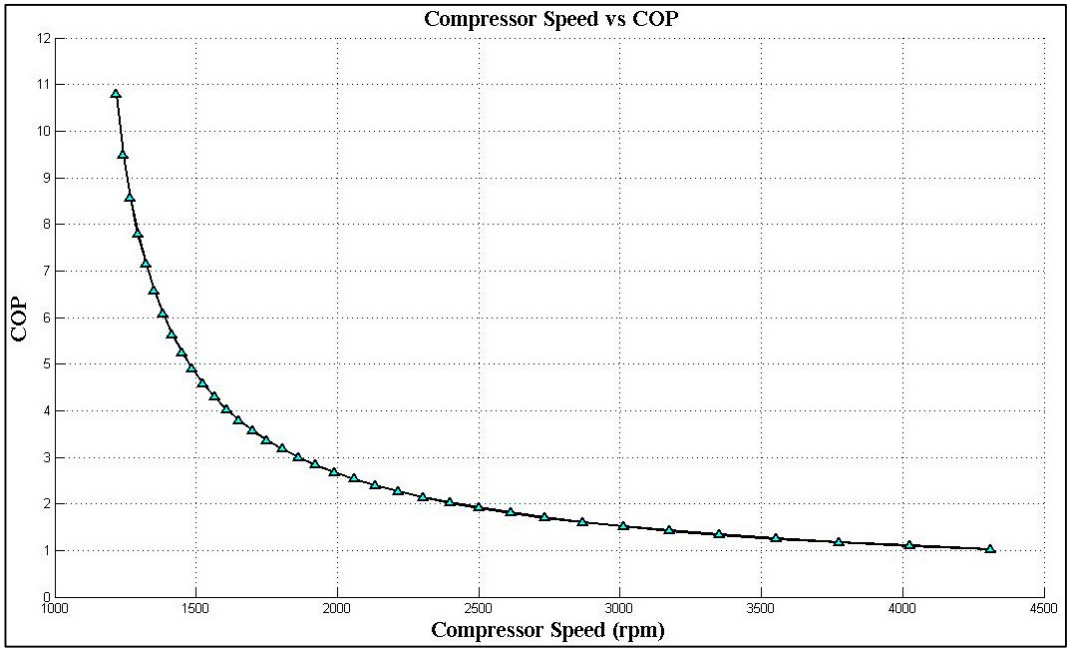

Figure 31 Compressor Speed vs COP

CHAPTER 3

EXPERIMENTS

Following chapter describes the details of the tests to be performed in the scope of understanding the dynamic behaviors of the refrigeration vapor compression cycle. Since the aim of current study is to determine the compression cycle characteristics under different load conditions on both the evaporator and the condenser as well as observe the particular mass flow rates considering the vapor and liquid phases of the refrigerant, cycling through the system, tests were performed according to the peculiar load status as following;

1. Condenser fan speed 50% of maximum & Evaporator fan switch on 1
2. Condenser fan speed 50% of maximum & Evaporator fan switch on 2
3. Condenser fan speed 50% of maximum & Evaporator fan switch on 3
4. Condenser fan speed 100% of maximum & Evaporator fan switch on 1
5. Condenser fan speed 100% of maximum & Evaporator fan switch on 2
6. Condenser fan speed 100% of maximum & Evaporator fan switch on 3

After system integration for the setup was completed, tests were implemented respectively. Component selection for the system was ended in the consideration of minimum work supplied to the compressor while ensuring the desired evaporator cooling capacity at the certain cycle operation point. In details, compressor speed and ambient air temperature were assured as same over the six tests. Compressor ran at a constant speed of 2650 ± 50 rpm. In addition, ambient air temperature at the inlet of the evaporator and condenser was same, and at around 33 °C with the humidity level of 30%-40%, since whole system stood in the same test chamber. Furthermore, the

utilized coolant in the cycle was determined as refrigerant R134a, commonly used in automotive A/C and HVAC industry. In addition, the sub-cool and super-heat temperatures were aimed to achieve as 5 °C and 10°C respectively in order to be consistent with that of performance analysis of the refrigeration cycle in section 2.3.

At the start of tests, measured temperatures and pressures at the inlet/outlet of the each components were waited for a certain time to approach to constant value in order to establish same system characteristics for each test startup.

3.1. TECHNICAL SPECIFICATIONS OF THE COMPONENTS

In this chapter, specifications of the equipment taken into operation in the experimental test setup are explained in terms of technical capabilities and general intention of usage. Indeed, compressors, condenser module with fans, evaporator module with receiver dryer and expansion valve are the main components of the A/C system. Additionally, pressure transmitters, thermocouples and flow meters were accompanied for measurements purposes. Besides, a data logger was connected to the pressure transmitters and thermocouples in order to record the relevant variables. Details of the equipment are as followings.

3.1.1. COMPRESSOR

For the experimental test setup of the refrigeration vapor compression cycle, a piston-type with swash plate compressor is used. Indeed, the compressor is powered with the diesel engine of the APU main unit, whose specifications are also indicated in the chapter 1, by using the belt system between the engine pulley and compressor clutch. The brand name and the model of the compressor are “Valeo TM16”. This type of compressors are commonly preferred in automotive, agricultural and refrigeration applications for providing prominent features such a light-weight & compactness, high efficiency & reliability and low vibrations. Figure 32 shows the “Valeo TM 16” piston-type with swash plate compressor used in the experimental setup.

Figure 32 Piston Type with Swash Plate Compressor - VALEO TM16 [34]

Moreover, referring the sub-cool and super-heat temperatures which were considered as 5 °C and 10°C respectively in the performance analysis of the refrigeration cycle, supplier is accordingly able to supply below performance table for TM16 in terms of changing evaporating and condensing temperatures.

Performance Table

TM16		Evaporating Temperature (℃)						
Cond Temp (℃)		-15	-10	-5	0	5	10	15
30	Q (kW)	-	8.06	-	-	-	-	-
	P (kW)	-	2.88	-	-	-	-	-
40	Q (kW)	-	6.94	9.14	11.36	-	-	-
	P (kW)	-	3.10	3.44	3.74	-	-	-
50	Q (kW)	-	5.84	7.77	9.69	11.92	14.78	-
	P (kW)	-	3.37	3.77	4.15	4.48	4.78	-
60	Q (kW)	-	4.76	6.41	8.02	9.91	12.41	-
	P (kW)	-	3.61	4.07	4.50	4.91	5.28	-
70	Q (kW)	-	3.69	5.05	6.34	7.89	10.01	-
	P (kW)	-	3.77	4.27	4.75	5.22	5.65	-

Q : Cooling Capacity, P : Power Consumption
Compressor rotation speed : 2650 rpm, Super heat temperature : 10 ℃, Subcooling temperature : 5 ℃

Figure 33 Performance Table - VALEO TM16 [36]

3.1.2. CONDENSER MODULE

Condenser module engaged into A/C system setup consists of a heat exchanger, being called condenser and two same DC powered axial fans. Indeed, condenser is conventionally manufactured with aluminum tubes encased in plate fins having same material with tubes as aluminum. Additionally, axial fans located onto top of condenser itself have the ambient air to pass through the passages of the condenser formed between the tubes and fins. This type of cooling operation can be named as cross-flow forced convection air-cooled condenser system, in which the components above are assembled into a package named as condenser module. In details, fans are the axial suction type driven by brushless DC motor, which are the product of "EBMpapts". Meanwhile, condenser itself is manufactured by "MAKEL Teknoloji", which is indeed the supplier of condenser module itself. Actually, module having fans and condenser itself can provide max. 13 kW heat rejection capacity considering the operation points of both compressor and evaporator in the cycle accordingly as well as the volumetric flow rate of the air crossing the condenser itself. As stated above, cooling load on the condenser was changed by adjusting the fans of condenser module as 50% and 100% of maximum fan speed, which can provide the opportunity to have mentioned test configurations. Below figure shows the components forming the condenser module and the air flow direction through it.

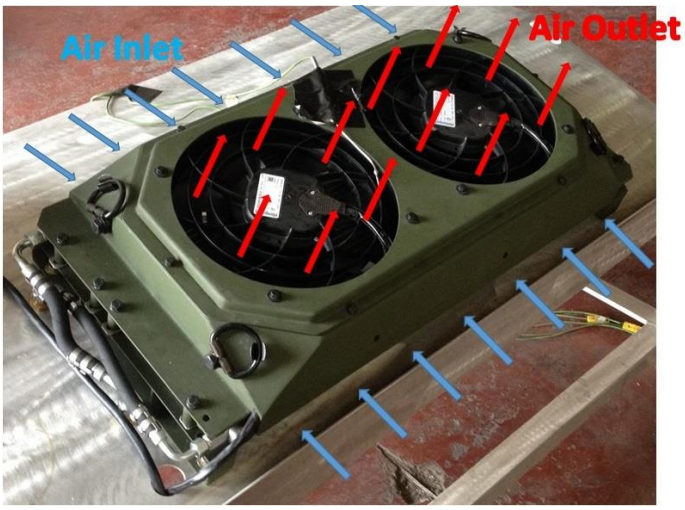

Figure 34 Forced-Convection & Air-Cooled Condenser Module

3.1.3. EVAPORATOR MODULE

Evaporator module consists of a heat changer, two double-wheel centrifugal fans positioned onto top of the heat exchanger which are both encased in the evaporator frame whereas receiver dryer and expansion valve are both installed on the module frame. Similar to case in the condenser module, heat exchanger is manufactured by using aluminum tubes and plate fins. Correspondingly, two double-wheel centrifugal fans suck the ambient air through the heat exchanger within the concept of cross-flow forced convection air-cooled cooling operation. Fans are the double-wheel centrifugal blower type driven by DC motors, which are the product of "SPAL Automotive". Also the heat exchanger as evaporator is manufactured by "Mobile Climate Control (MCC)", which is also the supplier of the evaporator module itself including the design of the module frame. For the overall performance of the evaporator module, it can provide max. 8.5 kW cooling capacity with the configuration of the fans and heat exchanger above, regarding the volumetric air flow rate supplied by fans through the module as well as the operation points of other components in the cycle. Additionally, the control unit of the A/C system is also positioned on the module frame, providing the ability to control both the compressor engage/disengage signal and the evaporator module fan speeds. Referring the test configurations above, fans speed control is managed via rotary switch on the control unit, allowing changing the load on the evaporator. Figure 35 indicates the evaporator module and A/C system control unit accordingly.

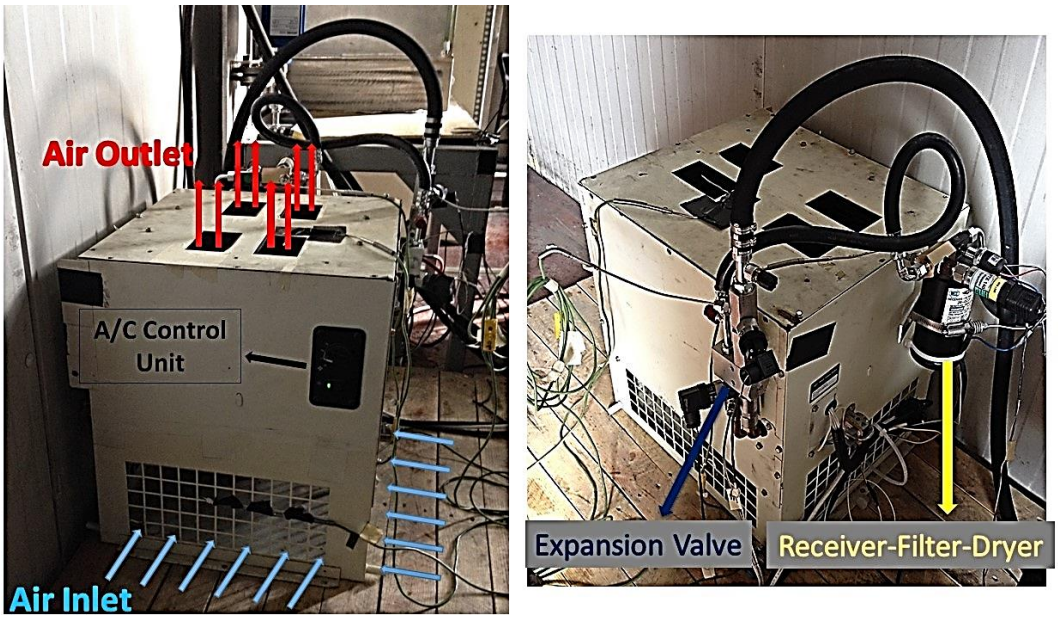

Figure 35 Evaporator Module with A/C Control Unit & Expansion Valve & Receiver – Filter – Dryer

3.1.4. EXPANSION VALVE

The thermal expansion valve is a metering or flow-restricting component in the A/C system, controlling the amount of refrigerant flow into the evaporator. Basically, restricting the cross sectional area of where the refrigerant passes from receiver dryer through the evaporator causes the increase of the refrigerant velocity hence decreases the pressure and corresponding temperature of the refrigerant flow. As the pressure and temperature of the refrigerant decrease, vapor-liquid mixture at the inlet of evaporator is obtained to enhance the heat transfer between ambient air and the refrigerant through the evaporator coils. In the experimental setup, block type thermal expansion valve is used, supplied by "Mobile Climate Control (MCC)". As details, block type valves have no external/internal pressure equalizing capability, meaning the readily available pressure information referring the pressure-enthalpy diagram of the refrigerant, at the outlet/inlet of the evaporator respectively. Instead, high pressure side of the A/C cycle is balanced with the spring force of the thermal expansion valve added to the pressure stemming into evaporator. While the refrigerant pressure in the evaporator is increased, the expansion valve needle position is caused to change as to allow the more liquid flow into the evaporator in order to absorb more heat which helps

decreasing the pressure. Block type thermal expansion valve seen in figure 36 is used in the experimental setup.

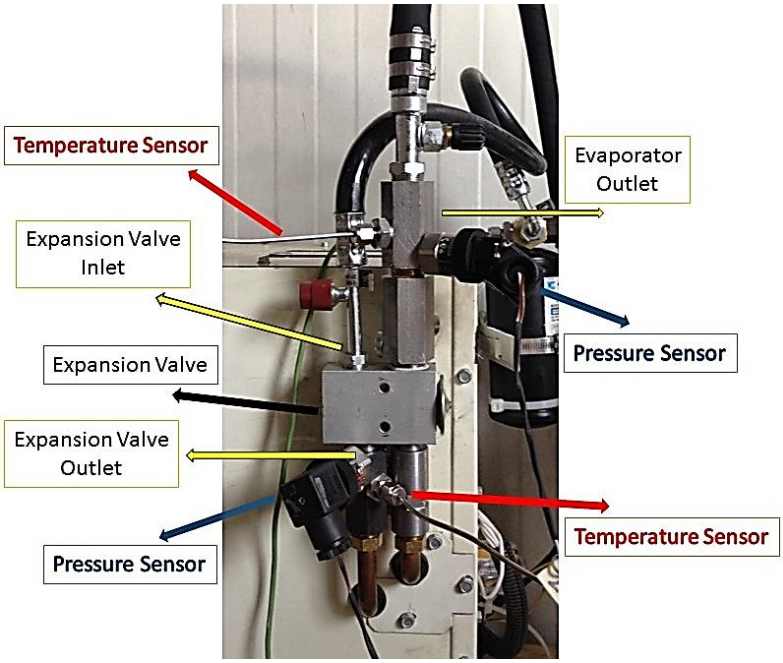

Figure 36 Thermal Expansion Valve - Block Type, MCC

3.1.5. RECEIVER DRYER

The receiver tank behaves as storage container for both liquid refrigerant and oil when A/C system may or may not require additional refrigerant flow through the components depending on the loads on the condenser and evaporator. Indeed, the receiver is located on the high pressure side of the system after the condenser in order to ensure that continuous refrigerant flow in liquid phase enters the expansion valve. While receiving the liquid refrigerant in order to maintain a certain level of liquid at the bottom at all times to feed the cycle, the receiver tank is additionally used for stabilizing the pressure on the evaporator and increases the system performance by enforcing the refrigerant to behave like in an ideal cycle. Furthermore, adding the desiccant tablets into the receiver tank, trans-changing the container as "receiver dryer", is purposed to trap and absorb the moisture in the refrigerant or oil, which is actually very harmful for components in the cycle. In fact, moisture may combine with the refrigerant to form the hydrochloric acid, which is extremely corrosive chemical

substance for the A/C system components. Below figure clarifies the inside mechanic of the receiver dryer tank with inlet/outlet port, filter and desiccant pellets schematically.

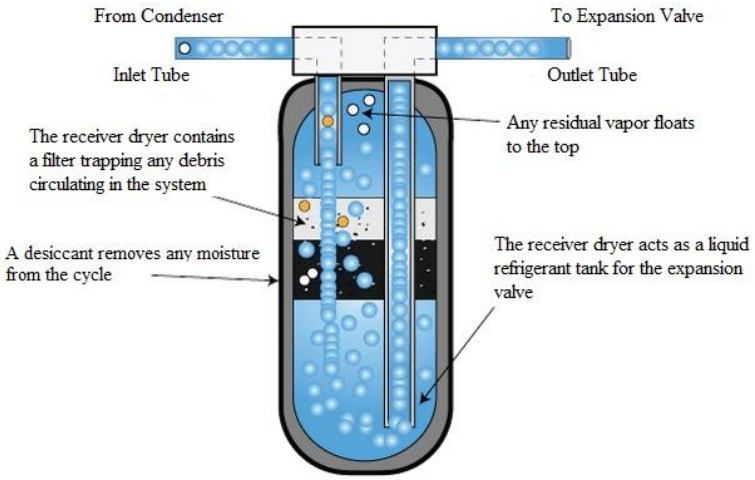

Figure 37 Schematic View of Receiver Dryer [37]

Also, the receiver dryer, which is the product of "Mobile Climate Control (MCC)", used in the experimental setup can be seen in figure 38 accordingly.

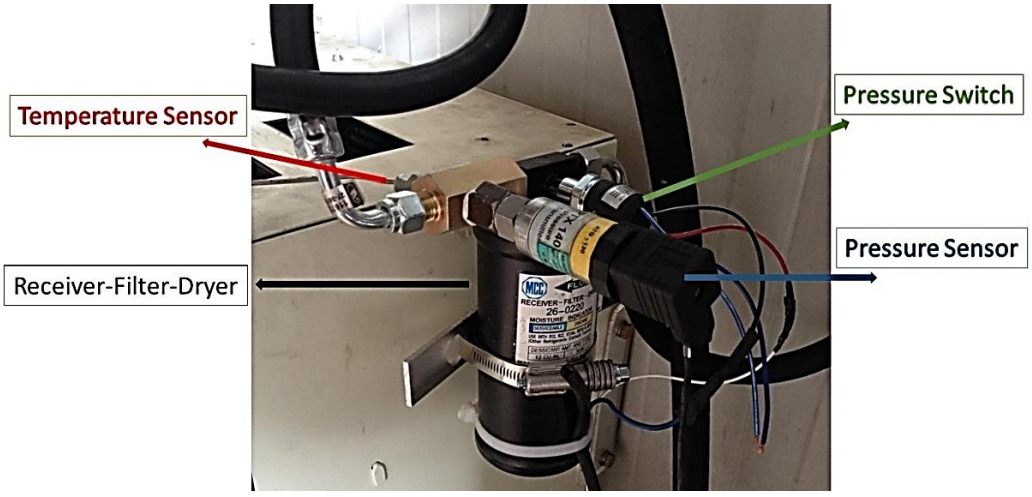

Figure 38 Receiver Filter Dryer – MCC

3.1.6. PRESSURE TRANSMITTERS

For the pressure measurements, six pressure transmitters are connected to the A/C system components' inlets/outlets accordingly whose positions are shown in the figure 44. The transmitters are the product of "GE Industrial, Sensing" with the model name "PTX1400". As details, transmitters used in the setup have two separate measurement ranges as 0-20 bars for low pressure side of the cycle and 0-40 bars for high pressure side of the cycle respectively. All six transmitters are connected to the data acquisition system for measurement recording. Apart from pressure ranges, other specifications for all six transmitters are same as stated in below table 5.

Table 5 Pressure Transmitter Specifications - PTX1400

Pressure Range (Low Side, High Side)	0-20, 0-40	bars
Temperature Range	-25 to 125	°C
Accuracy	± 0,15	%
Supply Voltage	9 to 28	VDC
Output Current	4 to 20	mA

Additionally, below figure 39 shows the picture of pressure transmitter "PTX1400" used in the experimental test setup.

Figure 39 Pressure Transmitter - PTX1400 [38]

3.1.7. THERMOCOUPLES

In the experimental test setup, ten thermocouples are used for the temperature measurements on relevant positions in the cycle. Indeed, six of ten are installed on the fittings which are used for in-cycle refrigerant side temperature measurements. Remaining are located at the inlets and the outlets of the evaporator and condenser module for the air side temperature measurements. Locations of the thermocouples are shown in figure 44. In details, thermocouples used in the cycle are the product of "Elimko" with straight K-type (NiCr-Ni) with model "E-MI04-1K30-20-K25-SS-TZ-G1/4 S-ME", 3 mm in prop diameter, which are actually known as fast responsive and considerably accurate in industry. Additionally, thermocouples temperature range varies between -200 °C to 1000 °C, which indeed entirely covers all the operation temperatures of A/C cycle. Besides, with an appropriate data acquisition system, straight type thermocouples are able to provide ±0.5% accuracy through its operation range. Similar to the pressure transmitters, thermocouples are also connected to the data acquisition system for recording the temperature values, read from the positions as shown in figure 44.

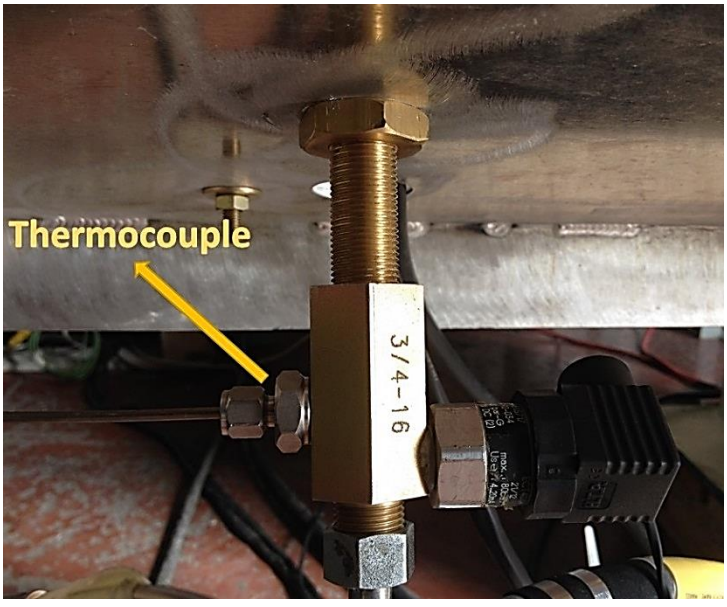

Figure 40 Thermocouple – inline @ Condenser Inlet – ELIMKO

3.1.8. FLOW METERS

As stated previously, one of the main claims of this thesis study is to experience different mass flow rate in liquid and vapor states of the refrigerant due to the component or system dynamics of the A/C cycle. For the purpose, there are two separate flow meters used in the cycle both calibrated for refrigerant R134a to measure the mass flow rate of the liquid and vapor phases of the fluid, whose positions are shown in figure 44 respectively. In details, flow meters are the product of "Krohne" with the model type "V40" used for vapor mass flow rate measurement and "H250" for liquid mass flow rate measurement. Both flow meters are designed for vertical usage, meaning that the flow direction should be from bottom to top since they employ the gravity to pull down the cone (measuring device) against the force created by flow itself. Below table 6 shows the specifications of the flow meters specified by the manufacturer.

Table 6 Flow Meter Specifications - VA40 & H250

SPECIFICATIONS	VA40 (Vapor)	H250 (Liquid)
Type	Glass Cone	Metal Cone
Operating Temperature	-20 °C to 100 °C	-196 °C to 300°C
Operating Pressure	up to 10 bars	up to 78 bars
Accuracy	1%	1.6%
Flow Measurement Scale	0.011 - 0.1 (kg/s)	0.011 - 0.1 (kg/s)
Connection	Screw type	Flange type

In details, measurements of the refrigerant mass flow rate in both vapor and liquid states are performed with above flow meters by using a camera to record the mass flow rate values seen on the each flow meters analog indicator. Indeed, flow meters with digital indicator, also suitable with data logger system below, are available in the market; however, their unit prices are so high to afford in the scope of test setup budget. Hence, the camera is located at the front side of the flow meters and they are synchronized with the data logger system time in order to cross-match the relevant

temperature-pressure values to corresponding vapor/liquid mass flow rate instantly. Below two figures 41&42 provide the pictures of both vapor and liquid mass flow meter used in the setup.

Figure 41 Vapor Mass Flow Meter KROHNE VA40 [39]

Figure 42 Liquid Mass Flow Meter KROHNE H250 [40]

3.1.9. DATA ACQUISITION SYSTEM

Data acquisition system used in the test setup is the product of “DEWEsoft” with model “Sirius-HD 16xLV” and the device uses readily available embedded software “DEWEsoft X”. Actually, all pressure and temperature values are recorded by using data acquisition system having connected to a computer with operation system “Windows 8”. In fact, hardware and software of the data logger system provides suitable interfaces for the pressure transmitters and thermocouples output signals and cable connections. Hence, the acquisition system manipulates all sensor data signals and transmits them to the computer in order to be recorded with desired units and in readable format, i.e. excel tables were created for the test results. In details, figure 43 shows frontal and rear views of the data acquisition device along with its analog input connectors embedded on the cover. Also, technical specifications of the data logger could be seen in table 7.

Figure 43 Data Acquisition System - DEWESOFT Sirius - HD 16xLV [41]

Table 7 Data Acquisition System Specifications - Sirius - HD 16xLV

SPECIFICATIONS		SIRIUS-HD 16xLV
Operating Temperature		-10 °C to 50 °C
Power Supply		6 to 36 VDC
Typical Power Consumption		11 W
Sensor Excitation		2 to 30 V bipolar, 0 to 24 V unipolar or max.0.2/2W
Connectors		16 Channel DSUB-9 Analog Input
DC Accuracy	100 V range 10 V range 1 V range 100 mV range	0.05% of value + 20 mV 0.05% of value + 2 mV 0.05% of value + 0.2 mV 0.05% of value + 0.1mV
Input Type		Voltage, Full Bridge Strain, Current (ext. Shunt)
Input Voltage		±100 V, ±10 V, ±1 V, ±100 mV
Data Rate / Channel [Hz]		200 k
Vertical Resolution		24 Bit - 200 Ks/sec
Advanced Functions		Low power, High input range, High sensor supply

3.2. TEST OBJECTIVES AND SETUP PREPARATION

As stated previously, since the primary objective of the air conditioning system is to achieve the temperature of air coming from evaporator at max. 18 °C, while considering the inlet air temperature entering the evaporator at 33 °C, the experimental test setup was prepared in a closed room whose air temperature was kept at around 33 °C constant through the tests.

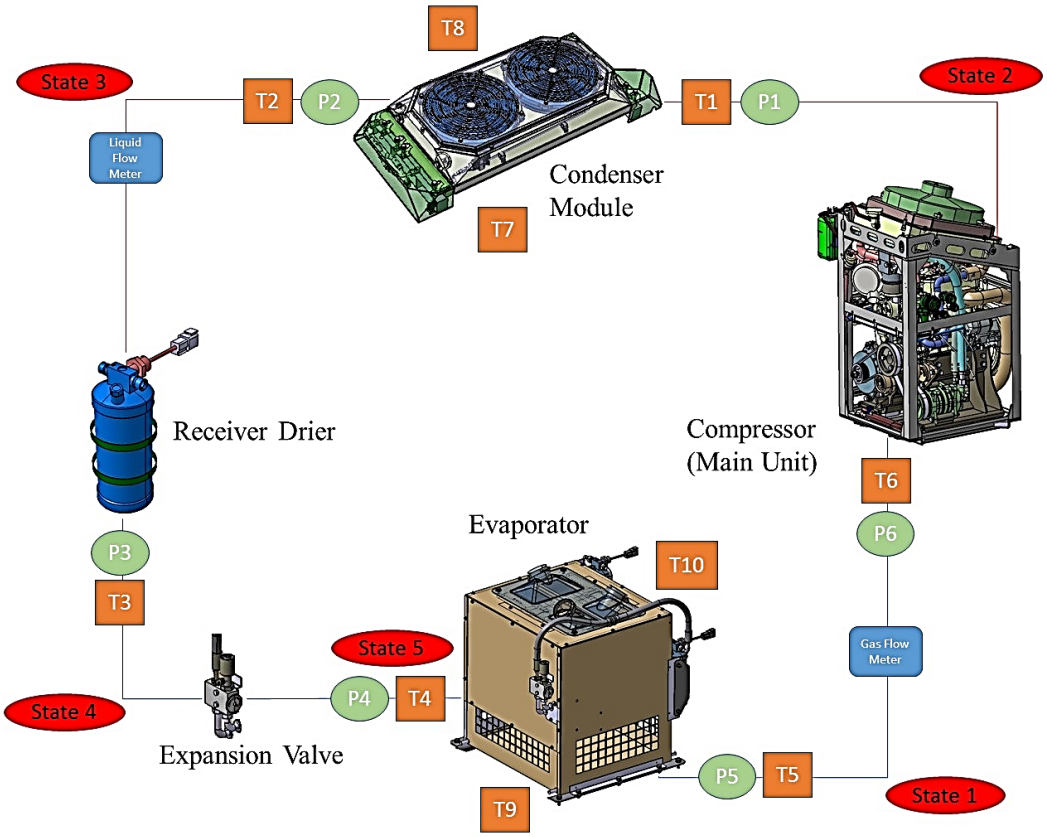

Figure 44 Component Layout of the Experimental Setup

Above figure shows the schematic drawing of the experimental setup components in all aspect. Indeed, according to the heat load changes both on the evaporator and condenser, temperature and pressure at each component's inlets and outlets as well as the vapor and liquid mass flow rate of the refrigerant were recorded accordingly. In the schematic, "P" represents the pressure transmitters and "T" represents the thermocouple for temperature readings. Additionally, as an important outcome of each test is expected that high-pressure side (liquid) and low-pressure side (vapor) mass flow rates through the cycle shall be same due to the system dynamics created by the

components, we have two different mass flow meters such as at the inlet of the compressor and the outlet of the condenser as shown in the figure 44. In detail, below table both clarifies the descriptions of each component accordingly and shows the variables recorded during each six tests.

Table 8 Experimental Test Setup - Recorded Variables

SENSORS	RECORDED VARIABLE	UNIT
P1 – T1	Compressor Outlet – Condenser Inlet Temperature – Pressure	°C - kPa
P2 – T2	Condenser Outlet Temperature – Pressure	°C - kPa
P3 – T3	Expansion Valve Inlet Temperature – Pressure	°C - kPa
P4 – T4	Expansion Valve Outlet – Evaporator Inlet Temperature – Pressure	°C - kPa
P5 – T5	Evaporator Outlet Temperature – Pressure	°C - kPa
P6 – T6	Compressor Inlet Temperature – Pressure	°C - kPa
T7 – T8	Condenser Air Side Inlet – Outlet Temperatures	°C
T9 – T10	Evaporator Air Side Inlet – Outlet Temperatures	°C
Vapor flow meter	Mass Flow Rate at the Inlet of the Compressor	kg/s
Liquid flow meter	Mass Flow Rate at the Outlet of the Condenser	kg/s

3.2.1. FUNCTIONAL SYSTEM STATES AND SETUP INSTALLATION

Referring the above conditions to be implemented to the test setup, six particular tests were performed for various load configurations on both the evaporator and the condenser modules accordingly. For the purpose, rotation speeds of the fans on the evaporator and the condenser were regulated to obtain different load configurations. Fan rotation speed adjustment methods will be indeed clarified in the further parts. Additionally, although the environment air temperature was tried to be kept at 33 °C constant, it was decided that keeping the air temperature at 33 °C at the inlet of the condenser and the evaporator would present more accountable and comprehensible results within the understanding of being economic and ease of control.

Before the tests, components were located in the test room considering the interaction between each component, especially between condenser and evaporator, not to use or to decrease the usage of inlet/outlet air from each other. Hence, components were located as far as possible on the test room ground. Additionally, a table, simulating the vehicle-condenser module interface, was designed and manufactured. Moreover, considering the usage of the both flow meters, which are indeed designed for vertical usage, they were inevitably needed to be mounted onto a separate platform shown in figure 45. Afterwards, A/C system components, which are the compressor embedded in APU main unit, the condenser, the evaporator with receiver dryer and expansion valve, were joined with appropriate hose connection including the fittings on which the pressure transmitters and thermocouples were installed. Besides, since the A/C system used in the experiments was an APU-driven system, electronic equipment were also connected into the system, which are electrical control box, man-machine interface panel (MMI) and also the batteries. For details, condenser module fans and MMI panel were operated by getting the electrical power directly from the electrical control box connected to the batteries. On the other hand, evaporator fans were powered by being directly connected to the batteries since they had separate control unit on the evaporator frame instead of MMI panel. Indeed, former was the properties of the APU electrical system architecture meaning that the control of MMI panel and the condenser fans were performed with accompanying the electrical control box of APU system.

In order to summarize the process that the refrigerant R134a experienced in the readily available A/C system components and also in the flow meters and fittings used for pressure and temperature measurements, it had better to cover up the followings in orderly by the help of figure 44. In the experimental setup, the refrigerant R134a is pressurized at a certain level of pressure and corresponding temperature value and comes to fitting at state 2 in figure 44 for measuring the temperature and pressure at the inlet of condenser; those were both recorded by the data taker. Indeed, installation order of the pressure transmitters and the thermocouples into all fitting was in the direction of refrigerant flow such that refrigerant comes firstly to pressure transmitter and then to the thermocouple in order not to allow the thermocouple to affect the

measurement of pressure transmitter. Below figure shows the details of fitting configuration used for pressure and temperature measurements.

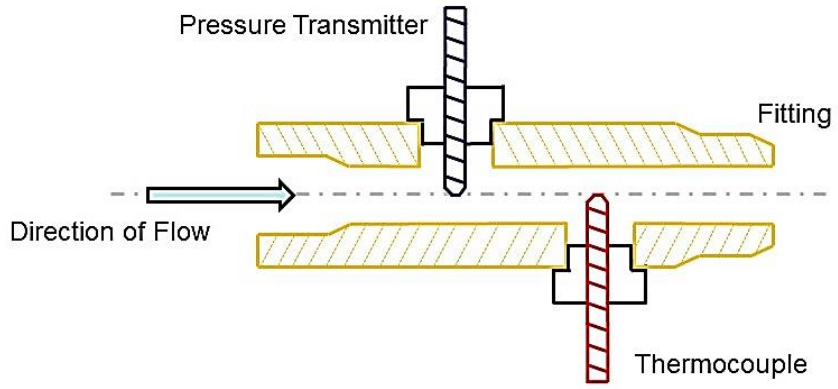

Figure 45 Schematic of the Fitting for Pressure and Temperature Measurements

After condensing to saturated or sub-cooled liquid in the condenser module itself, refrigerant comes to the fitting for temperature and pressure measurements at the outlet of condenser. Later on, refrigerant passes through the liquid mass flow rate meter while a fixed camera in front of the flow meter records the liquid mass flow rate accordingly. After leaving the liquid mass flow meter, refrigerant passes through the receiver dryer, expansion valve and evaporator respectively while being recorded its pressure and temperature at the inlet and outlet of each component accordingly as shown in figure 44. In details, since the expansion valve and the receiver dryer are installed on the evaporator frame by having short hose length between two, inlet pressure and temperature values for expansion valve were recorded at the outlet of the receiver dryer. Also, pressure and temperature at the inlet of the receiver dryer were not recorded due to the fact that they were not used in any calculation. However, temperature values at the outlet of the condenser could be taken into consideration as the parameters that of at the inlet of receiver dryer, if needed, by ignoring the losses in the hose between the condenser and the receiver dryer. Furthermore, while taking the way off from evaporator as reaching the super-heated vapor state, the refrigerant comes another fitting at the outlet of the evaporator module for related pressure and temperature measurements and passes to the vapor mass flow meter. Same camera in front of the mass flow meter records the instantaneous vapor mass flow rate of the refrigerant in kg/s. After the mass flow rate of the refrigerant is recorded as in vapor

state, it finally arrives the last fitting for pressure and temperature measurements at the inlet of the compressor and goes into the compressor to start the cycle again. For visual purposes, below pictures provide examples for installation of fitting used for pressure and temperature measurements and also the mass flow meters positions on the experimental test setup.

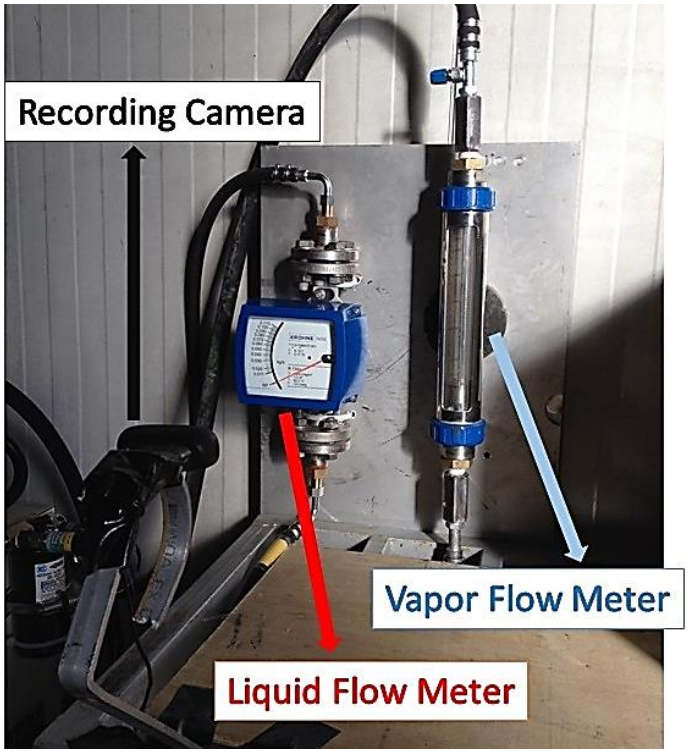

Figure 46 A View of Mass Flow Rate Meters

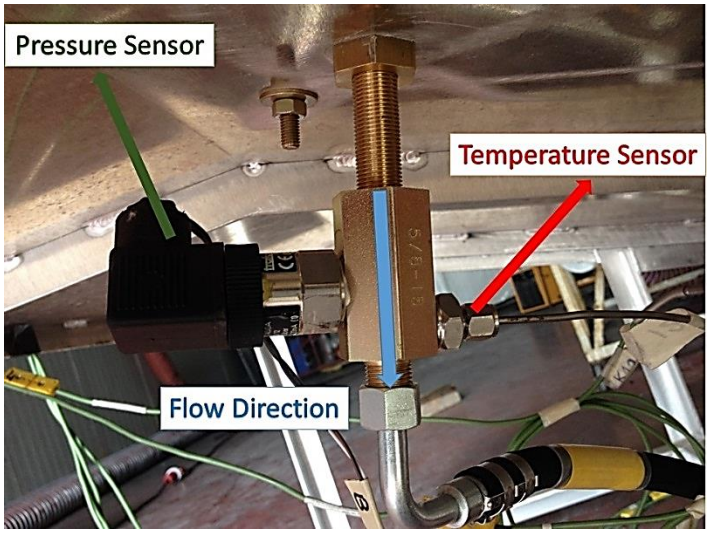

Figure 47 Fitting Installation Pressure & Temperature Measurement

Moreover as succeeding to reach reasonable results at the end of tests, amount of the refrigerant R134a in the cycle was another important factor needing to be considered in the perception of achieving the expected results that was one would aim to reach during design phase of the A/C system cycle. Indeed, charging R134a into the system, more or less than it should be, might result in performance decrease or damages on components. As stated in section 2.2, overcharge and undercharge of refrigerant R134a into the system shall cause the slugging and liquid shock on the compressor as well as the changing the system optimum operation point by affecting the super-heat or sub-cool temperatures that the system might experience continuously, which are actually not desired. For the purpose, amount of refrigerant in the cycle was determined according to the procedure, which was created by the evaporator module supplier "Mobile Climate Control (MCC)". In details, first step was the measuring ambient air temperature, which was stated previously as 33 °C (91.4 F). After that, adding 40 F to that temperature and specifying the corresponding pressure value from the pressure-enthalpy diagram of refrigerant R134a defined the pressure value that high side (compressor discharge) should have. According to the table below, 131 F corresponded to 200 psi (14 bar) which compressor discharge pressure value should be. Regarding this pressure value along with the super-heat and sub-cool temperatures, previously defined as 10 °C and 5 °C respectively, was also observed while refrigerant charging into the A/C system.

Pressure	**Temperature (F)**		**Pressure**	**Temperature (F)**	
psi	R-12	R134a	psi	R-12	R134a
(A)	(B)	(C)	(A)	(B)	(C)
95	87	85	150	117	112
100	90	88	155	119	114
105	93	90	160	121	116
110	96	93	165	123	118
115	99	96	170	126	120
120	102	98	175	128	122
125	104	100	180	130	123
130	107	103	185	132	125
135	109	105	190	134	127
140	112	107	195	136	129
145	114	109	200	138	131

Figure 48 Refrigerant Charging- Pressure vs Temperature

Following the above procedure by also considering the super-heat and sub-cool temperatures as well, amount of refrigerant to be charged into the system, which was clarified after some trial to reach 14 bar as discharge pressure, was determined as around 1600 grams.

In the scope of previously mentioned six separate test configurations, load on the both condenser and evaporator was changed regarding the list of test configurations in the introduction section of chapter 3. In fact, loads on the both components were adjusted by changing the fans rotation speed on related equipment, hence changing the overall heat transfer rate by regulating the volumetric flow rate of air passing through the condenser and evaporator heat exchangers. At the beginning of the tests, rate of the change of volumetric flow rate of the ambient air was uncertain due to not to know the relations between fans rotation speed and air volumetric flow rates that they provided at certain fan speed. For the purpose, outlet air flow speeds for both the condenser and evaporator for each test were recorded and presented in the result sections of related tests.

Before getting the details of adjusting fans rotation speeds of both the evaporator and the condenser modules, A/C system functional synthesis will be clarified. For the operation sequence of A/C system usage, once the APU engine is run and if the user needs to use APU-driven A/C system, button type switch of the controller unit on the evaporator module frame is set to ON state. After switch generates the “engage” signal to the compressor clutch through the electrical control box of the APU system, compressor clutch, driven by APU engine, is powered and engaged, and A/C system starts to operate. Meanwhile, a pressure switch on the receiver dryer unit simultaneously sends the pressure information at the outlet of the condenser to the electrical control box, which is also generating the “engage/disengage” signal for the compressor clutch, in order to control the high pressure side of the cycle regarding the high and low pressure values at which between the compressor clutch engages or disengages accordingly to maintain the system pressure. At the same time, during the A/C system operation, if the user needs more air flow from the evaporator blowers, rotary switch for evaporator fans can be set to “1”, “2” or “3” positions which can be

seen in figure 49 below. During the experimental tests for APU-driven A/C system, all three positions were used in order to adjust the fan speed, hence changing the load on the evaporator by affecting the volumetric flow rate of the air flow through the evaporator heat exchanger.

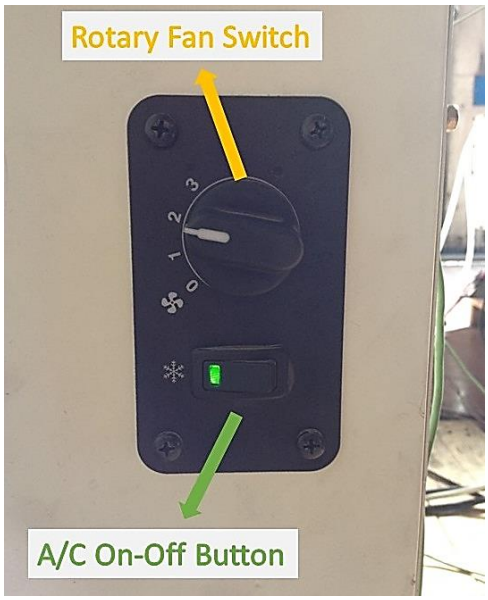

Figure 49 A/C System Control Unit - Evaporator Frame

For the condenser fans rotation speeds adjustment, a switch on the power cable of the fans was used. Indeed, the switch, in figure 50 below, has two state “Condenser Fan Rpm %50” and “Condenser Fan Rpm %50”, which allows the fans to rotate 50% speed of max. rotation speed and 100% speed of max. rotation speed respectively in order to change the heat transfer rate of the condenser module to the ambient air.

Figure 50 Condenser Fans Rotation Speed - Regulation Switch

Consequently, there were six load conditions on the evaporator and condenser modules considering the configurations generated with fans rotation speed regulations above. In detail, table in the next page shows the performed tests and relevant load configurations respectively.

Table 9 Heat Load Configurations – Experimental Matrix

TEST	CONDENSER FAN SPEED	EVAPORATOR FAN SPEED
Cond. Fan 50% & Evap. Fan "1"	50% of Maximum Fan Speed	Fan Switch on state "1"
Cond. Fan 50% & Evap. Fan "2"	50% of Maximum Fan Speed	Fan Switch on state "2"
Cond. Fan 50% & Evap. Fan "3"	50% of Maximum Fan Speed	Fan Switch on state "3"
Cond. Fan 100% & Evap. Fan "1"	100% of Maximum Fan Speed	Fan Switch on state "1"
Cond. Fan 100% & Evap. Fan "2"	100% of Maximum Fan Speed	Fan Switch on state "2"
Cond. Fan 100% & Evap. Fan "3"	100% of Maximum Fan Speed	Fan Switch on state "3"

Finally, experimental A/C system test setup was assembled by installing all necessary equipment, which are the APU system including the compressor in the APU main unit, condenser module and MMI panel to control the APU system operation. Additionally, evaporator module, consisting of heat exchanger with 2 centrifugal type of fans, receiver dryer and expansion valve installed on it, was connected to the A/C system. Meanwhile, ten thermocouples, six pressure transmitters, a vapor mass flow meter and a liquid mass flow meter were installed on the previously mentioned positions on the system for the measurement purposes. All these sensors were connected to a data logger system recording the pressure and temperature values instantaneously. Additionally, the camera was fixed in front of the flow meters to record the mass flow rates of the refrigerant inside the cycle. For visual clarification, below pictures show the final test setup layout and components' locations.

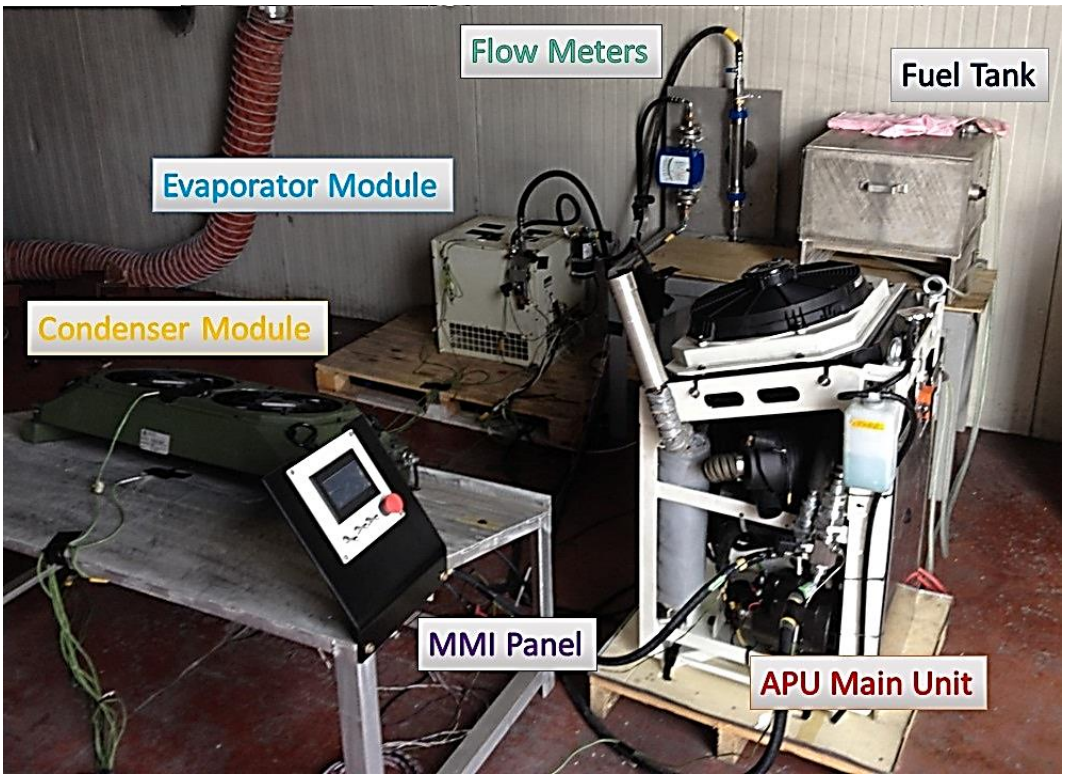

Figure 51 A View of Experimental Test Setup

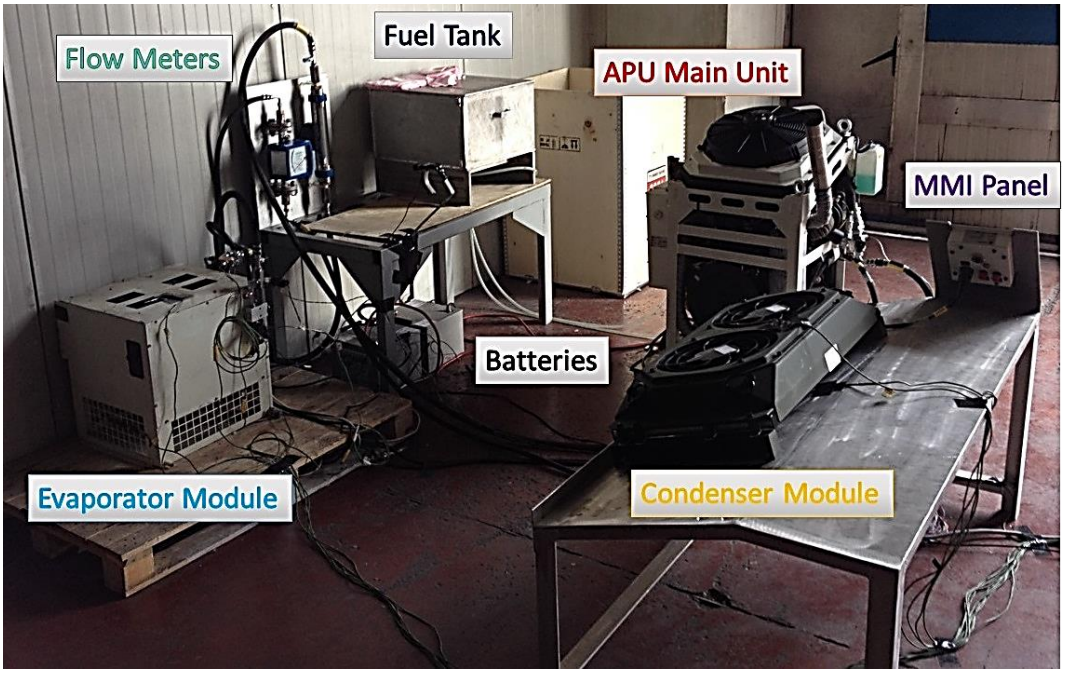

Figure 52 A View of the Experimental Test Setup

3.3. EXPERIMENTAL RESULTS

As stated previously, primary aim of the thesis study is to observe the dynamics behavior of the vapor compression refrigeration cycle while experiencing different heat load conditions on both condenser and evaporator modules. In addition, tendency of liquid and vapor phase mass flow rates of the refrigerant are important in order to characterize the effect of changing load conditions. For the purpose, temperature and pressure values at the points, defined in figure 44, were recorded by the data acquisition system seen in figure 53 as well as the particular mass flow rates of liquid and vapor phase while refrigeration cycle experienced six different load configurations clarified in table 9.

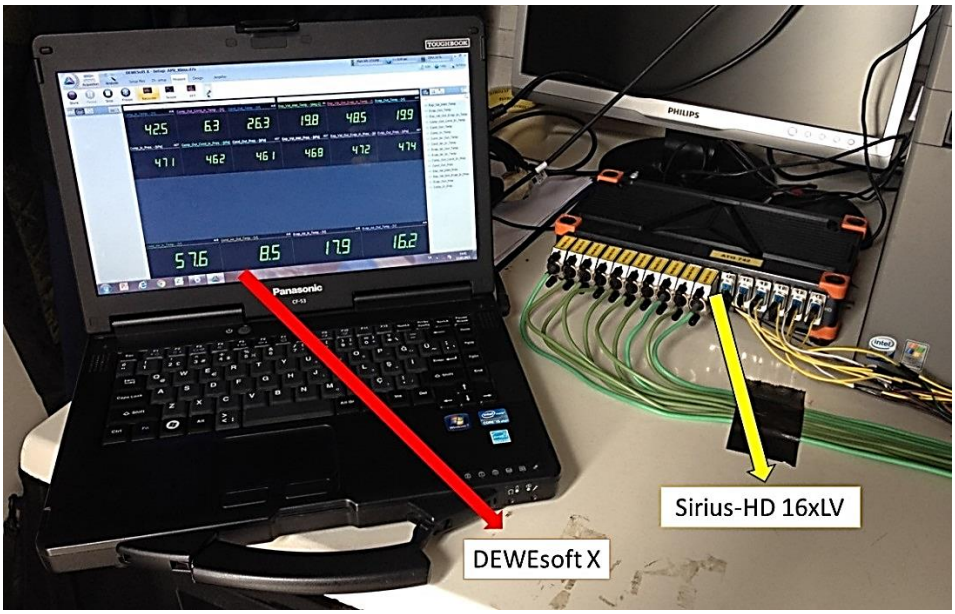

Figure 53 Data Acquisition System – DEWEsoft

Furthermore, one of the main criteria taken into account during design phase of the refrigeration cycle is to obtain max. 18 °C air side outlet temperature from evaporator while inlet air temperature is at around 33 °C. Obviously, this requirement can be met only when optimum operation condition is satisfied, Cond. Fan 100% & Evap. Fan "3" in this case. In details, changing load on the both condenser and evaporator will result in different air side outlet temperature from evaporator even if the air side inlet temperature entering evaporator remains constant and at around 33 °C. For

clarification, evaporator air side outlet temperatures of six particular tests are shown in figure 54 accordingly while air side inlet temperatures were kept as 33±2 °C throughout all six tests.

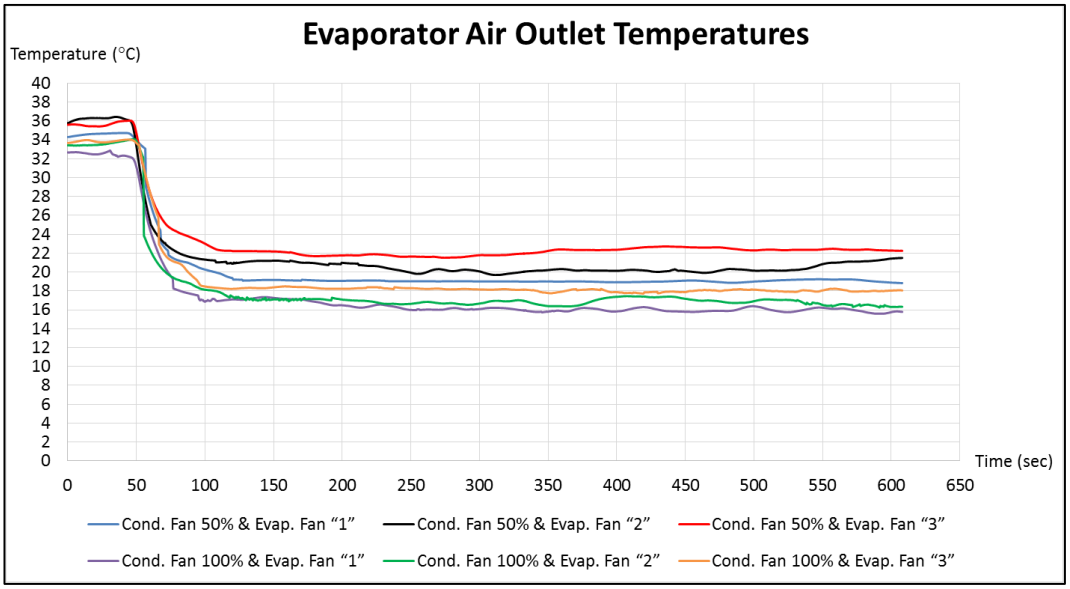

Figure 54 Air Side Outlet Temperatures (°C) - Evaporator

For the following section, six particular tests results will be shown in the consideration of pressure, temperature, vapor and liquid mass flow rates in graphical representations. In addition, corresponding calculated compressor work, evaporator cooling capacity and condenser heat rejection will also be presented in the same manner. For the purpose, a MATLAP® code, called 'test_results.m', is accompanied in order to prepare graphical representations of the tests results. Also, code is able to calculate the relevant information as COP, isentropic, volumetric and exergetic efficiencies, compressor work, condenser heat rejection, evaporator cooling capacity, exergy destruction. Also refrigerant pressure and temperature comparisons at related point can be produced and seen by the help of 'test_results.m'. The idea to run the code is similar with the analysis code, 'analysis.m', as for the proper usage of the 'test_results.m', the 'refpropm.m' should be located in the same directory with it. For further details, the code "test_results.m" is provided in the Appendix B.

3.3.1. Cond. Fan 50% & Evap. Fan “1”

As the first test of the experiments, Cond. Fan 50% & Evap. Fan “1” configuration was performed. For the purpose, condenser fan switch was adjusted as to rotate the condenser fans 50% of maximum rotation speed, which provided outlet air velocity around 12.5-14.5 m/s from condenser. Similarly, fan switch on the A/C control unit was adjusted to “1” supplying 18-19 m/s evaporator outlet air velocity.

In details, test was performed about 15 minutes. At the beginning, A/C switch was set to ON and hence compressor was engaged. After around 100 seconds, the cycle reached to steady state operation condition, which can be seen from figure 55. As shown below, pressures values at indicated points have oscillatory characteristics until around 100 sec. and then demonstrate wavy steady operation up until 400 sec. After that point, some disturbances occur in the system causing wavy operation with a bit high wave amplitude. Indeed, increase in amplitude is around 50 kPa in the high pressure side of the system. At the first sight, increase in amplitude may be caused from the difficulty of adjusting ambient temperature in the test chamber.

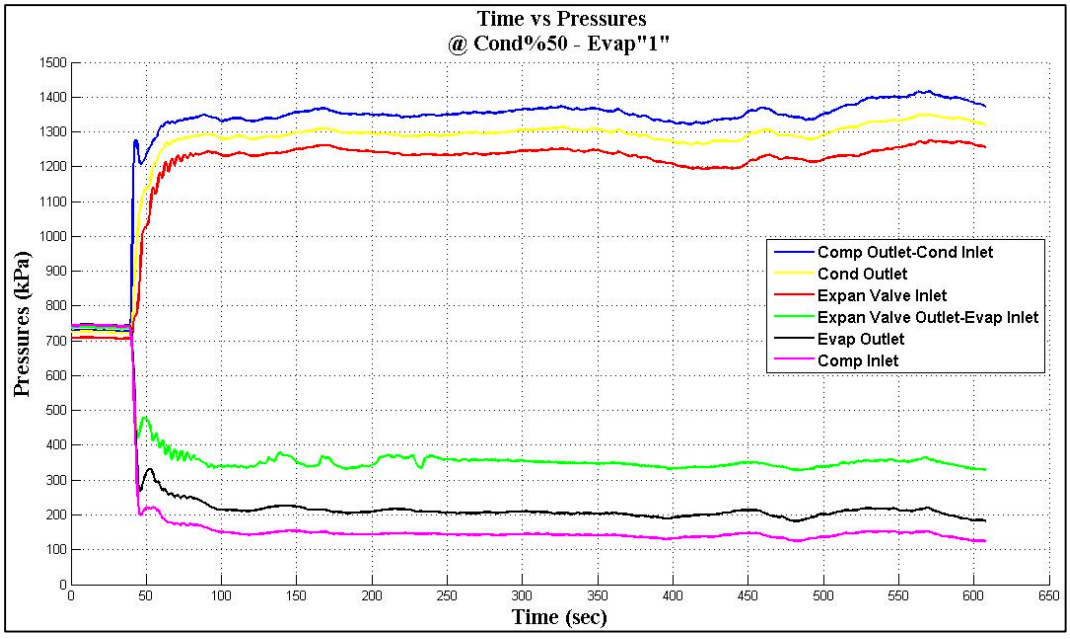

Figure 55 Pressure Measurements - Cond. Fan 50% & Evap. Fan “1”

Furthermore, total pressure loss in the condenser and evaporator can be found from figure 55 at around 75 kPa and 150 kPa in average respectively. In addition, pressure losses in the hose connections could be said as around 50-60 kPa in condenser to expansion valve and evaporator to compressor, which could be relatively considered as low values.

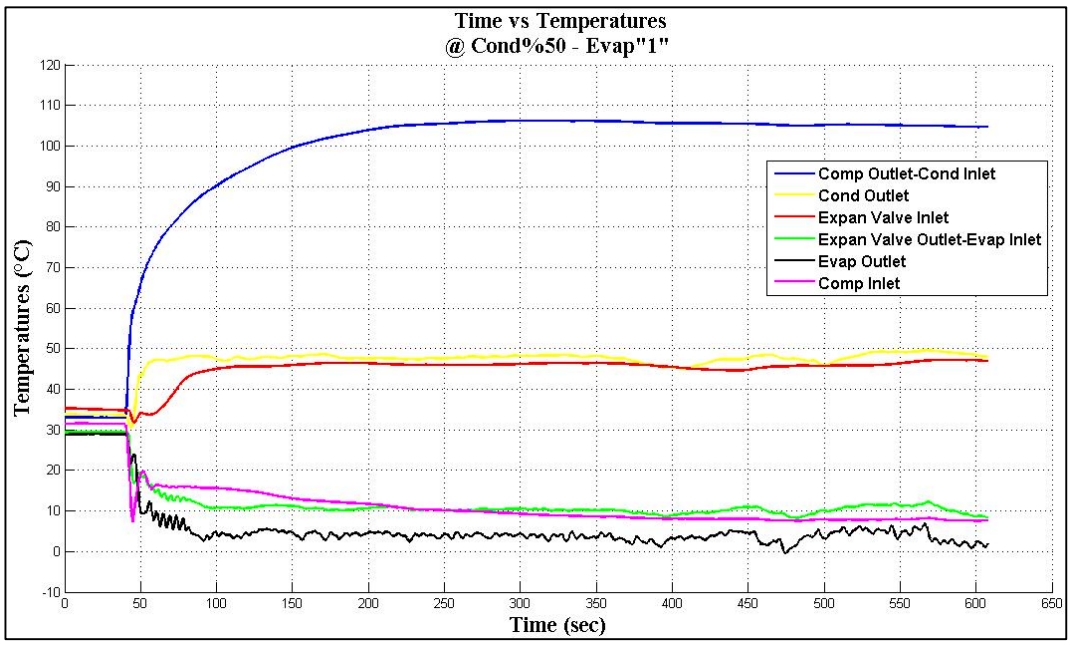

Figure 56 Temperature Measurements - Cond. Fan 50% & Evap. Fan "1"

In the same manner, temperature profiles could be found in figure 56. As it is seen, except for condenser inlet and outlet temperatures, remaining reach the steady state conditions at around 100 seconds. However, reaching the steady state for condenser inlet and outlet temperatures takes 200 sec. more time. Comparing the pressure characteristics of same points, these attitudes might be caused by the heat transfer to/from surroundings on the connection hoses, which are not indeed insulated. For clarification, pressure and temperature measurement points for inlet and outlet of the compressor were other tips of the hoses. Indeed, the reason could be observed from the characteristics of evaporator outlet and compressor inlet temperatures. In detail, there was 3 meters long hose connecting the evaporator and compressor which was not insulated. As seen from figure 56, temperature at the compressor inlet is higher than that of evaporator outlet, proving that there was heat transfer from surroundings to the hose.

Moreover, evaporator outlet temperature has wavier steady characteristic than others. As seen in figure 56, evaporator outlet temperature is fluctuating around 4-6 °C compared to that of other points, while being 0 °C at around 475 seconds, which is indeed instantaneous, being neglected. The most possible root cause for this behavior might be the effort of the expansion valve to adjust amount of liquid-vapor mixture inlet to the evaporator coils, which indeed affects considerably the evaporator outlet temperature while being incorporated with refrigerant phase change. Similarly, same wavy behavior could be seen at expansion valve outlet temperature as well.

For the mass flow rate measurements, below figure 57 shows the particular liquid and vapor mass flow rate, measured at the outlet of the condenser and at the inlet of compressor respectively. As seen, there are lot of fluctuations at the beginning of test up until at 100 sec. After that time, average steady state vapor mass flow rate is around 0.0385 kg/s while average steady state liquid mass is around 0.0375 kg/s. Indeed, since mass flow rates were recorded by a camera and matched with pressure-temperature values manually by user, they indicate step characteristics through the steady state operation.

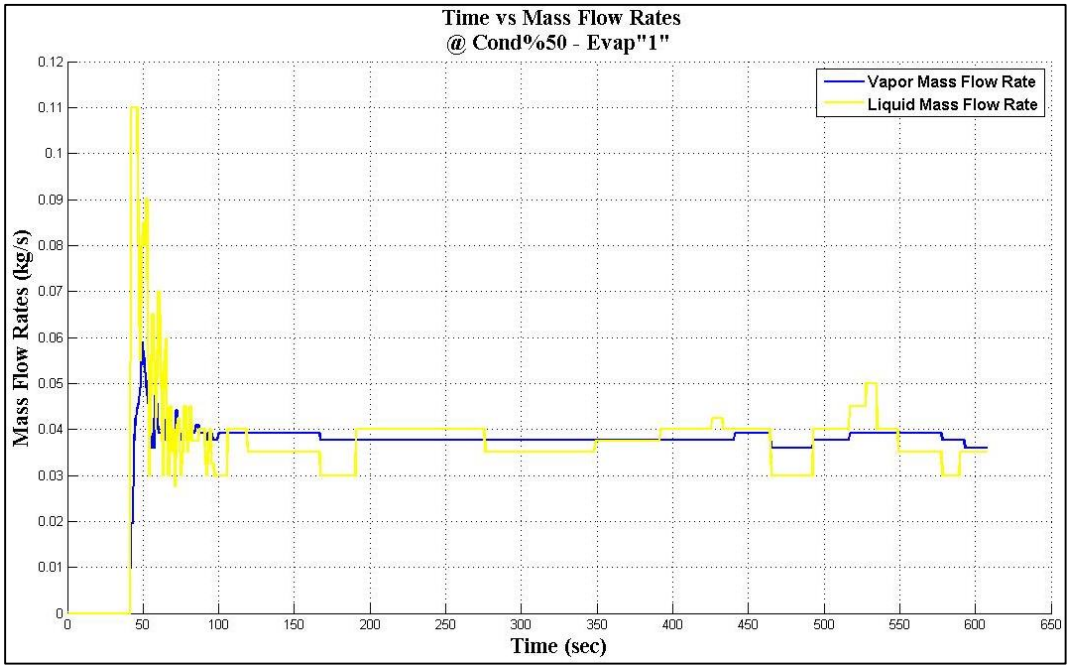

Figure 57 Mass Flow Rate Measurements - Cond. Fan 50% & Evap. Fan "1"

For the performance consideration, below figure 58 clarifies behaviors of the condenser heat rejection rate, evaporator cooling capacity and compressor work graphics, obtained by using formulas (8), (9) and (10). For the condenser heat rejection and evaporator cooling capacity, average of the vapor and liquid mass flow rates is considered since both components experience vapor and liquid flow through the cycle. Similarly, the compressor work is calculated by occupying again average of the vapor and liquid mass flow rates. Hence, characteristics of condenser heat rejection, evaporator cooling capacity and compressor work curves are almost similar and reflecting the behavior of the average of liquid and vapor mass flow rate curves. As seen figure 58, condenser heat rejection rate and evaporator cooling capacity are at around 8.2 kW and 5.3 kW respectively, and compressor work floats around 2.9 kW as well. Furthermore, similar to the behavior of pressure and temperature plot at the inlet/outlet of evaporator and condenser, heat values also reach steady state at around 100 seconds. Besides, considering the time for inlet/outlet compressor temperatures to reach steady state operation as at 300 sec., work curve also indicates same behavior with the temperatures rather than that of pressure values even if they reach steady state operation much earlier.

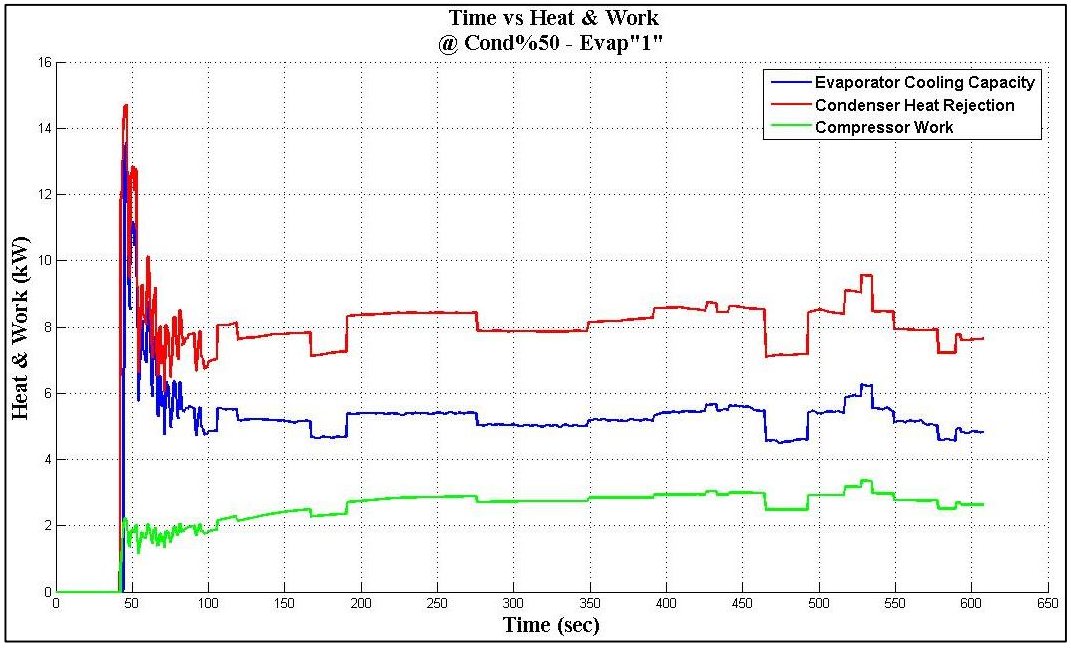

Figure 58 Heat & Work Calculations - Cond. Fan 50% & Evap. Fan "1"

3.3.2. Cond. Fan 50% & Evap. Fan “2”

For Cond. Fan 50% & Evap. Fan “2” test, fan switch on the A/C control unit was set to “2” in order to change the volumetric air flow rate through the evaporator module while keeping the condenser fan setting same with previous as 50%. In this condition, condenser side outlet air velocity remained same as 12.5-14.5 m/s while air velocity coming from the evaporator increased to 21-22 m/s. The test was performed about 15 min. and recorded values is as following.

As it is seen from figure 59, after A/C switch was set to ON, meaning that compressor was engaged, cycle tried to reach steady state operation at 100 seconds. However, high side pressures continued to increase by 100 kPa until 150 sec. and then decreased by same value at 250 seconds. Same behaviors could be seen at low side pressures as well at around 125 seconds. The possible reason for this behavior is that the evaporator air velocity is increased, which is increasing the load on the evaporator, while that of condenser remains same. While the pressure on the evaporator tries to be low, condenser cannot support that attitude and remains at relatively pressure high. To balance the increasing pressure on the evaporator at 125 sec., condenser reacts to increase its pressure until 150 sec. When the evaporator pressure reaches wavy steady operation condition at around 250 seconds, condenser still tries to cover up the pressure to its steady state condition. Finally, condenser reaches it wavy steady state operation at 400 seconds, which is 150 seconds after evaporator does. As it could be understood, the load increase on the evaporator starts some successive pressure fluctuations on both itself and condenser. When the pressure on the evaporator starts to increase, condenser reacts after 25 seconds. For the cover up period, pressure on the condenser settles down 150 seconds later when evaporator pressure reaches steady state condition.

For steady state operation, pressure oscillations, i.e. at compressor outlet, on the high pressure side are around 25 kPa. Also, pressure drop on the condenser and evaporator are same with previous as 75 kPa and 150 kPa in average respectively.

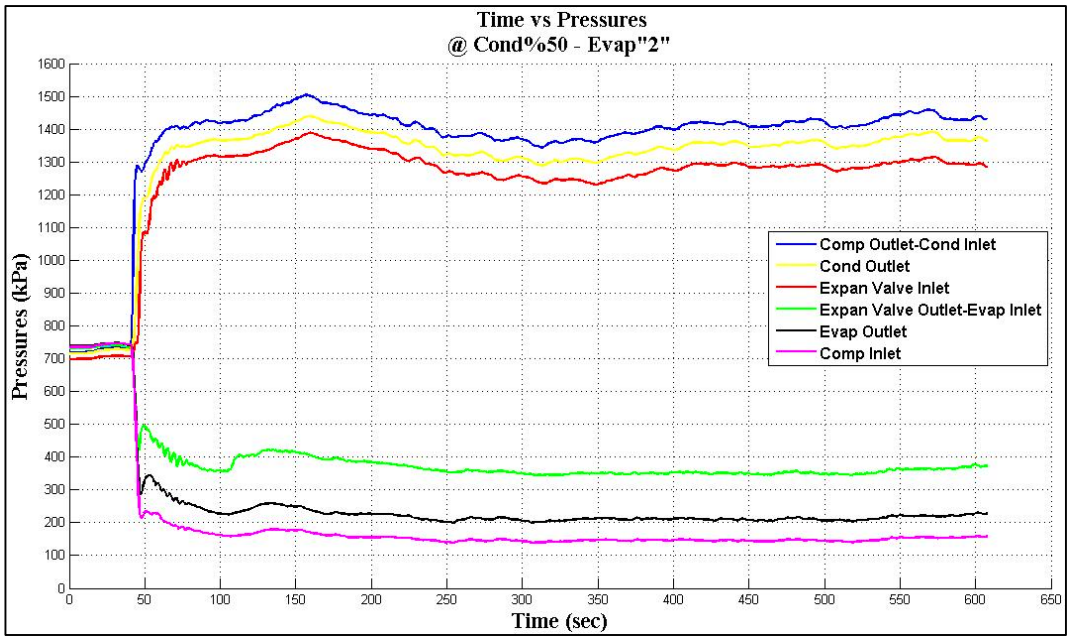

Figure 59 Pressure Measurements - Cond. Fan 50% & Evap. Fan "2"

For temperature measurements, same behaviors with previous test can also be observed as while compressor inlet/outlet temperatures reaches steady state at 300 seconds while remaining settle down at around 100 seconds as seen from figure 60.

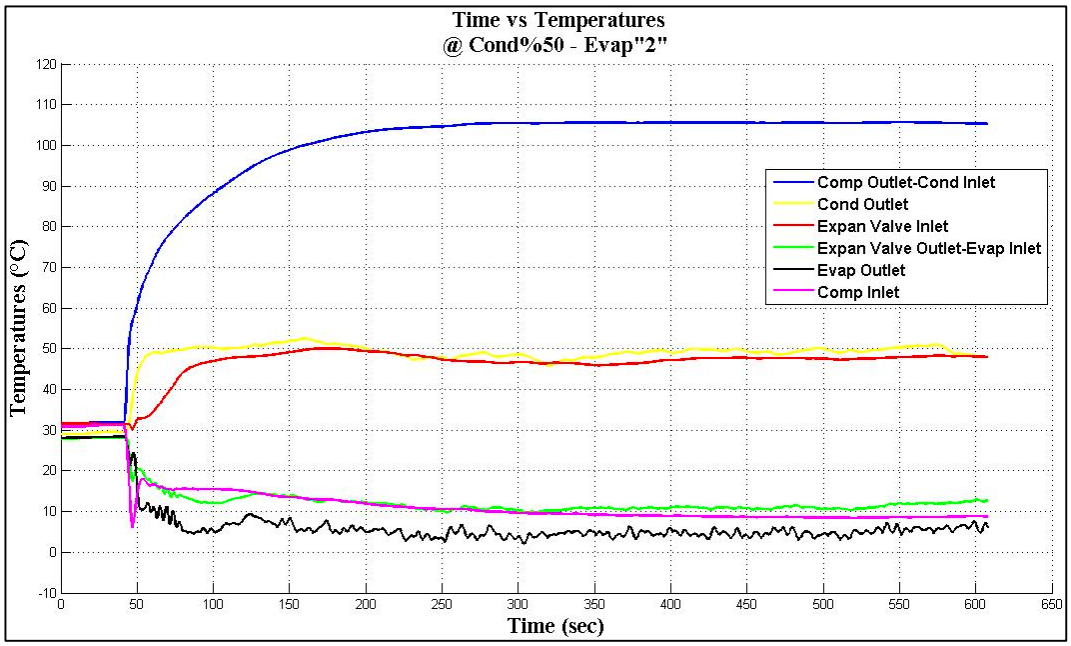

Figure 60 Temperature Measurements - Cond. Fan 50% & Evap. Fan "2"

Also, much waiver temperature characteristic at the inlet/outlet of evaporator are observed also for this test. Due to changing of expansion valve openings with regarding instantaneous phase change of the refrigerant, temperature fluctuations with shorter period could be seen for mentioned points.

For particular mass flow rates seen on figure 61, vapor mass flow rate shows fluctuations for start-up and seems to reaches it steady state at 100 seconds. On the other hand, liquid mass flow rate pretends to reach steady state at 100 seconds; however, some flow oscillations again start up until 125 seconds. Indeed, fluctuations on pressures could be directly linked to that behavior as the rapid pressure increments on the evaporator might result in sudden liquid mass flow rate decrease in the interval of 100 – 125 seconds. For average values flow rates, vapor mass flow rate is around 0.039 kg/s while liquid mass flow rate is fluctuating around 0.04 kg/s for steady state operation.

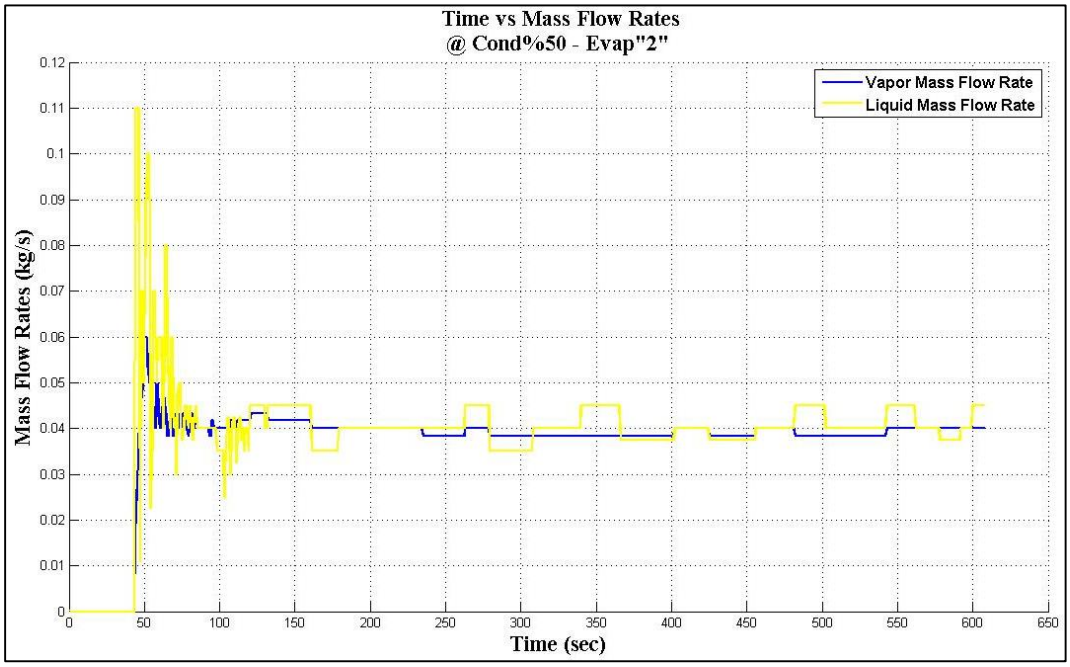

Figure 61 Mass Flow Rate Measurements - Cond. Fan 50% & Evap. Fan "2"

As coming up to performance of the test, condenser heat rejection, evaporator cooling capacity and compressor work behaviors could be seen in figure 62. In details, since the condenser heat rejection and evaporator cooling capacity calculations use the average of liquid and mass flow rates, both show the similar behaviors with the relevant flow characteristics. For the period of start-up, both seem to reach steady state operation condition as of 100 seconds. However, sudden liquid mass flow rate decrease due to abrupt pressure increase on the evaporator side directly affects the heat plots as well. Indeed, similar behavior with liquid mass flow rate graph could also be seen for condenser heat rejection and evaporator cooling capacity in the interval of 100 – 125 seconds. Furthermore, in the consideration of wavy steady state after 150 seconds, as step view of plots, condenser heat rejection and evaporator cooling capacity floats around 8.4 and 5.4 kW in average respectively. In addition to those, compressor work also indicates the similar plot characteristics with average of liquid and vapor mass flow rates. Besides, similar to previous test, compressor work reaches its steady state at around 300 seconds which is resulted from compressor inlet/outlet temperature characteristics. Also, average compressor work after that time could be seen as 3.0 kW in average.

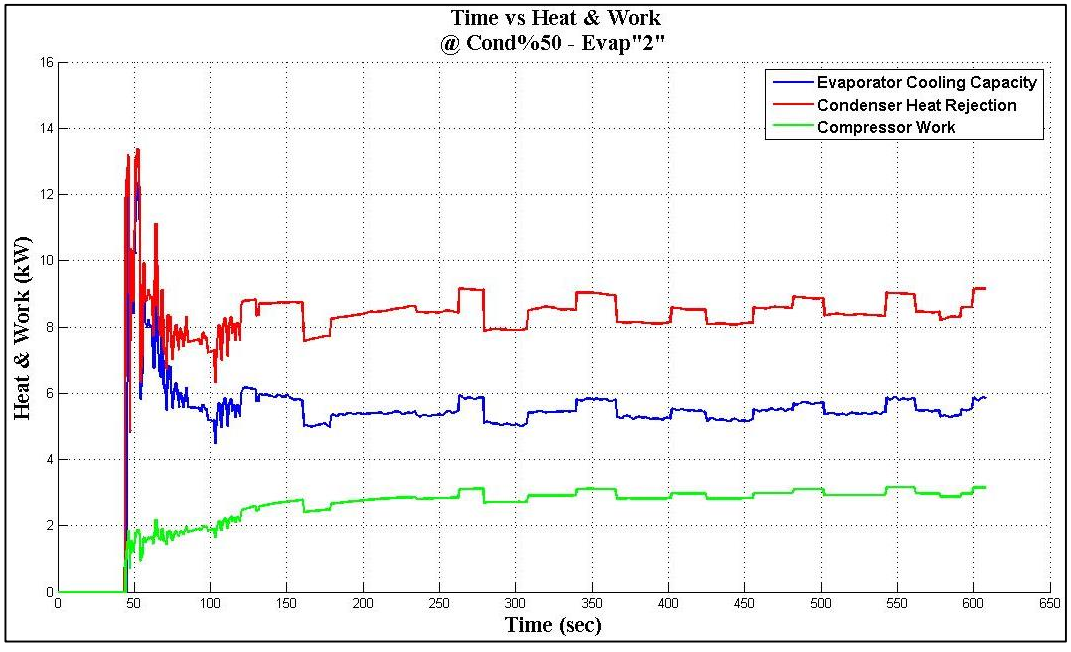

Figure 62 Heat & Work Calculations - Cond. Fan 50% & Evap. Fan "2"

3.3.3. Cond. Fan 50% & Evap. Fan “3”

For Cond. Fan 50% & Evap. Fan “3”, evaporator fan switch was set to ”3” in order to change the volumetric air flow rate through evaporator side by changing the air velocity coming from evaporator to 25-26 m/s. Similarly, condenser fan switch remained as same on %50 supplying 12.5-14.5 m/s air velocity at the outlet of the condenser. Additionally, test was performed about 20 min. along with the following recoded variables.

As seen from figure 63, after reaching the steady state operation at around 100 sec., both high and low pressure sides start to oscillate with considerably high periods through the end of the test. At the first sight, period for high pressure side is around 300 seconds with 100 kPa pressure amplitudes while low pressure side shows oscillations in the same interval with relatively low amplitudes as 25 kPa. Indeed, both sides also include small wavy fluctuations embedded in bigger cycle oscillations, which is probably due to compressor characteristic to be clarified in further sections.

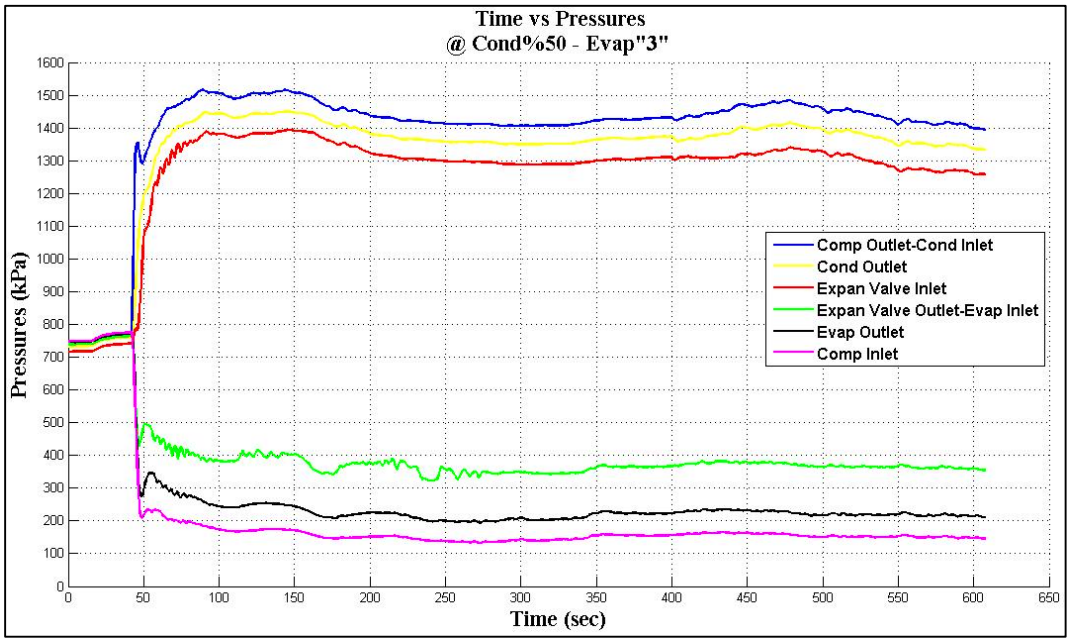

Figure 63 Pressure Measurements - Cond. Fan 50% & Evap. Fan “3”

Indeed, as the air velocity through the evaporator is increased thus increasing heat load on the evaporator while keeping the condenser load same, oscillations on the high and low pressure side, especially on high pressure side, become more clear. Considering the three tests above, pressure oscillations on the high pressure sides, also including small wavy fluctuations become more visible as from straight line to oscillatory behaviors. In addition to those, small wavy fluctuations existing in pressure line, i.e. compressor outlet, are around 15-20 kPa. Also, pressure drops through the condenser and evaporator are nearly same with previous tests as 75 kPa and 150 kPa in average respectively.

For temperature measurements in figure 64, reaching the steady state operation for compressor inlet/outlet temperatures again needs more time by comparing the remaining components as 200 seconds delay. Furthermore, more visible oscillatory behaviors could also be seen for the temperature plots of condenser outlet-expansion valve inlet and evaporator inlet-outlet with periods of around 300 seconds. Furthermore, along with the cycle oscillatory behavior on the evaporator, waiver fluctuations compared to the other components for temperature characteristic at the inlet/outlet points could again be observed as similar to the previous tests.

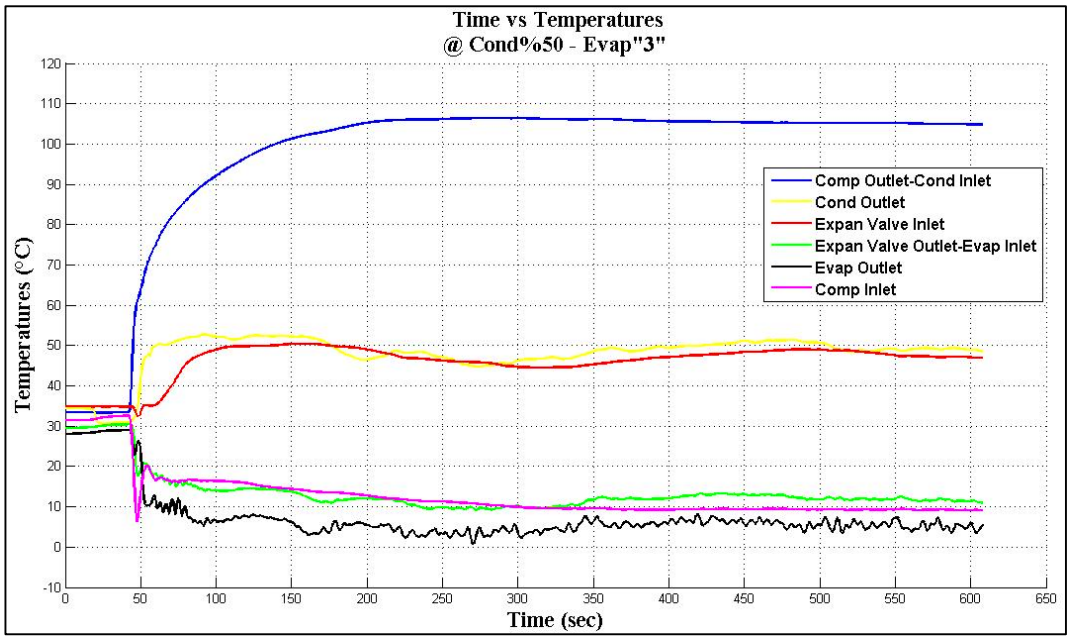

Figure 64 Temperature Measurements - Cond. Fan 50% & Evap. Fan "3"

For the mass flow rate measurements in figure 65, there is no remarkable change compared to the previous tests. As it is seen, both vapor and liquid mass flow rates reach steady state operation at around 100 seconds and oscillating in linear manner since pressure differences on the measurement points remain same although particular pressures show oscillatory behaviors. Furthermore for steady state operation, vapor mass flow rate is around 0.038 kg/s while liquid mass flow rate is about 0.0375 kg/s. Indeed, as the load on the evaporator is increased, it can be roughly said that vapor mass flow rate remains constant at 0.038 kg/s while liquid mass flow rate is fluctuating around 0.0375 kg/s.

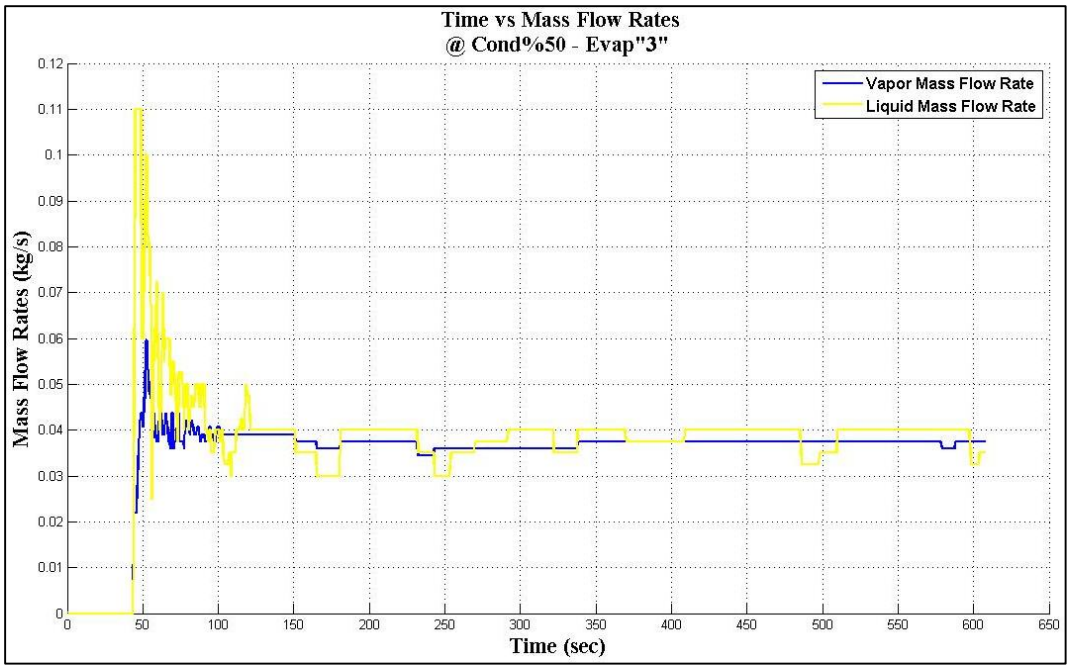

Figure 65 Mass Flow Rate Measurements - Cond. Fan 50% & Evap. Fan "3"

For performance characteristic of the related test in figure 66, time to reach steady state condition for compressor work is a bit late due to more time needed by the compressor inlet/outlet temperatures to reach to steady state operation. As it is seen from figure 66, condenser heat rejection and evaporator cooling capacity settle down to steady state operation at around 100 seconds while compressor work needs more time and it reaches to wavy steady state at around 300 seconds. Moreover, since flow in the condenser and evaporator is liquid-vapor mixture as stated previously, condenser heat rejection and evaporator cooling capacity plots show similar behaviors with average of the vapor-liquid plots. Hence, averages of the condenser heat rejection and evaporator cooling capacity are around 8 kW and 5.2 kW in steady state operation. For the compressor work, it also uses the average of liquid and vapor mass flow rates showing similar behavior with them, compressor work indicates more linear manner in steady state operation having 2.9 kW in average. Indeed, there is no such major difference while comparing above three tests in the scope of performance calculations. For the sake of clarification, tabulated results will be presented in the further sections indicating small variations of the plots.

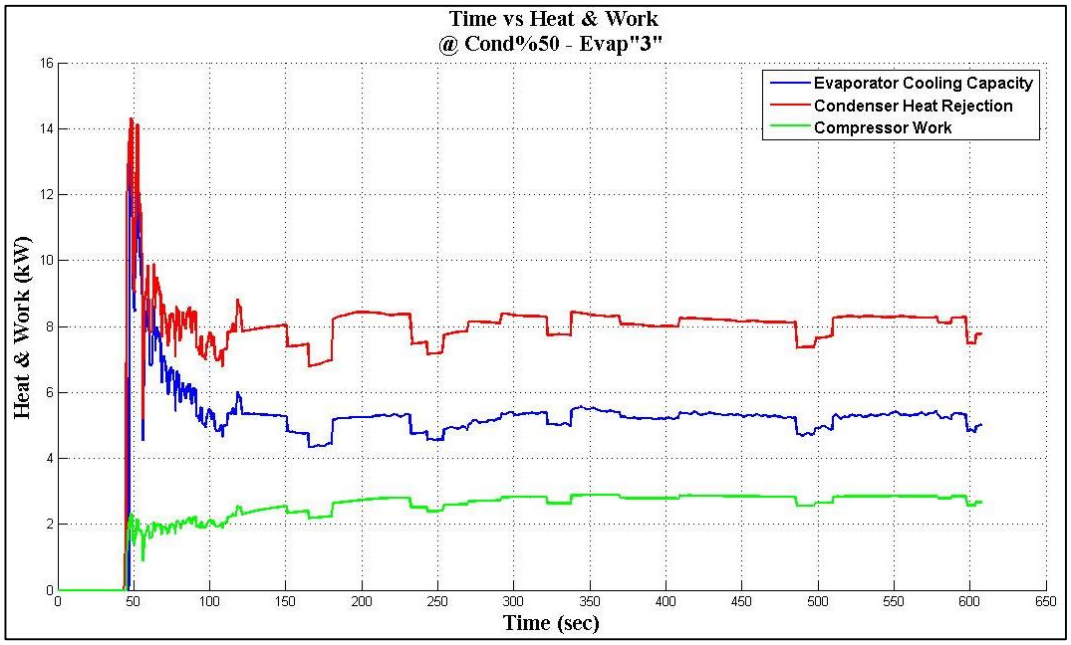

Figure 66 Heat & Work Calculations - Cond. Fan 50% & Evap. Fan "3"

3.3.4. Cond. Fan 100% & Evap. Fan “1”

For Cond. Fan 100% & Evap. Fan “1”, condenser fans were set to maximum speed by adjusting the fan switch position to 100% of maximum. In this case, air velocity coming from condenser was recorded around 19.4-21.8 m/s. Additionally, evaporator fans were set to initial position to “1”, at which the evaporator outlet velocity was around 18-19 m/s. Also, test was performed 15 minutes and the recorded results are as following.

Pressure measurements for the test are presented in figure 67. As it is seen, the cycle reaches quasi steady state around 100 seconds. However, pressures values for high side continue to increase up to 350 seconds with an increase of 100 kPa. On the other hand, low side pressures decrease with 25 kPa up to 350 seconds. After that time, cycle reaches steady state operation condition until the end of the test. Comparing pressure values of the test with Cond. Fan 50% & Evap. Fan “1” test, it can be seen that high pressure side, i.e. compressor outlet pressure, decreases considerably to a steady state value around 1100 kPa which is 250 kPa lower than that of Cond. Fan 50% & Evap. Fan “1”. In addition, low pressure side, i.e. compressor inlet, is 50 kPa lower than that of mentioned test.

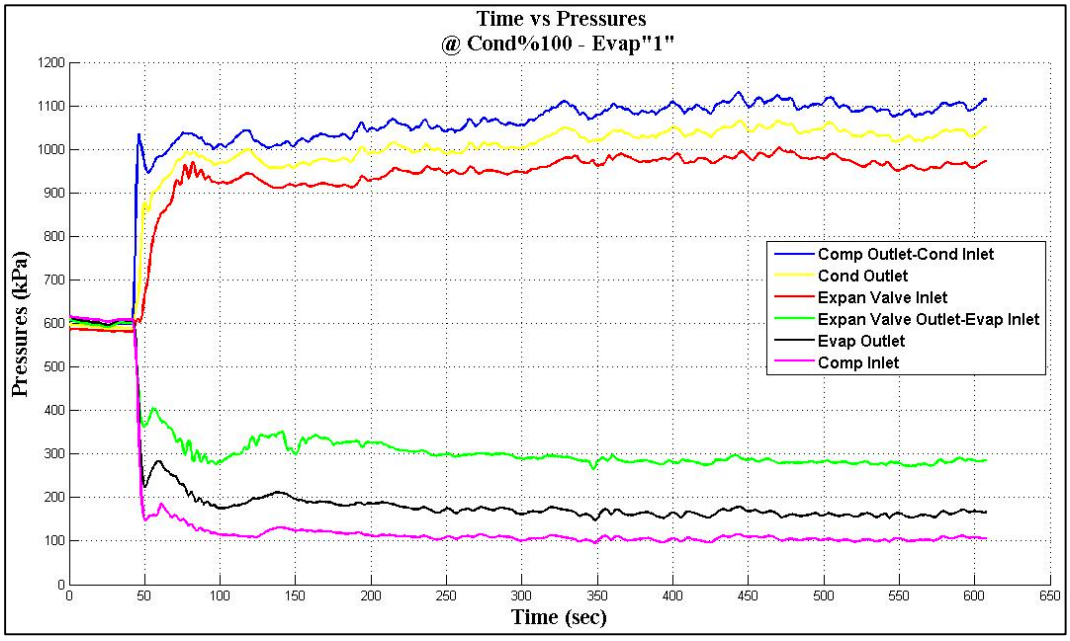

Figure 67 Pressure Measurements - Cond. Fan 100% & Evap. Fan “1”

Indeed, it can be said that increasing the condenser air velocity provides mentioned pressure drops above on the cycle as expected since condenser is able to provide more heat rejection with increasing air side volumetric flow rate. Furthermore, fluctuation in the steady state operation for high pressure side is around 25 kPa while low pressure side experiences about 10 kPa fluctuations instantaneously. Also, pressure drops in the condenser and evaporator are around 50 kPa and 125 kPa in average respectively. Indeed, since both pressure gradient seems to be lower than that of Cond. Fan 100% & Evap. Fan "1" test, lower mass flow rates for both liquid and vapor phases can be expected as well.

For temperature measurements in figure 68, cycle seems to reach steady state at around 100 seconds except compressor inlet/outlet temperatures, similar with previous tests. However, while compressor inlet temperature reaches steady state at around 300 sec., compressor outlet temperature continues to increase up to 450 second. In fact, non-isolated connection hoses between compressor and remaining components of the system might probably be the cause of that behavior as stated previously. Also, comparably high amplitude fluctuations in the inlet/outlet of the evaporator can be observed in the steady state operation period.

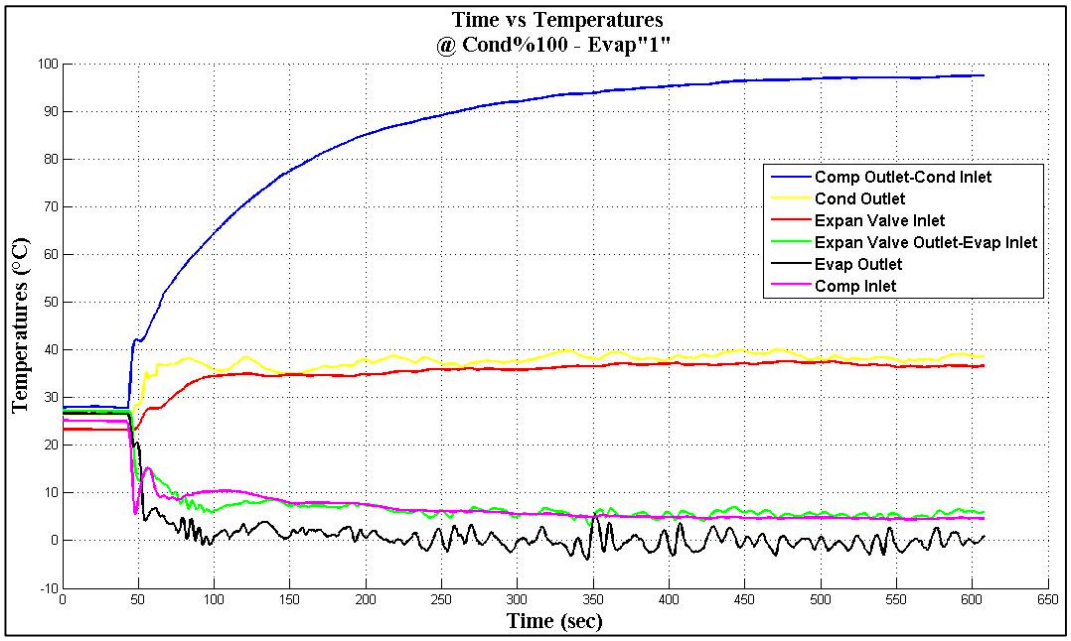

Figure 68 Temperature Measurements - Cond. Fan 100% & Evap. Fan "1"

For the particular mass flow rate seen in figure 69, vapor mass flow rate is around 0.037 kg/s while liquid mass flow rate is about 0.03 kg/s in average for steady state operation. As stated previously, since the pressure differences in the both condenser and evaporator are low compared to the previous tests stated above, it is expected that the particular mass flow rates for liquid and vapor phase should also be lower than that of previous tests. The reason for this idea comes from the relation between mass flow rate and pressure difference. Indeed, since the pressure difference in a system is the driving force to enforce mass flow rate to increase or decrease. As the pressure difference in a component, i.e. condenser or evaporator in this case, increases, it is expected that the mass flow rate is to increase in the same manner. Vice versa is also correct for the statement. Indeed, comparing the results of Cond. Fan 100% & Evap. Fan "1" and Cond. Fan 50% & Evap. Fan "1" tests, proportional relation between pressure difference and mass flow rate can be proven.

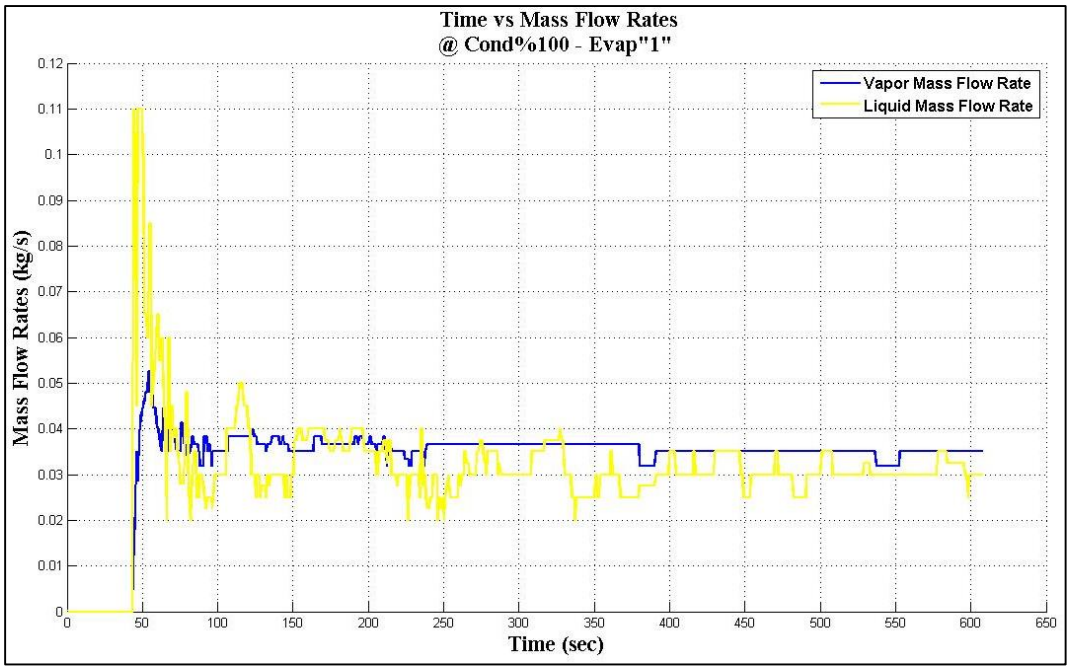

Figure 69 Mass Flow Rate Measurements - Cond. Fan 100% & Evap. Fan "1"

For performance variables of the test seen in figure 70, condenser heat rejection and evaporator cooling capacity seem to reach steady state operation at around 100 seconds. Indeed, oscillatory behavior in the interval 100 sec. to 300 sec. is most probably due to the oscillatory behavior of liquid mass flow rate experienced. Since both condenser heat rejection and evaporator cooling capacity is occupied with the average of the vapor and liquid mass flow rate, both plot show the characteristics of the liquid phase mass flow. In details, condenser heat rejection rate can be seen at around 7.5 kW in average and evaporator has 4.9 kW cooling capacity in average for steady state operation. In addition, compressor work reaches steady state at around 350 seconds as similar behavior seen in previous tests. Indeed, since the increase in temperature of the compressor outlet lasts up to 450 seconds while compressor inlet temperature reaches steady state at around 300 seconds, it can be obviously considered that compressor work behavior is directly related with compressor inlet/outlet temperatures. Also, compressor work shows the characteristic of vapor mass flow rate in steady state operation as from 350 second to 600 seconds. In details, compressor work could be taken as around 2.2 kW in average during the steady state operation.

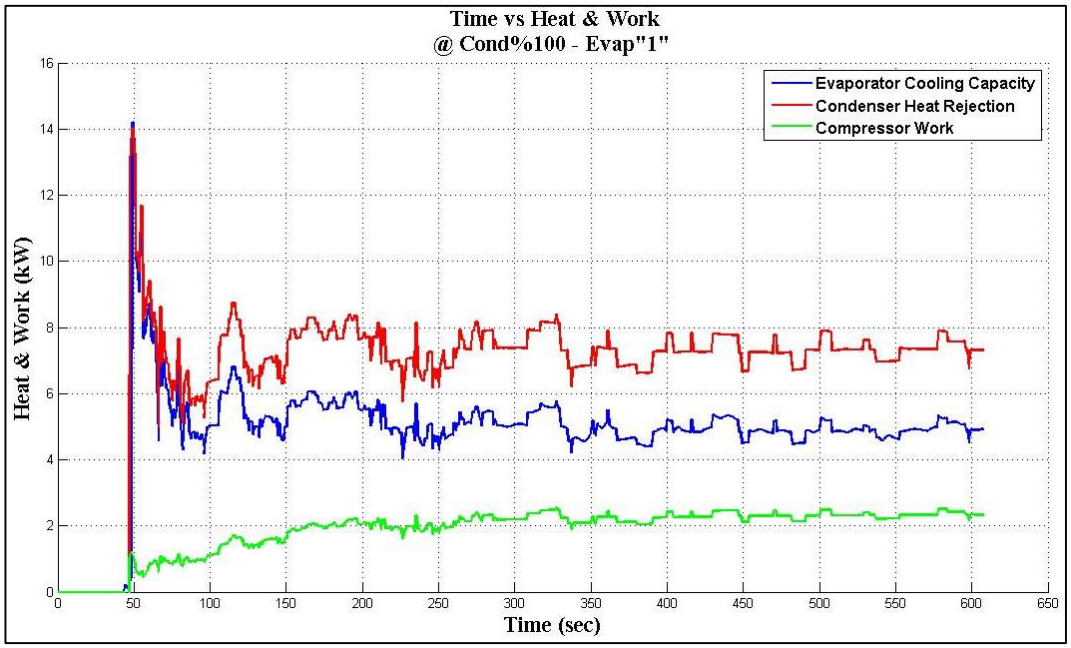

Figure 70 Heat & Work Calculations - Cond. Fan 100% & Evap. Fan "1"

3.3.5. Cond. Fan 100% & Evap. Fan “2”

For Cond. Fan 100% & Evap. Fan “2” test, evaporator fan switch was set to “2”, which increased the air outlet velocity from evaporator blowers by providing 21-22 m/s air velocity while condenser fans remained at %100 of maximum speed which supplied 19.4-21.8 m/s outlet air velocity on the condenser. The test was performed about 20 min. with presented results below.

In figure 71, pressure values for the high side and low side could be seen accordingly. Firstly, upon completion of the start-up duration up until 100 seconds, the pressure values tries to float around a certain value of a steady state operation. For the time interval of 100-150 seconds, both high and low pressure values decreases by 150 kPa and 25 kPa respectively. After 150 seconds, the system settle downs an oscillatory steady state operation with certain fluctuation periods. For the case, periods for both high and low pressure sides seem very same as around 225 seconds. Also, each pressure line shows internally wavy operation throughout the test, which are 20 kPa average for high pressure side and 10 kPa average for low pressure side.

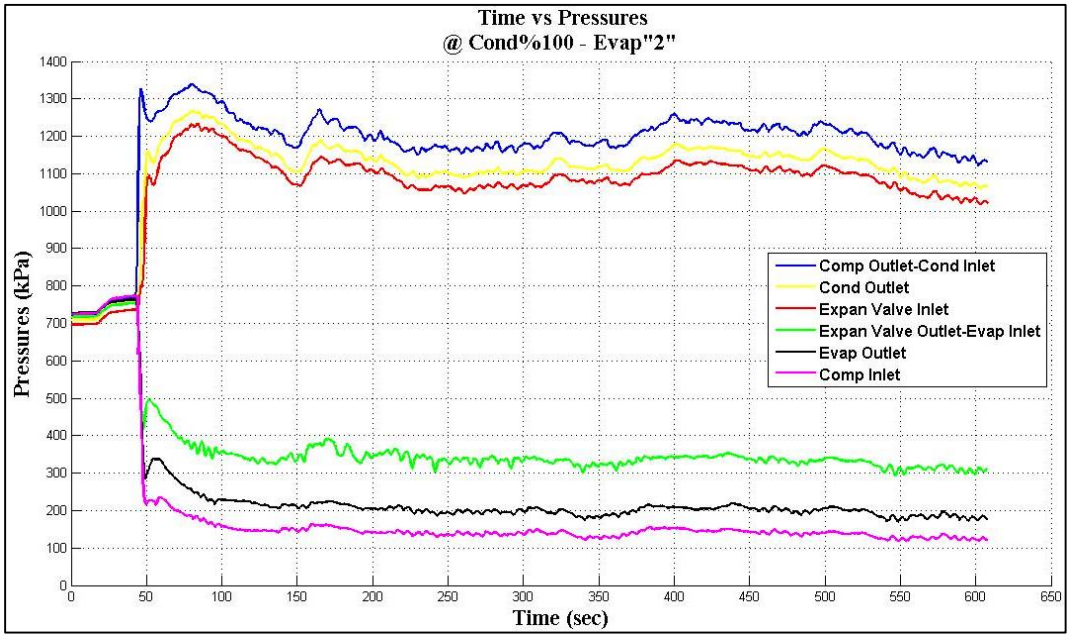

Figure 71 Pressure Measurements - Cond. Fan 100% & Evap. Fan “2”

Furthermore, comparing with the test “Cond. Fan 100% & Evap. Fan “1”, it can be found that as the load on the evaporator is increase by increasing the volumetric air flow rate through evaporator itself, pressures of both high and low side increases by 80 kPa and 50 kPa in average respectively. Also, an argument coming from the first three tests with condenser fan 50%, that is oscillations in the pressure plots become more visible when the evaporator outlet air velocity is increased, could also be agreed again. For the tests with condenser fan 100%, it is seen that system level oscillation is almost undetectable when evaporator fan set is “1”. When evaporator fan set is “2”, formless system level oscillations could be seen. Hence, it can be expected more regular oscillations when evaporator fan is set to position “3”.

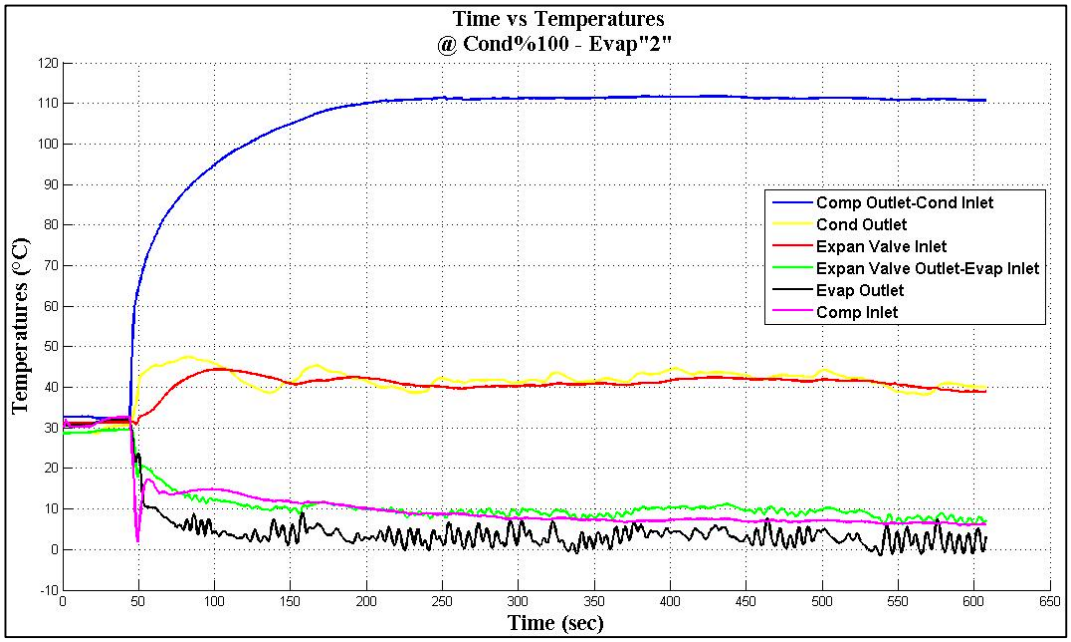

Figure 72 Temperature Measurements - Cond. Fan 100% & Evap. Fan “2”

For temperature measurement above in figure 72, the cycle reaches steady state operation at around 100 seconds except compressor inlet/outlet temperatures. Indeed, this behavior has been seen in all tests performed previously. For the compressor, both inlet and outlet temperatures settle down to steady state operation at about 250-300 seconds. For compressor inlet temperature, times to reach for steady state operation seem more or less similar with previous tests; however, compressor outlet temperature reaches steady state operation too early when the evaporator air outlet velocity is increased by comparing condenser fan 100% with evaporator fan test “1” and “2”.

Moreover, as encountered in previous four tests, relatively high amplitude fluctuations in the evaporator inlet/outlet temperatures also exist for this test. Indeed, fluctuations amplitude in evaporator outlet temperature is around 5-6 °C in average whereas evaporator inlet shows 1-2 °C temperature fluctuations.

For the mass flow rate in figure 73, both liquid and vapor mass flow rates seem to reach steady state operation at around 100 seconds. For the steady state, vapor mass flow rate is around 0.037 kg/s while liquid mass flow rate is floating around 0.035 in average. Additionally, both present oscillatory behaviors, including still small wavy fluctuations, during the steady state operation. Indeed, liquid mass flow rate oscillates having 0.02 kg/s amplitude with 100 seconds period while vapor mass flow rate is around 0.005 kg/s amplitude with 50 seconds at the first 250 seconds of steady state operation. After that time, amplitudes decrease to 0.005 kg/s for liquid phase and 0.002 for vapor phase while periods for both seem to remain same as 100 seconds.

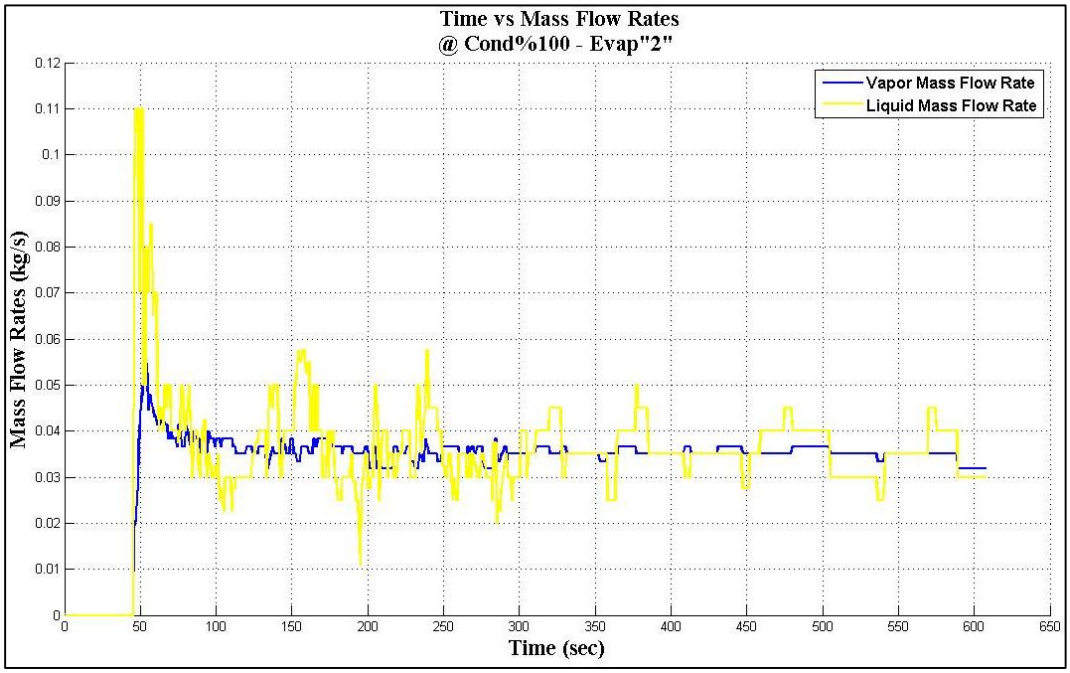

Figure 73 Mass Flow Rate Measurements - Cond. Fan 100% & Evap. Fan "2"

Indeed, the most possible reason for high amplitude mass flow rate oscillations in the beginning of steady state operation is the pressure oscillations for the same time interval seen in figure 71. Indeed, pressures should be separated into two different zones. What is understood from the results by regarding the different amplitudes in oscillations for liquid and vapor mass flow rates is that high pressure side seems to affect the behavior of liquid mass flow while low pressure side indeed has an impact on vapor mass flow rate. In details, amplitude of the system level oscillations in the high pressure side is much bigger than that of low pressure side as in the case of differences in the oscillation amplitudes of mass flow rates. When the high side pressures change around 100 kPa, low pressure side shows 10-15 kPa changes. Comparably, liquid mass flow rate changes by 0.02 kg/s when vapor mass flow rate floats with 0.005 kg/s. In addition to that, receiver dryer pretends as a reservoir which suppresses the high pressure oscillations coming from the high pressure side to affect the low pressure side. This effect of receiver dryer can be also seen on the behaviors of liquid and vapor mass flow rates.

For performance variables of the test seen in figure 74, condenser heat rejection and evaporator cooling capacity reach to steady state operation at around 100 seconds. Since they are calculated along with the average of liquid and vapor mass flow rates, both reflect the characteristics of primarily the liquid mass flow rate during the steady state oscillations. Indeed, if the effect of mass flow rate is removed from the related calculations, it is possible to see plots which are close to straight line, for both heats in steady state operation. The reason is that the temperature and pressure differences separately on condenser and evaporator remain same at any instant during steady state. Moreover, condenser heat rejection is floating around 8.2 kW while evaporator heat rejection is around 5 kW in average during steady state operation. Comparing with the test “Cond. Fan 100% & Evap. Fan “1”, both value seem to increase when the air velocity flowing through the evaporator is increased. Additionally, similar to the previous tests, compressor work can reach steady state operation 200 seconds late. The reason is that even if the compressor inlet/outlet pressures reach steady state at the similar time with other components, compressor inlet/outlet temperatures needs more time to accomplish steady state operation. Hence, this delay directly creates time effect

also on the compressor work to reach to steady state operation comparing with the other variables, i.e. condenser heat rejection. Also, compressor work is calculated by using the average of liquid and vapor mass flow rates, thus showing the similar graphical behavior with it. For steady state operation, compressor work is calculated as around 2.9 kW in average.

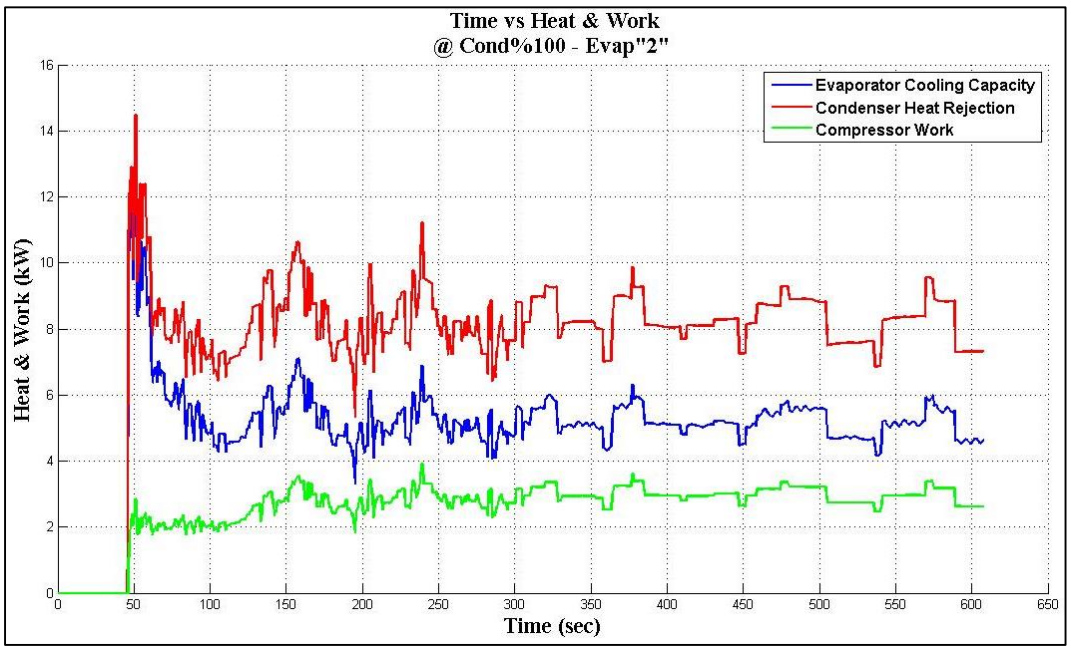

Figure 74 Heat & Work Calculations - Cond. Fan 100% & Evap. Fan "2"

3.3.6. Cond. Fan 100% & Evap. Fan “3”

For Cond. Fan 100% & Evap. Fan “3” test, evaporator fan switch on the A/C control unit was set to position “3”, which increased air velocity at the outlet of the evaporator coil to 25-26 m/s. At the same time, condenser fan was kept at 100% of maximum supplying 19.4-21.8 condenser outlet air velocity as same previous two tests. Meanwhile, test in this configuration was performed about 25 min. and results are as following.

In figure 75, it seems that the cycle reaches to steady state operation at around 150 seconds, which indeed takes a bit longer time compared with previous two tests. After completing start-up period, high pressure side shows more stable and visible oscillations, i.e. compressor outlet pressure, around 1300 kPa. As it is seen in the figure, oscillation occurs in the time interval 275-450 seconds with period of 175 seconds and 25-30 kPa amplitude. Actually, the idea, that is, oscillation on the pressure measurements become more visible as the evaporator air velocity increases, could again be supported by plots in figure 75.

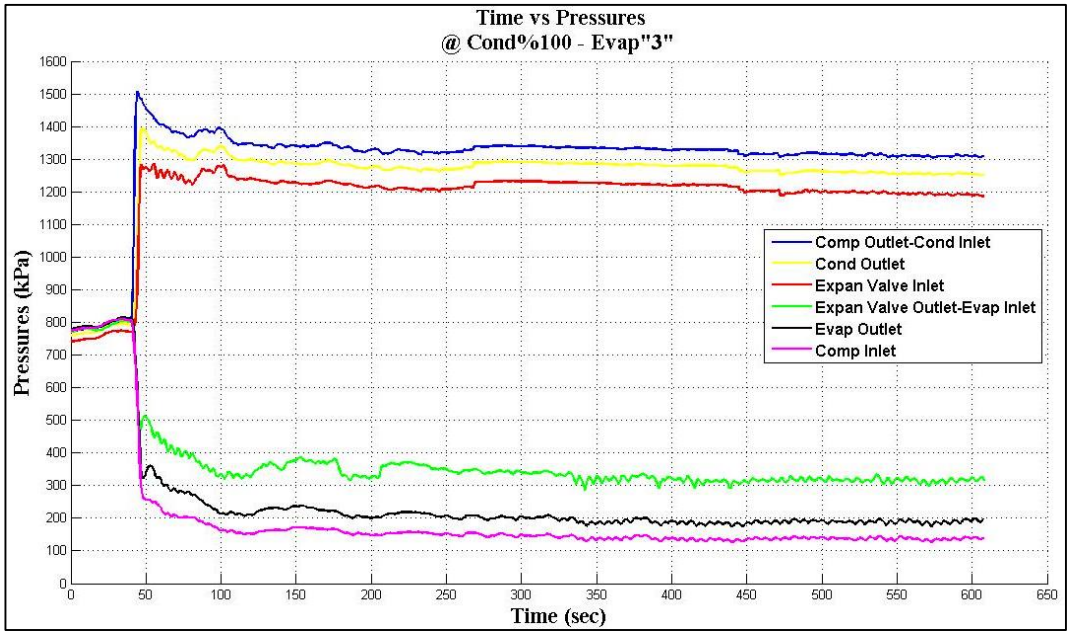

Figure 75 Pressure Measurements - Cond. Fan 100% & Evap. Fan “3”

In addition, pressure plots for both high and low sides oscillate internally with wavy fluctuations through the test and, indeed, periods of these fluctuations decrease through the end of the test. This behavior could be seen more clearly in the plots of low pressure side. In details, amplitude of fluctuations for high side is around 5-8 kPa while that of low side is around 15-20 kPa.

For temperature measurements in figure 76, the cycle seems to reach steady state at around 100-150 seconds while compressor inlet/outlet temperatures show slightly different characteristics. In details, compressor outlet temperature reaches steady state at around 250 seconds while compressor inlet temperature achieves steady state operation at around 350 seconds. In addition, comparably wavy behaviors of evaporator inlet/outlet temperatures could again be observed for the test. Indeed, amplitude of the fluctuations for evaporator inlet and outlet temperatures are around 2 °C and 5-6 °C respectively. Furthermore, decrease in the periods of the evaporator inlet and outlet temperature fluctuations through end of the test as in the interval of 350 to 600 seconds could also be observed as similar with that of in the pressure measurements.

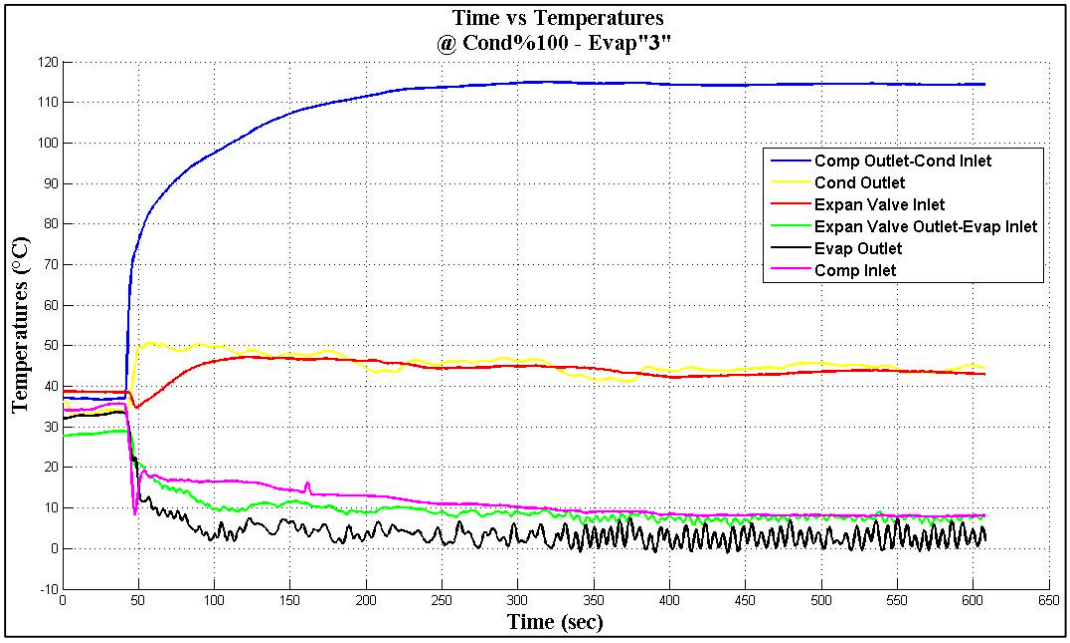

Figure 76 Temperature Measurements - Cond. Fan 100% & Evap. Fan "3

For the mass flow rate measurements below figure 77, vapor mass flow rate reaches steady state operation at around 100 seconds while liquid mass flow rate achieves steady state operation a bit late at 125 seconds. In details, average values of vapor and liquid mass flow rates are 0.03 kg/s and 0.032 kg/s in the steady state operation. Additionally, oscillations in the steady state operation don't seem to exist as in the case of previous test. The possible reason for that behavior comes from the stability of the pressure values through the steady state condition with very low oscillation values. However, there are still internally wavy fluctuations throughout the steady state operation with 0.0025 kg/s for vapor side and 0.005 for liquid side mass flow rate.

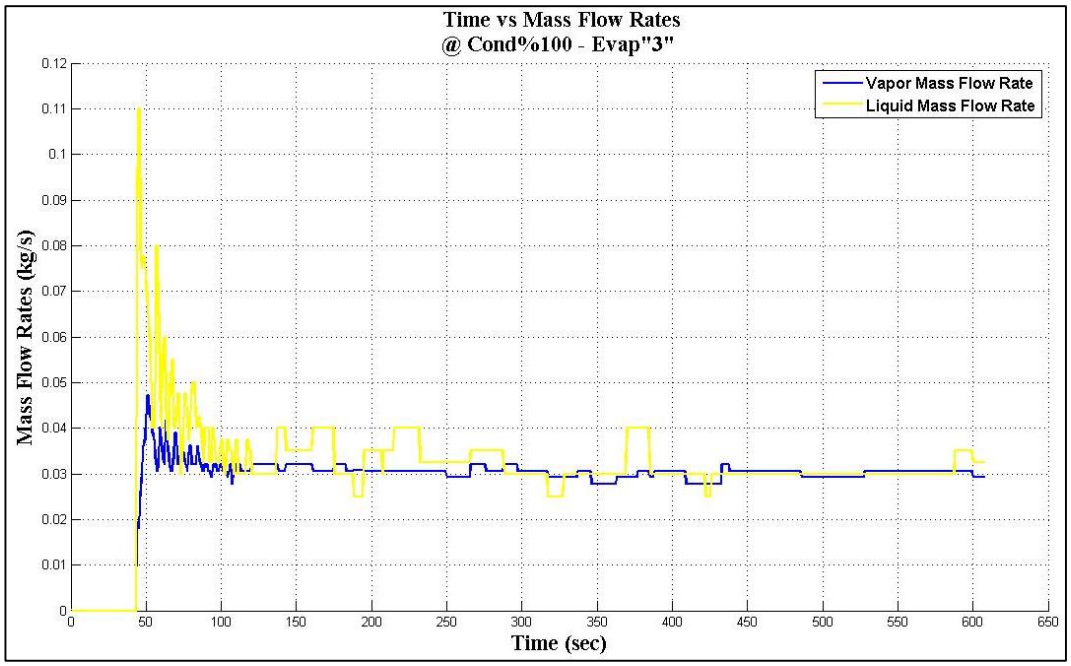

Figure 77 Mass Flow Rate Measurements - Cond. Fan 100% & Evap. Fan "3"

For performance variables of the test in below figure 78, it seems that condenser heat rejection and evaporator cooling capacity reach the steady state conditions at around 125-130 seconds. In addition, both plots show the characteristics of liquid and vapor mass flow rates average curve, which is indeed included in the calculation as similar with previous tests. In details, condenser heat rejection has average value of 7.2 kW for steady state operation while evaporator cooling capacity is around 4.2 kW in average for same period.

Futhermore, compressor work achieves the steady state operation at around 250 seconds due to the late responses of both compressor inlet/outlet temperatures even if the related pressure values reach steady state operation earlier. In details, the average value of compressor work for steady state operation is around 2.6 kW by simply reflecting the behavior of vapor mass flow rate curve. For the comparison purpose with previous test "Cond. Fan 100% & Evap. Fan "2", steady state condenser heat rejection and evaporator cooling capacity seem to decrease by 1 kW in average while compressor work remains at considerably same interval and averagely floats around 2.6 kW.

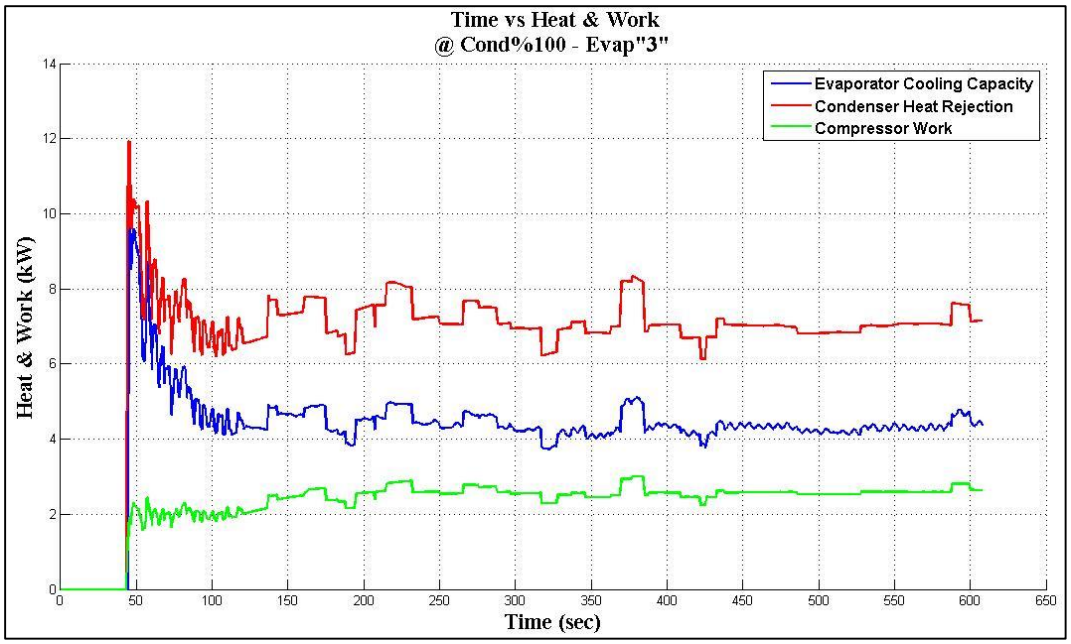

Figure 78 Heat & Work Calculations - Cond. Fan 100% & Evap. Fan "3"

CHAPTER 4

COMPARISON OF THE EXPERIMENT RESULTS

In this chapter, all six experiments are compared according to steady state operation conditions in terms of P-h operation diagram, COPs, volumetric efficiencies, isentropic efficiencies, exergetic efficiencies and finally average steady state performance variables are stated in the relevant evaluation table. Furthermore, performance of the each test configuration is tried to be analyzed in terms of consuming lowest power and supplying highest efficiency values based on the calculated performance variables in order to specify one of the experiment configuration as most prominent among others.

4.1. EXPERIMENTS ON P-h DIAGRAM

After measuring and recording the all temperature and pressure values of the experiments as well as relevant liquid and vapor mass flow rates, below graph is prepared in order to visualize the cycle behavior while changing the heat load on both the condenser and evaporator. For graphical presentation of the refrigeration cycle below figure 79, average values of temperatures and pressures of the experiments in the interval of 200 – 600 seconds are used while taking into account the comments from explanations of each test individually in chapter 3.

As it could be seen in figure 79, all six experiments are located in the P-h diagram of the refrigerant R134a. In details, black line shows the saturation line of R134a and blue tones and brown tones indicate the test configurations as Condenser Fan 50% and Condenser Fan 100% respectively.

At the beginning of the experiments, it was though that evaporator or condenser heat transfer rates could be increased by increasing the air velocity passing through them. However, as getting into details by using below figure 79, it can be seen that increasing the evaporator air velocity while keeping that of condenser same as Cond. Fan 50% & Evap. Fan "1", "2" and "3" tests, heat transfer rates on relevant components do not change considerably. Additionally, increasing the evaporator air velocity causes very low pressure raises on the high pressure side whereas pressure change for the low pressure side of the cycle could even be ignored as it could be understand by following the plots in blue tones. Furthermore, pressure drops in the condenser and evaporator could be assured that pressure drop on the condenser is around 50 kPa while that of evaporator is 150 kPa in average.

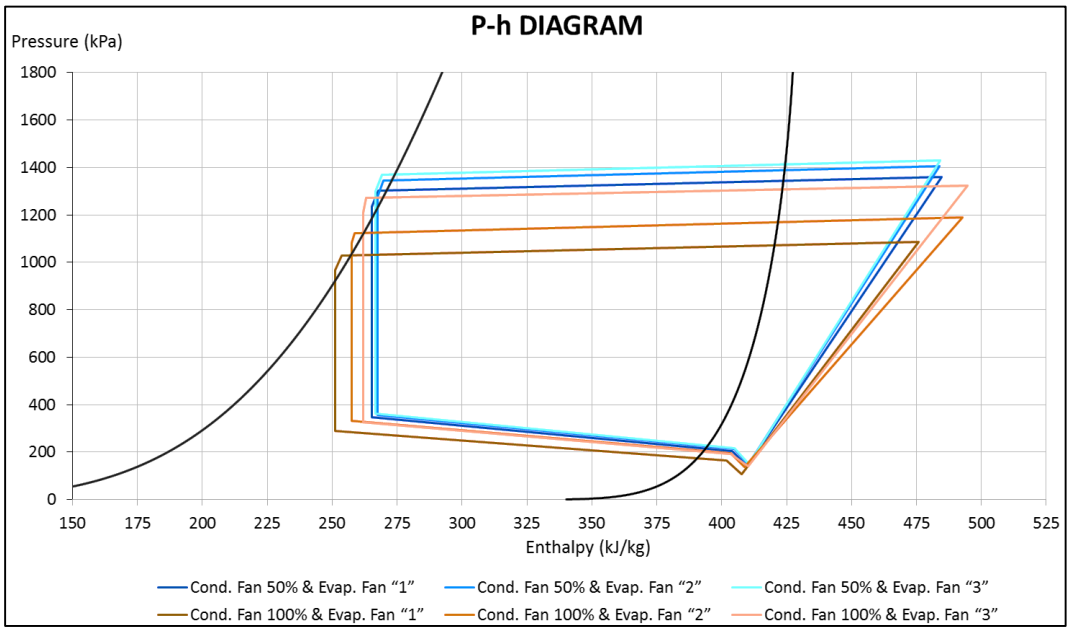

Figure 79 Experiments on P-h Diagram

Similarly, for tests as Cond. Fan 100% & Evap. Fan "1", "2" and "3", it can also be said that evaporator cooling capacities do not change considerably even if in the order of magnitude as 0.5 kW whereas condenser heat rejections show considerably high variations with increasing evaporator air velocity. Passing from "1" to "2", condenser heat rejection shows comparably small amount increase whereas passing from "2" to "3" cause condenser heat rejection rate to decrease. Indeed, change in the both evaporator cooling capacity and condenser heat rejection rates definitely depends on

the liquid and vapor mass flow rates as well. Related results will be indicated in table 10 orderly. In addition, change of the evaporator air velocity in the case of keeping condenser fan at 100% affects the cycle pressures as well if brown tone plots are followed. For the high pressure side, increasing the evaporator air velocity causes higher pressure increases than that of tests of condenser fan at 50%. Indeed, as evaporator fan switch passes from “1” through “3”, high pressure side increases from 1050 kPa to 1300 kPa in average. Controversially, low pressure side seems not to be affected so much, but still shows small amount of increase, by the evaporator air velocity increment. In addition to that, pressure drops on condenser and evaporator still could be seen as 50 kPa and 150 kPa in average for tests of condenser fan at 100%.

For the other side of view as, for example; keeping the evaporator switch at position “1” and changing the condenser air velocity from “50%” to “100%”, low pressure side shows comparably lower decrease as around 50 kPa than that of high pressure side. Moreover, as the evaporator switch is set to “1” through “3”, pressure difference between two tests, i.e. Cond. Fan 50% & Evap. Fan “3” and Cond. Fan 100% & Evap. Fan “3”, decrease up to 10-15 kPa accordingly. On the other side, pressure difference on the high pressure side of the cycle is around 250 kPa for the evaporator switch “1” tests. Similarly, setting the position of evaporator switch from “1” through “3” decreases to pressure difference up to 100 kPa. As expected, condenser fan 100% test pressure values on the high pressures side of the cycle are lower than that of condenser fan 50% tests. Theoretically, as keeping the remaining variables same, increasing the air velocity definitely decreases pressure on the condenser. Although condenser heat rejection for two tests, e.g. Cond. Fan 50% & Evap. Fan “3” and Cond. Fan 100% & Evap. Fan “3”, are 10.48 kW and 9.90 kW in average respectively which could indeed be assumed as same, it could be still said experimentally in figure 79 that, increasing the air velocity passing through the condenser decreases the average pressure value on it even if the condenser heat rejection rates for both tests are very similar as above.

4.2. PERFORMANCE PARAMETERS OF THE EXPERIMENTS

For the COP comparison of six experiments, formula (11) in chapter 2 is used. In details, coefficient of performance is the rate of the cycle providing evaporator cooling capacity with respect to given work to compressor. As it seen in below figure 80, COP values for condenser fan at 50% tests remain almost same as the evaporator air velocity is increased. Referring the table 10, it can be seen that evaporator cooling capacities and compressor works do not show considerable variations over the change of evaporator air velocity. For supporting that COP behavior for three tests of condenser fan at 50% tests, figure 55, 59 and 63 show that there is no significant change on the high and low pressure sides as well. Specific COP values for relevant three tests are 1.85, 1.86 and 1.88 respectively.

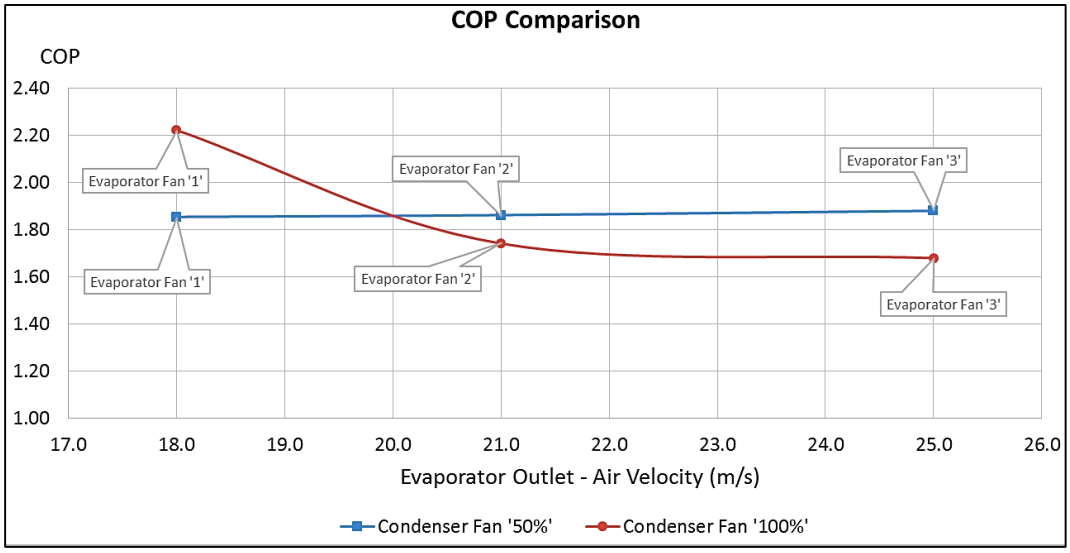

Figure 80 Comparison – COP

On the other hand, COP value is the highest for the Cond. Fan 100% & Evap. Fan "1" test as 2.20 and then decreases to 1.74 for evaporator fan switch on "2" and 1.68 for evaporator fan switch on "3" among condenser fan at 100% tests. Indeed, it can be said that after evaporator fan switch on "2" tests, COP value tends to remain same as the evaporator air velocity increases. In details, compressor work decreases almost 1 kW on each tests while the evaporator cooling capacity increases by 0.12 kW from evaporator fan switch on "1" to "2" and decreases by 0.55 from evaporator fan switch

on “2” to “3” test. Consequently, rate of change of COP values becomes less significant over the change of evaporator air velocity. Additionally, from figure 67, 71 and 75 above, it is observed that high pressure side values increase as the evaporator air velocity increases while low pressure side values experience small amount of increase through three tests accordingly.

For the performance evaluation of all six test in the concept of COP analysis, it seems that Cond. Fan 100% & Evap. Fan “1” is most effective test according to the figure 80 by having COP value as 2.22 stated in table 10. Indeed, this configuration provides considerably same evaporator cooling capacity regarding the remaining tests while requesting minimum power for compressor work.

In figure 81, corresponding compressor volumetric efficiencies of all six experiments could be seen. Related plots are obtained by using formula (6) in chapter 2. For condenser fan at %50 tests, three relevant volumetric efficiencies seem to be almost constant at around 68% in blue plot. Indeed, as stated previously, both high and low side pressure values indicates no remarkable change as the evaporator air velocity increases. Hence, it is expected no visible variations on volumetric efficiencies correspondingly. Besides for condenser fan at 100% tests, volumetric efficiency for evaporator fan switch on “1” is around 66% and then increases to 71.5% for evaporator fan switch on “2”. On the other hand, as the evaporator air velocity increases, volumetric efficiency drops to 69% for evaporator fan switch on “3”. In details, high pressure side values increases as the evaporator air velocity is increased. Similarly, low pressure side also shows low profile increments over the corresponding evaporator air velocity increase. Since the volumetric efficiency is the function of discharge pressure over suction pressure, rate of increase of both high and low pressure side values varies in terms of their corresponding ratios even if both sides show distinctive increases as well.

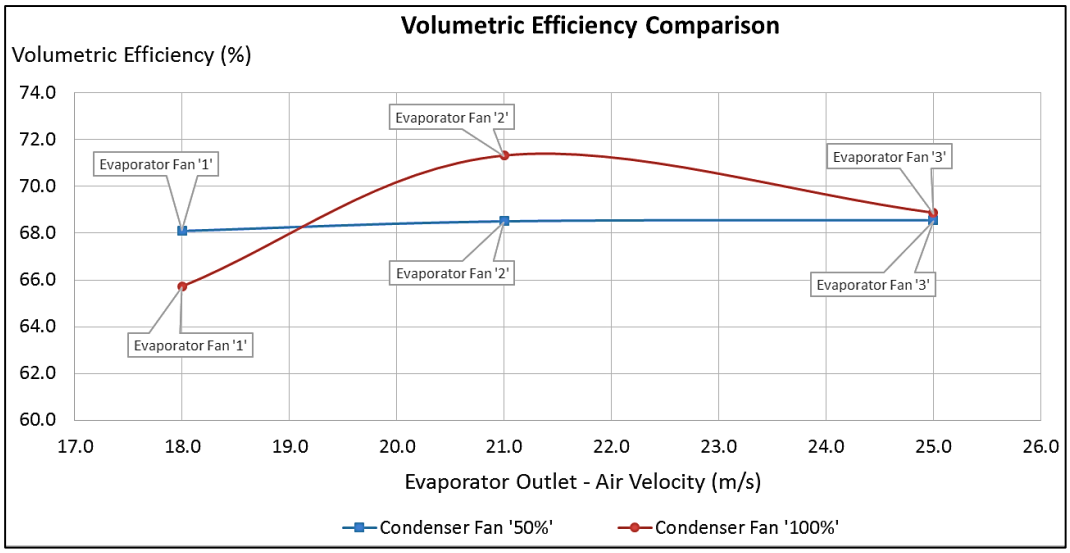

Figure 81 Comparison - Volumetric Efficiency

Furthermore, volumetric efficiency could be directly incorporated with vapor mass flow rates supplied by the compressor itself. Indeed, considering the mass flow rate formula (5) in chapter 2 and the plots in the figure 81, it could be expected that average vapor mass flow rates of condenser fan at 50% tests would not vary considerably and shows similar behavior with its volumetric efficiency plot with blue color. Indeed, if the vapor mass flow rate values in table 10 are checked, it is seen that vapor mass flow rates are increasing having low increase rate correspondingly. Similarly, behaviors of vapor mass flow rates for condenser fan at 100% tests in table 10 are same with the graphical representation with brown color as they decrease with respect to corresponding volumetric efficiency values for evaporator fan switch on “2” to “3”. Surprisingly, it is expected that evaporator fan switch “1” test should show lowest mass flow rate among three tests. However, values on the table show continuing decrease as the evaporator air velocity increases for condenser fan at 100% tests. This controversy case actually needs to be investigated.

In figure 82 below, isentropic efficiency comparisons of six experiments are presented. Plots in the graphical representation are obtained by using isentropic efficiency formula (1) in chapter 2. In details, isentropic efficiency is the ratio of isentropic work to the actual work. This parameter shows how actual compression process is close to the ideal isentropic compression process in the experiments. As the isentropic efficiency increases, compression process approaches to ideal behavior and thus

decreasing the exergy destruction through the process, which is indeed mostly desired operation condition. For condenser fan at 50% tests, it can be seen in figure 82 that the isentropic efficiencies with blue plot are around 72%-73% as the evaporator air velocity increases. Referring the table 10 below, actual compressor work for three tests with condenser fan at 50% are very close to each other and around 4.3 kW in average. Additionally, as it can be found in the figure 79, pressures (high pressure side) at the outlet of the compressor for three tests are around 1400 kPa and almost provide same enthalpy values as around 475 kJ/kg. Hence, what expected for three tests as showing same isentropic behaviors are proven in below figure 82 simultaneously. Indeed, increasing the evaporator air velocity do not also have considerable effect on the isentropic efficiency performances of the cycle as similar with COP and volumetric efficiency.

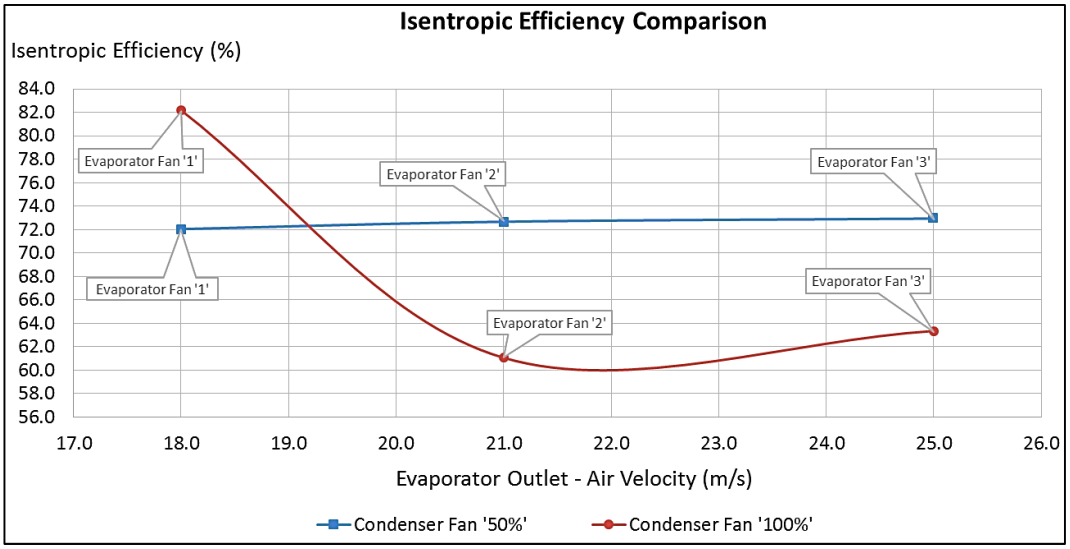

Figure 82 Comparison - Isentropic Efficiency

For condenser fan at 100% tests, values of isentropic efficiency illustrate different characteristics. Cond. Fan 100% & Evap. Fan "1" test seems to have most efficient operation during the experiments with the isentropic efficiency value as 82%. Furthermore, as the evaporator air velocity is increased to corresponding value of switch on "2", isentropic efficiency of related test shows rapid decrease to 61%. After that, setting the evaporator fan switch to position "3" recovers the final test to some extend with the isentropic efficiency value with 63.5%, which could be understood to

have tendency to steady operation. In details, comparing the all six tests in the concept of isentropic efficiency, it could be clearly resulted that the most efficient test is the Cond. Fan 100% & Evap. Fan "1" among all. To support that, lowest compressor work in the table 10 and lowest compressor outlet enthalpy value provided that enthalpies of all tests at the inlet of the compressor are very similar in figure 79 belong to mentioned test providing highest isentropic efficiency as 82% during the operation.

Exergetic efficiency evaluation of six tests is presented in figure 83. Plots are obtained by using exergetic efficiency formulation (17) in chapter 2. Indeed, exergetic efficiency can be simply described as the ratio of available reversible work to actual work. For the purpose, irreversibilities in compressor, condenser, expansion valve and evaporator are calculated with relevant formulas in chapter 2, and then formula (17) is used as remaining reversibility over actual compressor work through the operation. For clarification, exergetic efficiency values for condenser fan at 50% tests do not change considerably as the evaporator air velocity is increased. Indeed, relevant three exergetic efficiency values for the tests are around 13%. This behavior could be considered as similar with COP, isentropic and volumetric efficiency plots above for three tests with condenser fan at 50%. Referring the table 10, compressor works for relevant tests are very close to each other, hence deducing that the exergy destructions for each tests show also similar behaviors while evaporator air velocity is increased, regarding the figure 83 for condenser fan at 50% tests.

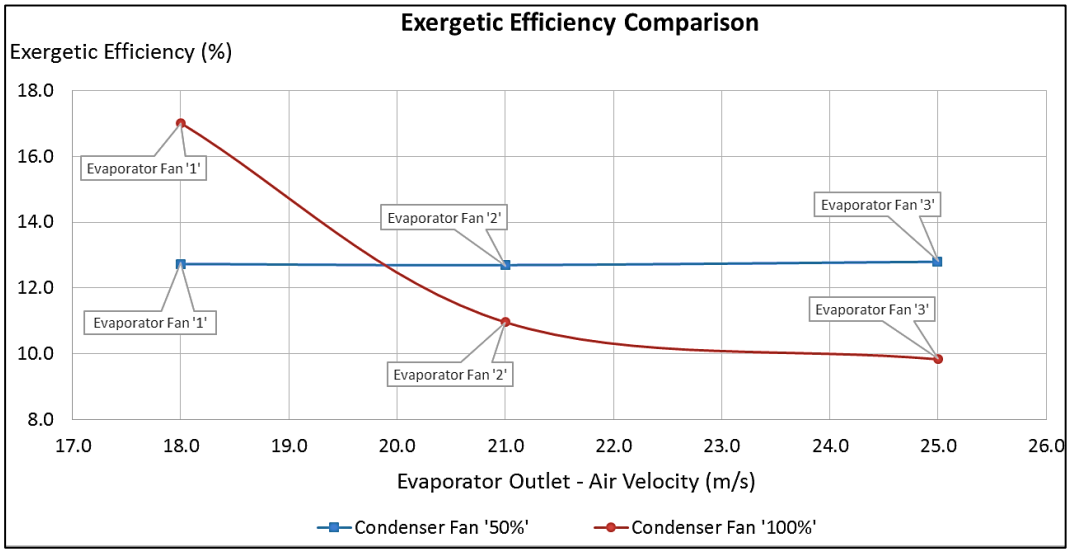

Figure 83 Comparison - Exergetic Efficiency

For condenser fan at 100% tests, as the evaporator air velocity increases, the exergetic efficiencies of the tests tend to decrease. In details, when the evaporator fan switch is at “1”, efficiency values are around 17%. As going further with getting the evaporator fan switch on “2”, exergetic efficiency shows rapid decrease to 11%. After that, the test with evaporator fan switch on “3” indicates lowest exergetic efficiency as around 10%. Indeed, behavior of the exergetic efficiency for condenser fan at 100% in brown color in above figure is very analog with the same configurations in above COP and isentropic efficiency graphs in terms of defining the most efficient test in the understating of cycle performance.

Furthermore, as it could be seen from figure 83 that Cond. Fan 100% & Evap. Fan “1” configuration provides the highest exergetic efficiency value among other tests. Indeed, this outcome supports the above inferences in COP and isentropic efficiency arguments that is, Cond. Fan 100% & Evap. Fan “1” test is the most efficient configuration considering the performance calculations of the experiments. Additionally, indicating such low values for exergetic efficiency, the vapor refrigeration compression cycle mainly shows the irreversible characteristic by considering the heat input and output to/from the refrigeration cycle. Eventually, average values of above performance parameters are tabulated in the table 10 below. For clarification, related values in the table are the averages of instantaneous performance calculation occurring during the steady state operation for each six tests. In the purpose of commonality, steady state operation duration is defined in the interval of 200 to 600 seconds.

Indeed, interrelations of the parameters and their respective behaviors are explained in the above discussions. In addition to these, change in the vapor and liquid mass flow rate characteristics referring each experiment configuration would be added. For condenser fans at 50% tests, vapor and liquid mass flow rates increase with increasing of evaporator air velocity when evaporator fan switch is set on “1” to “2” and then decreases for evaporator fan switch on “2” to “3” tests. On the other hand, condenser fan at 100% tests, vapor mass flow rate decreases as the evaporator air velocity increases. Additionally, liquid side shows similar behavior with that of condenser fan

at 50% tests. Indeed, it increases as evaporator fan switch is set on “1” to “2” and then similarly decreases from evaporator fan switch on “2” to “3” tests.

Table 10 Experiment Performance Variables - Averages

TEST / VARIABLE	Cond. Fan 50% Evap. Fan “1”	Cond. Fan 50% Evap. Fan “2”	Cond. Fan 50% Evap. Fan “3”	Cond. Fan 100% Evap. Fan “1”	Cond. Fan 100% Evap. Fan “2”	Cond. Fan 100% Evap. Fan “3”
Condenser Heat Rejection (kW)	8.17	8.49	8.09	7.30	8.24	7.12
Evaporator Cooling Capacity (kW)	5.23	5.44	5.20	4.96	5.14	4.35
Compressor Work (kW)	2.82	2.93	2.77	2.24	2.95	2.59
Volumetric Efficiency (%)	68.10	68.51	68.56	65.73	71.33	68.88
Isentropic Efficiency (%)	72.04	72.67	72.94	82.18	61.05	63.34
Exergetic Efficiency (%)	12.73	12.70	12.80	17.01	10.96	9.84
COP	1.85	1.86	1.88	2.22	1.74	1.68
Vapor Mass Flow Rate (kg/s)	0.0377	0.0390	0.0370	0.0354	0.0350	0.0300
Liquid Mass Flow Rate (kg/s)	0.0376	0.0402	0.0383	0.0303	0.0354	0.0314

In details, behavior of liquid and vapor mass flow rates can be directly linked with the pressure drops mainly occurring in evaporator and condenser due to dynamics of the refrigerant flow as well as the change of the corresponding operational pressure and temperature values on the relevant components. In the following section, more detailed evaluation of above relations will be studied. Moreover, when characteristics of vapor and liquid mass flow rates are as above by changing the evaporator air velocity with adjusting evaporator fan switch to related positions, it will also be better to look in the case when the condenser air velocities are changed. As stated in the table 10, changing the condenser fan configuration from 50% to 100% when keeping evaporator configuration same, e.g. evaporator fan switch on “1”, respective values of both vapor and liquid mass flow rates seem to decrease. Indeed, change factor for both vapor and liquid sides seems considerably higher when just increasing condenser air velocity while keeping evaporator configuration same than that of just increasing evaporator air velocity while keeping condenser configuration same.

4.3. INTERNAL PRESSURE FLUCTUATIONS

In this section, pressure fluctuations on both high and low pressure side are analyzed. As details, pressure plots in section 3.3 show the cyclic behaviors of the pressures at the relevant measurement points regarding as the system oscillations throughout each experiment. Indeed, internal fluctuations are also visible in mentioned graph above, it is better to magnify the pressure lines in order to understand the level of fluctuations. For the purpose, Cond. Fan 100% & Evap. Fan "3" test is taken into consideration for exemplifying the behavior of internal fluctuations. Time interval as 450 to 600 seconds is shown in the graph as a part of steady state operation for the test.

In figure 84 below, high pressure side of the refrigeration cycle is indicated. As it is seen, although the experiment reaches steady state operation by presenting some oscillatory behavior at the system level, it can also be possible to observe internal fluctuations. Indeed, order of magnitude of the pressure fluctuations is around 3-5 kPa for the high pressure side.

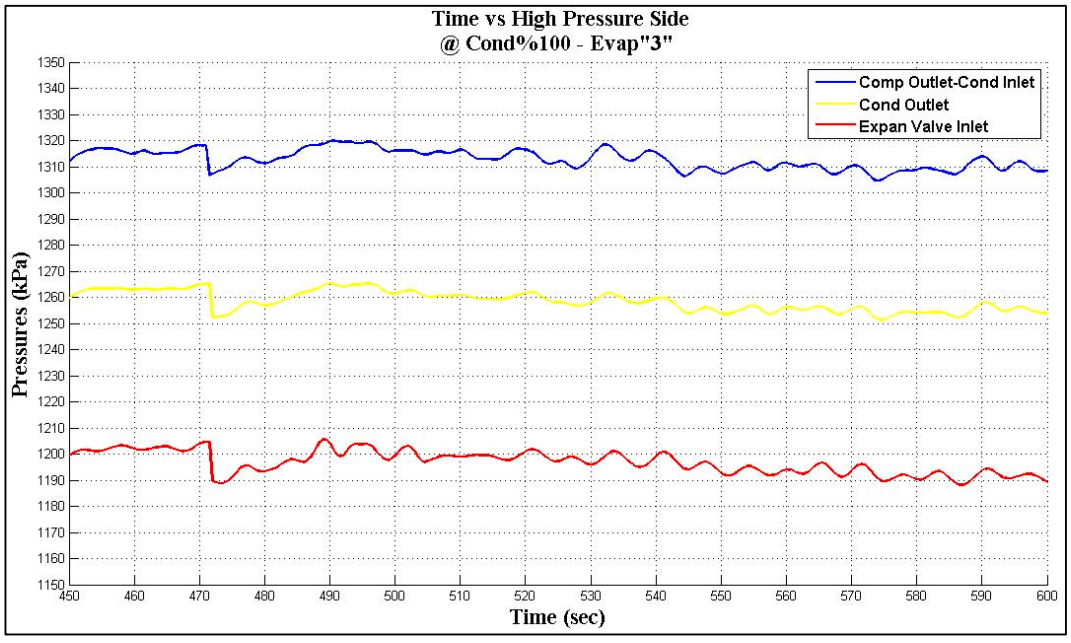

Figure 84 Internal Fluctuations - High Pressure Side

Additionally, although the pressure drops exist from compressor outlet to expansion valve inlet due to the hoses and condenser itself, behaviors of fluctuation seem very similar and ranging at the same level of amplitude.

Similarly, low pressure side of the refrigeration cycle shows paralles behaviour with the high pressur side plot. In figure 85 below, steady state pressure oscillations are fluctuate in the range of 10-15 kPa from expansion valve outlet to compressor inlet. Still having pressure drops due to hoses and mainly evaporator itself, it is very possible to say that internal fluctuations show very alike characteristics. Indeed, as going from the expansion valve outlet to compressor inlet, the amplitude of the fluctuations decreases to 5-10 kPa level.

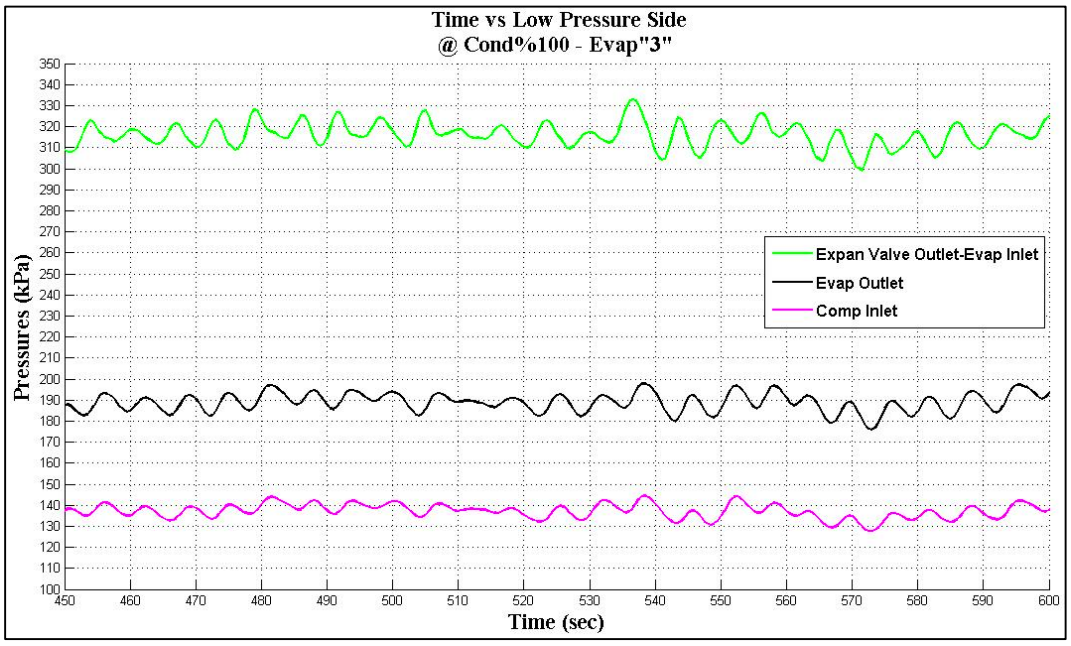

Figure 85 Internal Fluctuations - Low Pressure Side

The most likely reason for fluctuations could be said as compressor itself. Indeed, compressor used in the test is consisting of swash plate with 6 pistons. For every cycle for the compression of refrigerant in vapor phase, the pressure value increases and decreases instantaneously. If it is possible to have more pistons in the compressor structure, more linear pressure plot with lower fluctuation amplitude could be expected. Additionally, it is possible to say that comparing the figure 84 and 85 results, fluctuation amplitude in high pressure side is lower than that of low pressure side.

Indeed, fluctuation amplitude in high side do not change considerably while amplitude in low side decreases from 10-15 kPa to 5-10 kPa as going from expansion valve outlet to condenser inlet. Hence, it could be possible to say that expansion valve effort to stabilize the flow going into the evaporator causes more fluctuations to exist in the cycle. After leaving from evaporator, fluctuations have lower amplitudes up to compressor inlet. Indeed, when the refrigerant comes into hoses, fluctuation could be said to be suppressed or diminished. Furthermore, it is not possible to ignore the effect of unsteady characteristics of condensation and evaporation processes. Indeed, phase changes in the condenser and evaporator might support the increase of the fluctuation amplitudes as well. However, referring the pressure plots in chapter 3.3 again, condensation and evaporation processes are more likely to affect the behavior of system level oscillations. To remember, as the evaporator air velocity is increased, system level oscillations become more visible and stable while comparing with the messy behavior at the low evaporator air velocity configuration tests.

4.4. PERFORMANCE OF THE EXPERIMENTS

In the scope of result prosperity of the experiments based on the calculated values of performance variables listed in table 10, it can be concluded that one of the test configuration shall become prominent in terms of consuming lowest power and providing highest efficiencies among others. Actually, condenser heat rejections, evaporator cooling capacities and volumetric efficiencies of all six tests show no considerable changes upon adjusting the heat load configurations on the condenser and evaporator. Indeed, if Cond. Fan 100% & Evap. Fan "1" test results are specifically considered, it could be observed that the lowest compressor work, highest isentropic efficiency, highest exergetic efficiency and highest COP value show up in the mentioned test. Hence, Cond. Fan 100% & Evap. Fan "1" could be attributed as most efficient or optimum experimental configuration in terms of above performance variables. Following table indicates the respective values of variables and highlights the outstanding values for Cond. Fan 100% & Evap. Fan "1" test configuration.

Table 11 Performance Comparison of the Experiments

TEST / VARIABLE	Cond. Fan 50% Evap. Fan "1"	Cond. Fan 50% Evap. Fan "2"	Cond. Fan 50% Evap. Fan "3"	Cond. Fan 100% Evap. Fan "1"	Cond. Fan 100% Evap. Fan "2"	Cond. Fan 100% Evap. Fan "3"
Compressor Work (kW)	2.82	2.93	2.77	2.24	2.95	2.59
Isentropic Efficiency (%)	72.04	72.67	72.94	82.18	61.05	63.34
Exergetic Efficiency (%)	12.73	12.70	12.80	17.01	10.96	9.84
COP	1.85	1.86	1.88	2.22	1.74	1.68

4.5. UNCERTAINTY ANALYSIS

During the measurements of temperature and pressure values at the inlet/outlet of each A/C system components, as well as respective vapor and liquid mass flow rates, there occur some errors due to the imperfections existing in the measurement instruments. Obviously, the sensors for temperature and pressure measurements, and mass flow meters used in the experimental test setup may contain some calibration faults or by nature accuracies that cause systematical errors during measurements. Since these temperature and pressure values with vapor and liquid mass flow rates are used in the calculation of performance parameter of the tests, it is better to observe the level of uncertainties that may be preserved in the calculated values. For the purpose, Gauss' error propagation law is to be used to calculate the uncertainties of temperature, pressure and mass flow rates measurements. Also, uncertainty of "condenser heat rejection" is exemplified in order to understand the effects of temperature, pressure and mass flow meters uncertainties on the mentioned parameter. Finally, Cond. Fan 100% & Evap. Fan "1" test performance parameter are numerically tabulated with their respective uncertainties.

According to Gauss' propagation law, calculated value z is a function of measured values x and y, such as z=f(x, y), uncertainty in z is calculated as;

$$\sigma_z = \sqrt{\left(\frac{\partial f}{\partial x}\right)^2 \sigma_x + \left(\frac{\partial f}{\partial y}\right)^2 \sigma_y} \tag{18}$$

σ_z = Uncertainty in z
σ_x = Uncertainty in x
σ_y = Uncertainty in y

Thus, formula (9) is considered for condenser heat rejection uncertainty calculation as;

$$Q_{cond} = \dot{m}_{comp}(h_2 - h_3) \tag{9}$$

To start to calculation, the uncertainties in temperatures, pressures, mass flow meters and data logger system are listed as below;

σ_P $= 0.15\%$ of value

σ_T $= 0.5\%$ of value

σ_{flow} $= 1.6\%$ of value

σ_{logger} $= 0.05\%$ of value

Total uncertainty for temperature and pressure values is the sum of respective temperature/pressure and data logger uncertainties as;

$$\sigma_{T\_total} = \sqrt{(\sigma_T)^2 + \left(\sigma_{logger}\right)^2} \tag{19}$$

$$\sigma_{P\_total} = \sqrt{(\sigma_P)^2 + \left(\sigma_{logger}\right)^2} \tag{20}$$

Since h = h (T, P), the uncertainties in enthalpies at the inlet and outlet of the condenser can be calculated by using formula (21);

$$\sigma_h = \sqrt{\left(\frac{\partial h}{\partial T}\right)^2 \sigma_{T\_total} + \left(\frac{\partial h}{\partial P}\right)^2 \sigma_{P\_total}} \tag{21}$$

Partial derivatives of h with respect to T and P are calculated with finite difference method as following;

$$\frac{\partial h}{\partial T} = \frac{h_{t+1} - h_t}{T_{t+1} - T_t} \tag{22}$$

$$\frac{\partial h}{\partial P} = \frac{h_{t+1} - h_t}{P_{t+1} - P_t} \tag{23}$$

where, t is the time when the respective measurements are recorded.

Hence, considering formula (9) again, the uncertainty in condenser heat rejection could be obtained as following;

$$\sigma_{\text{cond}} = \left[\sqrt{\left(\frac{\sigma_{h2-h3}}{h_2-h_3}\right)^2 + \left(\frac{\sigma_{flow}}{\dot{m}_{\text{comp}}}\right)^2} \right] |Q_{cond}| \quad (24)$$

where, σ_{h2-h3} is the uncertainty in (h_2-h_3), which is indeed;

$$\sigma_{h2-h3} = \sqrt{(\sigma_{h2})^2 + (\sigma_{h3})^2} \quad (25)$$

Incorporating formula (25) into (24), uncertainty in condenser heat rejection calculation could be found accordingly as below;

$$\sigma_{\text{cond}} = \left[\sqrt{\left(\frac{\sqrt{(\sigma_{h2})^2+(\sigma_{h3})^2}}{(h_2-h_3)}\right)^2 + \left(\frac{\sigma_{flow}}{\dot{m}_{\text{comp}}}\right)^2} \right] |Q_{cond}| \quad (26)$$

In the highlight of above sample calculation for uncertainty in condenser heat rejection, other performance parameter for Cond. Fan 100% & Evap. Fan "1" experiment are calculated and listed in table 12 below.

Table 12 Uncertainty Analysis for "Cond. Fan 100% & Evap. Fan 1" Experiment

Cond. Fan 100% & Evap. Fan "1"	MEAN VALUE	UNCERTAINITY	UNIT
Condenser Heat Rejection	7.32	± 0.82	kW
Evaporator Cooling Capacity	4.89	± 0.53	kW
Compressor Work	2.31	± 0.61	kW
Volumetric Efficiency	64.96	± 2.63	%
Isentropic Efficiency	82.73	± 3.37	%
Exergetic Efficiency	16.97	± 0.96	%
COP	2.123	± 0.272	
Vapor Mass Flow Rate	0.0350	± 0.00035	kg/s
Liquid Mass Flow Rate	0.030	± 0.00056	kg/s

CHAPTER 5

CONCLUSION

5.1. SUMMARY AND CONCLUSION

The thesis study includes the experiments conducted on the vapor compression refrigeration process in the air conditioning system which is driven by an auxiliary power unit (APU) designed for an wheeled armored fighting vehicle. In addition, vapor compression cycle analysis was performed to clarify the change of performance characteristics as the compressor speed and condensing temperature change while keeping the evaporator cooling capacity between 8.4-8.6 kW.

Experiments were performed according to concept of changing the heat loads on both condenser and evaporator by adjusting the air velocities passing through the components. Indeed, there occurred six different load configurations, e.g. three for evaporator side and two for condenser side. Also, all pressure and temperature values of refrigerant were recorded by data acquisition system as well as particular vapor and liquid mass flow rates. Indeed, all data show purposeful behaviors regarding the changes on the heat loads. According the measured data, cycle performance variables, e.g. condenser heat rejection rates, evaporator cooling capacities, compressor works, COPs, isentropic, volumetric and exergetic efficiencies, were calculated and, respective results and discussions were presented. Furthermore, based on the calculated performance variables above, one of the experiment was specified as most efficient configuration in terms of consuming lowest power for compressor and providing highest isentropic and exergetic efficiencies along with the highest COP value.

One of the most important outcomes of the experiments is the difference between expected value of evaporator cooling capacity stemming from design phase and the relevant calculated values. During design phase, it is expected that evaporator cooling capacity is max. 8.5 kW at optimum operation condition; which should indeed be observed in the test of Cond. Fan 100% & Evap. Fan "3". However, calculated evaporator cooling capacity of mentioned test is 6.05 kW in average. Actually, this result may come from the average of the liquid and vapor mass flow rate that is used for calculating respective cooling capacities. In the base of individual test performances, Cond. Fan 100% & Evap. Fan "1" test becomes prominent among others while comparing the evaporator air outlet temperatures. Indeed, another design criterion is that the evaporator air outlet temperature should not exceed the 18 °C in the optimum operation condition. Although the tests with condenser fan 100% meet that requirement accordingly, it could be seen that Cond. Fan 100% & Evap. Fan "1" test provides the coolest air outlet among the six tests referring the figure 54. Indeed, table 10 shows that Cond. Fan 100% & Evap. Fan "1" does not provide the highest evaporator cooling capacity as well. Moreover in the purpose of providing the lowest work to the compressor, Cond. Fan 100% & Evap. Fan "1" test consumes the lowest power while supplying the lowest evaporator air outlet temperature. Meanwhile, the superior performance of the mentioned test could be also seen in regarding the COP, exergetic and isentropic efficiencies values. Among all six tests, Cond. Fan 100% & Evap. Fan "1" indicate the highest values for mentioned performance variables according to the table 11. Consequently, Cond. Fan 100% & Evap. Fan "1" could be considered as most efficient configuration.

While performances of the experiments are as above, system level oscillations and internal pressure fluctuations are another facts that need to be detailed. As clarified in chapter 3, system level pressure oscillations in both high and low pressure sides become more visible and regular as the evaporator air speed increases regardless of condenser fan configuration. Indeed, changing of condenser air velocity only affects the magnitude of high pressure side accordingly. As an example, when Cond. Fan 100% & Evap. Fan "3" fluctuates around 1300 kPa in average, Cond. Fan 50% & Evap. Fan "3" test fluctuates around 1375 kPa in average for the high pressure side.

Similarly, internal pressure fluctuations in the pressure plots could be observed in detail when magnifying the pressure graphs. In chapter 4, internal fluctuations in high and low pressure sides are exemplified with the results of Cond. Fan 100% & Evap. Fan “3” test. Indeed, main source of these fluctuations is the compressor itself which has the six pistons compressing the refrigerant. As it was said, more pistons the compressor has, lower amplitudes the fluctuations could be expected. Also, difference between amplitudes of high and low pressure sides was investigated and resulted that it might be most probably caused by the expansion valve effort to adjust the amount of refrigerant going into evaporator.

5.2. FUTURE WORK

This chapter includes the precautions and warnings that need to be taken into consideration while proceeding further studies in the same research area.

Firstly, adjusting the test room ambient temperature is one of the most effortful actions during the experiments. As stated previously, test chamber temperature needs be stable at 33 °C in order to achieve the desired performance of the refrigeration cycle. Although the experiments results indicate very stable environment temperature at around 33±2 °C, it could be advised that controlled test chamber, which is as big as just containing the experimental components and limited interface with outside ambient air, would be very beneficial.

Furthermore, observing the mass flow rate measurements manually recorded with a camera is very tough work to do and might contain considerable errors in readings. Since the both vapor and liquid mass flow rates are used in the relevant figures and performance variable calculations of the experiments, it is strongly advised to use digital mass flow meters to increase the accuracy of calculations and related graphics.

Finally, referring the above concern of mass flow rates, it will be very beneficial to measure the temperature and pressure information at few points in the condenser and evaporator if possible. Indeed, this will help to understand the internal dynamics of the refrigerant flow through the mentioned components while performing theoretical approach related with the interface of pressure drop versus mass flow rate. In details, observing the vapor quality of the fluid, flowing in the condenser or evaporator, would definitely enhance the accuracy of calculations and results in more realistic outcomes while comparing the actual test results and theoretical results accordingly.

REFERENCES

[1] Boxer, "http://en.wikipedia.org," [Online]. Available: http://en.wikipedia.org /wiki/Boxer_(armoured_fighting_vehicle). [Accessed 15 September 2014].

[2] FNSS Savunma Sistemleri A.Ş., "http://www.fnss.com.tr," FNSS Savunma Sistemleri A.Ş., 2014. [Online]. Available: http://www.fnss.com.tr/en/ product/pars-8x8#next. [Accessed 02 September 2014].

[3] Army-Technology, "http://www.army-technology.com," [Online]. Available: http://www.army-technology.com/projects/gpv/gpv11.html. [Accessed 17 Semtember 2014].

[4] Army-Recognition, "http://www.armyrecognition.com," [Online]. Available: http://www.armyrecognition.com/malaysia_malaysian_army_wheeled_armoured_vehicle_u/av8_av-8_8x8_armoured_vehicle_personnel_carrier_technical_data_sheet_specifications_pictures_video.html. [Accessed 07 September 2014].

[5] FNSS Savunma Sistemleri A.Ş, *Wheeled Armored Combat Vehicles Pars 8x8*, Ankara: FNSS Savunma Sistemleri A.Ş., 2014.

[6] "http://en.wikipedia.org," [Online]. Available: http://en.wikipedia.org/wiki/ Auxiliary_power_unit. [Accessed 12 September 2014].

[7] Willis Power Systems, "http://www.willisapu.com," [Online]. Available: http://www.willisapu.com/Product-Information/WPS-Premium.aspx. [Accessed 12 September 2014].

[8] Mitsubishi, "http://www.det-mitsubishi.com," [Online]. Available: http://www.det-mitsubishi.com/en/mitsubishi-diesel-engines/engines/l-series-4-17-kw/l3e-6-17-kw. [Accessed 14 September 2014].

[9] J. Humble, "Auxiliary Power Unit (APU) for Military Vehicles," General Dynamics Land Systems, Michigan, 2009.

[10] Marvin Land Systems, "Auxiliary Power Unit (APU) for the Expeditionary Fighting Vehicle (EFV)," Marvin Land Systems, California, 2011.

[11] Fisher Panda, "http://www.fischerpanda-defence.de," Fisher Panda, 2012. [Online]. Available: http://www.fischerpanda-defence.de/index.php?id=104&gid=6. [Accessed 15 September 2014].

[12] FNSS Savunma Sistemleri A.Ş., "http://www.fnss.com.tr," FNSS Savunma Sistemleri A.Ş., [Online]. Available: http://www.fnss.com.tr/en/corporate/about-us/introduction. [Accessed 14 September 2014].

[13] EDN Networks, "http://www.edn.com," [Online]. Available: http://www.edn.com/design/automotive/4403883/Fundamentals-of-the-automotive-cabin climate-control-system. [Accessed 14 September 2014].

[14] M. J. Moran and H. N. Shapiro, in *Fundementals of Engineering Thermodynamics 6.th Edition*, John Wiley & Sons, Inc., 2008, pp. 536, 545.

[15] "http://www.arca53.dsl.pipex.com," [Online]. Available: http://www.arca53.dsl.pipex.com/index_files/phrefrig.htm. [Accessed 18 September 2014].

[16] B. Li and A. G. Alleyne, "A dynamic model of a vapor compression cycle with shut-down and start-up operations," *International Journal of Refrigeration*, 2010.

[17] B. Li, S. Peuker, A. G. Alleyne and P. S. Hrnjak, "Refrigerant Migration Modeling During Shut-down And Start-up Cycling Transients," in *International Refrigeration and Air Conditioning Conference*, Purdue University, 2010.

[18] M. W. Browne and P. K. Bansal, "Transient simulation of vapour-compression packaged," *International Journal of Refrigeration*, no. 25, 22 June 2001.

[19] Z. Lei and M. Zaheeruddin, "Dynamic Simulation and Analysis of a Water Chiller Refrigeration System," *Applied Thermal Engineering*, 12 February 2005.

[20] K. A. Ismail, R. N. Koury and L. Machado, "Numerical Simulation of a Variable Speed Refrigeration System," *International Journey of Refrigeration,* 31 January 2001.

[21] M. Chandrasekharan, "Exergy Analysis of Vapor Compression Refrigeration System Using R12 and R134a as Refrigerants," *International Journal of Students' Research in Technology & Management,* pp. 134-139, June-July 2014.

[22] S. J. Wang and J. J. Gu, "Experimental Analysis of an Automotive Air Conditioning System With Two-Phase Flow Measurements," in *Internatinoal Refrigeration and Air Conditioning Conference*, Purdue University, 2014.

[23] M. Hoşöz, M. Direk, K. S. Yiğit, M. Çanakci, A. Türkcan and E. Alptekin, "R134a Soğutucu Akışkanlı Bir Otomobil İklimlendirme Sisteminin Performansına Çalışma Koşullarının Etkisinin Deneysel Olarak İncelenmesi," in *1. Ulusal İklimlendirme Soğutma Eğitimi Sempozyumu*, Balıkesir, 2012.

[24] M. Bahrami, "http://www.sfu.ca," [Online]. Available: http://www.sfu.ca/~mbahrami/ENSC%20461/Notes/Refrigeration%20Cycle.pdf. [Accessed 24 November 2014].

[25] "http://refrigerationbest.blogspot.com.tr," 02 2013. [Online]. Available: http://refrigerationbest.blogspot.com.tr/2013/02/vapor-compression-refrigeration.html. [Accessed 27 October 2014].

[26] E. W. Lemmon, M. L. Huber and M. O. McLinden, "miniREFPROP NIST Standart Reference Database 23, Version 9.1," National Institute of Standarts and Technology (NIST).

[27] K. Wait, "http://www.boulder.nist.gov," GE Home Business Solutions, 17 October 2013. [Online]. Available: http://www.boulder.nist.gov/div838/theory/refprop/Frequently_asked_questions.htm. [Accessed September 2014].

[28] S. Jain and C. W. Bullard, "Capacity and Efficiency in Variable Speed, Vapor Injection and Multi-Compressor System," University of Illinois at Urbana-Champaign, Illinois, 2004.

[29] K. Kianfar, R. Izadi-Zamanabadi and M. Saif, "Cascaded Control of Superheat Temperature of an HVAC System Via Super Twisting Sliding Mode Control," in *19th World Congress of the International Federation of Automatic Control*, Cape Town, 2014.

[30] Güntner AG &Co.KG, "Influence of Refrigerant Subcooling on the Refrigerant Plant Efficiency," Güntner, Fürstenfeldbruck, 2010.

[31] R. D. Holder, "Characteristics of Evaporators," National Technical Transfer Inc., Englewood, 2003.

[32] D. D. Silva, C. Hermes and C. Melo, "Experimental Study of Frost Accumulation on Fan-Supplied Tube-Fin Evaporators," in *International Refrigeration and Air Conditioning Conference*, Purdue, 2010.

[33] J. Sun, "Modelling and Intelligent Control of Vehicle Climatronic System," Nelson Mandela Metropolitan University, Port Elizabeth, 2009.

[34] Valeo Compressors, "www.valeocompressors.com," Valeo Compressors, 2014. [Online]. Available: http://www.valeocompressors.com/en/tm13-tm15-tm16. [Accessed 27 January 2015].

[35] W.-C. Wu and T.-S. Lee, "Energy and Exergy Analysis for Improving the Energy Performance of Air-Cooled Liquid Chillers by Different Condensing-Coil Configurations," *Entropy 2012*, pp. 517-532, 8 March 2012.

[36] Valeo Compressors, "valeocompressors.com," Valeo Compressors, 2014. [Online]. Available:http://valeocompressors.com/performance/. [Accessed 27 January 2015].

[37] Free Study Guides, "www.freeasestudyguides.com," [Online]. Available: http://www.freeasestudyguides.com/ac-receiver-drier.html. [Accessed 1 February 2015].

[38] GE Industrial, Sensing, "www.nicinst.co.za," [Online]. Available: http://www.nicinst.co.za/files/product_brochure/ptx-pmp_1400_0.pdf. [Accessed 1 February 2015].

[39] www.tecalemitflow.fi, "www.tecalemitflow.fi," [Online]. Available: http://www.tecalemitflow.fi/tuotteet/rotametrit-840/krohne-va-40-ja-45-117. [Accessed 6 February 2015].

[40] www.instrumart.com, "www.instrumart.com," [Online]. Available: https://www.instrumart.com/products/33899/krohne-h250-rr-variable-area-flow-meter. [Accessed 6 February 2015].

[41] www.dewesoft.com, "SIRIUS Technical Reference Manual," [Online]. Available: http://www.dewesoft.com/support/downloads#Manuals. [Accessed 12 February 2015].

[42] Wolverine Tube, Inc., "Two-Phase Pressure Drops - Engineering Data Book III," Wolverine Tube, Inc., 2006.

APPENDICES

A. MATLAB CODE (ANALYSIS.M) FOR REFRIGERATION CYCLE ANALYSIS

```
%%%%%%%%%%%%%%%%%%%%%%%%%%%%%%%%%%%%%%%%%%%%%%%%%%%%%%%%%%%%%%%%%%%%%%%%%%%%%%%%
% FILENAME          : analysis.m
% WRITTEN BY     : Alper KORKMAZ
% DATE                : JUNE 2015
% MATLAB REV.   : R2009b
% MIDDLE EAST TECHNICAL UNIVERSITY
%
% This code is written to analyze the refrigeration cycle properties as
% well as corresponding performance variables.
%
% The code shall be located in the same directory with "refpropm.m" and
% "rp_proto.m", which are the linking codes with program "RefpropMini" used
% for evaluating the refrigerant properties.
%
%%%%%%%%%%%%%%%%%%%%%%%%%%%%%%%%%%%%%%%%%%%%%%%%%%%%%%%%%%%%%%%%%%%%%%%%%%%%%%%%
clear all;
clc;

Tcondensing=20; % Initial condensation temperature assumption
Tevaporation=0; % Constant evaporation temperature
m=5; %Assumed percentage value of clearance volume
ns=0.8; % Estimated initial value of isentropic efficiency
Vs = 163*10^-6; % Compressor displacement volume (m^3/rev)
deltaT =2; % Condensation temperature increment
i=1;
j=1;
TH=33+273; % Hot reservoir temperature (K)
T0=33+273; % Cold reservoir temperature
Tsuperheat=10; % Assumed super-heating temperature
Tsubcool=5; % Assumed sub-cooling temperature
Pevaporation=refpropm('P','T',273+Tevaporation,'Q',1,'r134a'); % Corresponding evaporation pressure (Pa)
%%
%Matrices Allocation
Qevap=zeros(800,800);
T=zeros(800,800);
S=zeros(800,800);
mass=zeros(800,800);
voleff=zeros(800,800);
iseneff=zeros(800,800);
Psa=zeros(800,800);
COP=zeros(800,800);
Wcomp=zeros(800,800);
CondCap=zeros(800,800);
xtotal=zeros(800,800);
exeff=zeros(800,800);
%%
while Tcondensing<=90 % Calculation will be performed up until 90 °C

h1 = refpropm('H','T',273+Tevaporation+Tsuperheat,'P',Pevaporation,'r134a'); % Enthalpy at the compressor inlet
```

```
d1 = refpropm('D','T',273+Tevaporation+Tsuperheat,'P',Pevaporation,'r134a'); % Density at the compressor inlet
s1 = refpropm('S','T',273+Tevaporation+Tsuperheat,'P',Pevaporation,'r134a'); % Entropy at the compressor inlet
o1 = refpropm('O','T',273+Tevaporation+Tsuperheat,'P',Pevaporation,'r134a'); % Cv at the compressor inlet
c1 = refpropm('C','T',273+Tevaporation+Tsuperheat,'P',Pevaporation,'r134a'); % Cp at the compressor inlet

Pcondensing = refpropm('P','T',273+Tcondensing,'Q',0,'r134a'); % Corresponding condensation pressure
s2isen=s1;

h2isen = refpropm('H','P',Pcondensing,'S',s2isen,'r134a'); % Isentropic enthalpy at the compressor outlet
h2= ((h2isen-h1)/ns)+h1; % Actual enthalpy at the compressor outlet
s2 = refpropm('S','P',Pcondensing,'H',h2,'r134a'); % Entropy at the compressor outlet

h3 = refpropm('H','T',273+Tcondensing-Tsubcool,'P',Pcondensing,'r134a'); % Enthalpy at the condenser outlet
s3 = refpropm('S','T',273+Tcondensing-Tsubcool,'P',Pcondensing,'r134a'); % Entropy at the condenser outlet

h4=h3;
q4 = refpropm('Q','H',h4,'P',Pevaporation,'r134a'); % Vapor quality at the evaporator inlet
s4 = refpropm('S','T',273+Tevaporation,'Q',q4,'r134a'); % Entropy at the evaporator inlet

nvc = 100-m *((Pcondensing/Pevaporation)^(o1/c1)-1); % Volumetric efficiency (%)
%%
for Nrpm=600:1:7000 % Compressor rpm => between 600-7000 rpm
mr = Vs*(nvc/100)*d1*Nrpm/60; % Mass flow rate (kg/s)
Qevapcalculated = mr*(h1-h4)/1000; % Evaporator cooling capacity (kW)

%% Exergy Destruction
%for evaporator
xevap=T0*(mr*(s4-s1)+mr*(h1-h4)/T0);

%for compressor
xcomp=T0*mr*(s2-s1);

%for condenser
xcond= T0*(mr*(s3-s2)-mr*(h3-h2)/T0);
%for expansion valve
xexval=mr*T0*(s4-s3);

%Total system exergy destruction
xt= xevap+xcomp+xcond+xexval;

%%
ns1= -0.0123*(Pcondensing/Pevaporation)+0.8714;
ns2=-0.08*(Nrpm/3800)^2+0.1411*(Nrpm/3800)+0.9337;
ns=ns1*ns2; % Isentropic efficiency

if 8.4 <Qevapcalculated && Qevapcalculated < 8.6

Qevap(i,j)= Qevapcalculated; % Evaporator cooling capacity (kW)
Wcomp(i,j)= mr*(h2-h1)/1000; % Compressor work (kW)
CondCap(i,j)= mr*(h2-h3)/1000; % Condenser heat rejection rate (kW)
S(i,j)= Nrpm; % Compressor rpm
mass(i,j)= mr; % Refrigerant mass flow rate (kg/s)
T(i,j)= Tcondensing; % Condensation temperature (°C)
voleff(i,j)= nvc; % Volumetric efficiency (%)
Psa(i,j)= Pcondensing/100; % Condensation pressure (kPa)
COP(i,j)=(h1-h4)/(h2-h1); % System COP
iseneff(i,j)=ns*100; % Isentropic efficiency (%)
xtotal(i,j)=xt/1000; % Total exergy destruction (kW)
exeff(i,j)= (1-xtotal(i,j)/Wcomp(i,j))*100 ; % Exergetic efficiency (%)
i=i+1;
end

end
i=1;
j=j+1;
Tcondensing=Tcondensing+deltaT;
end

% Elimination zeros in the pre-allocated matrices
Qevap(Qevap==0)=nan;
T(T==0)=nan;
S(S==0)=nan;
mass(mass==0)=nan;
```

```
voleff(voleff==0)=nan;
Psa(Psa==0)=nan;
COP(COP==0)=nan;
Wcomp(Wcomp==0)=nan;
CondCap(CondCap==0)=nan;
iseneff(iseneff==0)=nan;
xtotal(xtotal==0)=nan;
exeff(exeff==0)=nan;

%%
figure (1)
surfc(S,T,Qevap);
xlabel('Compressor Speed (rpm)');
ylabel('Condensing Temperature (°C)');
zlabel('Evaporator Cooling Capacity (kW)');
title('\bf Comp. Speed & Temperature vs Evap. Cooling Cap.');
colormap cool;
grid on;
%%
figure (2)
SQ =plot(S,Qevap);
xlabel('Compressor Speed (rpm)');
ylabel('Evaporator Cooling Capacity (kW)');
title('\bf Compressor Speed vs Evap. Cooling Cap.');
set(SQ,'Color','black','Marker','>','Linewidth',1,'MarkerEdgeColor','k','MarkerFaceColor','y');
set(gca,'YLim',[8.38 8.62]);
set(gca,'YTick',8.38:0.01:8.62);
set(findall(gca,'type','text'),'fontSize',16,'fontWeight','bold','FontName','Times New Roman')
colormap cool;
grid on;
%%
figure (3)
[ax,h1,h2]=plotyy(T,CondCap,T,Wcomp,'plot');
set(get(ax(1),'Ylabel'),'String','Condenser Heat Rejection (kW)');
set(get(ax(2),'Ylabel'),'String','Compressor Work (kW)');
xlabel('Condensing Temperature (°C)');
title('\bf Condensing Temperature vs Cond. Heat Reject. & Comp. Work');
set(h1,'Color','green','Linewidth',4);
set(h2,'Color','blue','Linewidth',4);
set(ax,'XLim',[0 100]);
set(ax,'XTick',0:10:100);
L1=legend(ax(1),'Location',[0.65,0.18,0.3,0.05],'Condenser Heat Rejection');
legend(ax(1),'boxoff');
L2=legend(ax(2),'Location',[0.63,0.13,0.3,0.05],'Compressor Work');
legend(ax(2),'boxoff');
set(L1,'FontSize',10,'fontWeight','bold');
set(L2,'FontSize',10,'fontWeight','bold');
set(findall(ax(1),'type','text'),'fontSize',16,'fontWeight','bold','FontName','Times New Roman')
set(findall(ax(2),'type','text'),'fontSize',16,'fontWeight','bold','FontName','Times New Roman')
colormap cool;
grid on;
%%
figure (4)
[ax,h1,h2]=plotyy(S,CondCap,S,Wcomp,'plot');
set(get(ax(1),'Ylabel'),'String','Condenser Heat Rejection (kW)');
set(get(ax(2),'Ylabel'),'String','Compressor Work (kW)');
xlabel('Compressor Speed (rpm)');
title('\bf Compressor Speed vs Cond. Heat Reject. & Comp. Work');
set(h1,'Color','green','Linewidth',4);
set(h2,'Color','blue','Linewidth',4);
set(ax,'XLim',[0 5000]);
L1=legend(ax(1),'Location',[0.65,0.18,0.3,0.05],'Condenser Heat Rejection');
legend(ax(1),'boxoff');
L2=legend(ax(2),'Location',[0.63,0.13,0.3,0.05],'Compressor Work');
legend(ax(2),'boxoff');
set(L1,'FontSize',10,'fontWeight','bold');
set(L2,'FontSize',10,'fontWeight','bold');
set(findall(ax(1),'type','text'),'fontSize',16,'fontWeight','bold','FontName','Times New Roman')
set(findall(ax(2),'type','text'),'fontSize',16,'fontWeight','bold','FontName','Times New Roman')
colormap cool;
grid on;
%%
figure (5)
```

```
ctve =plot(S(1,:),voleff(1,:));
hold on;
ctie =plot(S(1,:),iseneff(1,:));
hold on;
ctee =plot(S(1,:),exeff(1,:));
hold on;
set(ctve,'Color','black','Marker','>','Linewidth',2,'MarkerEdgeColor','k','MarkerFaceColor','b');
set(ctie,'Color','black','Marker','s','Linewidth',2,'MarkerEdgeColor','k','MarkerFaceColor','y');
set(ctee,'Color','black','Marker','o','Linewidth',2,'MarkerEdgeColor','k','MarkerFaceColor','g');
L=legend('Volumetric Efficiency','Isentropic Efficiency','Exergetic Efficiency');
legend(L,'boxoff');
set(L,'FontSize',10,'fontWeight','bold');
set(gca,'YLim',[0 100]);
set(gca,'YTick',0:10:100);
xlabel('Compressor Speed (rpm)');
ylabel('Efficiency (%)');
title('\bf Compressor Speed vs Efficiency');
set(findall(gca,'type','text'),'fontSize',16,'fontWeight','bold','FontName','Times New Roman');
colormap cool;
grid on;
%%
figure (6)
ctve =plot(T(1,:),voleff(1,:));
hold on;
ctie =plot(T(1,:),iseneff(1,:));
hold on;
ctee =plot(T(1,:),exeff(1,:));
hold on;
set(ctve,'Color','black','Marker','>','Linewidth',2,'MarkerEdgeColor','k','MarkerFaceColor','b');
set(ctie,'Color','black','Marker','s','Linewidth',2,'MarkerEdgeColor','k','MarkerFaceColor','y');
set(ctee,'Color','black','Marker','o','Linewidth',2,'MarkerEdgeColor','k','MarkerFaceColor','g');
L=legend('Volumetric Efficiency','Isentropic Efficiency','Exergetic Efficiency');
legend(L,'boxoff');
set(L,'FontSize',10,'fontWeight','bold');
set(gca,'YLim',[0 100]);
set(gca,'YTick',0:10:100);
xlabel('Condensing Temperature (°C)');
ylabel('Efficiency (%)');
title('\bf Condensing Temperature vs Efficiency');
set(findall(gca,'type','text'),'fontSize',16,'fontWeight','bold','FontName','Times New Roman')
colormap cool;
grid on;

%%
figure (7)
cscop=line(S(1,:),COP(1,:));
xlabel('Compressor Speed (rpm)');
ylabel('COP');
title('\bf Compressor Speed vs COP');
set(cscop,'Color','black','Marker','^','Linewidth',2,'MarkerEdgeColor','k','MarkerFaceColor','c');
set(gca,'YLim',[0 12]);
set(gca,'YTick',0:1:12);
set(findall(gca,'type','text'),'fontSize',16,'fontWeight','bold','FontName','Times New Roman')
colormap cool;
grid on;

%%
figure (8)
tempcop =plot(T(1,:),COP(1,:));
xlabel('Condensing Temperature (°C)');
ylabel('COP');
title('\bf Condensing Temperature vs COP');
set(tempcop,'Color','black','Marker','^','Linewidth',2,'MarkerEdgeColor','k','MarkerFaceColor','c');
set(gca,'XLim',[10 100]);
set(gca,'XTick',10:10:100);
set(gca,'YLim',[0 12]);
set(gca,'YTick',0:1:12);
set(findall(gca,'type','text'),'fontSize',16,'fontWeight','bold','FontName','Times New Roman')
colormap cool;
grid on;
%%
figure (9)
ctve =plot(T(1,:),xtotal(1,:));
```

```
xlabel('Condensing Temperature (°C)');
ylabel('Exergy Destruction (kW)');
title('\bf Condensing Temperature vs Exergy Destruction');
set(ctve,'Color','black','Marker','h','Linewidth',2,'MarkerEdgeColor','k','MarkerFaceColor','g');
set(findall(gca,'type','text'),'fontSize',16,'fontWeight','bold','FontName','Times New Roman')
colormap cool;
grid on;
%%
figure (10)
ctve =plot(S(1,:),xtotal(1,:));
xlabel('Compressor Speed (rpm)');
ylabel('Exergy Destruction (kW)');
title('\bf Compressor Speed vs Exergy Destruction');
set(ctve,'Color','black','Marker','h','Linewidth',2,'MarkerEdgeColor','k','MarkerFaceColor','g');
set(findall(gca,'type','text'),'fontSize',16,'fontWeight','bold','FontName','Times New Roman')
colormap cool;
grid on;
%%
```

B. MATLAB CODE (TEST_RESULTS.M) FOR TEST RESULTS EVALUATION

```
%%%%%%%%%%%%%%%%%%%%%%%%%%%%%%%%%%%%%%%%%%%%%%%%%%%%%%%%%%%%%%%%%%%%%%%%%%%%%%%%
% FILENAME    : test_results.m
% WRITTEN BY  : Alper KORKMAZ
% DATE        : JUNE 2015
% MATLAB REV. : R2009b
% MIDDLE EAST TECHNICAL UNIVERSITY
%
% This code is written to evaluate the six particular test results and
% compare their performance variables accordingly.
%
% The code shall be located in the same directory with "refpropm.m" and
% "rp_proto.m", which are the linking codes with program "RefpropMini" used
% for evaluating the refrigerant properties.
%
%%%%%%%%%%%%%%%%%%%%%%%%%%%%%%%%%%%%%%%%%%%%%%%%%%%%%%%%%%%%%%%%%%%%%%%%%%%%%%%%

%%%%%% Variables %%%%%%
%Column 1 Time
%Column 2-3 Compressor Outlet-Condenser Inlet Temp-Press
%Column 4-5 Condenser Outlet Temp-Press
%Column 6-7 Expansion Valve Inlet Temp-Press
%Column 8-9 Expansion Valve Outlet-Evaporator Inlet Temp-Press
%Column 10-11 Evaporator Outlet Temp-Press
%Column 12-13 Compressor Inlet Temp-Press
%Column 14 Vapor Mass Flow Rate
%Column 15 Liquid Mass Flow Rate
%Column 16-17 Condenser Air Side Inlet-Outlet Temp
%Column 18 Condenser Fan Air Velocity
%Column 19-20 Evaporator Air Side Inlet-Outlet Temp
%Column 21 Evaporator Fan Air Velocity

%%%%%% Tests to be performed %%%%%%
%Condenser Fan Speed %50 ==> Evaporator Rotary Switch 1
%Condenser Fan Speed %50 ==> Evaporator Rotary Switch 2
%Condenser Fan Speed %50 ==> Evaporator Rotary Switch 3
%Condenser Fan Speed %100 ==> Evaporator Rotary Switch 1
%Condenser Fan Speed %100 ==> Evaporator Rotary Switch 2
%Condenser Fan Speed %100 ==> Evaporator Rotary Switch 3

%%%%%%%%%%%%%---------PLOTTING----------%%%%%%%%%%%%%%%%%%%%%%%%%%%%%%%%%%%%
function TestResult % Main function that calls the sub-functions below
clc;
clear all;

% Reading the test results from relevant excel files
for i=1:1:6
 if i==1
results=xlsread('test_cond50_evap1.xlsx');
D={'@ Cond%50 - Evap"1"'};
temperature(results,D);
pressure(results,D);
mass_flow(results,D);
heat(results,D);
 end
  if i==2
results=xlsread('test_cond50_evap2.xlsx');
D={'@ Cond%50 - Evap"2"'};
temperature(results,D);
pressure(results,D);
mass_flow(results,D);
heat(results,D);
end
```

```
  if i==3
results=xlsread('test_cond50_evap3.xlsx');
D={'@ Cond%50 - Evap"3"'};
temperature(results,D);
pressure(results,D);
mass_flow(results,D);
heat(results,D);
  end
  if i==4
results=xlsread('test_cond100_evap1.xlsx');
D={'@ Cond%100 - Evap"1"'};
temperature(results,D);
pressure(results,D);
mass_flow(results,D);
heat(results,D);
  end
  if i==5
results=xlsread('test_cond100_evap2.xlsx');
D={'@ Cond%100 - Evap"2"'};
temperature(results,D);
pressure(results,D);
mass_flow(results,D);
heat(results,D);
  end
  if i==6
results=xlsread('test_cond100_evap3.xlsx');
D={'@ Cond%100 - Evap"3"'};
temperature(results,D);
pressure(results,D);
mass_flow(results,D);
heat(results,D);
  end
end
tempcompare;
presscompare;
volumetriceffcompare;
heatcompare;
COPcompare;
isentropiceffcompare;
exergeticeffcompare_exergydestruction;
end
%%
function[figure_temperatures]= temperature(results,D) %Function that plots the temperatures
figure_temperatures=figure;
axes1 = axes('Parent',figure_temperatures);
hold(axes1,'all');
%%
compout_condin =plot(results(:,1),results(:,2));
set(compout_condin,'Color','blue','Linewidth',2,'DisplayName','Comp Outlet-Cond Inlet');
%%
condout =plot(results(:,1),results(:,4));
set(condout,'Color','yellow','Linewidth',2,'DisplayName','Cond Outlet');
%%
exin =plot(results(:,1),results(:,6));
set(exin,'Color','red','Linewidth',2,'DisplayName','Expan Valve Inlet');
%%
exout_evapin =plot(results(:,1),results(:,8));
set(exout_evapin,'Color','green','Linewidth',2,'DisplayName','Expan Valve Outlet-Evap Inlet');
%%
evapout =plot(results(:,1),results(:,10));
set(evapout,'Color','black','Linewidth',2,'DisplayName','Evap Outlet');
%%
compin =plot(results(:,1),results(:,12));
set(compin,'Color','magenta','Linewidth',2,'DisplayName','Comp Inlet');
%%
L=legend(axes1,'show');
set(L,'FontSize',12,'fontWeight','bold');
xlabel('Time (sec)');
set(axes1,'XLim',[0 650]);
set(axes1,'XTick',0:50:650);
ylabel('Temperatures (°C)');
title(['\bf Time vs Temperatures', D]);
set(findall(axes1,'type','text'),'fontSize',16,'fontWeight','bold','FontName','Times New Roman');
```

```
colormap cool;
grid on;
   end
%%
function[figure_pressure]= pressure(results,D) % Function that plots the pressures
figure_pressure=figure;
axes2 = axes('Parent',figure_pressure);
hold(axes2,'all');
%%
compout_condin =plot(results(:,1),results(:,3));
set(compout_condin,'Color','blue','Linewidth',2,'DisplayName','Comp Outlet-Cond Inlet');
%%
condout =plot(results(:,1),results(:,5));
set(condout,'Color','yellow','Linewidth',2,'DisplayName','Cond Outlet');
%%
exin =plot(results(:,1),results(:,7));
set(exin,'Color','red','Linewidth',2,'DisplayName','Expan Valve Inlet');
%%
exout_evapin =plot(results(:,1),results(:,9));
set(exout_evapin,'Color','green','Linewidth',2,'DisplayName','Expan Valve Outlet-Evap Inlet');
%%
evapout =plot(results(:,1),results(:,11));
set(evapout,'Color','black','Linewidth',2,'DisplayName','Evap Outlet');
%%
compin =plot(results(:,1),results(:,13));
set(compin,'Color','magenta','Linewidth',2,'DisplayName','Comp Inlet');
hold on;
%%
L=legend(axes2,'show');
set(L,'FontSize',12,'fontWeight','bold');
xlabel('Time (sec)');
set(axes2,'XLim',[0 650]);
set(axes2,'XTick',0:50:650);
ylabel('Pressures (kPa)');
title(['\bf Time vs Pressures', D,]);
set(findall(axes2,'type','text'),'fontSize',16,'fontWeight','bold','FontName','Times New Roman');
colormap cool;
grid on;
   end
%%
function[mass_gas,mass_liquid]= mass_flow(results,D) % Function that plots the mass flow rates
figure_mass=figure;
axes3 = axes('Parent',figure_mass);
hold(axes3,'all');
%%
mass_gas =plot(results(:,1),results(:,14));
set(mass_gas,'Color','blue','Linewidth',2,'DisplayName','Vapor Mass Flow Rate');
%%
mass_liquid =plot(results(:,1),results(:,15));
set(mass_liquid,'Color','yellow','Linewidth',2,'DisplayName','Liquid Mass Flow Rate');
%%
L=legend(axes3,'show');
set(L,'FontSize',12,'fontWeight','bold');
xlabel('Time (sec)');
ylabel('Mass Flow Rates (kg/s)');
set(axes3,'XLim',[0 650]);
set(axes3,'XTick',0:50:650);
set(axes3,'YLim',[0 0.12]);
set(axes3,'YTick',0:0.01:0.12);
title(['\bf Time vs Mass Flow Rates', D]);
set(findall(axes3,'type','text'),'fontSize',16,'fontWeight','bold','FontName','Times New Roman');
colormap cool;
grid on;
   end
%%
function[figure_heat]= heat(results,D) % Function that calculates and plots the evaporator cooling capacities, condenser heat
rejection rates and compressor works
figure_heat=figure;
axes4 = axes('Parent',figure_heat);
hold(axes4,'all');
[r,c] = size(results); % Size of the matrix (test results excel)
%%
for i=1:1:r
```

```
hevap_in(i,1)=refpropm('H','T',results(i,6)+273,'P',results(i,7),'r134a');
hevap_out(i,1) = refpropm('H','T',results(i,10)+273,'P',results(i,11),'r134a');
EvapCool(i,1)= ((results(i,14)+results(i,15))/2)*(hevap_out(i,1)-hevap_in(i,1));
end
Qevap =plot(results(:,1),EvapCool(:,1)/1000);
set(Qevap,'Color','blue','Linewidth',2,'DisplayName','Evaporator Cooling Capacity');
%%
for i=1:1:r
hcond_in(i,1) = refpropm('H','T',results(i,2)+273,'P',results(i,3),'r134a');
hcond_out(i,1) = refpropm('H','T',results(i,4)+273,'P',results(i,5),'r134a');
CondReject(i,1)= ((results(i,14)+results(i,15))/2)*(hcond_in(i,1)-hcond_out(i,1));
end
Qcond =plot(results(:,1),CondReject(:,1)/1000);
set(Qcond,'Color','red','Linewidth',2,'DisplayName','Condenser Heat Rejection');
%%
for i=1:1:r
hcomp_out(i,1) = refpropm('H','T',results(i,2)+273,'P',results(i,3),'r134a');
hcomp_in(i,1) = refpropm('H','T',results(i,12)+273,'P',results(i,13),'r134a');
Wcomp(i,1)= ((results(i,14)+results(i,15))/2)*(hcomp_out(i,1)-hcomp_in(i,1));
end
Wcomp =plot(results(:,1),Wcomp(:,1)/1000);
set(Wcomp,'Color','green','Linewidth',2,'DisplayName','Compressor Work');
%%
L=legend(axes4,'show');
set(L,'FontSize',12,'fontWeight','bold');
xlabel('Time (sec)');
set(axes4,'XLim',[0 650]);
set(axes4,'XTick',0:50:650);
ylabel('Heat & Work (kW)');
title(['\bf Time vs Heat & Work', D]);
set(findall(axes4,'type','text'),'fontSize',16,'fontWeight','bold','FontName','Times New Roman');
colormap cool;
grid on;
end
%%
function tempcompare % Function that compares and plots the temperatures at each measurement points
result1=xlsread('test_cond50_evap1.xlsx');
result2=xlsread('test_cond50_evap2.xlsx');
result3=xlsread('test_cond50_evap3.xlsx');
result4=xlsread('test_cond100_evap1.xlsx');
result5=xlsread('test_cond100_evap2.xlsx');
result6=xlsread('test_cond100_evap3.xlsx');
%%
tempcompare_compout_condin;
tempcompare_condout;
tempcompare_exin;
tempcompare_exout_evapin;
tempcompare_evapout;
tempcompare_compin;
%%
function[compout_condin1,compout_condin2,compout_condin3,compout_condin4,compout_condin5,compout_condin6]=
tempcompare_compout_condin
figure_tempcompare_compout_condin=figure;
axes5 = axes('Parent',figure_tempcompare_compout_condin);
hold(axes5,'all');
%%
compout_condin1 =plot(result1(:,1),result1(:,2));
set(compout_condin1,'Color','blue','Linewidth',2,'DisplayName','Cond%50 - Evap1');
%%
compout_condin2 =plot(result2(:,1),result2(:,2));
set(compout_condin2,'Color','yellow','Linewidth',2,'DisplayName','Cond%50 - Evap2');
%%
compout_condin3 =plot(result3(:,1),result3(:,2));
set(compout_condin3,'Color','red','Linewidth',2,'DisplayName','Cond%50 - Evap3');
%%
compout_condin4 =plot(result4(:,1),result4(:,2));
set(compout_condin4,'Color','green','Linewidth',2,'DisplayName','Cond%100 - Evap1');
%%
compout_condin5 =plot(result5(:,1),result5(:,2));
set(compout_condin5,'Color','black','Linewidth',2,'DisplayName','Cond%100 - Evap2');
%%
compout_condin6 =plot(result6(:,1),result6(:,2));
set(compout_condin6,'Color','magenta','Linewidth',2,'DisplayName','Cond%100 - Evap3');
```

```
%%
L=legend(axes5,'show');
xlabel('Time (sec)');
ylabel('Compressor Outlet-Condenser Inlet (°C)');
title('\bf Time vs Temperatures');
set(L,'FontSize',12,'fontWeight','bold');
set(axes5,'XLim',[0 650]);
set(axes5,'XTick',0:50:650);
set(findall(axes5,'type','text'),'fontSize',16,'fontWeight','bold','FontName','Times New Roman');
colormap cool;
grid on;
end
%%
function[condout1,condout2,condout3,condout4,condout5,condout6]= tempcompare_condout
figure_tempcompare_condout=figure;
axes6 = axes('Parent',figure_tempcompare_condout);
hold(axes6,'all');
%%
condout1 =plot(result1(:,1),result1(:,4));
set(condout1,'Color','blue','Linewidth',2,'DisplayName','Cond%50 - Evap1');
%%
condout2 =plot(result2(:,1),result2(:,4));
set(condout2,'Color','yellow','Linewidth',2,'DisplayName','Cond%50 - Evap2');
%%
condout3 =plot(result3(:,1),result3(:,4));
set(condout3,'Color','red','Linewidth',2,'DisplayName','Cond%50 - Evap3');
%%
condout4 =plot(result4(:,1),result4(:,4));
set(condout4,'Color','green','Linewidth',2,'DisplayName','Cond%100 - Evap1');
%%
condout5 =plot(result5(:,1),result5(:,4));
set(condout5,'Color','black','Linewidth',2,'DisplayName','Cond%100 - Evap2');
%%
condout6 =plot(result6(:,1),result6(:,4));
set(condout6,'Color','magenta','Linewidth',2,'DisplayName','Cond%100 - Evap3');
%%
L=legend(axes6,'show');
xlabel('Time (sec)');
ylabel('Condenser Outlet (°C)');
title('\bf Time vs Temperatures');
set(L,'FontSize',12,'fontWeight','bold');
set(axes6,'XLim',[0 650]);
set(axes6,'XTick',0:50:650);
set(findall(axes6,'type','text'),'fontSize',16,'fontWeight','bold','FontName','Times New Roman');
colormap cool;
grid on;
end
%%
function[exin1,exin2,exin3,exin4,exin5,exin6]= tempcompare_exin
figure_tempcompare_exin=figure;
axes7 = axes('Parent',figure_tempcompare_exin);
hold(axes7,'all');
%%
exin1 =plot(result1(:,1),result1(:,6));
set(exin1,'Color','blue','Linewidth',2,'DisplayName','Cond%50 - Evap1');
%%
exin2 =plot(result2(:,1),result2(:,6));
set(exin2,'Color','yellow','Linewidth',2,'DisplayName','Cond%50 - Evap2');
%%
exin3 =plot(result3(:,1),result3(:,6));
set(exin3,'Color','red','Linewidth',2,'DisplayName','Cond%50 - Evap3');
%%
exin4 =plot(result4(:,1),result4(:,6));
set(exin4,'Color','green','Linewidth',2,'DisplayName','Cond%100 - Evap1');
%%
exin5 =plot(result5(:,1),result5(:,6));
set(exin5,'Color','black','Linewidth',2,'DisplayName','Cond%100 - Evap2');
%%
exin6 =plot(result6(:,1),result6(:,6));
set(exin6,'Color','magenta','Linewidth',2,'DisplayName','Cond%100 - Evap3');
%%
L=legend(axes7,'show');
xlabel('Time (sec)');
```

```
ylabel('Expansion Valve Inlet (°C)');
title('\bf Time vs Temperatures');
set(L,'FontSize',12,'fontWeight','bold');
set(axes7,'XLim',[0 650]);
set(axes7,'XTick',0:50:650);
set(findall(axes7,'type','text'),'fontSize',16,'fontWeight','bold','FontName','Times New Roman');
colormap cool;
grid on;
end
%%
function[exout_evapin1,exout_evapin2,exout_evapin3,exout_evapin4,exout_evapin5,exout_evapin6]=
tempcompare_exout_evapin
figure_tempcompare_exout_evapin=figure;
axes8 = axes('Parent',figure_tempcompare_exout_evapin);
hold(axes8,'all');
%%
exout_evapin1 =plot(result1(:,1),result1(:,8));
set(exout_evapin1,'Color','blue','Linewidth',2,'DisplayName','Cond%50 - Evap1');
%%
exout_evapin2 =plot(result2(:,1),result2(:,8));
set(exout_evapin2,'Color','yellow','Linewidth',2,'DisplayName','Cond%50 - Evap2');
%%
exout_evapin3 =plot(result3(:,1),result3(:,8));
set(exout_evapin3,'Color','red','Linewidth',2,'DisplayName','Cond%50 - Evap3');
%%
exout_evapin4 =plot(result4(:,1),result4(:,8));
set(exout_evapin4,'Color','green','Linewidth',2,'DisplayName','Cond%100 - Evap1');
%%
exout_evapin5 =plot(result5(:,1),result5(:,8));
set(exout_evapin5,'Color','black','Linewidth',2,'DisplayName','Cond%100 - Evap2');
%%
exout_evapin6 =plot(result6(:,1),result6(:,8));
set(exout_evapin6,'Color','magenta','Linewidth',2,'DisplayName','Cond%100 - Evap3');
%%
L=legend(axes8,'show');
xlabel('Time (sec)');
ylabel('Expansion Valve Outlet-Evaporator Inlet (°C)');
title('\bf Time vs Temperatures');
set(L,'FontSize',12,'fontWeight','bold');
set(axes8,'XLim',[0 650]);
set(axes8,'XTick',0:50:650);
set(findall(axes8,'type','text'),'fontSize',16,'fontWeight','bold','FontName','Times New Roman');
colormap cool;
grid on;
end
%%
function[evapout1,evapout2,evapout3,evapout4,evapout5,evapout6]= tempcompare_evapout
figure_tempcompare_evapout=figure;
axes9 = axes('Parent',figure_tempcompare_evapout);
hold(axes9,'all');
%%
evapout1 =plot(result1(:,1),result1(:,10));
set(evapout1,'Color','blue','Linewidth',2,'DisplayName','Cond%50 - Evap1');
%%
evapout2 =plot(result2(:,1),result2(:,10));
set(evapout2,'Color','yellow','Linewidth',2,'DisplayName','Cond%50 - Evap2');
%%
evapout3 =plot(result3(:,1),result3(:,10));
set(evapout3,'Color','red','Linewidth',2,'DisplayName','Cond%50 - Evap3');
%%
evapout4 =plot(result4(:,1),result4(:,10));
set(evapout4,'Color','green','Linewidth',2,'DisplayName','Cond%100 - Evap1');
%%
evapout5 =plot(result5(:,1),result5(:,10));
set(evapout5,'Color','black','Linewidth',2,'DisplayName','Cond%100 - Evap2');
%%
evapout6 =plot(result6(:,1),result6(:,10));
set(evapout6,'Color','magenta','Linewidth',2,'DisplayName','Cond%100 - Evap3');
%%
L=legend(axes9,'show');
xlabel('Time (sec)');
ylabel('Evaporator Outlet (°C)');
title('\bf Time vs Temperatures');
```

```
set(L,'FontSize',12,'fontWeight','bold');
set(axes9,'XLim',[0 650]);
set(axes9,'XTick',0:50:650);
set(findall(axes9,'type','text'),'fontSize',16,'fontWeight','bold','FontName','Times New Roman');
colormap cool;
grid on;
end
%%
function[compin1,compin2,compin3,compin4,compin5,compin6]= tempcompare_compin
figure_tempcompare_compin=figure;
axes10 = axes('Parent',figure_tempcompare_compin);
hold(axes10,'all');
%%
compin1 =plot(result1(:,1),result1(:,12));
set(compin1,'Color','blue','Linewidth',2,'DisplayName','Cond%50 - Evap1');
%%
compin2 =plot(result2(:,1),result2(:,12));
set(compin2,'Color','yellow','Linewidth',2,'DisplayName','Cond%50 - Evap2');
%%
compin3 =plot(result3(:,1),result3(:,12));
set(compin3,'Color','red','Linewidth',2,'DisplayName','Cond%50 - Evap3');
%%
compin4 =plot(result4(:,1),result4(:,12));
set(compin4,'Color','green','Linewidth',2,'DisplayName','Cond%100 - Evap1');
%%
compin5 =plot(result5(:,1),result5(:,12));
set(compin5,'Color','black','Linewidth',2,'DisplayName','Cond%100 - Evap2');
%%
compin6 =plot(result6(:,1),result6(:,12));
set(compin6,'Color','magenta','Linewidth',2,'DisplayName','Cond%100 - Evap3');
%%
L=legend(axes10,'show');
xlabel('Time (sec)');
ylabel('Compressor Inlet (°C)');
title('\bf Time vs Temperatures');
set(L,'FontSize',12,'fontWeight','bold');
set(axes10,'XLim',[0 650]);
set(axes10,'XTick',0:50:650);
set(findall(axes10,'type','text'),'fontSize',16,'fontWeight','bold','FontName','Times New Roman');
colormap cool;
grid on;
end
%%
end
%%
function presscompare % Function that compares and plots the pressures at each measurement points
result1=xlsread('test_cond50_evap1.xlsx');
result2=xlsread('test_cond50_evap2.xlsx');
result3=xlsread('test_cond50_evap3.xlsx');
result4=xlsread('test_cond100_evap1.xlsx');
result5=xlsread('test_cond100_evap2.xlsx');
result6=xlsread('test_cond100_evap3.xlsx');
%%
presscompare_compout_condin;
presscompare_condout;
presscompare_exin;
presscompare_exout_evapin;
presscompare_evapout;
presscompare_compin;
%%
function[compout_condin1,compout_condin2,compout_condin3,compout_condin4,compout_condin5,compout_condin6]=
presscompare_compout_condin
figure_presscompare_compout_condin=figure;
axes11 = axes('Parent',figure_presscompare_compout_condin);
hold(axes11,'all');
%%
compout_condin1 =plot(result1(:,1),result1(:,3));
set(compout_condin1,'Color','blue','Linewidth',2,'DisplayName','Cond%50 - Evap1');
%%
compout_condin2 =plot(result2(:,1),result2(:,3));
set(compout_condin2,'Color','yellow','Linewidth',2,'DisplayName','Cond%50 - Evap2');
%%
compout_condin3 =plot(result3(:,1),result3(:,3));
```

```
set(compout_condin3,'Color','red','Linewidth',2,'DisplayName','Cond%50 - Evap3');
%%
compout_condin4 =plot(result4(:,1),result4(:,3));
set(compout_condin4,'Color','green','Linewidth',2,'DisplayName','Cond%100 - Evap1');
%%
compout_condin5 =plot(result5(:,1),result5(:,3));
set(compout_condin5,'Color','black','Linewidth',2,'DisplayName','Cond%100 - Evap2');
%%
compout_condin6 =plot(result6(:,1),result6(:,3));
set(compout_condin6,'Color','magenta','Linewidth',2,'DisplayName','Cond%100 - Evap3');
%%
L=legend(axes11,'show');
xlabel('Time (sec)');
ylabel('Compressor Outlet-Condenser Inlet (kPa)');
title('\bf Time vs Pressures');
set(L,'FontSize',12,'fontWeight','bold');
set(axes11,'XLim',[0 650]);
set(axes11,'XTick',0:50:650);
set(findall(axes11,'type','text'),'fontSize',16,'fontWeight','bold','FontName','Times New Roman');
colormap cool;
grid on;
end
%%
function[condout1,condout2,condout3,condout4,condout5,condout6]= presscompare_condout
figure_presscompare_condout=figure;
axes12 = axes('Parent',figure_presscompare_condout);
hold(axes12,'all');
%%
condout1 =plot(result1(:,1),result1(:,5));
set(condout1,'Color','blue','Linewidth',2,'DisplayName','Cond%50 - Evap1');
%%
condout2 =plot(result2(:,1),result2(:,5));
set(condout2,'Color','yellow','Linewidth',2,'DisplayName','Cond%50 - Evap2');
%%
condout3 =plot(result3(:,1),result3(:,5));
set(condout3,'Color','red','Linewidth',2,'DisplayName','Cond%50 - Evap3');
%%
condout4 =plot(result4(:,1),result4(:,5));
set(condout4,'Color','green','Linewidth',2,'DisplayName','Cond%100 - Evap1');
%%
condout5 =plot(result5(:,1),result5(:,5));
set(condout5,'Color','black','Linewidth',2,'DisplayName','Cond%100 - Evap2');
%%
condout6 =plot(result6(:,1),result6(:,5));
set(condout6,'Color','magenta','Linewidth',2,'DisplayName','Cond%100 - Evap3');
%%
L=legend(axes12,'show');
xlabel('Time (sec)');
ylabel('Condenser Outlet (kPa)');
title('\bf Time vs Pressures');
set(L,'FontSize',12,'fontWeight','bold');
set(axes12,'XLim',[0 650]);
set(axes12,'XTick',0:50:650);
set(findall(axes12,'type','text'),'fontSize',16,'fontWeight','bold','FontName','Times New Roman');
colormap cool;
grid on;
end
%%
function[exin1,exin2,exin3,exin4,exin5,exin6]= presscompare_exin
figure_presscompare_exin=figure;
axes13 = axes('Parent',figure_presscompare_exin);
hold(axes13,'all');
%%
exin1 =plot(result1(:,1),result1(:,7));
set(exin1,'Color','blue','Linewidth',2,'DisplayName','Cond%50 - Evap1');
%%
exin2 =plot(result2(:,1),result2(:,7));
set(exin2,'Color','yellow','Linewidth',2,'DisplayName','Cond%50 - Evap2');
%%
exin3 =plot(result3(:,1),result3(:,7));
set(exin3,'Color','red','Linewidth',2,'DisplayName','Cond%50 - Evap3');
%%
exin4 =plot(result4(:,1),result4(:,7));
```

```
set(exin4,'Color','green','Linewidth',2,'DisplayName','Cond%100 - Evap1');
%%
exin5 =plot(result5(:,1),result5(:,7));
set(exin5,'Color','black','Linewidth',2,'DisplayName','Cond%100 - Evap2');
%%
exin6 =plot(result6(:,1),result6(:,7));
set(exin6,'Color','magenta','Linewidth',2,'DisplayName','Cond%100 - Evap3');
%%
L=legend(axes13,'show');
xlabel('Time (sec)');
ylabel('Expansion Valve Inlet (kPa)');
title('\bf Time vs Pressures');
set(L,'FontSize',12,'fontWeight','bold');
set(axes13,'XLim',[0 650]);
set(axes13,'XTick',0:50:650);
set(findall(axes13,'type','text'),'fontSize',16,'fontWeight','bold','FontName','Times New Roman');
colormap cool;
grid on;
end
%%
function[exout_evapin1,exout_evapin2,exout_evapin3,exout_evapin4,exout_evapin5,exout_evapin6]=
presscompare_exout_evapin
figure_presscompare_exout_evapin=figure;
axes14 = axes('Parent',figure_presscompare_exout_evapin);
hold(axes14,'all');
%%
exout_evapin1 =plot(result1(:,1),result1(:,9));
set(exout_evapin1,'Color','blue','Linewidth',2,'DisplayName','Cond%50 - Evap1');
%%
exout_evapin2 =plot(result2(:,1),result2(:,9));
set(exout_evapin2,'Color','yellow','Linewidth',2,'DisplayName','Cond%50 - Evap2');
%%
exout_evapin3 =plot(result3(:,1),result3(:,9));
set(exout_evapin3,'Color','red','Linewidth',2,'DisplayName','Cond%50 - Evap3');
%%
exout_evapin4 =plot(result4(:,1),result4(:,9));
set(exout_evapin4,'Color','green','Linewidth',2,'DisplayName','Cond%100 - Evap1');
%%
exout_evapin5 =plot(result5(:,1),result5(:,9));
set(exout_evapin5,'Color','black','Linewidth',2,'DisplayName','Cond%100 - Evap2');
%%
exout_evapin6 =plot(result6(:,1),result6(:,9));
set(exout_evapin6,'Color','magenta','Linewidth',2,'DisplayName','Cond%100 - Evap3');
%%
L=legend(axes14,'show');
xlabel('Time (sec)');
ylabel('Expansion Valve Outlet-Evaporator Inlet (kPa)');
title('\bf Time vs Pressures');
set(L,'FontSize',12,'fontWeight','bold');
set(axes14,'XLim',[0 650]);
set(axes14,'XTick',0:50:650);
set(findall(axes14,'type','text'),'fontSize',16,'fontWeight','bold','FontName','Times New Roman');
colormap cool;
grid on;
end
%%
function[evapout1,evapout2,evapout3,evapout4,evapout5,evapout6]= presscompare_evapout
figure_presscompare_evapout=figure;
axes15 = axes('Parent',figure_presscompare_evapout);
hold(axes15,'all');
%%
evapout1 =plot(result1(:,1),result1(:,11));
set(evapout1,'Color','blue','Linewidth',2,'DisplayName','Cond%50 - Evap1');
%%
evapout2 =plot(result2(:,1),result2(:,11));
set(evapout2,'Color','yellow','Linewidth',2,'DisplayName','Cond%50 - Evap2');
%%
evapout3 =plot(result3(:,1),result3(:,11));
set(evapout3,'Color','red','Linewidth',2,'DisplayName','Cond%50 - Evap3');
%%
evapout4 =plot(result4(:,1),result4(:,11));
set(evapout4,'Color','green','Linewidth',2,'DisplayName','Cond%100 - Evap1');
%%
```

```
evapout5 =plot(result5(:,1),result5(:,11));
set(evapout5,'Color','black','Linewidth',2,'DisplayName','Cond%100 - Evap2');
%%
evapout6 =plot(result6(:,1),result6(:,11));
set(evapout6,'Color','magenta','Linewidth',2,'DisplayName','Cond%100 - Evap3');
%%
L=legend(axes15,'show');
xlabel('Time (sec)');
ylabel('Evaporator Outlet (kPa)');
title('\bf Time vs Pressures');
set(L,'FontSize',12,'fontWeight','bold');
set(axes15,'XLim',[0 650]);
set(axes15,'XTick',0:50:650);
set(findall(axes15,'type','text'),'fontSize',16,'fontWeight','bold','FontName','Times New Roman');
colormap cool;
grid on;
end
%%
function[compin1,compin2,compin3,compin4,compin5,compin6]= presscompare_compin
figure_presscompare_compin=figure;
axes16 = axes('Parent',figure_presscompare_compin);
hold(axes16,'all');
%%
compin1 =plot(result1(:,1),result1(:,13));
set(compin1,'Color','blue','Linewidth',2,'DisplayName','Cond%50 - Evap1');
%%
compin2 =plot(result2(:,1),result2(:,13));
set(compin2,'Color','yellow','Linewidth',2,'DisplayName','Cond%50 - Evap2');
%%
compin3 =plot(result3(:,1),result3(:,13));
set(compin3,'Color','red','Linewidth',2,'DisplayName','Cond%50 - Evap3');
%%
compin4 =plot(result4(:,1),result4(:,13));
set(compin4,'Color','green','Linewidth',2,'DisplayName','Cond%100 - Evap1');
%%
compin5 =plot(result5(:,1),result5(:,13));
set(compin5,'Color','black','Linewidth',2,'DisplayName','Cond%100 - Evap2');
%%
compin6 =plot(result6(:,1),result6(:,13));
set(compin6,'Color','magenta','Linewidth',2,'DisplayName','Cond%100 - Evap3');
%%
L=legend(axes16,'show');
xlabel('Time (sec)');
ylabel('Compressor Inlet (kPa)');
title('\bf Time vs Pressures');
set(L,'FontSize',12,'fontWeight','bold');
set(axes16,'XLim',[0 650]);
set(axes16,'XTick',0:50:650);
set(findall(axes16,'type','text'),'fontSize',16,'fontWeight','bold','FontName','Times New Roman');
colormap cool;
grid on;
end
%%
end
%%
function[figure_volumetriceffcompare]= volumetriceffcompare % Function that compares and plots the volumetric efficiencies
result1=xlsread('test_cond50_evap1.xlsx');
result2=xlsread('test_cond50_evap2.xlsx');
result3=xlsread('test_cond50_evap3.xlsx');
result4=xlsread('test_cond100_evap1.xlsx');
result5=xlsread('test_cond100_evap2.xlsx');
result6=xlsread('test_cond100_evap3.xlsx');
[r,c] = size(result1); % Size of the matrix (test results excel)
m=5; % Assumed percentage value of clearance volume

figure_volumetriceffcompare=figure;
axes17 = axes('Parent',figure_volumetriceffcompare);
hold(axes17,'all');
%%
for i=1:1:r
O11(i,1) = refpropm('O','T',result1(i,12)+273,'P',result1(i,13),'r134a');
C11(i,1) = refpropm('C','T',result1(i,12)+273,'P',result1(i,13),'r134a');
P1comp_out(i,1)=result1(i,3);
```

```
P1comp_in(i,1)=result1(i,13);
volumetric_eff1(i,1)=100-m *((P1comp_out(i,1)/P1comp_in(i,1))^(O11(i,1)/C11(i,1))-1);
end
eff_cond50_evap1 =plot(result1(:,1),volumetric_eff1(:,1));
set(eff_cond50_evap1,'Color','blue','Linewidth',2,'DisplayName','Cond%50 - Evap1');
%%
for i=1:1:r
O21(i,1) = refpropm('O','T',result2(i,12)+273,'P',result2(i,13),'r134a');
C21(i,1) = refpropm('C','T',result2(i,12)+273,'P',result2(i,13),'r134a');
P2comp_out(i,1)=result2(i,3);
P2comp_in(i,1)=result2(i,13);
volumetric_eff2(i,1)=100-m *((P2comp_out(i,1)/P2comp_in(i,1))^(O21(i,1)/C21(i,1))-1);
end
eff_cond50_evap2 =plot(result2(:,1),volumetric_eff2(:,1));
set(eff_cond50_evap2,'Color','yellow','Linewidth',2,'DisplayName','Cond%50 - Evap2');
%%
for i=1:1:r
O31(i,1) = refpropm('O','T',result3(i,12)+273,'P',result3(i,13),'r134a');
C31(i,1) = refpropm('C','T',result3(i,12)+273,'P',result3(i,13),'r134a');
P3comp_out(i,1)=result3(i,3);
P3comp_in(i,1)=result3(i,13);
volumetric_eff3(i,1)=100-m *((P3comp_out(i,1)/P3comp_in(i,1))^(O31(i,1)/C31(i,1))-1);
end
eff_cond50_evap3 =plot(result3(:,1),volumetric_eff3(:,1));
set(eff_cond50_evap3,'Color','red','Linewidth',2,'DisplayName','Cond%50 - Evap3');
%%
for i=1:1:r
O41(i,1) = refpropm('O','T',result4(i,12)+273,'P',result4(i,13),'r134a');
C41(i,1) = refpropm('C','T',result4(i,12)+273,'P',result4(i,13),'r134a');
P4comp_out(i,1)=result4(i,3);
P4comp_in(i,1)=result4(i,13);
volumetric_eff4(i,1)=100-m *((P4comp_out(i,1)/P4comp_in(i,1))^(O41(i,1)/C41(i,1))-1);
end
eff_cond100_evap1 =plot(result4(:,1),volumetric_eff4(:,1));
set(eff_cond100_evap1,'Color','green','Linewidth',2,'DisplayName','Cond%100 - Evap1');
%%
for i=1:1:r
O51(i,1) = refpropm('O','T',result5(i,12)+273,'P',result5(i,13),'r134a');
C51(i,1) = refpropm('C','T',result5(i,12)+273,'P',result5(i,13),'r134a');
P5comp_out(i,1)=result5(i,3);
P5comp_in(i,1)=result5(i,13);
volumetric_eff5(i,1)=100-m *((P5comp_out(i,1)/P5comp_in(i,1))^(O51(i,1)/C51(i,1))-1);
end
eff_cond100_evap2 =plot(result5(:,1),volumetric_eff5(:,1));
set(eff_cond100_evap2,'Color','black','Linewidth',2,'DisplayName','Cond%100 - Evap2');
%%
for i=1:1:r
O61(i,1) = refpropm('O','T',result6(i,12)+273,'P',result6(i,13),'r134a');
C61(i,1) = refpropm('C','T',result6(i,12)+273,'P',result6(i,13),'r134a');
P6comp_out(i,1)=result6(i,3);
P6comp_in(i,1)=result6(i,13);
volumetric_eff6(i,1)=100-m *((P6comp_out(i,1)/P6comp_in(i,1))^(O61(i,1)/C61(i,1))-1);
end
eff_cond100_evap3 =plot(result6(:,1),volumetric_eff6(:,1));
set(eff_cond100_evap3,'Color','magenta','Linewidth',2,'DisplayName','Cond%100 - Evap3');
%%
L=legend(axes17,'show');
xlabel('Time (sec)');
ylabel('Volumetric Efficiencies (%)');
title('\bf Time vs Efficiencies');
set(L,'FontSize',12,'fontWeight','bold');
set(axes17,'XLim',[0 650]);
set(axes17,'XTick',0:50:650);
set(findall(axes17,'type','text'),'fontSize',16,'fontWeight','bold','FontName','Times New Roman');
colormap cool;
grid on;

xlswrite('volumetriceff.xlsx',volumetric_eff1,1,'A1');
xlswrite('volumetriceff.xlsx',volumetric_eff2,1,'B1');
xlswrite('volumetriceff.xlsx',volumetric_eff3,1,'C1');
xlswrite('volumetriceff.xlsx',volumetric_eff4,1,'D1');
xlswrite('volumetriceff.xlsx',volumetric_eff5,1,'E1');
xlswrite('volumetriceff.xlsx',volumetric_eff6,1,'F1');
```

```
end
%%
function heatcompare % Function that compares and plots the evaporator cooling capacities, condenser heat rejection rates and
compressor works for each tests.
result1=xlsread('test_cond50_evap1.xlsx');
result2=xlsread('test_cond50_evap2.xlsx');
result3=xlsread('test_cond50_evap3.xlsx');
result4=xlsread('test_cond100_evap1.xlsx');
result5=xlsread('test_cond100_evap2.xlsx');
result6=xlsread('test_cond100_evap3.xlsx');
%%
heatcompare_evaporator;
heatcompare_condenser;
heatcompare_compressor;

%%
function[figure_heatcompare_evaporator]= heatcompare_evaporator
[r,c] = size(result1); % Size of the matrix (test results excel)
figure_heatcompare_evaporator=figure;
axes18 = axes('Parent',figure_heatcompare_evaporator);
hold(axes18,'all');
%%
for i=1:1:r
hevap_out1(i,1) = refpropm('H','T',result1(i,10)+273,'P',result1(i,11),'r134a');
hexval_in1(i,1)=refpropm('H','T',result1(i,6)+273,'P',result1(i,7),'r134a');
hevap_in1(i,1) = hexval_in1(i,1);
heat_evap1(i,1)= ((result1(i,14)+result1(i,15))/2)*(hevap_out1(i,1)-hevap_in1(i,1));
end
heat_evap11 =plot(result1(:,1),heat_evap1(:,1)/1000);
set(heat_evap11,'Color','blue','Linewidth',2,'DisplayName','Cond%50 - Evap1');
%%
for i=1:1:r
hevap_out2(i,1) = refpropm('H','T',result2(i,10)+273,'P',result2(i,11),'r134a');
hexval_in2(i,1)=refpropm('H','T',result2(i,6)+273,'P',result3(i,7),'r134a');
hevap_in2(i,1) = hexval_in2(i,1);
heat_evap2(i,1)= ((result2(i,14)+result2(i,15))/2)*(hevap_out2(i,1)-hevap_in2(i,1));
end
heat_evap21 =plot(result2(:,1),heat_evap2(:,1)/1000);
set(heat_evap21,'Color','yellow','Linewidth',2,'DisplayName','Cond%50 - Evap2');
%%
for i=1:1:r
hevap_out3(i,1) = refpropm('H','T',result3(i,10)+273,'P',result3(i,11),'r134a');
hexval_in3(i,1)=refpropm('H','T',result3(i,6)+273,'P',result3(i,7),'r134a');
hevap_in3(i,1) = hexval_in3(i,1);
heat_evap3(i,1)= ((result3(i,14)+result3(i,15))/2)*(hevap_out3(i,1)-hevap_in3(i,1));
end
heat_evap31 =plot(result3(:,1),heat_evap3(:,1)/1000);
set(heat_evap31,'Color','red','Linewidth',2,'DisplayName','Cond%50 - Evap3');
%%
for i=1:1:r
hevap_out4(i,1) = refpropm('H','T',result4(i,10)+273,'P',result4(i,11),'r134a');
hexval_in4(i,1)=refpropm('H','T',result4(i,6)+273,'P',result4(i,7),'r134a');
hevap_in4(i,1) = hexval_in4(i,1);
heat_evap4(i,1)= ((result4(i,14)+result4(i,15))/2)*(hevap_out4(i,1)-hevap_in4(i,1));
end
heat_evap41 =plot(result4(:,1),heat_evap4(:,1)/1000);
set(heat_evap41,'Color','green','Linewidth',2,'DisplayName','Cond%100 - Evap1');
%%
for i=1:1:r
hevap_out5(i,1) = refpropm('H','T',result5(i,10)+273,'P',result5(i,11),'r134a');
hexval_in5(i,1)=refpropm('H','T',result5(i,6)+273,'P',result5(i,7),'r134a');
hevap_in5(i,1) = hexval_in5(i,1);
heat_evap5(i,1)= ((result5(i,14)+result5(i,15))/2)*(hevap_out5(i,1)-hevap_in5(i,1));
end
heat_evap51 =plot(result4(:,1),heat_evap5(:,1)/1000);
set(heat_evap51,'Color','black','Linewidth',2,'DisplayName','Cond%100 - Evap2');
%%
for i=1:1:r
hevap_out6(i,1) = refpropm('H','T',result6(i,10)+273,'P',result6(i,11),'r134a');
hexval_in6(i,1)=refpropm('H','T',result6(i,6)+273,'P',result6(i,7),'r134a');
hevap_in6(i,1) = hexval_in6(i,1);
heat_evap6(i,1)= ((result6(i,14)+result6(i,15))/2)*(hevap_out6(i,1)-hevap_in6(i,1));
end
```

```
heat_evap61 =plot(result6(:,1),heat_evap6(:,1)/1000);
set(heat_evap61,'Color','magenta','Linewidth',2,'DisplayName','Cond%100 - Evap3');
%%
L=legend(axes18,'show');
xlabel('Time (sec)');
ylabel('Evaporator Cooling Capacity(kW)');
title('\bf Time vs Heats');
set(L,'FontSize',12,'fontWeight','bold');
set(axes18,'XLim',[0 650]);
set(axes18,'XTick',0:50:650);
set(findall(axes18,'type','text'),'fontSize',16,'fontWeight','bold','FontName','Times New Roman');
colormap cool;
grid on;

xlswrite('evapheat.xlsx',heat_evap1,1,'A1');
xlswrite('evapheat.xlsx',heat_evap2,1,'B1');
xlswrite('evapheat.xlsx',heat_evap3,1,'C1');
xlswrite('evapheat.xlsx',heat_evap4,1,'D1');
xlswrite('evapheat.xlsx',heat_evap5,1,'E1');
xlswrite('evapheat.xlsx',heat_evap6,1,'F1');
end
%%
function[figure_heatcompare_condenser]= heatcompare_condenser
[r,c] = size(result1); % Size of the matrix (test results excel)
figure_heatcompare_condenser=figure;
axes19 = axes('Parent',figure_heatcompare_condenser);
hold(axes19,'all');

for i=1:1:r
hcond_in1(i,1) = refpropm('H','T',result1(i,2)+273,'P',result1(i,3),'r134a');
hcond_out1(i,1) = refpropm('H','T',result1(i,4)+273,'P',result1(i,5),'r134a');
heat_cond1(i,1)= ((result1(i,14)+result1(i,15))/2)*(hcond_in1(i,1)-hcond_out1(i,1));
end
heat_cond11 =plot(result1(:,1),heat_cond1(:,1)/1000);
set(heat_cond11,'Color','blue','Linewidth',2,'DisplayName','Cond%50 - Evap1');
%%
for i=1:1:r
hcond_in2(i,1) = refpropm('H','T',result2(i,2)+273,'P',result2(i,3),'r134a');
hcond_out2(i,1) = refpropm('H','T',result2(i,4)+273,'P',result2(i,5),'r134a');
heat_cond2(i,1)= ((result2(i,14)+result2(i,15))/2)*(hcond_in2(i,1)-hcond_out2(i,1));
end
heat_cond21 =plot(result2(:,1),heat_cond2(:,1)/1000);
set(heat_cond21,'Color','yellow','Linewidth',2,'DisplayName','Cond%50 - Evap2');
%%
for i=1:1:r
hcond_in3(i,1) = refpropm('H','T',result3(i,2)+273,'P',result3(i,3),'r134a');
hcond_out3(i,1) = refpropm('H','T',result3(i,4)+273,'P',result3(i,5),'r134a');
heat_cond3(i,1)= ((result3(i,14)+result3(i,15))/2)*(hcond_in3(i,1)-hcond_out3(i,1));
end
heat_cond31 =plot(result3(:,1),heat_cond3(:,1)/1000);
set(heat_cond31,'Color','red','Linewidth',2,'DisplayName','Cond%50 - Evap3');
%%
for i=1:1:r
hcond_in4(i,1) = refpropm('H','T',result4(i,2)+273,'P',result4(i,3),'r134a');
hcond_out4(i,1) = refpropm('H','T',result4(i,4)+273,'P',result4(i,5),'r134a');
heat_cond4(i,1)= ((result4(i,14)+result4(i,15))/2)*(hcond_in4(i,1)-hcond_out4(i,1));
end
heat_cond41 =plot(result4(:,1),heat_cond4(:,1)/1000);
set(heat_cond41,'Color','green','Linewidth',2,'DisplayName','Cond%100 - Evap1');
%%
for i=1:1:r
hcond_in5(i,1) = refpropm('H','T',result5(i,2)+273,'P',result5(i,3),'r134a');
hcond_out5(i,1) = refpropm('H','T',result5(i,4)+273,'P',result5(i,5),'r134a');
heat_cond5(i,1)= ((result5(i,14)+result5(i,15))/2)*(hcond_in5(i,1)-hcond_out5(i,1));
end
heat_cond51 =plot(result5(:,1),heat_cond5(:,1)/1000);
set(heat_cond51,'Color','black','Linewidth',2,'DisplayName','Cond%100 - Evap2');
%%
for i=1:1:r
hcond_in6(i,1) = refpropm('H','T',result6(i,2)+273,'P',result6(i,3),'r134a');
hcond_out6(i,1) = refpropm('H','T',result6(i,4)+273,'P',result6(i,5),'r134a');
heat_cond6(i,1)= ((result6(i,14)+result6(i,15))/2)*(hcond_in6(i,1)-hcond_out6(i,1));
end
```

```
heat_cond61 =plot(result5(:,1),heat_cond6(:,1)/1000);
set(heat_cond61,'Color','magenta','Linewidth',2,'DisplayName','Cond%100 - Evap3');
%%
L=legend(axes19,'show');
xlabel('Time (sec)');
ylabel('Condenser Heat Rejection (kW)');
title('\bf Time vs Heats');
set(L,'FontSize',12,'fontWeight','bold');
set(axes19,'XLim',[0 650]);
set(axes19,'XTick',0:50:650);
set(findall(axes19,'type','text'),'fontSize',16,'fontWeight','bold','FontName','Times New Roman');
colormap cool;
grid on;

xlswrite('condheat.xlsx',heat_cond1,1,'A1');
xlswrite('condheat.xlsx',heat_cond2,1,'B1');
xlswrite('condheat.xlsx',heat_cond3,1,'C1');
xlswrite('condheat.xlsx',heat_cond4,1,'D1');
xlswrite('condheat.xlsx',heat_cond5,1,'E1');
xlswrite('condheat.xlsx',heat_cond6,1,'F1');
end
%%
function[figure_heatcompare_compressor]= heatcompare_compressor
[r,c] = size(result1); % Size of the matrix (test results excel)
figure_heatcompare_compressor=figure;
axes20 = axes('Parent',figure_heatcompare_compressor);
hold(axes20,'all');

for i=1:1:r
hcomp_out1(i,1) = refpropm('H','T',result1(i,2)+273,'P',result1(i,3),'r134a');
hcomp_in1(i,1) = refpropm('H','T',result1(i,12)+273,'P',result1(i,13),'r134a');
heat_comp1(i,1)= ((result1(i,14)+result1(i,15))/2)*(hcomp_out1(i,1)-hcomp_in1(i,1));
end
heat_comp11 =plot(result1(:,1),heat_comp1(:,1)/1000);
set(heat_comp11,'Color','blue','Linewidth',2,'DisplayName','Cond%50 - Evap1');
%%
for i=1:1:r
hcomp_out2(i,1) = refpropm('H','T',result2(i,2)+273,'P',result2(i,3),'r134a');
hcomp_in2(i,1) = refpropm('H','T',result2(i,12)+273,'P',result2(i,13),'r134a');
heat_comp2(i,1)= ((result2(i,14)+result2(i,15))/2)*(hcomp_out2(i,1)-hcomp_in2(i,1));
end
heat_comp21 =plot(result2(:,1),heat_comp2(:,1)/1000);
set(heat_comp21,'Color','yellow','Linewidth',2,'DisplayName','Cond%50 - Evap2');
%%
for i=1:1:r
hcomp_out3(i,1) = refpropm('H','T',result3(i,2)+273,'P',result3(i,3),'r134a');
hcomp_in3(i,1) = refpropm('H','T',result3(i,12)+273,'P',result3(i,13),'r134a');
heat_comp3(i,1)= ((result3(i,14)+result3(i,15))/2)*(hcomp_out3(i,1)-hcomp_in3(i,1));
end
heat_comp31 =plot(result3(:,1),heat_comp3(:,1)/1000);
set(heat_comp31,'Color','red','Linewidth',2,'DisplayName','Cond%50 - Evap3');
%%
for i=1:1:r
hcomp_out4(i,1) = refpropm('H','T',result4(i,2)+273,'P',result4(i,3),'r134a');
hcomp_in4(i,1) = refpropm('H','T',result4(i,12)+273,'P',result4(i,13),'r134a');
heat_comp4(i,1)= ((result4(i,14)+result4(i,15))/2)*(hcomp_out4(i,1)-hcomp_in4(i,1));
end
heat_comp41 =plot(result4(:,1),heat_comp4(:,1)/1000);
set(heat_comp41,'Color','green','Linewidth',2,'DisplayName','Cond%100 - Evap1');
%%
for i=1:1:r
hcomp_out5(i,1) = refpropm('H','T',result5(i,2)+273,'P',result5(i,3),'r134a');
hcomp_in5(i,1) = refpropm('H','T',result5(i,12)+273,'P',result5(i,13),'r134a');
heat_comp5(i,1)= ((result5(i,14)+result5(i,15))/2)*(hcomp_out5(i,1)-hcomp_in5(i,1));
end
heat_comp51 =plot(result5(:,1),heat_comp5(:,1)/1000);
set(heat_comp51,'Color','black','Linewidth',2,'DisplayName','Cond%100 - Evap2');
%%
for i=1:1:r
hcomp_out6(i,1) = refpropm('H','T',result6(i,2)+273,'P',result6(i,3),'r134a');
hcomp_in6(i,1) = refpropm('H','T',result6(i,12)+273,'P',result6(i,13),'r134a');
heat_comp6(i,1)= ((result6(i,14)+result6(i,15))/2)*(hcomp_out6(i,1)-hcomp_in6(i,1));
end
```

```
heat_comp61 =plot(result6(:,1),heat_comp6(:,1)/1000);
set(heat_comp61,'Color','magenta','Linewidth',2,'DisplayName','Cond%100 - Evap3');
%%
L=legend(axes20,'show');
xlabel('Time (sec)');
ylabel('Compressor Work (kW)');
title('\bf Time vs Works');
set(L,'FontSize',12,'fontWeight','bold');
set(axes20,'XLim',[0 650]);
set(axes20,'XTick',0:50:650);
set(findall(axes20,'type','text'),'fontSize',16,'fontWeight','bold','FontName','Times New Roman');
colormap cool;
grid on;

xlswrite('compwork.xlsx',heat_comp1,1,'A1');
xlswrite('compwork.xlsx',heat_comp2,1,'B1');
xlswrite('compwork.xlsx',heat_comp3,1,'C1');
xlswrite('compwork.xlsx',heat_comp4,1,'D1');
xlswrite('compwork.xlsx',heat_comp5,1,'E1');
xlswrite('compwork.xlsx',heat_comp6,1,'F1');

end
%%
end
%%
function[figure_COPcompare]= COPcompare % Function that compares and plots the COP values
result1=xlsread('test_cond50_evap1.xlsx');
result2=xlsread('test_cond50_evap2.xlsx');
result3=xlsread('test_cond50_evap3.xlsx');
result4=xlsread('test_cond100_evap1.xlsx');
result5=xlsread('test_cond100_evap2.xlsx');
result6=xlsread('test_cond100_evap3.xlsx');

[r,c] = size(result1); % Size of the matrix (test results excel)
figure_COPcompare=figure;
axes21 = axes('Parent',figure_COPcompare);
hold(axes21,'all');

for i=1:1:r
comp_out1(i,1) = refpropm('H','T',result1(i,2)+273,'P',result1(i,3),'r134a');
comp_in1(i,1) = refpropm('H','T',result1(i,12)+273,'P',result1(i,13),'r134a');
evap_out1(i,1) = refpropm('H','T',result1(i,10)+273,'P',result1(i,11),'r134a');
exval_in1(i,1)=refpropm('H','T',result1(i,6)+273,'P',result1(i,7),'r134a');
evap_in1(i,1) = exval_in1(i,1);
COP1(i,1) = (evap_out1(i,1)-evap_in1(i,1))/(comp_out1(i,1)-comp_in1(i,1));
end
COP11 =plot(result1(:,1),COP1(:,1));
set(COP11,'Color','blue','Linewidth',2,'DisplayName','Cond%50 - Evap1');
%%
for i=1:1:r
comp_out2(i,1) = refpropm('H','T',result2(i,2)+273,'P',result2(i,3),'r134a');
comp_in2(i,1) = refpropm('H','T',result2(i,12)+273,'P',result2(i,13),'r134a');
evap_out2(i,1) = refpropm('H','T',result2(i,10)+273,'P',result2(i,11),'r134a');
exval_in2(i,1)=refpropm('H','T',result2(i,6)+273,'P',result2(i,7),'r134a');
evap_in2(i,1) = exval_in2(i,1);
COP2(i,1) = (evap_out2(i,1)-evap_in2(i,1))/(comp_out2(i,1)-comp_in2(i,1));
end
COP22 =plot(result2(:,1),COP2(:,1));
set(COP22,'Color','yellow','Linewidth',2,'DisplayName','Cond%50 - Evap2');
%%
for i=1:1:r
comp_out3(i,1) = refpropm('H','T',result3(i,2)+273,'P',result3(i,3),'r134a');
comp_in3(i,1) = refpropm('H','T',result3(i,12)+273,'P',result3(i,13),'r134a');
evap_out3(i,1) = refpropm('H','T',result3(i,10)+273,'P',result3(i,11),'r134a');
exval_in3(i,1)=refpropm('H','T',result3(i,6)+273,'P',result3(i,7),'r134a');
evap_in3(i,1) = exval_in3(i,1);
COP3(i,1) = (evap_out3(i,1)-evap_in3(i,1))/(comp_out3(i,1)-comp_in3(i,1));
end
COP33 =plot(result3(:,1),COP3(:,1));
set(COP33,'Color','red','Linewidth',2,'DisplayName','Cond%50 - Evap3');
%%
for i=1:1:r
comp_out4(i,1) = refpropm('H','T',result4(i,2)+273,'P',result4(i,3),'r134a');
```

```
comp_in4(i,1) = refpropm('H','T',result4(i,12)+273,'P',result4(i,13),'r134a');
evap_out4(i,1) = refpropm('H','T',result4(i,10)+273,'P',result4(i,11),'r134a');
exval_in4(i,1)=refpropm('H','T',result4(i,6)+273,'P',result4(i,7),'r134a');
evap_in4(i,1) = exval_in4(i,1);
COP4(i,1) = (evap_out4(i,1)-evap_in4(i,1))/(comp_out4(i,1)-comp_in4(i,1));
end
COP44 =plot(result4(:,1),COP4(:,1));
set(COP44,'Color','green','Linewidth',2,'DisplayName','Cond%100 - Evap1');
%%
for i=1:1:r
comp_out5(i,1) = refpropm('H','T',result5(i,2)+273,'P',result5(i,3),'r134a');
comp_in5(i,1) = refpropm('H','T',result5(i,12)+273,'P',result5(i,13),'r134a');
evap_out5(i,1) = refpropm('H','T',result5(i,10)+273,'P',result5(i,11),'r134a');
exval_in5(i,1)=refpropm('H','T',result5(i,6)+273,'P',result5(i,7),'r134a');
evap_in5(i,1) = exval_in5(i,1);
COP5(i,1) = (evap_out5(i,1)-evap_in5(i,1))/(comp_out5(i,1)-comp_in5(i,1));
end
COP55 =plot(result5(:,1),COP5(:,1));
set(COP55,'Color','black','Linewidth',2,'DisplayName','Cond%100 - Evap2');
%%
for i=1:1:r
comp_out6(i,1) = refpropm('H','T',result6(i,2)+273,'P',result6(i,3),'r134a');
comp_in6(i,1) = refpropm('H','T',result6(i,12)+273,'P',result6(i,13),'r134a');
evap_out6(i,1) = refpropm('H','T',result6(i,10)+273,'P',result6(i,11),'r134a');
exval_in6(i,1)=refpropm('H','T',result6(i,6)+273,'P',result6(i,7),'r134a');
evap_in6(i,1) = exval_in6(i,1);
COP6(i,1) = (evap_out6(i,1)-evap_in6(i,1))/(comp_out6(i,1)-comp_in6(i,1));
end
COP66 =plot(result6(:,1),COP6(:,1));
set(COP66,'Color','magenta','Linewidth',2,'DisplayName','Cond%100 - Evap3');
%%
L=legend(axes21,'show');
xlabel('Time (sec)');
ylabel('COP');
title('\bf Time vs COP');
set(L,'FontSize',12,'fontWeight','bold');
set(axes21,'XLim',[0 650]);
set(axes21,'XTick',0:50:650);
set(findall(axes21,'type','text'),'fontSize',16,'fontWeight','bold','FontName','Times New Roman');
colormap cool;
grid on;

xlswrite('COP.xlsx',COP1,1,'A1');
xlswrite('COP.xlsx',COP2,1,'B1');
xlswrite('COP.xlsx',COP3,1,'C1');
xlswrite('COP.xlsx',COP4,1,'D1');
xlswrite('COP.xlsx',COP5,1,'E1');
xlswrite('COP.xlsx',COP6,1,'F1');
end
%%
function[figure_isentropiceffcompare]= isentropiceffcompare % Function that compares and plots the isentropic efficiencies

result1=xlsread('test_cond50_evap1.xlsx');
result2=xlsread('test_cond50_evap2.xlsx');
result3=xlsread('test_cond50_evap3.xlsx');
result4=xlsread('test_cond100_evap1.xlsx');
result5=xlsread('test_cond100_evap2.xlsx');
result6=xlsread('test_cond100_evap3.xlsx');
[r,c] = size(result1); % Size of the matrix (test results excel)

figure_isentropiceffcompare=figure;
axes22 = axes('Parent',figure_isentropiceffcompare);
hold(axes22,'all');
%%
for i=1:1:r
H11_actual(i,1) = refpropm('H','T',result1(i,12)+273,'P',result1(i,13),'r134a');
S11_actual(i,1) = refpropm('S','T',result1(i,12)+273,'P',result1(i,13),'r134a');
H12_actual(i,1) = refpropm('H','T',result1(i,2)+273,'P',result1(i,3),'r134a');
H12_ideal(i,1) = refpropm('H','P',result1(i,3),'S',S11_actual(i,1),'r134a');
isentropic_eff1(i,1)=(H12_ideal(i,1)-H11_actual(i,1))/(H12_actual(i,1)-H11_actual(i,1))*100;
end
iseneff_cond50_evap1 =plot(result1(:,1),isentropic_eff1(:,1));
set(iseneff_cond50_evap1,'Color','blue','Linewidth',2,'DisplayName','Cond%50 - Evap1');
```

```
%%
for i=1:1:r
H21_actual(i,1) = refpropm('H','T',result2(i,12)+273,'P',result2(i,13),'r134a');
S21_actual(i,1) = refpropm('S','T',result2(i,12)+273,'P',result2(i,13),'r134a');
H22_actual(i,1) = refpropm('H','T',result2(i,2)+273,'P',result2(i,3),'r134a');
H22_ideal(i,1) = refpropm('H','P',result2(i,3),'S',S21_actual(i,1),'r134a');
isentropic_eff2(i,1)=(H22_ideal(i,1)-H21_actual(i,1))/(H22_actual(i,1)-H21_actual(i,1))*100;
end
iseneff_cond50_evap2 =plot(result2(:,1),isentropic_eff2(:,1));
set(iseneff_cond50_evap2,'Color','yellow','Linewidth',2,'DisplayName','Cond%50 - Evap2');
%%
for i=1:1:r
H31_actual(i,1) = refpropm('H','T',result3(i,12)+273,'P',result3(i,13),'r134a');
S31_actual(i,1) = refpropm('S','T',result3(i,12)+273,'P',result3(i,13),'r134a');
H32_actual(i,1) = refpropm('H','T',result3(i,2)+273,'P',result3(i,3),'r134a');
H32_ideal(i,1) = refpropm('H','P',result3(i,3),'S',S31_actual(i,1),'r134a');
isentropic_eff3(i,1)=(H32_ideal(i,1)-H31_actual(i,1))/(H32_actual(i,1)-H31_actual(i,1))*100;
end
iseneff_cond50_evap3 =plot(result3(:,1),isentropic_eff3(:,1));
set(iseneff_cond50_evap3,'Color','red','Linewidth',2,'DisplayName','Cond%50 - Evap3');
%%
for i=1:1:r
H41_actual(i,1) = refpropm('H','T',result4(i,12)+273,'P',result4(i,13),'r134a');
S41_actual(i,1) = refpropm('S','T',result4(i,12)+273,'P',result4(i,13),'r134a');
H42_actual(i,1) = refpropm('H','T',result4(i,2)+273,'P',result4(i,3),'r134a');
H42_ideal(i,1) = refpropm('H','P',result4(i,3),'S',S41_actual(i,1),'r134a');
isentropic_eff4(i,1)=(H42_ideal(i,1)-H41_actual(i,1))/(H42_actual(i,1)-H41_actual(i,1))*100;
end
iseneff_cond100_evap1 =plot(result4(:,1),isentropic_eff4(:,1));
set(iseneff_cond100_evap1,'Color','green','Linewidth',2,'DisplayName','Cond%100 - Evap1');
%%
for i=1:1:r
H51_actual(i,1) = refpropm('H','T',result5(i,12)+273,'P',result5(i,13),'r134a');
S51_actual(i,1) = refpropm('S','T',result5(i,12)+273,'P',result5(i,13),'r134a');
H52_actual(i,1) = refpropm('H','T',result5(i,2)+273,'P',result5(i,3),'r134a');
H52_ideal(i,1) = refpropm('H','P',result5(i,3),'S',S51_actual(i,1),'r134a');
isentropic_eff5(i,1)=(H52_ideal(i,1)-H51_actual(i,1))/(H52_actual(i,1)-H51_actual(i,1))*100;
end
iseneff_cond100_evap2 =plot(result5(:,1),isentropic_eff5(:,1));
set(iseneff_cond100_evap2,'Color','black','Linewidth',2,'DisplayName','Cond%100 - Evap2');
%%
for i=1:1:r
H61_actual(i,1) = refpropm('H','T',result6(i,12)+273,'P',result6(i,13),'r134a');
S61_actual(i,1) = refpropm('S','T',result6(i,12)+273,'P',result6(i,13),'r134a');
H62_actual(i,1) = refpropm('H','T',result6(i,2)+273,'P',result6(i,3),'r134a');
H62_ideal(i,1) = refpropm('H','P',result6(i,3),'S',S61_actual(i,1),'r134a');
isentropic_eff6(i,1)=(H62_ideal(i,1)-H61_actual(i,1))/(H62_actual(i,1)-H61_actual(i,1))*100;
end
iseneff_cond100_evap3 =plot(result6(:,1),isentropic_eff6(:,1));
set(iseneff_cond100_evap3,'Color','magenta','Linewidth',2,'DisplayName','Cond%100 - Evap3');
%%
L=legend(axes22,'show');
xlabel('Time (sec)');
ylabel('Isentropic Efficiencies (%)');
title('\bf Time vs Efficiencies');
set(L,'FontSize',12,'fontWeight','bold');
set(axes22,'XLim',[0 650]);
set(axes22,'XTick',0:50:650);
set(findall(axes22,'type','text'),'fontSize',16,'fontWeight','bold','FontName','Times New Roman');
colormap cool;
grid on;

xlswrite('isentropiceff.xlsx',isentropic_eff1,1,'A1');
xlswrite('isentropiceff.xlsx',isentropic_eff2,1,'B1');
xlswrite('isentropiceff.xlsx',isentropic_eff3,1,'C1');
xlswrite('isentropiceff.xlsx',isentropic_eff4,1,'D1');
xlswrite('isentropiceff.xlsx',isentropic_eff5,1,'E1');
xlswrite('isentropiceff.xlsx',isentropic_eff6,1,'F1');
end
%%
function[figure_exergeticeffcompare,figure_exerdest]= exergeticeffcompare_exergydestruction % Function that compares and plots the exergy destructions and relevant exergetic efficiencies
```

```
result1=xlsread('test_cond50_evap1.xlsx');
result2=xlsread('test_cond50_evap2.xlsx');
result3=xlsread('test_cond50_evap3.xlsx');
result4=xlsread('test_cond100_evap1.xlsx');
result5=xlsread('test_cond100_evap2.xlsx');
result6=xlsread('test_cond100_evap3.xlsx');
[r,c] = size(result1); % Size of the matrix (test results excel)
T0=33+273;

figure_exergeticeffcompare=figure;
axes24 = axes('Parent',figure_exergeticeffcompare);
hold(axes24,'all');

%%
for i=1:1:r
mr_1(i,1)=(result1(i,14)+result1(i,15))/2;
hexval_in_1(i,1)=refpropm('H','T',result1(i,6)+273,'P',result1(i,7),'r134a');
hevap_in_1(i,1) = hexval_in_1(i,1);
hevap_out_1(i,1) = refpropm('H','T',result1(i,10)+273,'P',result1(i,11),'r134a');
sevap_in_1(i,1) = refpropm('S','H',hevap_in_1(i,1),'P',result1(i,9),'r134a');
sevap_out_1(i,1) = refpropm('S','T',result1(i,10)+273,'P',result1(i,11),'r134a');
hcomp_in_1(i,1) = refpropm('H','T',result1(i,12)+273,'P',result1(i,13),'r134a');
hcomp_out_1(i,1) = refpropm('H','T',result1(i,2)+273,'P',result1(i,3),'r134a');
scomp_in_1(i,1) = refpropm('S','T',result1(i,12)+273,'P',result1(i,13),'r134a');
scomp_out_1(i,1) = refpropm('S','T',result1(i,2)+273,'P',result1(i,3),'r134a');
hcond_in_1(i,1) = refpropm('H','T',result1(i,2)+273,'P',result1(i,3),'r134a');
hcond_out_1(i,1) = refpropm('H','T',result1(i,4)+273,'P',result1(i,5),'r134a');
scond_in_1(i,1) = refpropm('S','T',result1(i,2)+273,'P',result1(i,3),'r134a');
scond_out_1(i,1) = refpropm('S','T',result1(i,4)+273,'P',result1(i,5),'r134a');
sexval_in_1(i,1) = refpropm('S','T',result1(i,6)+273,'P',result1(i,7),'r134a');
sexval_out_1(i,1) = refpropm('S','H',hevap_in_1(i,1),'P',result1(i,9),'r134a');
xevap_1(i,1)=T0*(mr_1(i,1)*(hevap_in_1(i,1)-hevap_out_1(i,1))/T0+mr_1(i,1)*(sevap_out_1(i,1)-sevap_in_1(i,1)));
xcomp_1(i,1)=T0*mr_1(i,1)*(scomp_out_1(i,1)-scomp_in_1(i,1));
xcond_1(i,1)=T0*(mr_1(i,1)*(hcond_in_1(i,1)-hcond_out_1(i,1))/T0+mr_1(i,1)*(scond_out_1(i,1)-scond_in_1(i,1)));
xexval_1(i,1)=mr_1(i,1)*T0*(sexval_out_1(i,1)-sexval_in_1(i,1));
xt_1(i,1)= xevap_1(i,1)+xcomp_1(i,1)+xcond_1(i,1)+xexval_1(i,1);
Wcomp_1(i,1)= mr_1(i,1)*(hcomp_out_1(i,1)-hcomp_in_1(i,1));
exergetic_eff_1(i,1)= (1-xt_1(i,1)/Wcomp_1(i,1))*100 ;
end
exer_eff_1_cond50_evap1 =plot(result1(:,1),exergetic_eff_1(:,1));
set(exer_eff_1_cond50_evap1,'Color','blue','Linewidth',2,'DisplayName','Cond%50 - Evap1');
%%
for i=1:1:r
mr_2(i,1)=(result2(i,14)+result2(i,15))/2;
hexval_in_2(i,1)=refpropm('H','T',result2(i,6)+273,'P',result2(i,7),'r134a');
hevap_in_2(i,1) = hexval_in_2(i,1);
hevap_out_2(i,1) = refpropm('H','T',result2(i,10)+273,'P',result2(i,11),'r134a');
sevap_in_2(i,1) = refpropm('S','H',hexval_in_2(i,1),'P',result2(i,9),'r134a');
sevap_out_2(i,1) = refpropm('S','T',result2(i,10)+273,'P',result2(i,11),'r134a');
hcomp_in_2(i,1) = refpropm('H','T',result2(i,12)+273,'P',result2(i,13),'r134a');
hcomp_out_2(i,1) = refpropm('H','T',result2(i,2)+273,'P',result2(i,3),'r134a');
scomp_in_2(i,1) = refpropm('S','T',result2(i,12)+273,'P',result2(i,13),'r134a');
scomp_out_2(i,1) = refpropm('S','T',result2(i,2)+273,'P',result2(i,3),'r134a');
hcond_in_2(i,1) = refpropm('H','T',result2(i,2)+273,'P',result2(i,3),'r134a');
hcond_out_2(i,1) = refpropm('H','T',result2(i,4)+273,'P',result2(i,5),'r134a');
scond_in_2(i,1) = refpropm('S','T',result2(i,2)+273,'P',result2(i,3),'r134a');
scond_out_2(i,1) = refpropm('S','T',result2(i,4)+273,'P',result2(i,5),'r134a');
sexval_in_2(i,1) = refpropm('S','T',result2(i,6)+273,'P',result2(i,7),'r134a');
sexval_out_2(i,1) = refpropm('S','H',hexval_in_2(i,1),'P',result2(i,9),'r134a');
xevap_2(i,1)=T0*(mr_2(i,1)*(hevap_in_2(i,1)-hevap_out_2(i,1))/T0+mr_2(i,1)*(sevap_out_2(i,1)-sevap_in_2(i,1)));
xcomp_2(i,1)=T0*mr_2(i,1)*(scomp_out_2(i,1)-scomp_in_2(i,1));
xcond_2(i,1)=T0*(mr_2(i,1)*(hcond_in_2(i,1)-hcond_out_2(i,1))/T0+mr_2(i,1)*(scond_out_2(i,1)-scond_in_2(i,1)));
xexval_2(i,1)=mr_2(i,1)*T0*(sexval_out_2(i,1)-sexval_in_2(i,1));
xt_2(i,1)= xevap_2(i,1)+xcomp_2(i,1)+xcond_2(i,1)+xexval_2(i,1);
Wcomp_2(i,1)= mr_2(i,1)*(hcomp_out_2(i,1)-hcomp_in_2(i,1));
exergetic_eff_2(i,1)= (1-xt_2(i,1)/Wcomp_2(i,1))*100 ;
end
exer_eff_2_cond50_evap2 =plot(result2(:,1),exergetic_eff_2(:,1));
set(exer_eff_2_cond50_evap2,'Color','yellow','Linewidth',2,'DisplayName','Cond%50 - Evap2');
%%
for i=1:1:r
mr_3(i,1)=(result3(i,14)+result3(i,15))/2;
hexval_in_3(i,1)=refpropm('H','T',result3(i,6)+273,'P',result3(i,7),'r134a');
```

```
hevap_in_3(i,1) = hexval_in_3(i,1);
hevap_out_3(i,1) = refpropm('H','T',result3(i,10)+273,'P',result3(i,11),'r134a');
sevap_in_3(i,1) = refpropm('S','H',hevap_in_3(i,1),'P',result3(i,9),'r134a');
sevap_out_3(i,1) = refpropm('S','T',result3(i,10)+273,'P',result3(i,11),'r134a');
hcomp_in_3(i,1) = refpropm('H','T',result3(i,12)+273,'P',result3(i,13),'r134a');
hcomp_out_3(i,1) = refpropm('H','T',result3(i,2)+273,'P',result3(i,3),'r134a');
scomp_in_3(i,1) = refpropm('S','T',result3(i,12)+273,'P',result3(i,13),'r134a');
scomp_out_3(i,1) = refpropm('S','T',result3(i,2)+273,'P',result3(i,3),'r134a');
hcond_in_3(i,1) = refpropm('H','T',result3(i,2)+273,'P',result3(i,3),'r134a');
hcond_out_3(i,1) = refpropm('H','T',result3(i,4)+273,'P',result3(i,5),'r134a');
scond_in_3(i,1) = refpropm('S','T',result3(i,2)+273,'P',result3(i,3),'r134a');
scond_out_3(i,1) = refpropm('S','T',result3(i,4)+273,'P',result3(i,5),'r134a');
sexval_in_3(i,1) = refpropm('S','T',result3(i,6)+273,'P',result3(i,7),'r134a');
sexval_out_3(i,1) = refpropm('S','H',hevap_in_3(i,1),'P',result3(i,9),'r134a');
xevap_3(i,1)=T0*(mr_3(i,1)*(hevap_in_3(i,1)-hevap_out_3(i,1))/T0+mr_3(i,1)*(sevap_out_3(i,1)-sevap_in_3(i,1)));
xcomp_3(i,1)=T0*mr_3(i,1)*(scomp_out_3(i,1)-scomp_in_3(i,1));
xcond_3(i,1)=T0*(mr_3(i,1)*(hcond_in_3(i,1)-hcond_out_3(i,1))/T0+mr_3(i,1)*(scond_out_3(i,1)-scond_in_3(i,1)));
xexval_3(i,1)=mr_3(i,1)*T0*(sexval_out_3(i,1)-sexval_in_3(i,1));
xt_3(i,1)= xevap_3(i,1)+xcomp_3(i,1)+xcond_3(i,1)+xexval_3(i,1);
Wcomp_3(i,1)= mr_3(i,1)*(hcomp_out_3(i,1)-hcomp_in_3(i,1));
exergetic_eff_3(i,1)= (1-xt_3(i,1)/Wcomp_3(i,1))*100 ;
end
exer_eff_3_cond50_evap3 =plot(result3(:,1),exergetic_eff_3(:,1));
set(exer_eff_3_cond50_evap3,'Color','red','Linewidth',2,'DisplayName','Cond%50 - Evap3');
%%
for i=1:1:r
mr_4(i,1)=(result4(i,14)+result4(i,15))/2;
hexval_in_4(i,1)=refpropm('H','T',result4(i,6)+273,'P',result4(i,7),'r134a');
hevap_in_4(i,1) = hexval_in_4(i,1);
hevap_out_4(i,1) = refpropm('H','T',result4(i,10)+273,'P',result4(i,11),'r134a');
sevap_in_4(i,1) = refpropm('S','H',hevap_in_4(i,1),'P',result4(i,9),'r134a');
sevap_out_4(i,1) = refpropm('S','T',result4(i,10)+273,'P',result4(i,11),'r134a');
hcomp_in_4(i,1) = refpropm('H','T',result4(i,12)+273,'P',result4(i,13),'r134a');
hcomp_out_4(i,1) = refpropm('H','T',result4(i,2)+273,'P',result4(i,3),'r134a');
scomp_in_4(i,1) = refpropm('S','T',result4(i,12)+273,'P',result4(i,13),'r134a');
scomp_out_4(i,1) = refpropm('S','T',result4(i,2)+273,'P',result4(i,3),'r134a');
hcond_in_4(i,1) = refpropm('H','T',result4(i,2)+273,'P',result4(i,3),'r134a');
hcond_out_4(i,1) = refpropm('H','T',result4(i,4)+273,'P',result4(i,5),'r134a');
scond_in_4(i,1) = refpropm('S','T',result4(i,2)+273,'P',result4(i,3),'r134a');
scond_out_4(i,1) = refpropm('S','T',result4(i,4)+273,'P',result4(i,5),'r134a');
sexval_in_4(i,1) = refpropm('S','T',result4(i,6)+273,'P',result4(i,7),'r134a');
sexval_out_4(i,1) = refpropm('S','H',hevap_in_4(i,1),'P',result4(i,9),'r134a');
xevap_4(i,1)=T0*(mr_4(i,1)*(hevap_in_4(i,1)-hevap_out_4(i,1))/T0+mr_4(i,1)*(sevap_out_4(i,1)-sevap_in_4(i,1)));
xcomp_4(i,1)=T0*mr_4(i,1)*(scomp_out_4(i,1)-scomp_in_4(i,1));
xcond_4(i,1)=T0*(mr_4(i,1)*(hcond_in_4(i,1)-hcond_out_4(i,1))/T0+mr_4(i,1)*(scond_out_4(i,1)-scond_in_4(i,1)));
xexval_4(i,1)=mr_4(i,1)*T0*(sexval_out_4(i,1)-sexval_in_4(i,1));
xt_4(i,1)= xevap_4(i,1)+xcomp_4(i,1)+xcond_4(i,1)+xexval_4(i,1);
Wcomp_4(i,1)= mr_4(i,1)*(hcomp_out_4(i,1)-hcomp_in_4(i,1));
exergetic_eff_4(i,1)= (1-xt_4(i,1)/Wcomp_4(i,1))*100 ;
end
exer_eff_4_cond100_evap1 =plot(result4(:,1),exergetic_eff_4(:,1));
set(exer_eff_4_cond100_evap1,'Color','green','Linewidth',2,'DisplayName','Cond%100 - Evap1');
%%
for i=1:1:r
mr_5(i,1)=(result5(i,14)+result5(i,15))/2;
hexval_in_5(i,1)=refpropm('H','T',result5(i,6)+273,'P',result5(i,7),'r134a');
hevap_in_5(i,1) = hexval_in_5(i,1);
hevap_out_5(i,1) = refpropm('H','T',result5(i,10)+273,'P',result5(i,11),'r134a');
sevap_in_5(i,1) = refpropm('S','H',hevap_in_5(i,1),'P',result5(i,9),'r134a');
sevap_out_5(i,1) = refpropm('S','T',result5(i,10)+273,'P',result5(i,11),'r134a');
hcomp_in_5(i,1) = refpropm('H','T',result5(i,12)+273,'P',result5(i,13),'r134a');
hcomp_out_5(i,1) = refpropm('H','T',result5(i,2)+273,'P',result5(i,3),'r134a');
scomp_in_5(i,1) = refpropm('S','T',result5(i,12)+273,'P',result5(i,13),'r134a');
scomp_out_5(i,1) = refpropm('S','T',result5(i,2)+273,'P',result5(i,3),'r134a');
hcond_in_5(i,1) = refpropm('H','T',result5(i,2)+273,'P',result5(i,3),'r134a');
hcond_out_5(i,1) = refpropm('H','T',result5(i,4)+273,'P',result5(i,5),'r134a');
scond_in_5(i,1) = refpropm('S','T',result5(i,2)+273,'P',result5(i,3),'r134a');
scond_out_5(i,1) = refpropm('S','T',result5(i,4)+273,'P',result5(i,5),'r134a');
sexval_in_5(i,1) = refpropm('S','T',result5(i,6)+273,'P',result5(i,7),'r134a');
sexval_out_5(i,1) = refpropm('S','H',hevap_in_5(i,1),'P',result5(i,9),'r134a');
xevap_5(i,1)=T0*(mr_5(i,1)*(hevap_in_5(i,1)-hevap_out_5(i,1))/T0+mr_5(i,1)*(sevap_out_5(i,1)-sevap_in_5(i,1)));
xcomp_5(i,1)=T0*mr_5(i,1)*(scomp_out_5(i,1)-scomp_in_5(i,1));
xcond_5(i,1)=T0*(mr_5(i,1)*(hcond_in_5(i,1)-hcond_out_5(i,1))/T0+mr_5(i,1)*(scond_out_5(i,1)-scond_in_5(i,1)));
```

```
xexval_5(i,1)=mr_5(i,1)*T0*(sexval_out_5(i,1)-sexval_in_5(i,1));
xt_5(i,1)= xevap_5(i,1)+xcomp_5(i,1)+xcond_5(i,1)+xexval_5(i,1);
Wcomp_5(i,1)= mr_5(i,1)*(hcomp_out_5(i,1)-hcomp_in_5(i,1));
exergetic_eff_5(i,1)= (1-xt_5(i,1)/Wcomp_5(i,1))*100 ;
end
exer_eff_5_cond100_evap2 =plot(result5(:,1),exergetic_eff_5(:,1));
set(exer_eff_5_cond100_evap2,'Color','black','Linewidth',2,'DisplayName','Cond%100 - Evap2');
%%
for i=1:1:r
mr_6(i,1)=(result6(i,14)+result6(i,15))/2;
hexval_in_6(i,1)=refpropm('H','T',result6(i,6)+273,'P',result6(i,7),'r134a');
hevap_in_6(i,1) = hexval_in_6(i,1);
hevap_out_6(i,1) = refpropm('H','T',result6(i,10)+273,'P',result6(i,11),'r134a');
sevap_in_6(i,1) = refpropm('S','H',hevap_in_6(i,1),'P',result6(i,9),'r134a');
sevap_out_6(i,1) = refpropm('S','T',result6(i,10)+273,'P',result6(i,11),'r134a');
hcomp_in_6(i,1) = refpropm('H','T',result6(i,12)+273,'P',result6(i,13),'r134a');
hcomp_out_6(i,1) = refpropm('H','T',result6(i,2)+273,'P',result6(i,3),'r134a');
scomp_in_6(i,1) = refpropm('S','T',result6(i,12)+273,'P',result6(i,13),'r134a');
scomp_out_6(i,1) = refpropm('S','T',result6(i,2)+273,'P',result6(i,3),'r134a');
hcond_in_6(i,1) = refpropm('H','T',result6(i,2)+273,'P',result6(i,3),'r134a');
hcond_out_6(i,1) = refpropm('H','T',result6(i,4)+273,'P',result6(i,5),'r134a');
scond_in_6(i,1) = refpropm('S','T',result6(i,2)+273,'P',result6(i,3),'r134a');
scond_out_6(i,1) = refpropm('S','T',result6(i,4)+273,'P',result6(i,5),'r134a');
sexval_in_6(i,1) = refpropm('S','T',result6(i,6)+273,'P',result6(i,7),'r134a');
sexval_out_6(i,1) = refpropm('S','H',hevap_in_6(i,1),'P',result6(i,9),'r134a');
xevap_6(i,1)=T0*(mr_6(i,1)*(hevap_in_6(i,1)-hevap_out_6(i,1))/T0+mr_6(i,1)*(sevap_out_6(i,1)-sevap_in_6(i,1)));
xcomp_6(i,1)=T0*mr_6(i,1)*(scomp_out_6(i,1)-scomp_in_6(i,1));
xcond_6(i,1)=T0*(mr_6(i,1)*(hcond_in_6(i,1)-hcond_out_6(i,1))/T0+mr_6(i,1)*(scond_out_6(i,1)-scond_in_6(i,1)));
xexval_6(i,1)=mr_6(i,1)*T0*(sexval_out_6(i,1)-sexval_in_6(i,1));
xt_6(i,1)= xevap_6(i,1)+xcomp_6(i,1)+xcond_6(i,1)+xexval_6(i,1);
Wcomp_6(i,1)= mr_6(i,1)*(hcomp_out_6(i,1)-hcomp_in_6(i,1));
exergetic_eff_6(i,1)= (1-xt_6(i,1)/Wcomp_6(i,1))*100 ;
end
exer_eff_6_cond100_evap3 =plot(result6(:,1),exergetic_eff_6(:,1));
set(exer_eff_6_cond100_evap3,'Color','magenta','Linewidth',2,'DisplayName','Cond%100 - Evap3');
%%
L=legend(axes24,'show');
xlabel('Time (sec)');
ylabel('Exergetic Efficiencies (%)');
title('\bf Time vs Efficiencies');
set(L,'FontSize',12,'fontWeight','bold');
set(axes24,'XLim',[0 650]);
set(axes24,'XTick',0:50:650);
set(findall(axes24,'type','text'),'fontSize',16,'fontWeight','bold','FontName','Times New Roman');
colormap cool;
grid on;

xlswrite('exergeticeff.xlsx',exergetic_eff_1,1,'A1');
xlswrite('exergeticeff.xlsx',exergetic_eff_2,1,'B1');
xlswrite('exergeticeff.xlsx',exergetic_eff_3,1,'C1');
xlswrite('exergeticeff.xlsx',exergetic_eff_4,1,'D1');
xlswrite('exergeticeff.xlsx',exergetic_eff_5,1,'E1');
xlswrite('exergeticeff.xlsx',exergetic_eff_6,1,'F1');
%%
figure_exerdest=figure;
axes25 = axes('Parent',figure_exerdest);
hold(axes25,'all');

%%
exergydest_1 =plot(result1(:,1),xt_1(:,1)/1000);
set(exergydest_1,'Color','blue','Linewidth',2,'DisplayName','Cond%50 - Evap1');
%%
exergydest_2 =plot(result2(:,1),xt_2(:,1)/1000);
set(exergydest_2 ,'Color','yellow','Linewidth',2,'DisplayName','Cond%50 - Evap2');
%%
exergydest_3 =plot(result3(:,1),xt_3(:,1)/1000);
set(exergydest_3,'Color','red','Linewidth',2,'DisplayName','Cond%50 - Evap3');
%%
exergydest_4 =plot(result4(:,1),xt_4(:,1)/1000);
set(exergydest_4,'Color','green','Linewidth',2,'DisplayName','Cond%100 - Evap1');
%%
exergydest_5 =plot(result5(:,1),xt_5(:,1)/1000);
set(exergydest_5,'Color','black','Linewidth',2,'DisplayName','Cond%100 - Evap2');
```

```
%%
exergydest_6 =plot(result6(:,1),xt_6(:,1)/1000);
set(exergydest_6,'Color','magenta','Linewidth',2,'DisplayName','Cond%100 - Evap3');
%%
L=legend(axes25,'show');
xlabel('Time (sec)');
ylabel('Exergy Destruction (kW)');
title('\bf Time vs Exergy Destruction');
set(L,'FontSize',12,'fontWeight','bold');
set(axes25,'XLim',[0 650]);
set(axes25,'XTick',0:50:650);
set(findall(axes25,'type','text'),'fontSize',16,'fontWeight','bold','FontName','Times New Roman');
colormap cool;
grid on;
end
%%
```

C. RECORDED EXPERIMENTAL DATA

Table 13 Cond. Fan 50% & Evap. Fan "1" Recorded Data

Time (sec.)	Comp_Out_Cond_In_Temp (°C)	Comp_Out_Cond_In_Pres (kPa)	Cond_Out_Temp (°C)	Cond_Out_Pres (kPa)	Exp_Val_Inlet_Temp (°C)	Exp_Val_Inlet_Pres (kPa)	Exp_Val_Out_Evap_In_Temp (°C)	Exp_Val_Out_Evap_In_Pres (kPa)	Evap_Out_Temp (°C)	Evap_Out_Pres (kPa)	Comp_In_Temp (°C)	Comp_In_Pres (kPa)	m_vapor (kg/s)	m_liquid (kg/s)
0	33.1	728.6	33.8	725.3	35.3	708.1	29.4	738.4	28.8	745.2	31.5	743.4	0	0
10	33.1	730.3	33.7	726.3	35.2	709.3	29.4	740.0	28.9	746.3	31.5	744.9	0	0
20	33.0	728.3	33.7	724.7	35.0	707.9	29.4	737.7	29.0	744.5	31.5	743.1	0	0
30	33.0	726.4	33.6	723.0	34.9	706.5	29.4	736.8	28.9	743.4	31.5	741.2	0	0
40	33.1	798.7	33.6	726.4	34.8	708.5	29.5	726.3	28.9	721.6	31.1	703.6	0	0
50	65.9	1235.7	43.2	1135.3	34.1	1027.3	18.6	475.4	9.6	321.4	18.9	219.2	0.056	0.085
60	75.1	1316.0	47.3	1247.4	34.2	1169.8	14.5	405.1	9.4	274.7	16.3	196.8	0.039	0.07
70	80.1	1326.8	47.2	1273.9	38.1	1219.5	13.7	372.7	7.7	254.6	15.8	175.7	0.038	0.04
80	84.3	1338.7	48.0	1287.5	42.7	1236.5	12.6	360.3	5.1	250.2	16.0	173.1	0.038	0.035
90	87.6	1347.2	48.1	1292.1	44.3	1241.5	11.5	346.0	3.1	230.8	15.7	163.4	0.039	0.04
100	90.1	1329.8	47.4	1280.3	45.0	1232.3	10.8	339.2	4.4	215.0	15.6	151.2	0.039	0.03
110	92.4	1338.6	47.5	1287.7	45.5	1238.7	10.8	338.4	3.5	213.1	15.3	147.1	0.039	0.04
120	94.4	1330.6	47.4	1278.6	45.6	1231.3	10.7	339.2	4.4	211.7	14.9	143.8	0.039	0.035
130	96.4	1339.6	47.9	1286.5	45.6	1237.0	11.2	350.2	5.3	220.9	14.4	147.6	0.039	0.035
140	98.2	1343.6	47.8	1287.8	45.7	1240.2	11.4	374.7	5.0	226.4	13.7	152.6	0.039	0.035
150	99.6	1356.4	48.2	1298.3	46.0	1250.1	11.2	350.7	4.5	223.9	13.1	154.2	0.039	0.035
160	100.7	1361.4	48.4	1302.6	46.2	1255.8	10.5	340.2	4.5	214.2	12.6	148.9	0.039	0.035
170	101.7	1365.8	48.6	1308.9	46.4	1261.5	10.5	363.0	3.2	213.5	12.4	150.5	0.038	0.03
180	102.4	1352.6	47.9	1297.7	46.5	1250.5	10.2	334.3	3.1	207.0	12.2	145.6	0.038	0.03
190	103.1	1350.3	47.6	1296.9	46.5	1246.4	10.3	336.6	4.4	205.8	11.9	143.8	0.038	0.03
200	103.9	1348.9	47.5	1295.8	46.4	1243.3	10.6	342.8	4.7	208.9	11.7	143.9	0.038	0.04
210	104.5	1348.0	47.6	1294.7	46.2	1241.2	10.9	370.0	4.4	215.2	11.4	146.0	0.038	0.04
220	104.9	1341.2	47.5	1286.4	46.1	1233.2	10.8	365.6	4.4	215.7	10.9	146.8	0.038	0.04
230	105.1	1343.6	47.4	1287.3	46.0	1232.8	10.2	343.4	4.1	208.9	10.4	144.8	0.038	0.04
240	105.3	1349.4	47.7	1290.5	46.0	1234.8	10.3	369.6	4.0	209.1	10.3	146.1	0.038	0.04
250	105.5	1350.6	47.6	1291.5	45.9	1234.7	10.1	359.8	4.3	205.7	10.1	143.9	0.038	0.04
260	105.7	1355.4	47.8	1296.2	45.9	1236.1	10.3	358.1	4.0	206.5	10.0	143.8	0.038	0.04
270	105.9	1355.0	48.0	1297.9	46.0	1237.2	10.2	357.7	4.4	204.7	9.9	142.6	0.038	0.04
280	106.0	1354.4	48.0	1297.0	46.0	1237.7	10.3	357.4	3.3	206.6	9.7	142.3	0.038	0.035
290	106.1	1359.6	47.9	1299.5	46.1	1239.5	10.4	357.6	4.5	207.6	9.4	143.3	0.038	0.035
300	106.2	1364.4	48.2	1305.3	46.2	1245.0	10.5	356.3	4.4	209.4	9.3	144.3	0.038	0.035

Table 13 Cond. Fan 50% & Evap. Fan "1" Recorded Data - Continued

Time (sec.)	Comp_Out_Cond_In_Temp (°C)	Comp_Out_Cond_In_Pres (kPa)	Cond_Out_Temp (°C)	Cond_Out_Pres (kPa)	Exp_Val_Inlet_Temp (°C)	Exp_Val_Inlet_Pres (kPa)	Exp_Val_Out_Evap_In_Temp (°C)	Exp_Val_Out_Evap_In_Pres (kPa)	Evap_Out_Temp (°C)	Evap_Out_Pres (kPa)	Comp_In_Temp (°C)	Comp_In_Pres (kPa)	m_vapor (kg/s)	m_liquid (kg/s)
310	106.2	1366.9	48.2	1306.8	46.3	1245.9	10.5	352.0	3.8	208.7	9.1	145.2	0.038	0.035
320	106.2	1369.6	48.3	1311.0	46.4	1250.8	10.0	351.5	3.3	203.8	8.9	142.4	0.038	0.035
330	106.1	1368.0	48.4	1310.5	46.5	1250.5	10.2	348.8	2.5	205.3	8.8	143.4	0.038	0.035
340	106.1	1363.6	48.0	1303.6	46.4	1243.0	10.2	348.7	4.2	204.0	8.7	141.5	0.038	0.035
350	106.1	1365.5	48.2	1306.8	46.5	1246.9	10.2	346.1	3.2	203.5	8.6	141.4	0.038	0.0375
360	106.0	1358.0	47.6	1299.4	46.3	1237.1	10.4	349.3	3.8	205.3	8.6	142.3	0.038	0.0375
370	105.9	1349.3	47.4	1292.5	46.2	1231.7	9.9	345.9	2.4	200.9	8.4	138.8	0.038	0.0375
380	105.8	1346.2	46.4	1290.3	46.0	1226.8	9.5	341.6	2.4	197.4	8.2	136.2	0.038	0.0375
390	105.6	1334.6	45.7	1279.1	45.7	1214.6	9.1	338.1	1.6	193.2	8.1	133.1	0.038	0.0375
400	105.5	1327.7	45.3	1273.3	45.5	1208.2	8.9	333.2	3.3	191.6	8.1	132.2	0.038	0.04
410	105.5	1322.6	45.1	1265.3	45.1	1197.6	9.3	336.1	3.4	196.7	8.1	136.1	0.038	0.04
420	105.5	1324.3	46.1	1264.4	44.9	1193.6	9.6	337.7	3.0	201.1	8.0	137.8	0.038	0.04
430	105.5	1334.4	47.2	1274.3	44.7	1197.3	9.8	340.2	4.2	202.0	7.9	138.6	0.038	0.0425
440	105.4	1338.3	47.3	1272.3	44.6	1195.1	10.6	345.2	4.9	209.9	8.0	144.2	0.038	0.04
450	105.4	1357.9	47.7	1291.1	44.8	1212.7	10.9	350.0	4.5	213.6	8.0	147.4	0.039	0.04
460	105.3	1368.5	48.4	1305.7	45.3	1229.4	10.3	347.5	1.9	206.6	7.8	142.2	0.039	0.04
470	105.1	1349.1	47.9	1290.0	45.7	1222.8	9.4	340.3	3.0	193.5	7.6	133.9	0.036	0.03
480	105.0	1342.5	47.5	1287.7	45.8	1223.7	8.3	329.5	1.2	182.9	7.6	126.2	0.036	0.03
490	105.0	1335.5	47.0	1279.4	45.8	1215.2	9.1	331.1	3.9	190.3	7.7	131.2	0.036	0.03
500	105.1	1351.4	45.8	1291.6	45.7	1221.1	10.1	337.7	3.2	202.7	7.9	137.1	0.038	0.04
510	105.2	1367.5	47.3	1307.5	45.9	1231.5	10.5	343.7	4.8	209.0	7.7	142.7	0.038	0.04
520	105.2	1377.4	48.0	1313.3	45.9	1231.5	11.0	350.1	5.2	212.9	7.7	146.9	0.039	0.045
530	105.2	1397.0	49.0	1327.3	45.9	1240.7	11.6	355.9	4.8	219.5	7.8	152.5	0.039	0.05
540	105.1	1398.0	49.2	1329.3	46.0	1247.9	11.5	355.8	5.0	218.0	7.8	152.2	0.039	0.04
550	105.0	1398.3	49.2	1332.1	46.4	1255.0	11.2	353.4	3.9	213.4	7.9	148.6	0.039	0.035
560	105.0	1406.4	49.3	1340.1	46.8	1264.0	11.4	355.5	6.1	212.3	7.9	148.7	0.039	0.035
570	105.0	1416.1	49.5	1349.5	47.1	1273.1	12.0	360.0	2.9	219.7	8.2	151.9	0.039	0.035
580	104.9	1399.3	49.1	1340.8	47.2	1270.8	10.4	347.8	2.4	202.6	7.7	138.5	0.038	0.03
590	104.7	1397.3	48.8	1340.1	47.2	1272.2	9.4	340.2	1.5	192.1	7.6	132.2	0.038	0.035
600	104.6	1383.6	48.4	1329.1	47.2	1263.9	8.6	332.8	2.3	184.1	7.5	125.1	0.036	0.035
608	104.7	1372.7	47.9	1319.2	47.0	1255.0	8.3	329.3	1.9	182.5	7.6	124.5	0.036	0.035

Table 14 Cond. Fan 50% & Evap. Fan "2" Recorded Data

Time (sec.)	Comp_Out_Cond_In_Temp (°C)	Comp_Out_Cond_In_Pres (kPa)	Cond_Out_Temp (°C)	Cond_Out_Pres (kPa)	Exp_Val_Inlet_Temp (°C)	Exp_Val_Inlet_Pres (kPa)	Exp_Val_Out_Evap_In_Temp (°C)	Exp_Val_Out_Evap_In_Pres (kPa)	Evap_Out_Temp (°C)	Evap_Out_Pres (kPa)	Comp_In_Temp (°C)	Comp_In_Pres (kPa)	m_vapor (kg/s)	m_liquid (kg/s)
0	31.8	718.7	29.0	715.2	31.6	698.0	27.9	731.4	28.0	738.4	30.8	734.8	0	0
10	31.8	719.7	29.0	716.5	31.6	699.1	28.0	732.3	28.1	739.3	30.9	736.1	0	0
20	31.8	728.8	29.3	724.6	31.5	705.4	28.1	737.1	28.2	744.0	31.1	742.1	0	0
30	31.9	733.4	29.5	729.0	31.5	708.5	28.1	740.5	28.3	747.2	31.3	746.5	0	0
40	31.9	730.1	29.5	726.2	31.5	706.5	28.1	732.7	28.4	739.9	31.2	743.2	0	0
50	60.6	1293.7	43.7	1190.4	32.6	1084.9	20.5	492.6	14.8	329.8	14.0	232.5	0.06	0.065
60	71.3	1374.9	49.0	1304.0	34.3	1238.0	16.7	430.1	10.3	307.4	16.6	219.3	0.04	0.06
70	77.5	1406.4	49.2	1342.0	39.0	1285.5	15.4	400.4	10.1	272.4	15.5	191.9	0.038	0.04
80	81.7	1409.8	49.7	1347.8	44.0	1300.2	13.5	377.1	5.2	256.4	15.6	180.6	0.04	0.045
90	85.2	1425.4	50.4	1362.4	46.1	1315.5	12.4	361.5	5.1	238.0	15.4	169.4	0.04	0.04
100	88.1	1418.2	50.2	1365.2	47.0	1315.4	12.1	358.1	5.2	228.2	15.5	162.0	0.04	0.035
110	90.8	1424.6	50.1	1368.2	47.7	1318.1	12.7	395.2	6.8	230.2	15.3	160.0	0.04	0.04
120	93.3	1432.2	50.4	1372.1	48.0	1322.1	13.6	405.6	8.1	242.4	15.1	164.6	0.04	0.045
130	95.7	1454.1	50.8	1387.2	48.2	1334.8	14.4	419.6	8.4	257.9	14.5	177.1	0.04	0.04
140	97.5	1471.2	51.5	1406.8	48.6	1354.6	14.1	417.6	6.9	254.8	13.8	178.1	0.04	0.045
150	98.9	1491.2	51.9	1422.6	49.1	1370.4	13.8	414.4	8.3	248.5	13.5	176.3	0.04	0.045
160	100.0	1499.8	52.5	1438.0	49.7	1388.4	13.0	404.0	5.2	237.7	13.2	169.8	0.04	0.045
170	100.9	1480.4	51.6	1422.5	50.0	1372.6	12.5	392.2	6.2	226.6	12.9	161.5	0.04	0.035
180	101.9	1469.1	51.2	1415.2	50.0	1363.2	12.7	394.3	5.4	227.6	12.8	159.8	0.04	0.04
190	102.6	1453.7	50.8	1400.9	49.8	1350.5	12.4	386.9	6.2	224.4	12.3	154.6	0.04	0.04
200	103.2	1442.6	50.1	1389.2	49.4	1339.4	12.2	384.5	4.9	227.3	11.9	155.3	0.04	0.04
210	103.7	1438.7	49.4	1384.6	49.2	1334.7	11.9	380.5	5.7	225.6	11.5	156.2	0.04	0.04
220	104.1	1414.9	48.5	1361.0	48.8	1312.4	11.5	374.7	5.4	220.6	11.2	153.1	0.04	0.04
230	104.3	1420.6	47.3	1365.4	48.4	1312.3	10.9	367.4	4.2	213.2	10.9	148.9	0.04	0.04
240	104.5	1401.2	47.6	1344.9	48.0	1291.4	10.5	359.9	4.4	207.4	10.7	146.5	0.038	0.04
250	104.6	1379.3	47.9	1323.3	47.3	1267.5	10.1	353.5	3.5	202.1	10.6	140.3	0.038	0.04
260	104.9	1377.9	47.9	1321.0	47.0	1264.0	10.6	355.6	4.9	209.1	10.6	144.5	0.038	0.04
270	105.2	1386.7	48.7	1326.9	46.8	1263.7	11.0	359.1	4.5	213.4	10.3	145.9	0.04	0.045
280	105.4	1369.5	48.8	1312.0	46.7	1255.0	10.5	355.1	6.0	209.2	10.0	144.7	0.038	0.035
290	105.5	1366.4	48.2	1305.7	46.4	1248.3	10.8	354.4	3.0	213.6	9.9	147.9	0.038	0.035
300	105.5	1368.1	48.5	1311.7	46.7	1255.2	10.2	350.6	3.9	205.3	9.6	143.1	0.038	0.035

Table 14 Cond. Fan 50% & Evap. Fan "2" Recorded Data - Continued

Time (sec.)	Comp_Out_Cond_In_Temp (°C)	Comp_Out_Cond_In_Pres (kPa)	Cond_Out_Temp (°C)	Cond_Out_Pres (kPa)	Exp_Val_Inlet_Temp (°C)	Exp_Val_Inlet_Pres (kPa)	Exp_Val_Out_Evap_In_Temp (°C)	Exp_Val_Out_Evap_In_Pres (kPa)	Evap_Out_Temp (°C)	Evap_Out_Pres (kPa)	Comp_In_Temp (°C)	Comp_In_Pres (kPa)	m_vapor (kg/s)	m_liquid (kg/s)
310	105.4	1348.2	47.5	1292.6	46.5	1238.4	9.9	344.8	3.6	201.7	9.5	139.6	0.038	0.04
320	105.5	1359.8	45.8	1301.9	46.4	1244.1	10.2	345.4	3.9	205.2	9.5	142.2	0.038	0.04
330	105.5	1363.1	47.3	1305.0	46.5	1246.0	10.4	347.5	4.6	207.7	9.4	143.6	0.038	0.04
340	105.6	1366.8	47.6	1305.5	46.3	1240.7	10.9	352.2	4.9	212.2	9.4	146.4	0.038	0.045
350	105.6	1361.4	47.8	1298.8	45.9	1232.0	10.9	349.4	4.7	214.2	9.3	147.2	0.038	0.045
360	105.5	1378.9	48.6	1315.2	46.0	1244.9	10.9	349.5	4.2	213.3	9.2	147.6	0.038	0.045
370	105.5	1388.1	49.1	1328.0	46.3	1259.9	10.4	346.5	4.0	208.4	9.0	144.3	0.038	0.0375
380	105.5	1391.5	48.8	1327.9	46.4	1261.2	10.7	349.9	5.1	209.8	9.0	145.3	0.038	0.0375
390	105.5	1406.9	49.5	1344.6	46.9	1278.9	10.8	349.3	4.3	211.2	8.9	147.2	0.038	0.0375
400	105.5	1397.5	49.0	1336.1	47.2	1273.7	11.0	353.0	5.7	211.9	8.9	146.8	0.038	0.0375
410	105.6	1417.2	49.6	1354.1	47.4	1287.6	11.2	354.7	5.1	213.0	8.9	148.2	0.04	0.04
420	105.6	1418.8	49.8	1357.9	47.7	1293.2	10.9	350.8	4.4	209.7	8.8	145.3	0.04	0.04
430	105.5	1414.7	49.6	1353.6	47.7	1289.0	11.0	352.1	5.3	210.8	8.7	146.1	0.038	0.0375
440	105.6	1422.4	49.9	1362.1	47.7	1297.2	10.7	348.3	3.6	209.4	8.7	145.3	0.038	0.0375
450	105.5	1406.3	49.3	1346.5	47.8	1284.4	10.8	350.4	4.1	208.4	8.6	143.8	0.038	0.0375
460	105.5	1406.9	49.1	1348.7	47.6	1285.4	10.6	346.2	3.7	206.4	8.6	143.1	0.04	0.04
470	105.5	1410.5	48.5	1350.1	47.7	1283.5	11.0	351.2	4.9	210.7	8.7	146.3	0.04	0.04
480	105.6	1423.3	49.0	1360.2	47.7	1288.0	11.4	356.4	6.1	214.2	8.6	148.2	0.04	0.04
490	105.6	1430.4	49.7	1364.7	47.6	1290.3	11.1	352.7	5.0	212.1	8.5	147.3	0.038	0.045
500	105.5	1420.7	50.0	1358.5	47.6	1287.2	10.6	349.0	4.5	206.5	8.5	143.7	0.038	0.045
510	105.5	1408.8	49.0	1342.7	47.3	1273.3	10.8	347.0	3.6	208.8	8.5	144.6	0.038	0.04
520	105.4	1408.8	49.6	1348.6	47.5	1280.7	10.5	347.6	5.3	204.7	8.4	140.6	0.038	0.04
530	105.5	1417.1	49.5	1353.7	47.5	1283.3	10.9	350.6	4.9	210.8	8.5	145.4	0.038	0.04
540	105.6	1434.7	49.9	1370.4	47.8	1296.4	11.3	354.8	5.7	214.4	8.5	148.9	0.038	0.04
550	105.6	1443.3	50.2	1375.3	47.9	1298.5	12.1	362.7	5.2	223.4	8.6	155.7	0.04	0.045
560	105.6	1447.9	50.6	1382.7	48.0	1305.9	11.9	363.9	6.2	219.4	8.6	154.3	0.04	0.045
570	105.6	1458.4	50.8	1390.2	48.2	1312.6	12.1	364.7	5.8	219.9	8.6	154.9	0.04	0.04
580	105.5	1431.2	50.1	1366.5	48.3	1296.5	11.9	364.9	6.2	218.9	8.7	152.9	0.04	0.0375
590	105.4	1427.8	48.8	1364.7	48.1	1293.4	12.2	368.1	6.4	221.6	8.7	154.1	0.04	0.0375
600	105.3	1436.3	48.2	1371.2	48.0	1291.5	12.9	376.8	7.2	228.3	8.9	158.0	0.04	0.045
608	105.3	1433.3	48.1	1366.3	47.9	1284.4	12.7	373.0	6.1	228.6	8.8	159.0	0.04	0.045

Table 15 Cond. Fan 50% & Evap. Fan "3" Recorded Data

Time (sec.)	Comp_Out_Cond_In_Temp (°C)	Comp_Out_Cond_In_Pres (kPa)	Cond_Out_Temp (°C)	Cond_Out_Pres (kPa)	Exp_Val_Inlet_Temp (°C)	Exp_Val_Inlet_Pres (kPa)	Exp_Val_Out_Evap_In_Temp (°C)	Exp_Val_Out_Evap_In_Pres (kPa)	Evap_Out_Temp (°C)	Evap_Out_Pres (kPa)	Comp_In_Temp (°C)	Comp_In_Pres (kPa)	m_vapor (kg/s)	m_liquid (kg/s)
0	33.4	738.6	34.4	732.3	34.9	716.5	29.5	739.0	28.0	746.6	31.5	748.5	0	0
10	33.4	739.0	34.4	733.4	34.9	717.2	29.6	740.0	28.2	747.3	31.5	749.1	0	0
20	33.4	752.3	32.4	745.9	34.9	727.1	29.8	749.7	28.5	756.8	31.8	760.4	0	0
30	33.4	763.6	30.8	757.1	34.9	738.2	30.3	760.3	28.9	767.8	32.3	772.3	0	0
40	33.4	766.6	30.9	759.8	34.8	741.3	30.4	763.8	29.0	771.4	32.5	775.4	0	0
50	63.8	1297.8	41.6	1189.0	33.5	1065.1	19.4	491.4	22.5	293.7	13.5	216.8	0.041	0.06
60	75.2	1410.3	50.0	1328.8	35.3	1251.0	18.3	453.2	11.0	319.7	16.6	230.4	0.038	0.05
70	81.6	1464.2	50.5	1393.0	39.7	1314.6	15.5	419.7	10.7	279.6	16.2	199.6	0.036	0.055
80	85.9	1485.4	51.9	1415.7	45.3	1355.7	16.1	406.5	9.1	277.4	16.4	198.1	0.041	0.04
90	89.4	1514.8	52.6	1445.0	47.7	1382.7	14.5	389.8	6.3	257.4	16.4	184.4	0.039	0.05
100	92.1	1505.9	52.2	1443.5	49.0	1381.6	14.1	382.8	6.3	244.1	16.4	174.0	0.039	0.04
110	94.4	1488.4	51.5	1430.4	49.7	1372.1	14.0	381.1	6.6	241.3	16.2	167.8	0.039	0.035
120	96.6	1501.3	52.1	1440.4	49.8	1379.7	14.5	407.5	7.6	249.9	15.9	169.7	0.039	0.0475
130	98.6	1506.5	52.4	1442.7	49.9	1383.6	14.4	395.0	7.7	253.9	15.1	174.0	0.039	0.04
140	100.1	1511.4	52.3	1447.6	50.1	1389.3	14.2	396.6	6.9	251.0	14.7	174.4	0.039	0.04
150	101.3	1507.3	52.2	1445.8	50.4	1390.4	13.7	403.9	6.2	243.7	14.4	170.8	0.039	0.04
160	102.2	1497.8	52.1	1439.8	50.4	1385.9	12.4	370.3	3.4	227.6	14.0	159.8	0.038	0.035
170	102.9	1469.2	51.2	1417.4	50.2	1365.5	11.1	345.6	4.3	210.7	13.6	147.6	0.036	0.03
180	103.7	1458.3	49.1	1405.5	49.7	1348.5	11.6	366.2	5.9	214.4	13.5	148.4	0.036	0.03
190	104.6	1454.2	47.2	1401.8	49.5	1343.1	11.9	376.1	5.5	220.0	13.2	148.9	0.038	0.04
200	105.3	1436.2	46.5	1381.2	49.0	1321.2	12.1	378.4	5.5	224.9	12.7	151.9	0.038	0.04
210	105.7	1430.9	47.3	1375.3	48.2	1314.6	11.9	383.3	5.4	224.5	12.2	153.3	0.038	0.04
220	105.9	1421.9	48.6	1366.4	47.4	1306.7	11.3	383.1	4.5	218.7	11.9	150.9	0.038	0.04
230	106.0	1421.0	48.2	1365.3	46.9	1305.1	10.5	365.2	4.2	208.7	11.6	144.8	0.038	0.04
240	106.0	1415.8	48.1	1360.8	46.6	1301.9	9.5	323.2	3.0	198.4	11.3	139.0	0.034	0.035
250	106.2	1412.4	47.1	1357.6	46.3	1298.5	9.8	356.6	3.3	200.6	11.3	138.5	0.036	0.03
260	106.3	1411.9	45.9	1357.1	46.0	1297.2	9.7	344.6	3.6	198.3	11.0	135.9	0.036	0.035
270	106.4	1412.1	44.9	1357.0	45.8	1296.3	9.6	349.7	0.6	199.4	10.8	136.3	0.036	0.0375
280	106.5	1410.7	45.2	1355.8	45.7	1295.0	9.5	345.3	2.8	199.3	10.5	134.8	0.036	0.0375
290	106.5	1405.8	45.6	1349.9	45.0	1288.7	9.9	346.7	5.1	203.9	10.2	137.3	0.036	0.0375
300	106.4	1406.6	46.3	1349.9	44.6	1287.7	10.3	348.7	3.4	209.6	9.9	144.0	0.036	0.04

Table 15 Cond. Fan 50% & Evap. Fan "3" Recorded Data - Continued

Time (sec.)	Comp_Out_Cond_In_Temp (°C)	Comp_Out_Cond_In_Pres (kPa)	Cond_Out_Temp (°C)	Cond_Out_Pres (kPa)	Exp_Val_Inlet_Temp (°C)	Exp_Val_Inlet_Pres (kPa)	Exp_Val_Out_Evap_In_Temp (°C)	Exp_Val_Out_Evap_In_Pres (kPa)	Evap_Out_Temp (°C)	Evap_Out_Pres (kPa)	Comp_In_Temp (°C)	Comp_In_Pres (kPa)	m_vapor (kg/s)	m_liquid (kg/s)
310	106.3	1406.6	46.6	1350.0	44.5	1288.0	9.6	344.5	3.6	202.2	9.7	139.1	0.036	0.04
320	106.2	1407.7	46.9	1351.2	44.5	1289.0	9.8	342.6	4.4	204.0	9.6	141.2	0.036	0.04
330	106.1	1407.5	46.6	1350.6	44.6	1288.8	10.1	344.1	3.8	206.6	9.5	143.7	0.036	0.035
340	106.1	1413.3	47.3	1356.2	44.8	1293.2	10.4	347.3	5.4	208.4	9.5	143.9	0.038	0.04
350	106.2	1422.4	48.6	1364.3	45.3	1299.3	11.7	361.5	6.3	222.6	9.6	155.3	0.038	0.04
360	106.2	1427.0	49.3	1369.0	45.7	1303.5	12.1	364.6	5.0	227.0	9.5	158.0	0.038	0.04
370	106.0	1424.6	48.8	1366.6	46.2	1303.2	11.8	363.9	5.9	221.9	9.3	155.3	0.038	0.0375
380	105.8	1426.4	48.7	1368.0	46.5	1305.1	12.0	364.6	5.5	222.5	9.2	155.1	0.038	0.0375
390	105.7	1429.7	49.5	1372.0	46.9	1308.9	12.0	365.5	6.1	222.7	9.2	155.1	0.038	0.0375
400	105.6	1431.5	49.4	1373.6	47.1	1310.3	12.0	366.4	6.0	223.7	9.3	156.3	0.038	0.0375
410	105.6	1435.8	49.8	1366.0	47.4	1313.2	12.7	374.2	6.6	229.9	9.4	160.5	0.038	0.04
420	105.6	1437.9	49.9	1367.3	47.6	1307.1	13.2	381.7	7.7	233.5	9.4	163.3	0.038	0.04
430	105.5	1446.3	50.2	1377.3	47.8	1307.5	13.2	381.8	7.4	233.7	9.4	163.5	0.038	0.04
440	105.4	1458.5	50.5	1387.2	48.0	1314.0	13.1	377.2	6.0	232.6	9.4	162.1	0.038	0.04
450	105.3	1468.0	51.2	1399.9	48.4	1319.9	13.1	379.0	5.5	233.1	9.4	163.8	0.038	0.04
460	105.3	1470.5	50.8	1399.5	48.5	1320.3	12.9	379.4	7.3	229.2	9.4	160.1	0.038	0.04
470	105.2	1476.1	51.2	1407.0	48.8	1331.2	12.8	378.0	6.2	228.3	9.4	159.9	0.038	0.04
480	105.2	1478.9	51.4	1413.4	49.0	1338.9	12.4	371.7	5.3	223.6	9.4	156.0	0.038	0.04
490	105.2	1468.3	50.8	1402.1	49.0	1333.5	11.9	365.7	3.6	218.7	9.3	152.9	0.038	0.0325
500	105.2	1456.4	50.6	1394.0	49.0	1327.8	11.8	364.4	5.2	218.1	9.3	151.0	0.038	0.035
510	105.2	1454.1	49.3	1391.3	48.8	1321.9	11.8	365.4	5.0	218.5	9.3	152.2	0.038	0.04
520	105.2	1449.3	48.5	1386.7	48.7	1315.0	11.6	362.4	5.0	217.2	9.2	151.3	0.038	0.04
530	105.2	1442.3	48.6	1376.2	48.3	1299.1	12.0	365.5	4.5	220.2	9.3	153.3	0.038	0.04
540	105.2	1432.7	48.9	1367.2	48.0	1290.5	11.7	362.5	5.3	217.3	9.2	150.1	0.038	0.04
550	105.1	1410.7	49.1	1345.0	47.5	1269.7	12.0	367.8	7.1	220.3	9.3	152.8	0.038	0.04
560	105.1	1417.7	49.0	1351.0	47.4	1272.4	11.8	362.2	4.0	219.6	9.3	152.4	0.038	0.04
570	105.0	1414.8	49.3	1348.7	47.3	1270.5	11.7	361.0	5.1	217.8	9.2	151.4	0.038	0.04
580	105.0	1412.9	48.9	1345.1	47.1	1264.3	12.1	365.4	5.6	222.2	9.3	153.6	0.036	0.04
590	104.9	1411.4	49.3	1347.4	47.2	1268.9	11.3	360.3	5.6	213.3	9.1	146.4	0.038	0.04
600	104.8	1398.1	48.9	1336.3	47.1	1259.6	11.4	360.1	5.9	213.9	9.1	147.9	0.038	0.0325
608	104.8	1392.4	48.5	1331.3	47.0	1258.2	11.0	355.0	5.5	211.0	9.1	145.3	0.038	0.035

Table 16 Cond. Fan 100% & Evap. Fan "1" Recorded Data

Time (sec.)	Comp_Out_Cond_In_Temp (°C)	Comp_Out_Cond_In_Pres (kPa)	Cond_Out_Temp (°C)	Cond_Out_Pres (kPa)	Exp_Val_Inlet_Temp (°C)	Exp_Val_Inlet_Pres (kPa)	Exp_Val_Out_Evap_In_Temp (°C)	Exp_Val_Out_Evap_In_Pres (kPa)	Evap_Out_Temp (°C)	Evap_Out_Pres (kPa)	Comp_In_Temp (°C)	Comp_In_Pres (kPa)	m_vapor (kg/s)	m_liquid (kg/s)
0	27.9	607.0	26.4	597.5	23.4	587.5	27.2	608.6	26.7	614.4	25.2	615.9	0	0
10	28.0	603.7	26.4	594.4	23.3	585.8	27.2	600.0	26.6	605.8	25.1	611.1	0	0
20	28.1	600.6	26.5	591.5	23.3	583.8	27.1	595.6	26.6	601.2	25.1	608.1	0	0
30	28.0	598.7	26.4	590.2	23.2	581.8	27.1	596.5	26.6	601.7	25.0	606.9	0	0
40	27.8	598.1	26.5	589.5	23.2	581.7	27.1	600.8	26.6	605.8	25.0	608.3	0	0
50	41.9	964.1	28.5	878.3	24.0	665.6	12.6	363.2	19.6	224.2	8.7	148.0	0.045	0.1
60	46.8	983.4	34.6	913.9	27.7	846.6	13.9	380.1	6.7	282.7	12.0	179.2	0.04	0.065
70	53.1	1016.2	36.8	964.2	29.3	916.0	11.0	337.2	3.5	249.1	8.8	159.1	0.04	0.04
80	57.3	1035.9	37.9	988.4	31.8	939.9	9.2	324.3	4.0	209.0	9.1	135.8	0.033	0.0325
90	60.9	1012.0	37.4	977.1	33.8	930.7	7.4	297.4	2.7	187.1	10.0	122.4	0.032	0.0275
100	64.4	1010.7	35.7	969.3	34.5	922.5	6.3	282.3	0.9	175.0	10.3	114.5	0.035	0.03
110	67.6	1025.2	35.9	981.9	34.7	930.1	7.4	299.9	0.6	181.6	10.4	113.9	0.038	0.04
120	70.5	1038.8	38.4	998.0	34.9	943.5	8.2	329.9	3.1	193.1	10.1	110.0	0.038	0.04
130	73.0	1005.6	36.8	962.2	34.7	920.9	7.9	340.5	3.6	202.3	9.3	120.0	0.037	0.0275
140	75.4	1008.8	35.3	957.0	34.4	911.1	8.6	349.3	2.2	210.9	8.7	130.9	0.038	0.03
150	77.4	1011.0	35.1	958.9	34.8	915.7	7.3	299.3	0.9	195.8	7.9	124.5	0.035	0.03
160	79.2	1021.2	35.3	965.5	34.6	914.5	7.2	335.9	1.5	189.7	7.9	123.9	0.035	0.04
170	81.0	1032.9	36.3	977.2	34.7	920.8	7.3	336.4	2.2	189.4	7.9	122.2	0.037	0.04
180	82.5	1031.5	36.3	976.1	34.6	915.7	7.0	324.3	1.0	182.5	7.8	118.1	0.037	0.0375
190	83.8	1041.2	36.6	985.1	34.4	916.6	7.7	329.3	2.6	185.3	7.8	118.1	0.037	0.04
200	85.0	1048.0	37.9	992.2	34.8	929.4	7.4	325.6	0.5	186.0	7.6	112.5	0.037	0.035
210	86.1	1053.4	37.9	1000.5	34.9	939.3	7.0	321.2	0.6	187.8	7.1	113.1	0.038	0.0375
220	86.9	1057.7	38.6	1007.0	35.4	951.5	5.9	308.1	0.0	178.2	6.5	110.6	0.035	0.03
230	87.6	1050.8	37.6	994.0	35.4	944.0	5.7	305.8	0.6	172.6	6.3	108.9	0.035	0.03
240	88.5	1047.4	38.3	999.0	35.8	954.4	5.1	296.8	-2.2	169.5	6.2	106.4	0.037	0.0225
250	89.1	1041.1	37.0	989.0	35.9	944.6	6.3	299.5	0.7	174.9	6.2	109.9	0.037	0.02
260	89.8	1045.8	36.8	991.3	35.8	943.2	6.1	296.6	2.0	171.8	6.1	109.9	0.037	0.03
270	90.6	1053.7	37.2	1000.8	36.1	946.2	6.7	300.6	3.2	173.2	6.1	112.4	0.037	0.03
280	91.2	1067.1	37.6	1012.4	36.0	951.6	6.1	297.7	0.1	171.1	6.0	108.2	0.037	0.035
290	91.7	1056.6	37.3	1001.7	35.8	942.3	6.5	299.1	-0.9	174.0	5.9	109.4	0.037	0.03
300	92.0	1056.4	37.5	1003.0	35.8	947.3	5.0	288.7	-0.2	161.8	5.5	100.8	0.037	0.03

Table 16 Cond. Fan 100% & Evap. Fan "1" Recorded Data - Continued

Time (sec.)	Comp_Out_Cond_In_Temp (°C)	Comp_Out_Cond_In_Pres (kPa)	Cond_Out_Temp (°C)	Cond_Out_Pres (kPa)	Exp_Val_Inlet_Temp (°C)	Exp_Val_Inlet_Pres (kPa)	Exp_Val_Out_Evap_In_Temp (°C)	Exp_Val_Out_Evap_In_Pres (kPa)	Evap_Out_Temp (°C)	Evap_Out_Pres (kPa)	Comp_In_Temp (°C)	Comp_In_Pres (kPa)	m_vapor (kg/s)	m_liquid (kg/s)
310	92.5	1071.8	37.9	1015.9	35.9	955.5	5.4	289.2	-0.4	167.4	5.5	105.8	0.037	0.035
320	93.0	1094.6	38.9	1033.7	36.1	965.3	6.7	295.6	0.2	177.8	5.6	112.6	0.037	0.0375
330	93.4	1106.4	39.6	1049.0	36.4	981.1	6.0	293.0	-0.8	170.6	5.4	107.0	0.037	0.03
340	93.6	1083.3	39.0	1027.2	36.6	969.2	5.0	284.2	0.6	159.1	5.0	100.5	0.037	0.025
350	93.8	1079.1	38.2	1021.3	36.5	962.5	4.8	283.1	4.3	151.4	4.9	98.8	0.037	0.025
360	94.3	1102.7	39.2	1041.2	36.8	975.7	5.9	297.3	3.1	162.3	5.1	103.6	0.037	0.03
370	94.5	1091.4	39.2	1036.0	37.2	983.0	5.0	281.3	-0.7	159.4	5.0	100.8	0.037	0.025
380	94.8	1087.9	38.1	1030.4	36.8	972.4	5.7	284.1	0.2	165.6	5.0	105.7	0.032	0.0275
390	95.0	1084.3	38.2	1030.1	37.0	974.5	4.5	277.5	-2.3	155.7	4.9	98.8	0.032	0.0275
400	95.2	1109.5	38.0	1052.5	37.0	982.8	5.8	280.8	-1.4	165.1	5.0	105.5	0.035	0.035
410	95.4	1090.1	38.3	1031.6	36.9	968.2	6.1	284.2	0.1	167.6	4.9	107.1	0.035	0.03
420	95.6	1091.9	38.6	1038.0	37.0	978.8	4.4	275.8	-2.3	156.8	4.7	99.5	0.035	0.03
430	95.8	1104.3	38.7	1044.5	36.7	973.4	6.1	286.9	2.9	167.6	4.7	106.6	0.035	0.035
440	96.2	1116.7	39.6	1053.1	37.0	979.2	6.8	296.3	2.6	173.8	4.9	112.7	0.035	0.035
450	96.4	1097.2	39.8	1042.5	37.2	981.3	6.0	286.0	0.1	168.2	4.7	109.4	0.035	0.025
460	96.5	1107.9	39.2	1050.0	37.1	987.7	5.7	286.6	1.0	164.8	4.6	109.1	0.035	0.03
470	96.5	1122.9	40.0	1064.7	37.4	1003.2	4.9	278.6	-3.2	159.3	4.7	104.0	0.035	0.035
480	96.6	1107.6	39.5	1052.6	37.5	993.5	5.4	279.9	-1.1	160.9	4.8	104.0	0.035	0.03
490	96.7	1096.8	38.1	1039.4	37.2	977.9	5.6	282.0	0.3	160.0	4.8	104.8	0.035	0.025
500	96.8	1107.2	38.1	1049.9	37.3	978.3	5.6	282.5	0.8	159.3	4.8	102.6	0.035	0.03
510	97.0	1096.8	38.7	1041.3	37.5	980.8	5.2	280.6	-0.6	157.5	4.7	100.4	0.035	0.03
520	97.0	1086.7	38.1	1030.5	37.1	968.4	4.7	276.9	-1.6	156.0	4.7	98.5	0.035	0.03
530	97.1	1097.6	38.0	1039.0	36.7	966.4	5.5	278.2	-2.0	163.2	4.7	103.1	0.035	0.0325
540	97.0	1091.1	38.4	1031.3	36.7	964.5	5.5	275.9	-1.6	162.4	4.6	103.3	0.032	0.03
550	97.1	1080.0	37.9	1019.9	36.4	951.5	5.5	278.8	-1.2	163.9	4.6	106.1	0.032	0.03
560	97.0	1076.3	37.8	1020.2	36.6	958.7	4.7	272.6	-0.1	155.0	4.4	100.3	0.035	0.03
570	97.0	1085.7	37.9	1027.5	36.4	956.6	5.0	273.2	-1.9	158.7	4.5	102.5	0.035	0.03
580	97.2	1105.9	38.2	1043.2	36.5	966.2	6.0	280.0	-1.0	168.2	4.7	109.9	0.035	0.035
590	97.3	1107.1	39.0	1044.6	36.6	965.8	6.5	290.5	1.6	169.0	4.7	110.6	0.035	0.0325
600	97.4	1093.3	38.7	1031.5	36.4	958.0	6.2	285.0	-0.3	168.3	4.7	108.8	0.035	0.03
608	97.4	1114.7	38.6	1051.8	36.7	973.7	6.1	284.9	0.7	166.8	4.6	107.8	0.035	0.03

Table 17 Cond. Fan 100% & Evap. Fan "2" Recorded Data

Time (sec.)	Comp_Out_Cond_In_Temp (℃)	Comp_Out_Cond_In_Pres (kPa)	Cond_Out_Temp (℃)	Cond_Out_Pres (kPa)	Exp_Val_Inlet_Temp (℃)	Exp_Val_Inlet_Pres (kPa)	Exp_Val_Out_Evap_In_Temp (℃)	Exp_Val_Out_Evap_In_Pres (kPa)	Evap_Out_Temp (℃)	Evap_Out_Pres (kPa)	Comp_In_Temp (℃)	Comp_In_Pres (kPa)	m_vapor (kg/s)	m_liquid (kg/s)
0	32.7	718.6	28.7	708.1	31.2	696.1	28.6	717.2	30.6	727.0	30.4	724.2	0	0
10	32.7	720.4	28.8	709.3	31.2	697.6	28.8	718.3	30.7	729.0	30.3	725.7	0	0
20	32.5	737.6	28.8	724.1	31.2	708.6	29.0	729.6	31.0	739.8	30.6	740.3	0	0
30	32.3	762.5	30.2	751.3	31.3	731.1	29.4	749.2	31.9	758.5	32.3	767.6	0	0
40	32.4	767.3	30.6	757.1	31.3	735.6	29.5	753.5	32.1	762.7	32.6	772.2	0	0
50	64.6	1249.6	40.4	1145.6	32.2	1058.4	18.4	481.9	23.5	294.3	3.4	216.3	0.045	0.08
60	76.5	1268.7	45.3	1189.0	34.7	1143.5	18.4	448.0	10.3	330.6	16.1	232.0	0.043	0.07
70	83.4	1312.3	46.1	1239.8	39.0	1201.1	15.4	399.0	7.1	282.3	13.6	200.8	0.04	0.04
80	88.1	1338.2	47.3	1267.1	41.8	1232.3	13.2	364.3	4.9	253.4	14.1	181.8	0.041	0.04
90	91.8	1317.1	46.7	1254.7	43.5	1218.7	11.7	355.0	4.8	228.5	14.7	167.5	0.038	0.035
100	94.9	1292.2	45.8	1232.4	44.3	1200.1	12.1	358.5	4.5	228.0	14.8	158.4	0.038	0.03
110	97.5	1241.0	43.9	1193.2	44.2	1168.1	11.7	347.9	3.5	225.2	14.3	148.1	0.038	0.0225
120	99.6	1223.6	41.0	1178.6	43.7	1151.7	10.7	340.1	3.7	219.6	13.4	145.3	0.037	0.03
130	101.7	1217.8	39.3	1161.6	42.9	1130.6	10.1	325.5	1.8	213.2	12.5	144.9	0.037	0.04
140	103.5	1204.8	39.0	1139.4	42.1	1104.1	10.4	341.2	6.4	213.6	11.9	151.2	0.035	0.05
150	105.0	1170.4	41.3	1105.5	40.9	1070.3	9.4	337.0	3.8	207.1	11.8	145.1	0.038	0.04
160	106.4	1244.5	44.4	1171.5	41.2	1124.8	10.7	368.8	4.7	221.5	11.6	163.5	0.037	0.0525
170	107.8	1233.8	45.0	1167.8	41.6	1132.8	11.6	390.0	5.7	223.6	11.6	161.4	0.038	0.03
180	108.8	1217.6	43.8	1164.4	42.1	1129.7	11.0	347.6	5.1	216.7	11.1	152.3	0.037	0.025
190	109.4	1220.5	42.2	1159.4	42.5	1126.7	10.2	331.6	1.6	206.9	10.7	143.2	0.035	0.029
200	110.0	1193.3	41.5	1138.2	42.3	1108.2	10.0	343.7	3.0	204.7	10.1	141.4	0.035	0.0275
210	110.6	1194.0	39.9	1134.0	41.8	1099.5	10.0	362.3	4.0	205.8	9.7	141.5	0.032	0.04
220	110.7	1161.6	39.8	1101.6	41.1	1072.3	9.0	338.2	2.8	203.9	9.3	138.7	0.035	0.035
230	110.9	1150.0	38.7	1087.4	40.5	1056.9	9.1	344.5	2.9	201.4	8.8	141.5	0.033	0.03
240	111.1	1172.3	39.1	1097.5	40.2	1061.2	8.8	324.8	0.5	195.8	8.9	138.4	0.035	0.045
250	111.4	1162.9	42.2	1101.6	40.1	1065.7	8.6	326.1	1.3	194.8	8.7	136.7	0.037	0.0325
260	111.2	1155.7	41.4	1089.7	39.7	1048.9	9.1	340.3	4.9	194.2	8.8	134.5	0.035	0.035
270	111.0	1170.4	41.7	1103.7	39.9	1066.8	8.9	324.7	0.6	196.5	8.4	137.4	0.035	0.0325
280	111.1	1172.7	41.7	1104.2	40.1	1063.9	9.9	342.8	4.3	200.7	8.1	140.5	0.032	0.03
290	111.2	1169.6	41.8	1102.7	40.2	1063.8	8.9	330.0	1.4	195.1	7.6	135.8	0.037	0.0325
300	111.2	1178.8	41.1	1106.0	40.3	1068.9	8.4	332.5	2.5	196.0	7.7	135.7	0.035	0.03

Table 17 Cond. Fan 100% & Evap. Fan "2" Recorded Data - Continued

Time (sec.)	Comp_Out_Cond_In_Temp (°C)	Comp_Out_Cond_In_Pres (kPa)	Cond_Out_Temp (°C)	Cond_Out_Pres (kPa)	Exp_Val_Inlet_Temp (°C)	Exp_Val_Inlet_Pres (kPa)	Exp_Val_Out_Evap_In_Temp (°C)	Exp_Val_Out_Evap_In_Pres (kPa)	Evap_Out_Temp (°C)	Evap_Out_Pres (kPa)	Comp_In_Temp (°C)	Comp_In_Pres (kPa)	m_vapor (kg/s)	m_liquid (kg/s)
310	111.3	1172.5	41.8	1104.7	40.4	1066.1	9.5	337.8	1.8	205.8	7.7	147.4	0.035	0.035
320	111.2	1208.2	42.3	1133.7	40.6	1093.7	8.3	324.6	2.3	191.7	7.4	138.1	0.035	0.045
330	111.3	1182.6	42.9	1119.9	40.8	1085.4	9.5	334.8	1.5	195.9	7.7	139.4	0.035	0.03
340	111.2	1176.3	41.3	1115.1	40.7	1080.9	7.0	300.6	0.9	176.0	7.3	122.7	0.035	0.035
350	111.3	1182.6	41.4	1117.9	40.8	1082.1	7.7	318.6	0.7	182.4	7.4	126.1	0.035	0.035
360	111.4	1170.6	42.1	1109.9	40.8	1075.7	8.5	317.7	0.3	191.2	7.2	129.9	0.035	0.025
370	111.5	1182.2	41.3	1109.1	40.5	1069.4	8.8	332.6	5.6	192.4	6.7	135.2	0.037	0.04
380	111.6	1216.6	43.5	1143.5	40.9	1097.9	9.8	343.4	5.7	208.5	7.0	146.5	0.035	0.045
390	111.6	1227.8	43.3	1146.2	41.0	1101.7	10.2	342.5	4.5	211.4	7.0	151.4	0.035	0.035
400	111.6	1259.5	44.3	1176.3	41.6	1130.8	10.4	341.1	4.0	209.6	7.2	153.0	0.035	0.035
410	111.6	1237.5	43.7	1163.4	42.0	1123.3	10.5	342.8	3.2	206.0	7.5	148.4	0.035	0.03
420	111.6	1239.2	43.7	1165.8	42.3	1125.0	10.4	344.6	4.0	205.1	7.5	145.5	0.035	0.035
430	111.7	1236.9	43.7	1167.6	42.4	1126.1	10.7	348.6	5.8	207.9	7.4	145.6	0.035	0.035
440	111.7	1232.8	43.5	1161.2	42.2	1121.8	10.9	348.1	3.1	217.9	7.4	147.6	0.037	0.035
450	111.4	1213.8	43.0	1147.3	42.0	1109.4	9.5	338.8	3.4	204.0	6.8	141.9	0.035	0.0275
460	111.3	1231.9	41.9	1157.4	41.9	1117.1	9.6	327.3	0.8	205.3	7.1	141.8	0.035	0.04
470	111.3	1228.0	42.8	1156.9	42.0	1118.1	9.0	332.6	1.6	201.7	7.0	139.9	0.035	0.04
480	111.1	1211.8	42.8	1142.4	41.7	1103.8	9.2	327.2	2.4	197.1	6.8	139.8	0.037	0.04
490	111.1	1211.4	42.5	1137.4	41.5	1094.4	8.8	334.7	5.0	191.5	7.0	135.4	0.037	0.04
500	111.3	1232.8	44.1	1166.2	41.9	1121.5	9.8	338.3	4.5	205.3	7.1	140.4	0.037	0.04
510	111.4	1211.4	43.0	1144.3	41.6	1104.6	9.7	334.3	1.7	205.2	7.0	139.8	0.035	0.03
520	111.3	1207.5	42.2	1139.6	41.6	1102.3	9.3	330.8	2.2	202.4	6.8	139.9	0.035	0.03
530	111.2	1197.0	41.7	1130.5	41.6	1093.1	8.9	328.6	0.1	196.3	6.9	133.3	0.035	0.03
540	111.0	1168.3	40.7	1109.5	41.0	1074.1	6.3	301.8	0.4	175.8	6.3	121.9	0.033	0.025
550	110.8	1150.9	38.8	1088.6	40.6	1053.0	7.7	311.7	3.5	178.3	6.4	121.3	0.035	0.035
560	110.9	1152.0	38.6	1084.3	40.2	1045.2	7.6	315.3	2.0	185.0	6.6	128.5	0.035	0.035
570	110.9	1164.4	38.3	1087.4	39.7	1040.3	8.0	313.9	3.1	184.8	6.5	126.2	0.035	0.045
580	111.1	1154.1	40.9	1080.1	39.3	1038.3	8.5	312.6	-0.2	194.8	6.7	133.9	0.035	0.04
590	110.9	1133.0	40.6	1066.5	39.0	1022.5	7.4	312.7	3.6	177.5	6.1	120.8	0.032	0.03
600	110.7	1133.3	40.2	1072.4	39.0	1034.0	6.2	298.9	-0.1	176.7	6.1	121.2	0.032	0.03
608	110.8	1131.3	39.9	1065.0	38.9	1020.8	7.2	310.7	3.1	177.2	6.2	119.9	0.032	0.03

Table 18 Cond. Fan 100% & Evap. Fan "3" Recorded Data

Time (sec.)	Comp_Out_Cond_In_Temp (℃)	Comp_Out_Cond_In_Pres (kPa)	Cond_Out_Temp (℃)	Cond_Out_Pres (kPa)	Exp_Val_Inlet_Temp (℃)	Exp_Val_Inlet_Pres (kPa)	Exp_Val_Out_Evap_In_Temp (℃)	Exp_Val_Out_Evap_In_Pres (kPa)	Evap_Out_Temp (℃)	Evap_Out_Pres (kPa)	Comp_In_Temp (℃)	Comp_In_Pres (kPa)	m_vapor (kg/s)	m_liquid (kg/s)
0	37.2	771.8	36.1	760.4	38.7	741.5	27.8	771.0	32.0	779.9	34.1	775.0	0	0
10	36.9	779.3	33.1	767.2	38.6	748.6	28.1	780.4	32.8	788.4	34.1	782.5	0	0
20	36.8	788.4	33.3	776.4	38.6	756.9	28.2	776.9	32.7	787.0	34.3	789.4	0	0
30	36.8	803.9	34.1	792.8	38.6	772.0	28.7	797.6	33.2	806.9	35.5	806.3	0	0
40	37.0	802.3	34.0	791.3	38.5	770.3	28.9	801.0	33.5	811.0	35.6	806.3	0	0
50	75.7	1453.0	49.5	1383.6	35.0	1275.1	20.8	508.8	14.4	341.1	14.6	256.8	0.043	0.07
60	84.4	1405.5	50.5	1338.7	37.6	1267.3	17.1	429.1	9.7	317.2	18.0	230.4	0.036	0.04
70	89.0	1383.6	49.6	1325.4	40.6	1253.8	14.5	399.8	8.4	283.9	16.7	206.6	0.036	0.0425
80	92.6	1370.6	48.8	1298.1	43.3	1225.7	13.7	392.6	8.1	271.5	16.7	202.4	0.032	0.0475
90	95.3	1391.1	50.4	1328.7	45.1	1262.8	11.5	362.3	5.5	240.6	16.3	180.8	0.032	0.04
100	97.5	1392.2	49.7	1337.0	46.1	1275.3	9.7	336.3	3.6	213.8	16.5	162.6	0.032	0.0375
110	99.7	1346.7	49.0	1299.2	46.7	1238.7	9.5	334.7	4.1	210.2	16.5	154.0	0.032	0.0375
120	101.8	1348.3	48.4	1299.0	47.1	1241.4	9.4	327.9	4.6	209.8	16.3	151.9	0.032	0.03
130	104.0	1342.0	48.3	1291.0	47.0	1232.5	11.1	358.8	6.0	228.9	16.0	161.9	0.032	0.03
140	105.8	1345.0	47.0	1292.2	46.9	1231.9	10.6	348.1	3.6	229.0	14.9	163.3	0.031	0.04
150	107.3	1340.4	48.0	1287.0	46.8	1227.7	11.4	377.2	6.4	236.5	14.4	171.5	0.032	0.035
160	108.4	1340.8	47.5	1284.6	46.5	1222.7	11.2	376.6	4.2	232.6	14.4	170.7	0.032	0.035
170	109.3	1349.6	48.3	1294.5	46.7	1232.6	10.2	365.9	4.8	222.4	13.2	165.2	0.031	0.04
180	110.0	1332.3	48.2	1281.3	46.6	1224.6	9.6	333.0	1.4	212.7	13.2	158.7	0.032	0.03
190	110.7	1325.0	46.4	1273.9	46.4	1216.9	9.3	331.3	4.5	206.4	13.0	152.9	0.031	0.025
200	111.5	1328.6	44.5	1275.8	46.2	1215.1	8.7	324.4	3.8	199.8	13.0	147.1	0.031	0.035
210	112.2	1317.3	43.8	1266.9	46.0	1209.0	9.9	360.7	5.3	211.6	12.8	153.1	0.031	0.035
220	112.9	1327.3	43.6	1274.1	45.7	1211.8	10.2	366.6	4.6	218.6	12.4	155.6	0.031	0.04
230	113.3	1319.3	46.3	1267.2	45.2	1206.0	10.0	364.8	3.5	217.7	11.7	156.9	0.031	0.04
240	113.5	1321.6	45.7	1267.7	44.6	1206.9	9.3	351.9	1.5	211.1	11.3	152.9	0.031	0.0325
250	113.7	1321.0	45.6	1267.9	44.4	1207.4	9.0	350.1	1.9	207.8	11.0	153.9	0.029	0.0325
260	113.8	1322.9	46.0	1271.1	44.6	1211.2	7.8	341.1	4.9	195.6	10.9	144.0	0.029	0.0325
270	114.2	1339.7	45.8	1289.3	44.5	1229.8	9.3	349.5	2.6	208.1	11.0	154.1	0.032	0.035
280	114.3	1339.6	46.2	1289.8	44.6	1230.5	8.4	338.2	3.2	199.2	10.7	146.6	0.031	0.035
290	114.6	1341.1	47.0	1292.0	45.0	1232.6	8.7	344.6	2.6	201.6	10.6	148.2	0.032	0.03
300	114.7	1339.8	46.2	1290.3	44.8	1231.4	9.0	340.1	1.7	205.6	10.2	149.8	0.031	0.03

Table 18 Cond. Fan 100% & Evap. Fan "3" Recorded Data - Continued

Time (sec.)	Comp_Out_Cond_In_Temp (°C)	Comp_Out_Cond_In_Pres (kPa)	Cond_Out_Temp (°C)	Cond_Out_Pres (kPa)	Exp_Val_Inlet_Temp (°C)	Exp_Val_Inlet_Pres (kPa)	Exp_Val_Out_Evap_In_Temp (°C)	Exp_Val_Out_Evap_In_Pres (kPa)	Evap_Out_Temp (°C)	Evap_Out_Pres (kPa)	Comp_In_Temp (°C)	Comp_In_Pres (kPa)	m_vapor (kg/s)	m_liquid (kg/s)
310	114.9	1339.4	46.6	1290.7	45.0	1232.1	8.7	340.0	3.9	202.5	9.9	146.1	0.031	0.03
320	115.0	1337.5	45.8	1288.0	44.7	1229.0	9.1	340.1	0.5	204.7	9.9	147.2	0.029	0.025
330	114.9	1337.1	43.4	1287.9	44.7	1228.8	7.8	333.3	4.6	195.0	9.3	144.0	0.029	0.03
340	114.7	1334.0	42.7	1285.2	44.5	1227.0	8.0	318.0	0.4	189.8	9.2	138.4	0.031	0.03
350	114.6	1333.7	41.6	1285.1	44.4	1226.6	7.1	329.4	5.1	181.2	9.0	133.9	0.028	0.03
360	114.6	1332.7	41.9	1283.8	44.0	1225.1	7.0	321.0	3.6	183.2	9.1	134.6	0.028	0.03
370	114.7	1332.2	41.3	1282.5	43.2	1222.5	7.9	317.4	0.4	195.2	9.1	142.1	0.029	0.04
380	114.8	1333.1	42.9	1283.2	43.1	1223.1	8.4	334.4	5.2	198.0	9.1	144.8	0.031	0.04
390	114.6	1331.0	44.3	1281.3	42.6	1222.3	7.5	308.8	-0.7	187.4	8.7	136.0	0.031	0.03
400	114.3	1327.6	43.8	1278.2	42.2	1218.8	8.0	321.2	2.0	192.0	8.5	140.3	0.031	0.03
410	114.3	1328.9	44.4	1280.0	42.3	1219.8	6.8	325.5	4.8	181.0	8.3	130.3	0.028	0.03
420	114.2	1328.8	44.2	1279.8	42.4	1221.5	6.8	304.9	0.0	183.9	8.1	134.6	0.028	0.03
430	114.2	1328.8	43.9	1279.4	42.5	1220.3	7.3	315.9	3.9	185.5	8.2	135.5	0.028	0.03
440	114.2	1324.7	43.7	1274.7	42.7	1215.9	5.6	300.2	2.1	174.3	8.1	127.9	0.031	0.03
450	114.1	1311.8	44.2	1259.8	42.7	1199.4	7.3	308.9	3.0	187.5	8.1	137.2	0.031	0.03
460	114.3	1315.0	44.4	1262.9	42.9	1202.0	7.4	318.6	3.9	185.0	8.3	134.9	0.031	0.03
470	114.3	1318.2	44.4	1264.8	42.9	1203.8	7.4	310.3	0.0	190.4	8.2	138.7	0.031	0.03
480	114.4	1311.3	45.2	1256.9	43.2	1193.4	8.3	324.2	6.3	192.9	8.1	140.1	0.031	0.03
490	114.4	1319.7	45.6	1265.3	43.4	1204.0	7.1	314.2	1.3	187.6	8.2	137.4	0.029	0.03
500	114.5	1316.1	45.6	1261.5	43.6	1199.4	8.2	317.8	1.2	193.9	8.2	141.9	0.029	0.03
510	114.5	1316.5	45.2	1260.8	43.7	1198.9	7.7	318.6	2.0	189.0	8.1	137.2	0.029	0.03
520	114.5	1316.5	45.2	1261.6	43.8	1201.0	7.2	310.3	-0.4	188.5	8.1	135.4	0.029	0.03
530	114.5	1313.4	44.9	1257.9	43.9	1195.9	7.3	317.3	4.9	185.6	7.9	135.2	0.031	0.03
540	114.5	1315.3	45.0	1259.5	43.8	1199.1	7.9	308.3	-0.5	193.5	8.2	140.8	0.031	0.03
550	114.4	1307.3	44.2	1253.8	43.7	1192.7	7.5	323.2	7.2	185.5	7.7	134.5	0.031	0.03
560	114.4	1311.4	43.5	1256.2	43.6	1194.0	7.5	317.1	0.9	190.9	8.1	137.3	0.031	0.03
570	114.3	1310.2	43.5	1255.4	43.5	1193.4	7.3	304.5	0.1	188.7	7.9	134.7	0.031	0.03
580	114.3	1308.9	43.5	1254.0	43.4	1190.2	7.3	317.7	4.8	184.6	7.9	133.9	0.031	0.03
590	114.4	1313.8	44.4	1257.8	43.2	1193.7	7.2	310.1	0.3	190.1	8.0	136.0	0.031	0.035
600	114.4	1308.4	45.1	1253.6	43.1	1189.2	8.0	325.0	4.6	193.3	8.0	137.8	0.029	0.0325
608	114.4	1311.1	44.5	1252.7	42.9	1187.8	8.3	317.1	1.9	198.3	8.1	140.2	0.029	0.0325